

**WestminsterResearch**

<http://www.westminster.ac.uk/research/westminsterresearch>

**The role of cancer stem cells in osteosarcoma**

**Andrew D. Jenks**

Faculty of Science and Technology

This is an electronic version of a PhD thesis awarded by the University of Westminster. © The Author, 2014.

This is an exact reproduction of the paper copy held by the University of Westminster library.

---

The WestminsterResearch online digital archive at the University of Westminster aims to make the research output of the University available to a wider audience. Copyright and Moral Rights remain with the authors and/or copyright owners.

Users are permitted to download and/or print one copy for non-commercial private study or research. Further distribution and any use of material from within this archive for profit-making enterprises or for commercial gain is strictly forbidden.

---

Whilst further distribution of specific materials from within this archive is forbidden, you may freely distribute the URL of WestminsterResearch:  
(<http://westminsterresearch.wmin.ac.uk/>).

In case of abuse or copyright appearing without permission e-mail  
[repository@westminster.ac.uk](mailto:repository@westminster.ac.uk)

# **THE ROLE OF CANCER STEM CELLS IN OSTEOSARCOMA**

Andrew D. Jenks

A THESIS SUBMITTED IN PARTIAL FULFILMENT OF THE  
REQUIREMENTS OF THE UNIVERSITY OF WESTMINSTER  
FOR THE DEGREE OF DOCTOR OF PHILOSOPHY

MAY 2014

## Abstract

Osteosarcoma (OS) is the most common bone malignancy often producing aggressive tumours in adolescents. OS aetiology is poorly understood, however, recent studies suggest OS cancers contain a small population of cancer stem cells (CSC) which initiate tumour growth. The cancer stem cell hypothesis describes cancers as a hierarchical population of heterogeneous cells. It has been proposed that CSC are at the base of this hierarchy and are responsible for the initiation, growth and spread of the tumour and pose a therapeutic challenge due to enhanced chemotherapy resistance. This project had three aims: identifying whether OS cell lines contain subpopulations of putative CSC, identifying if CSC contribute to chemotherapeutic resistance and to elucidate paracrine cell signals controlling OS tumour growth.

Eight OS cell lines (143B, Cal72, G292, HOS, MG63, MNNG-HOS, U2OS and SaOS-2) along with the breast cancer cell line MCF7 have been analysed for the presence of subpopulation of cells expressing putative CSC markers (aldehyde dehydrogenase and CD117). The intracellular enzyme aldehyde dehydrogenase (ALDH) and tyrosine kinase receptor CD117 were found to be heterogeneously expressed amongst the cell lines. All cell lines when plated at low density could recapitulate the colony hierarchies based on variation in colony morphology (holoclones, meroclones and paraclones), this was originally observed in carcinoma cell lines and is further putative evidence a CSC hierarchy exists within these cell lines. ALDH expressing cells were found to be confined to the holoclones (in cell lines with ALDH populations comprising less than 10 % of the total population) indicating that putative CSCs reside within this population. All OS cell lines also expressed mesenchymal markers (high vimentin and CD44 expression and low e-cadherin expression) suggesting they are a progenitor of mesenchymal stem cells. The expression of CD117 was found to negatively correlate with cisplatin chemotherapy resistance whereas ALDH inhibition using the specific antagonist diethylaminobenzaldehyde sensitised different cell lines to opposing chemotherapeutics, suggesting a heterogeneous response of OS ALDH cells to cytotoxic compounds.

All OS cell lines, except 143B and HOS, were found to secrete a paracrine growth factor which was capable of significantly enhancing their own growth. U2OS conditioned media was also able to enhance the growth of the breast cancer cell line MCF7 and a fibrosarcoma cell line (HT1080). Analysis of the cytokine expression profile of OS cell lines (HOS, MG63 and U2OS) demonstrated these cells secrete a broad range of cytokines associated with inflammation. The cytokine CCL-2 was identified as the putative OS paracrine growth factor as determined by the response to recombinant CCL-2, receptor antagonism and CCL-2 RNA interference. Genes with altered expression in response to CCL-2 were associated with transcription, suggesting that CCL-2 enhances proliferation through its downstream effect on transcription.

Overall this thesis has contributed to the field of oncology by further defining the populations of putative CSC within a panel of OS cell lines. In addition the identification of a novel OS growth factor provides a possible adjuvant therapeutic target, which could aid in the reduction of OS proliferation.

<b>Section</b>	<b>Page</b>
Title.....	1
Abstract.....	2
Table of contents.....	3
List of figures.....	8
List of tables.....	13
Acknowledgements.....	14
Author's declaration.....	15
List of abbreviations.....	16

## **CHAPTER 1 GENERAL INTRODUCTION**

1.1 Introduction to cancer.....	19
1.1.1 Cancer associated mutations.....	20
1.1.2 Classification of cancer.....	21
1.1.3 Osteosarcoma .....	23
1.2 Stem cells and cancer.....	26
1.2.1 Evidence supporting the cancer stem cell theory .....	28
1.2.2 Markers of CSCs.....	29
1.2.3 Cancer cell hierarchy.....	32
1.2.4 Epithelial to mesenchymal transition.....	33
1.2.5 Cancer stem cells and epithelial mesenchymal transition .....	35
1.3 Osteosarcoma chemotherapy treatment.....	37
1.3.1 Doxorubicin resistance .....	37
1.3.2 Platinum based by chemotherapy resistance.....	39
1.3.3 Methotrexate resistance.....	39
1.3.4 Cancer stem cells and chemotherapy resistance.....	40
1.4 Cell signalling networks.....	42
1.4.1 Signalling networks in healthy bone.....	43
1.4.2 Influence of the microenvironment upon cancer.....	44
1.4.3 Osteosarcoma signaling networks.....	45
1.4.4 CCL2 expression in cancer.....	45
1.4.5 IL-8 expression in cancer.....	46
1.4.6 Targeted cancer therapeutics.....	47
1.5 Thesis aims.....	49

## **CHAPTER 2 MATERIALS AND METHODS**

2.1 Materials.....	52
2.2 Cell lines.....	52
2.2.1 Cell culture.....	53
2.2.2 Passaging cell lines.....	53
2.2.3 Cell line trypsinisation and counting.....	54

2.2.4 Spherical colony assay.....	54
2.2.5 Soft agarose assay.....	55
<b>2.3 Chemotoxicity analysis .....</b>	<b>56</b>
2.3.1 Assessment of median lethal doses in response to chemotherapeutics and DEAB.....	56
2.3.2 Clonogenicity of chemotherapy treated cells .....	56
2.3.3 Combined DEAB and chemotherapy exposure .....	57
<b>2.4 Paracrine growth experiments.....</b>	<b>58</b>
2.4.1 Conditioned media collection.....	58
2.4.2 Conditioned media effect on colony formation .....	58
2.4.3 96 well proliferation assay .....	58
2.4.4 CXCR1, CXCR2 and CCR2 receptor antagonist experiment .....	59
<b>2.5 Cytokine expression.....</b>	<b>60</b>
2.5.1 Cytokine array.....	60
2.5.2 CCL-2 and IL-8 ELISA .....	60
<b>2.6 CCL-2 RNA gene interference.....</b>	<b>61</b>
2.6.1 Transforming bacterial competent cells.....	62
2.6.2 Plasmid preparation.....	62
2.6.3 CCL-2 stable knockdown.....	62
<b>2.7 Gene expression analysis .....</b>	<b>64</b>
2.7.1 RNA extraction.....	64
2.7.2 Reverse transcription.....	64
2.7.3 Quantitative real time PCR.....	64
2.7.4 Gene microarray.....	65
<b>2.8 Flow cytometry .....</b>	<b>66</b>
2.8.1 Extracellular antibody staining.....	66
2.8.2 Intracellular antibody staining.....	67
2.8.3 Aldehyde dehydrogenase staining (ALDH) .....	68
2.8.4 Living cell discrimination .....	68
2.8.5 Flow cytometric analysis.....	68
2.8.6 CSC marker expression of chemotherapy treated cells.....	69
2.8.7 ALDH cell density expression.....	69
<b>2.9 Confocal microscopy.....</b>	<b>70</b>
 <b>CHAPTER 3 CHARACTERISATION OF OSTEOSARCOMA STEM CELLS</b>	
<b>3.1 Introduction.....</b>	<b>72</b>
<b>3.2 Expression of cancer stem cell markers.....</b>	<b>75</b>
3.2.1 ALDH staining optimisation.....	75
3.2.2 Analysis of ALDH expression in OS cell lines and MCF7.....	77
3.2.3 CD117 staining optimisation .....	78
3.2.4 Analysis of CD117 expression in OS cell lines and MCF7.....	79
3.2.5 Analysis of CD44 expression in OS cell lines and MCF7.....	80
<b>3.3 Analysis of expression of EMT markers in OS cell lines and MCF7.....</b>	<b>81</b>

3.4 CD44 and EMT marker co-expression analysis.....	83
3.4.1 Optimisation of method used to assess CD44 and e-cadherin expression.....	83
3.4.2 Characterisation of CD44/e-cadherin phenotypes in OS cell lines and MCF7.....	84
3.4.3 Characterisation of CD44/vimentin phenotypes in OS cell lines and MCF7.....	88
3.5 Identification of the colony hierarchies within OS cell lines and MCF7.....	91
3.6 Presence of cells expressing CSC markers within colony hierarchies .....	94
3.6.1 Location of ALDH expressing cells within OS cell lines and MCF7 colony hierarchies .....	94
3.6.2: Location of CD117 expressing cells within colony hierachy of 143B .....	99
3.6.3: Location of CD44 and e-cadherin expressing cells within colony hierachy.....	101
3.7 Evaluation of sarcosphere forming ability of OS cell lines and MCF7.....	104
3.7.1 Evaluation of primary sarcosphere sizes in OS cell lines and MCF.....	107
3.7.2 Evaluation of secondary sarcospheres in OS cell lines and MCF7.....	109
3.7.3 Correlation of CSC marker expression with sarcosphere forming effciency.....	111
3.8 Presence of ALDH and CD117 expressing cell within sarcosphere colonies .....	112
3.8.1 ALDH expression within 143B sarcosphere .....	112
3.8.2 CD117 expression within 143B sarcosphere .....	114
3.9 Discussion .....	116
<b>CHAPTER 4 THE ROLE OF PUTATIVE OSTEOSARCOMA CANCER STEM CELL IN CHEMOTHERAPY RESISTANCE</b>	
4.1 Introduction.....	127
4.2 Chemotherapy sensitivity of OS cell lines and MCF7.....	130
4.3 Clonogenicity assessment of cisplatin and doxorubicin treated cells in selected OS cell lines and MCF7.....	135
4.4 Analysis of putative CSC marker expression in cisplatin and doxorubicin treated cells in selected OS cell lines and MCF7.....	138
4.5 Growth rates of methotrexate exposed cell in selected OS cell lines and MCF7.....	140
4.6 Presence of putative cancer stem cells in methotrexate treated OS and MCF7 cells Lines.....	143
4.6.1 Cancer stem markers expressed by methotrexate treated cell lines.....	143
4.7 Effect of cell density on ALDH expression in selected OS cell lines and MCF7.....	147
4.8 Correlation of cancer stem cell marker expression with chemotherapeutic resistance in osteosarcoma cell lines and MCF7.....	149
4.9 Sarcosphere forming ability of MG63 methotrexate exposed cells.....	154

4.10 Effect of ALDH inhibition on methotrexate sensitivity upon selected OS cell lines and MCF7 .....	158
4.11 Discussion.....	162
<b>CHAPTER 5 CHARACTERISATION OF PARACRINE GROWTH SIGNALLING UTILISED BY OSTEOSARCOMA CELLS</b>	
5.1 Introduction.....	172
5.2 Paracrine signaling in OS cell lines and MCF7 in response to 24 hour conditioned media.....	174
5.3 Assessment cell density during 24 hour media conditioning for HOS, MG63, U2OS and MCF7 .....	177
5.4 Analysis of paracrine growth signaling in sarcoma cell lines.....	178
5.5 Analysis of U2OS cell confluency and cell exposure time upon the growth enhancing properties of conditioned media.....	180
5.6 Paracrine signaling in OS cell lines and MCF7 in response to 72 hour conditioned media.....	182
5.7 Analysis of the growth response of U2OS and HOS cells to 72 hour conditioned media within a 96 well assay.....	184
5.8 Assessment of colony hierarchy frequency in response to conditioned media in HOS, U2OS and MCF7 cells.....	186
5.9 Cytokine profiling of HOS, MG63, U2OS and MCF7 72 hour conditioned media ....	188
5.10 Expression profile of CCL-2 and IL-8 from sarcoma cell lines and MCF7.....	193
5.11 Discussion .....	198
<b>CHAPTER 6 ASSESSMENT OF IL-8 AND CCL-2 IN OSTEOSARCOMA PROLIFERATION</b>	
6.1 Introduction.....	205

6.2 Effect of IL-8 and CCL-2 receptor anatagonism on HOS and U2OS growth rates.....	207
6.3 Growth reponse of HOS, MCF7 and MG63 cells to IL-8 and CCL-2.....	212
6.4 Growth response of HOS and U2OS to recombinant CCL-2 in a 96 well growth assay.....	213
6.5 Assessment of soft agarose colony formation in response to recombinant IL-8 and CCL-2 in the OS cell lines MG63 and U2OS .....	215
6.6 Assessment of sarcosphere formation in response to recombinant IL-8 and CCL-2 in the OS cell line MG63.....	218
6.7 Analysis of CXCR1, CXCR2 and CCR2 expression in OS cell lines and MCF7.....	221
6.8 RNA inference of CCL-2 gene expression in U2OS cells.....	224
6.9 Assessment of the U2OS CCL-2 knockdown cell lines proliferation rate.....	227
6.10 U2OS CCL-2 knockdown cell lines in low attachment conditions.....	231
6.11 Identification of genes with altered expression in U2OS cells in response to CCL-2 and U2OS conditioned media.....	234
6.12 Discussion.....	241
<b>CHAPTER 7 GENERAL DISCUSSION</b>	
7.1 General discussion .....	251
7.2 Conclusions .....	257
7.3 Future work.....	258
Appendix.....	260
References.....	268



<b>Figure</b>	<b>Page</b>
<b>Figure 1.1:</b> Cancer stem cell evolution model.....	27
<b>Figure 1.2:</b> Holoclone, meroclone and paraclone morphologies in the malignant cell line VB6.....	33
<b>Figure 1.3:</b> Doxorubicin (Dox) resistance mechanisms .....	38
<b>Figure 1.4:</b> Autocrine, paracrine, endocrine and juxtacrine signalling Mechanisms .....	42
<b>Figure 2.1:</b> Diagram of pLKO.1 vector map used for the RNA interference . of CCL-2 .....	61
<b>Figure 3.1:</b> Removal of two cells (duplets) passing through the flow cytometer laser at once.....	75
<b>Figure 3.2:</b> Optimisation of live/dead cells in ALDH staining.....	76
<b>Figure 3.3:</b> Analysis of ALDH positive population.....	76
<b>Figure 3.4:</b> Evaluation of the percentage of ALDH positive cells (ALDH <sup>+</sup> ) in OS and MCF7 cell lines .....	77
<b>Figure 3.5:</b> Gating of dead cells using PE channel.....	78
<b>Figure 3.6:</b> Evaluation of the percentage of CD117 positive cells in the cell line 143B.....	78
<b>Figure 3.7:</b> Evaluation of the percentage of cells expressing CD117 in OS and MCF7 cell lines .....	79
<b>Figure 3.8:</b> Evaluation of the percentage of cells expressing CD44 in OS and MCF7 cell lines .....	80
<b>Figure 3.9:</b> Evaluation of cell lines expressing e-cadherin in OS and MCF7 cell lines .....	81
<b>Figure 3.10:</b> Evaluation of cell lines expressing vimentin in OS and MCF7 cell lines .....	81
<b>Figure 3.11:</b> Evaluation of CD44 and e-cadherin populations in OS and MCF7 cell lines .....	84
<b>Figure 3.12:</b> Evaluation of CD44 and e-cadherin expression in OS and MCF7 cell lines .....	86
<b>Figure 3.13:</b> Evaluation of CD44 and vimentin expression of OS cell lines and MCF7 .....	89
<b>Figure 3.14:</b> Colony hierarchies present within each cell line.....	92
<b>Figure 3.15:</b> Colony morphologies containing ALDH positive cells OS cell lines and MCF7 .....	98
<b>Figure 3.16:</b> Colony morphologies containing CD117 positive cells in 143B at low density .....	99
<b>Figure 3.17:</b> Colony morphologies containing CD117 positive cells in 143B at high density. ....	100
<b>Figure 3.18:</b> Colony morphologies containing CD44 and e-cad positive cells in G292 and MCF7 .....	103
<b>Figure 3.19:</b> Images of sarcospheres produced from OS cell lines and MCF7.....	105
<b>Figure 3.20:</b> Analysis of primary sarcosphere sizes in OS cell lines and MCF7.....	108
<b>Figure 3.21:</b> Analysis of number of cells present after passage of primary sarcospheres .....	108

<b>Figure</b>	<b>Page</b>
<b>Figure 3.22:</b> Analysis of cell line relative sarcosphere sizes of and sarcosphere forming efficiency (SFE) of secondary sarcospheres .....	110
<b>Figure 3.23:</b> Cells expressing ALDH within a large 143B sarcosphere.....	113
<b>Figure 3.24:</b> Cells expressing CD117 within a 143B sarcosphere .....	115
<b>Figure 4.1:</b> Dose response curves for Cisplatin (A and B) and Doxorubicin (C and D) and methotrexate (D and E) dose response curves for OS cell lines and MCF7 .....	131
<b>Figure 4.2:</b> Appearance of OS cell lines and MCF7 after 48 hours of cisplatin or doxorubicin LD25 exposure.....	136
<b>Figure 4.3:</b> U2OS cells exposed to LD25 of either cisplatin or doxorubicin.....	137
<b>Figure 4.4:</b> MG63 cells exposed to LD25 of either cisplatin or doxorubicin.....	137
<b>Figure 4.5:</b> Auto-fluorescence of doxorubicin and cisplatin exposed cells detected by flow cytometry analysis in HOS cell line.....	139
<b>Figure 4.6:</b> Images of OS cell lines (HOS, MG63 and U2OS) and MCF7 in response to methotrexate exposure at 0, 5 and 50 nM.....	141
<b>Figure 4.7:</b> Assessment of colony size of HOS, MG63, U2OS and MCF7 exposed to MTX concentrations (0, 5 and 50 nM) .....	142
<b>Figure 4.8:</b> Analysis of the frequency of the colony hierarchies in methotrexate treated HOS, MG63, U2OS and MCF7 cells.....	145
<b>Figure 4.9:</b> Presence of ALDH expressing cells in MG63, U2OS and MCF7 MTX treated cells.....	146
<b>Figure 4.10:</b> Presence of CD117 expressing cells in MG63, U2OS and MCF7 MTX treated cells.....	146
<b>Figure 4.11:</b> Analysis of effect of cell density upon ALDH expression.....	148
<b>Figure 4.12:</b> Linear regression analysis of cell line (143B, Cal72, G292, HOS, MG63 U2OS, SaOS-2 and MCF7) cisplatin LD <sub>50</sub> concentration against ALDH expression.....	150
<b>Figure 4.13:</b> Linear regression analysis of cell line (143B, Cal72, G292, HOS, MG63 U2OS, SaOS-2 and MCF7) doxorubicin LD <sub>50</sub> concentration against ALDH expression .....	150
<b>Figure 4.14:</b> Linear regression analysis of cell line (143B, Cal72, G292, HOS, MG63, U2OS, SaOS-2 and MCF7) methotrexate LD <sub>50</sub> concentration against ALDH expression.....	151
<b>Figure 4.15:</b> Linear regression analysis of cell line (143B, Cal72, G292, HOS, MG63, U2OS, SaOS-2 and MCF7) cisplatin LD <sub>50</sub> concentration against CD117 expression .....	151
<b>Figure 4.16:</b> Linear regression analysis of cell line (143B, Cal72, G292, HOS, MG63, U2OS, SaOS-2 and MCF7) doxorubicin LD <sub>50</sub> concentration against CD117 expression .....	152
<b>Figure 4.17:</b> Linear regression analysis of cell line (143B, Cal72, G292, HOS, MG63, U2OS, SaOS-2 and MCF7) methotrexate LD <sub>50</sub> concentration against CD117 expression .....	152
<b>Figure 4.18:</b> MG63 methotrexate treated sarcosphere assay procedure.....	155
<b>Figure 4.19:</b> Images of MG63 sarcospheres in response to methotrexate exposure.....	156
<b>Figure 4.20:</b> Analysis of primary sarcosphere size in MG63.....	157

<b>Figure</b>	<b>Page</b>
<b>Figure 4.21:</b> Analysis of secondary sarcosphere forming efficiency.....	157
<b>Figure 4.22:</b> DEAB dose response curve of HOS, MG63, U2OS and MCF7.....	159
<b>Figure 4.23:</b> Cell sensitivity to MTX LD <sub>25</sub> and DEAB LD <sub>50</sub> in HOS, MG63, U2OS and MCF7 .....	160
<b>Figure 4.24:</b> Cell sensitivity to cis LD <sub>25</sub> and DEAB LD <sub>50</sub> in HOS and U2OS.....	161
<b>Figure 4.25:</b> Cell sensitivity to dox LD <sub>25</sub> and DEAB LD <sub>50</sub> in HOS and U2OS.....	161
<b>Figure 5.1:</b> Average colony size of OS cell lines and MCF7 exposed to either conditioned (collected after 24 hours exposure to confluent cells) or unconditioned media.....	175
<b>Figure 5.2:</b> Response of HOS, MG63, U2OS and MCF7 cells to 24 hour conditioned media from growth increasing and non-growth responsive conditioned media.....	176
<b>Figure 5.3:</b> Cell density of HOS, MG63, U2OS and MCF7 for 24 hour conditioned media collection.....	177
<b>Figure 5.4:</b> Growth response of sarcoma cell lines (HT1080 and SKLNS1) and U2OS to conditioned media from U2OS and sarcoma cell lines.....	179
<b>Figure 5.5:</b> Growth effect of U2OS conditioned media taken after 24 hours exposure to U2OS cells at 70, 90 and 100 % confluency.....	181
<b>Figure 5.6:</b> Growth effect of U2OS conditioned media collected from confluent U2OS cells after 24, 48 and 72 hours .....	181
<b>Figure 5.7:</b> Response of HOS, MG63, U2OS and MCF7 cells to 24 hour and 72 hour conditioned media from growth increasing and non-growth responsive conditioned media.....	183
<b>Figure 5.8:</b> Response of HOS and U2OS cells to 72 hour conditioned media from HOS, MG63, U2OS and MCF7 in a 96 well assay.....	185
<b>Figure 5.9:</b> Colony hierarchy frequency in response to 24 hour conditioned media in HOS, U2OS and MCF7 cell lines.....	187
<b>Figure 5.10:</b> Images of the cytokine array of HOS, MG63, U2OS and MCF7 72 hour conditioned media.....	189
<b>Figures 5.11:</b> Densitometry analysis of cytokines present on the cytokine array of HOS, MG63, U2OS and MCF7 72 hour conditioned media.....	192
<b>Figure 5.12:</b> Analysis of CCL-2 and IL-8 concentration of conditioned media from sarcoma cell lines and MCF7 and the growth response of each cell line to its conditioned media.....	194
<b>Figure 5.13:</b> Concentration of IL-8 in 24 hour conditioned media from sarcoma cell lines and MCF7.....	195
<b>Figure 5.14:</b> Comparison of IL-8 concentration of 24 hour and 72 hour conditioned media from MG63, U2OS, HOS and MCF7.....	195
<b>Figure 5.15:</b> Concentration of CCL-2 in 24 hour conditioned media from sarcoma cell lines and MCF7.....	196
<b>Figure 5.16:</b> Comparison of CCL-2 concentration of 24 hour and 72 hour conditioned media from MG63, U2OS, HOS and MCF7.....	196
<b>Figure 5.17:</b> Linear regression analysis of CCL-2 or IL-8 concentration of OS cell line and MCF7 24 hour conditioned media against colony size change in response to growth in conditioned media .....	197

<b>Figure</b>	<b>Page</b>
<b>Figure 6.1:</b> IL-8 receptor anatagonism of U2OS and HOS cells growth in unconditioned, U2OS and MG63 72 hour conditioned media in the presence or absence of 200 ng/ml CXCR1 and CXCR2 inhibitory antibodies .....	208
<b>Figure 6.2:</b> IL-8 receptor anatagonism of U2OS and HOS cells growth in unconditioned, U2OS and MG63 72 hour conditioned media in the presence or absence of 2 µg/ml CXCR1 inhibitory antibody.....	209
<b>Figure 6.3:</b> RS 504393 CCR2 receptor antagonism (1 µM) of U2OS and HOS cells growth in unconditioned, U2OS and MG63 72 hour conditioned media.....	210
<b>Figure 6.4:</b> CCR2 receptor antagonism (10 µM) of U2OS and HOS cells growth in unconditioned, U2OS and MG63 72 hour conditioned media.....	211
<b>Figure 6.5:</b> Growth reponse of HOS, MCF7 and MG63 to CCL-2 and IL-8.....	212
<b>Figure 6.6:</b> Supplementation of recombinant CCL-2 in to complete media to assess the growth affect upon U2OS cells .....	214
<b>Figure 6.7:</b> Supplementation of recombinant CCL-2 in to complete media to assess the growth affect upon HOS cells.....	214
<b>Figure 6.8:</b> Appearance of MG63 and U2OS soft agarose colonies formed in the absence and presence of recombinant CCL-2 and IL-8.....	214
<b>Figure 6.9:</b> Number of U2OS colonies present in the soft agarose assay in response to CCL-2 and IL-8.....	217
<b>Figure 6.10:</b> Number of MG63 colonies present in the soft agarose assay in Response to CCL-2 and IL-8.....	217
<b>Figure 6.11:</b> Appearance of MG63 primary and secondary sarcosphere formed in the absence and presence of recombinant CCL-2 and IL-8.....	219
<b>Figure 6.12:</b> Analysis of primary sarcosphere sizes in MG63 in response to IL-8 and CCL-2.....	220
<b>Figure 6.13:</b> Analysis of secondary sarcosphere forming efficiency of MG63 cells in response to IL-8 and CCL2.....	220
<b>Figure 6.14:</b> Flow cytometry overlay analysis of CXCR1, CXCR2 and CCR2 expression from the cell lines HOS, MG63, U2OS and MCF7.....	222
<b>Figure 6.15:</b> Relative mRNA expression of CCL-2 compared to 18S rRNA expression from U2OS empty vector cells and CCL-2 knockdown 1 and 2 cells.....	225
<b>Figure 6.16:</b> Analysis of CCL-2 concentration of 24 hour conditioned media taken from normal U2OS cells along with U2OS CCL-2 knockdown lines.....	225
<b>Figure 6.17:</b> Analysis of CCL-2 concentration of 72 hour conditioned media taken from normal U2OS cells along with U2OS CCL-2 gene knockdown cell lines.....	226
<b>Figure 6.18:</b> Analysis of U2OS empty vector control and CCL-2 knockdown cell lines growth rates.....	228

<b>Figure</b>	<b>Page</b>
<b>Figure 6.19:</b> Assessment U2OS CCL-2 knockdown cell lines growth response to CCL-2 (100 ng/ml) and conditioned media from empty vector and CCL-2 knockdown cell lines.....	229
<b>Figure 6.20:</b> The growth effect of supplementing CCL-2 in to knockdown 2 conditioned media upon knockdown 1 and 2 cell lines .....	230
<b>Figure 6.21:</b> Comparison of soft agarose colonies formed by U2OS CCL-2 Knockdown cell lines and empty vector control in the absence (unconditioned) and presence of CCL-2 at 36.4 ng/ml.....	232
<b>Figure 6.22:</b> Assessment of colonies formed by U2OS CCL-2 knockdown cell lines and empty vector control in the soft agarose assay.....	233
<b>Figure 6.23:</b> Assessment of colonies formed by U2OS CCL-2 knockdown cell lines and empty vector control in the soft agarose assay.....	233
<b>Figure 6.24:</b> Heatmap of genes expressed in U2OS cells in response to unconditioned (DMEM), CCL-2 (MCP-1) and U2OS conditioned media.....	235
<b>Figure 6.25:</b> Volcano plots of genes with altered expression in CCL-2 conditioned or U2OS conditioned cells compared to unconditioned cells.....	236
<b>Figure 6.26:</b> Venn diagram of genes with altered expression compared to unconditioned cells in CCL-2 conditioned and U2OS conditioned cells.....	236
<b>Figure 7.1:</b> Proposed signal transduction of homodimeric CCR2 and heterodimeric CCR2 and CCR5 .....	255
<b>Figure I:</b> Negative control confocal microscopy images of ALDH and CD44 co-stained images.....	260
<b>Figure II:</b> Negative control confocal microscopy image of CD117 and CD44 co-stained image .....	261
<b>Figure III:</b> Calibration curves of CCL-2 and IL-8 concentration.....	262
<b>Figure IV:</b> Real time PCR primer efficiencies.....	263
<b>Figure V:</b> Melting curves of 18s rRNA primers.....	264
<b>Figure VI:</b> Melting curves of CCL-2 primers .....	265
<b>Figure VII:</b> Box plot of samples tested in using the affymetrix gene microarray.....	267
<b>Figure VIII:</b> Multi-dimensional plot of genes expressed by microarray samples.....	267

<b>Table</b>	<b>Page</b>
<b>Table 1.1:</b> Human OS cell lines.....	24
<b>Table 1.2:</b> CSC identified using a CD44 phenotype.....	30
<b>Table 2.1:</b> Osteosarcoma cell lines utilised within study.....	53
<b>Table 2.2:</b> shRNA lentiviral sequences used to assess stable knockdown of CCL-2 in U2OS cells.....	62
<b>Table 2.3:</b> Comparison of primary antibodies used for assessment of cell marker expression in flow cytometry.....	66
<b>Table 2.4:</b> Antibodies used to stain for CSC markers, EMT status and expression of cytokine receptors.....	67
<b>Table 3.1:</b> CD44/e-cadherin phenotypes in OS cell lines and MCF7 .....	87
<b>Table 3.2:</b> CD44/e-cadherin phenotypes in OS cell lines and MCF7.....	90
<b>Table 3.3:</b> Pearson's correlation coefficient analysis of primary or secondary spherical colony formation with CSC marker expression.....	111
<b>Table 4.1:</b> Comparison of cisplatin, doxorubicin and methotrexate median lethal doses (LD <sub>50</sub> ) in OS cell lines and MCF7.....	134
<b>Table 4.2:</b> Identification of CD44 positive populations of HOS cells when comparing untreated cells with cis and dox exposed cells.....	139
<b>Table 4.3:</b> Pearson's correlation coefficient of cell lines CSC marker expression and chemotherapy LD <sub>50</sub> .....	153
<b>Table 4.4:</b> DEAB LD <sub>50</sub> concentrations and percentage of cells expressing ALDH HOS, MG63, U2OS and MCF7.....	159
<b>Table 5.1:</b> Position of cytokines in cytokine array used in figure 5.10.....	190
<b>Table 5.2:</b> Pearson's correlation coefficient of sarcoma cell lines and MCF7 colony size change in response to auto conditioning with either CCL-2 or IL-8 24 hour conditioned media concentration.....	197
<b>Table 6.1:</b> CXCR1, CXCR2 and CCR2 expression in the cell lines HOS, MG63, U2OS and MCF7.....	223
<b>Table 6.2:</b> Comparison of CCL-2 concentrations of conditioned media taken from U2OS cell, empty vector and knockdown 1 and 2 at 24 and 72 hours.....	226
<b>Table 6.3:</b> Transcription genes with shared altered expression in U2OS cells in response to recombinant CCL-2 and U2OS conditioned.....	237
<b>Table 6.4:</b> Transcription genes with altered expression in U2OS cells in response to recombinant CCL-2.....	237
<b>Table 6.5:</b> Apoptosis inhibiting genes with altered expression in U2OS cells in response to U2OS conditioned media.....	237
<b>Table 6.6:</b> Cancer signalling genes with altered expression in U2OS cells in response to U2OS conditioned media.....	238
<b>Table 6.7:</b> Locomotion genes with altered expression in U2OS cells in response to U2OS conditioned media.....	240
<b>Table I:</b> Primer efficiencies (E) for 18s rRNA and CCL-2.....	265
<b>Table II:</b> Melting temperatures of 18s rRNA primers tested with U2OS CCL-2 knockdown cell lines reverse transcribed RNA.....	265
<b>Table III:</b> Melting temperatures of CCL-2 primers tested with U2OS CCL-2 knockdown cell lines reverse transcribed RNA.....	266

**Acknowledgements**

The past 4 years have been the most rewarding of my life and have culminated in the completion of this PhD, which has been facilitated by the University of Westminster research scholarship. The achievements would not have been possible without the support and guidance of a number of individuals for which my gratitude is the least I can offer.

Firstly I would like to sincerely thank my director of studies Mark Clements for his constant guidance and support throughout the PhD. His help has been invaluable and I am very grateful to have had opportunity to work alongside him. It has been also been a privilege to work with my second supervisor Caroline Smith who has provided guidance throughout my project, I would also like to thank Dr Vin Patel and Dr Francesc Miralles (St George's University) for kindly providing the assistance with genetic manipulation techniques and the Illumina microarray. I am very grateful to Dr Anatoliy Markiv for his patience with assisting me with my confocal microscopy analysis. I would also like to thank the university of Westminster technical staff, in particular Kim Storey for her assistance with the flow cytometer.

I would like to thank fellow PhD students at the University of Westminster including Myrsini Tsimon who has helped to get me through the lab work and Faye Bowker, Katie Wright, Brad Elliott, Rana Ammache and everyone else in office C4.03 who have made the whole process more fun.

Finally, I would like to thank my family for their all their support and especially my fiancée Camilla for always believing in me.

## **AUTHOR'S DECLARATION**

I declare that the present work was out in accordance with the guidelines and regulations of the University of Westminster. The work is original except where indicated by reference in the text.

The submission as a whole or part is substantially the same as any that I previously or am currently making, whether in published or unpublished form, for a degree diploma or similar qualification at university of similar institution.

Until the outcome of the current application to the University of Westminster is known, the work will not be submitted for any such qualification at another university or similar institution.

Any views expressed in this work are those of the author and in no way represent those of University of Westminster.

**Signed:**

**Date**



The list of abbreviations used in this thesis are as follows:

<b>Abbreviation</b>	<b>Full name</b>
ALDH	Aldehyde dehydrogenase
APC	Allophycocyanin
AP-1	Activator protein 1
BRCA1	Breast cancer 1, early onset
Cis	Cisplatin
CSC	Cancer stem cell
DEAB	Diethylaminobenzaldehyde
DHFR	Dihydrofolate reductase
DMSO	Dimethyl sulfoxide
Dox	Doxorubicin
DTL	Denticleless protein homolog
E-cad	E-cadherin
EGF	Epidermal growth factor
EMT	Epithelial to mesenchymal transition
ESA	Epithelial specific antigen
FACS	Fluorescence activated cell sorting
FC	Folate receptor
FGFR2IIc	Fibroblast growth receptor 2IIc
FITC	Fluorescein isothiocyanate
FOXC1	Forkhead box
GIST	Gastrointestinal stromal tumours
GSTP1	Glutathione S-transferase
HER2	Human epidermal growth receptor 2
HMEC	Human mammary epithelial cells
IL-8	Interleukin 8
MDM2	Murine double minute 2
MET	Mesenchymal epithelial transition
MIF	Macrophage inhibitory factor
MNNG	<i>N</i> -methyl- <i>N'</i> -nitro- <i>N</i> -nitrosoguanidine
MTT	Thiazolyl blue tetrazolium bromide
MTX	Methotrexate
NFκB	Nuclear factor kappa-light-chain-enhancer of activated B cells
nm	Nanometer
nM	Nanomolar
OS	Osteosarcoma
OSP	Osteoprotegerin
PGI	Phosphoglucose isomerase
PI3K	Phosphatidylinositol-3-kinase
PE	Phycocyanin
PEI	Polyethylenimine
PI	Propidium iodide
RANK	Receptor activator of nuclear factor κ B

RANTES	Regulated on Activation, Normal T Cell Expressed and Secreted
Rb	Retinoblastoma
RNAi	RNA interference
SC	Stem cell
SCF	Stem cell factor
SDF-1	Stomal derived factor 1
TAM	Tumour associated macrophage
TNF $\alpha$	Tumour necrosis factor $\alpha$
shRNA	Short hairping RNR
Vim	Vimentin
$\mu\text{m}$	Micrometer
$\mu\text{M}$	Micromolar

# **Chapter 1**

## **General Introduction**

## 1.1 Introduction to cancer

Cancer is a broad range of diseases all with varying characteristics and prognoses, which are classified based upon the tissue of origin. There are the four cancer types; carcinomas of the epithelium, sarcomas of the connective tissue (Mackall et al., 2002), tumours of the nervous system (Louis et al., 2007) and lymphomas and leukaemias which arise from the haematopoietic lineage (Vardiman et al., 2009, Harris et al., 1999). In order for a cell to become cancerous it must acquire six characteristics; chronic proliferation, evasion of contact inhibition, the ability to resist cell death, replicative immortality, sustained angiogenesis and the ability to invade surrounding tissues and metastasise to distant organs (Hanahan and Weinberg, 2011). A cell which acquires these six characteristics will develop in to a malignant cancer, however, benign tumours can also develop if a cell acquires the same hallmarks excluding the ability to invade and metastasise (Lazebnik, 2010). Benign tumours can still grow large in size but lack these most fatal aspects of cancer, which are often attributed to treatment complications and cancer related fatalities (Ford et al., 1994).

Improvements in cancer therapy have been made since the first chemotherapeutic was discovered and used to induce a remission in 1947 (Farber and Diamond, 1948). The use of combined chemotherapy regimens in combination with surgery, has dramatically reduced tumour reoccurrence (Jaffe et al., 1974). However due to the toxic nature of these chemotherapeutics (Shapiro et al., 1998) and the enhanced risk of leukaemia following treatment (Curtis et al., 1992), this has led to the introduction of cancer treatments which have a reduced toxicity to non-cancerous cells. These targeted therapies are now able to distinguish cancer cells from healthy cells, using agents which inhibit the signaling networks required for maintenance of a malignant phenotype. These treatment strategies, even when used as single agents, have been found to induce high rates of tumour suppression and are associated with low rates of toxicity (Kantarjian et al., 2002). However, cancer is still a leading cause of death worldwide, predictions in 2012 estimate 14.1 million new cancer cases within that year and 8.2 million cancer related deaths (GLOBOCAN, 2014). This figure is only likely to rise with the increased proportion of elderly people within developed

countries (Croce, 2008), making improved cancer therapies a necessity to reduce mortality rates.

### 1.1.1 Cancer associated mutations

The evolution of a normal healthy cell into an invasive tumour is often a gradual process which requires a number of genetic insults. Cancer driving mutations occur with either the loss of tumour suppressors; genes involved in regulating the cell cycle or a mutation which may enhance the expression of an oncogene, the result of which will force a cell to divide. These mutations are usually acquired somatically, however in some rare cases germline mutations can also predispose cells towards cancer (Gayther et al., 1997). One of the most common somatic mutations is the loss of the tumour suppressor *P53* which occurs in up to 50 % of head and neck, ovarian, oesophageal, colorectal and lung cancers (Jones and Baylin, 2002). One of the first germline mutations associated with cancer to be identified was the tumour suppressor breast cancer 1, early onset gene (*BRCA1*) where individuals carrying a mutation causing the loss of one *BRCA1* allele have an elevated risk of cancer with an 80 % chance of developing breast cancer and increased risk of ovarian and secondary cancers (Ford et al., 1994).

The heterogenous nature of cancers is highlighted by the finding that the somatic mutation rate can vary from 0.001 to 400 mutations per megabase even in cancers of the same type (Stefanska et al., 2011). Although mutations do play a significant role in tumour formation altering gene expression via epigenetic mechanisms has also been shown to be important. Gene silencing via methylation of CpG islands upstream of gene promoters is commonly observed in the silencing of tumour suppressors such as *BRCA1* (Jones and Baylin, 2002). Conversely regions of the genome containing oncogenes can become hypomethylated and this can lead to increased gene expression resulting in neoplasias (Feinberg and Tycko, 2004). Analysis of gene methylation in liver cancer found that hypermethylated genes were involved in growth, angiogenesis and metastasis (Stefanska et al., 2011), which are crucial for cancer formation. In addition genome wide hypomethylation has been found to induce chromosome instability, which has been proposed as a mechanism by which cancer cells can gain mutations and lose heterozygosity in areas containing tumour suppressors (Chen et al., 1998).

### 1.1.2 Classification of cancer

Excluding embryonic tumours, cancers can be broadly classed in to either carcinomas, haematologic neoplasms, neuronal cancers and sarcomas. Carcinomas originate from epithelial cells, and are the most common cancer type. Lung cancer is an example of a carcinoma and alone is the most frequently diagnosed cancer worldwide, contributing to  $\geq 50\%$  of all cancer related deaths (Jemal et al., 2010). The high incidence of carcinomas is possibly a result of the large abundance of these cells as well as a consequence of their exposure to the external environment. Organs such as the lungs, skin and alimentary tract are in constant interaction with an environment frequently containing carcinogens, increasing the likelihood of tumour formation (Berman, 2004). Carcinomas can effect all organs containing epithelial or endothelial cells, therefore, comprise a diverse collection of cancers. In the breast for example a collection of neoplasias have been characterised which have distinct clinical outcomes (Vargo-Gogola and Rosen, 2007). Currently six different breast cancer subtypes have been identified using gene microarrays, these include normal breast like, basal like, epidermal growth factor 2 expressing (EGFR2 +), and the luminal types which are comprised of the A,B and C subtypes (Sorlie et al., 2006).

The haematologic neoplasms more commonly called leukaemia, encompass any tumour arising from the haematopoietic stem cells which reside in the bone marrow. These stem cells give rise to all the blood cells of the body, therefore neoplasms can be either lymphoid, myeloid or histiocytic (Harris et al., 1999). All leukaemias can be divided in to acute and chronic diseases. Acute forms are characterised by a high percentage of haematopoietic progenitor cells more commonly called blast cells, which have lost their ability to differentiate (Estey and Dohner, 2006). In contrast chronic forms contain more differentiated leukaemic cells, however these diseases can progress in to a blast phase, whereby differentiated leukaemic cells are replaced by blast cells (Sawyers, 1999). Myeloid leukaemias encompass neoplasias originating in either the granulocyte (neutrophils, basophils and eosinophils), monocytes/macrophages, megakaryocytes or mast lineage of cells (Vardiman et al., 2009). Although all age groups can be effected by chronic myeloid leukaemia on average people in their 50s are effected and the disease is usually diagnosed at a fairly benign phase, however this can progress to a fatal blast crisis (Calabretta and Perrotti, 2004, Sawyers, 1999). Acute myeloid leukaemias are characterised by the *de novo*

presentation of a blast count 20 % or greater (Vardiman et al., 2009). The build up of these immature myeloid cells can rapidly lead to fatal infection, internal bleeding or organ infiltration if left untreated (Estey and Dohner, 2006).

Neuronal cancers include brain tumours which can be divided in to either medulloblastomas arising from a neuronal progenitor or astrocytoma and oligodendroglioma originating from a glioma precursor (Mischel et al., 2004). Medulloblastoma and glioblastomas (the most malignant form of astrocytoma) have an incidence in the US of around 10 % and are associated with poor prognosis. Even with improved treatment strategies the long term (5 year) survival rate has not improved for 20 years (Deorah et al., 2006) and in particular glioma survival rates are very poor with a median survival time post diagnosis of 12 – 15 months (Wen and Kesari, 2008). One issue that makes treating brain tumours a challenge is the effect of the blood brain barrier to inhibit anti-cancer drugs reaching the central nervous system. In order for treatment strategies to be improved it will be important to design drugs with enhanced lipophilicity or packaging in to liposomes (Huse and Holland, 2010).

Sarcomas arise from the connective tissue (bone, cartilage, fat and muscle) and account for around 5 % of adult cancers and 20 % of paediatric cancers (Mackall et al., 2002). Classifying sarcomas can often be a challenge because tumours display little similarity to differentiated connective tissue (Henderson et al., 2005). As a consequence tumour location is often less important in sarcoma diagnosis, emphasis is instead placed on molecular pathology. This has led to sarcomas being broadly classified in to either a tumour with either a simple or complex karyotypic defects (Berman, 2004). Simple karyotypic sarcomas include tumours with a disease specific translocation giving rise to a fusion protein which plays an active role in tumour formation. In 85 % of Ewing's sarcomas a fusion of chromosome 22 to either chromosome 2, 7, 11, 17 and 21 occurs leading to the expression of a fusion protein which enhances cellular proliferation (Riggi et al., 2005). In contrast, complex neoplasias contain extensive chromosomal rearrangements and are commonly associated with genetic abnormalities including the loss of tumour suppressors such as *P53*, murine double minute 2 (*MDM2*) and especially retinoblastoma (*Rb*) which is commonly mutated (Wang et al., 1995). In some sarcomas mesenchymal precursor cells have been identified as the

initiating cell (Riggi et al., 2005), which is also hypothesised to be the case in other sarcomas such as osteosarcoma (Tang et al., 2008).

### 1.1.3 Osteosarcoma

Osteosarcoma (OS) describes malignancies characterised by direct formation of bone or osteoid tissue from tumour cells (Schajowicz et al., 1995). It primarily affects adolescents and has been found to have a bimodal age distribution with the highest incidence at 10 - 19 years and a subsequent increase at >70 years (Jawad *et al.*, 2010). In adolescents the peak incidence of OS has been linked to the ages of highest growth velocity (Hems, 1970). Although rare, OS is the most common malignant primary bone tumour with an estimated incidence of 1 case per 500,000 persons per year (Klein and Siegal, 2006). It has a poor clinical outcome, even with improved treatment strategies still only 40 - 50 % of patients achieve long term survival of 10 years (Bielack et al., 2002, Petrilli et al., 2006).

OS is a collection of lesions which are classified according to their histological features and grade. Different tumour types produce variable quantities of cartilage matrix or fibrous tissue. This has given rise to three classical subdivisions: osteoblastic, chondroblastic and fibroblastic tumours. In reality all OS tumours contain a variety of cell types and matrices so classification is based on >50 % predominance of any histologic type (Klein and Siegal, 2006). The cellular origin of OS is still unclear, the origin of an alternative sarcoma (Ewing's sarcoma) has been identified as bone marrow derived mesenchymal cells (Riggi et al., 2005). A similar cellular origin has been hypothesised in OS (Tang et al., 2008), however, further research is required to substantiate this theory. To aid with the study of OS a variety of cell lines are available which mimic the different tumour morphologies. These cell lines include Saos-2 and U2OS which contain cells of an epithelial morphology, MG63 is a fibroblastic cell line and there are also mixed morphology cell lines such as 143B, HOS and MNNG-HOS (Table 1.1).



**Table 1.1:** Human OS cell lines. \* indicates cell lines derived from HOS by Ki-ras transformation (\*1) and by *N*-methyl-*N'*-nitro-*N*-nitrosoguanidine (MNNG) treatment (\*2). # indicates ATCC® bank line not available; cell line derived from Rochet *et al* 1999.

OS Cell line	Phenotype	ATCC number®
CAL 72	Epithelia	#
G-292	Fibroblastic	CRL_1423
HOS	Mixed	CRL_1543
143B* <sup>1</sup>	Mixed	CRL_8303
MMNG HOS* <sup>2</sup>	Mixed	CRL_1547
U2OS	Epithelia	HTB_96
MG63	Fibroblastic	CRL_1427
Saos-2	Epithelia	HTB_85

The aetiology of OS is poorly understood, the disease has no familial patterns and is classed as a complex karyotype sarcoma with a host of different genetic abnormalities observed within tumours (Hansen, 2002). Several common OS associated mutations include the loss of the tumour suppressors such as *P53* and *Rb* (Diller et al., 1990, Miller et al., 1996). Loss of *Rb* leads to a significant increase in OS incidence (Lueder et al., 1986), with the protein product of *Rb* (pRb) promoting osteoblast cell cycle arrest and differentiation when dephosphorylated (Lipinski and Jacks, 1999, Thomas et al., 2001). In osteosarcoma ectopic expression of pRB in the OS cell line SaOS-2 was found to lead to cell senescence and apoptosis by inhibiting E2F transcription factors, which inhibits entry into S phase of the cell cycle (Tiemann and Hinds, 1998). p16ink4 is an inhibitor of cyclin dependant kinases 4 and 6 which are involved in the deactivation of pRb via phosphorylation. OS U2OS cells transfected with p16ink4 become senescent (Dai and Enders, 2000) highlighting that pRb can be inactivated via alternative mechanisms rather than just loss of gene function. The activator protein 1 (AP-1) transcription factors c-fos and c-jun are commonly overexpressed in OS (Franchi et al., 1998) with c-fos playing an important role in osteoblast activity (Grigoriadis et al., 1993). When c-fos and c-jun are both overexpressed in transgenic mice this enhances OS formation (Wang et al., 1995), through the increased expression of genes

associated with proliferation and survival (Angel and Karin, 1991). When c-jun and c-fos form a heterodimeric protein they bind genes containing promoters with AP-1 transcription activation elements 25 times more efficiently than homodimeric proteins (Halazonetis et al., 1988), which indicates why overexpression of both these proteins can lead to osteosarcoma formation.

## 1.2 Stem cells and cancer

Stem cells (SC) have the capability to undergo self-renewal and to produce progeny which can differentiate into separate cell lineages (Hall and Watt, 1989). The potency of a SC refers to how many cellular lineages it can give rise to. Totipotency describes cells with the greatest potency such as the zygote, with the ability to produce every cell in the body, whereas pluripotency refers to cells able to produce any adult or embryonic cell (Mitalipov and Wolf, 2009). Multipotency is a cell which can give rise to a limited number of cell lineages and these are found in the later stages of embryo development as well as throughout adult life which is why they are often referred to as adult stem cells. Adult SCs have been identified in a wide range of organs including the epidermis, intestine, liver, brain (Hall and Watt, 1989, Weissman, 2000) and two distinct populations (mesenchymal and haematopoietic cells) found within the bone marrow (Delorme et al., 2008). Within these organs the SCs reside in specific niches which provide a suitable environment for a stem cell population and provide substrates to control their self-renewal and progeny production (Spradling et al., 2001). Control over SCs is vital in order for them to effectively fulfill their purpose of maintaining the number of differentiated cells and ensuring that any tissue damage can be repaired (Hall and Watt, 1989). Adult SCs use clonal succession in order to maintain cell populations. This is achieved by a small percentage of SCs dividing either asymmetrically to replenish differentiated progeny or symmetrically to produce daughter SCs. The remaining SCs population is dormant and acts like a reserve only dividing when a replacement or extra SCs are required (Abkowitz et al., 1990).

Traditionally the stochastic model was used to describe cancer formation; this theory states that any cell within an organ can become tumorigenic, giving rise to a homogenous population of cells all with equal tumorigenicity (Odox et al., 2008, Patel et al., 2010). Recent findings contradict this idea and indicate that many cancers are in fact composed of a hierarchical population of cells with a mutated progenitor cell driving the initiation and maintenance of neoplastic growth (Siclari and Qin, 2010). Mutated progenitor cells have been aptly named cancer stem cells (CSC), because like stem cells they have plasticity and divide to produce either a daughter CSC or progeny which will mature and recapitulate the original tumour heterogeneity (Mackenzie, 2008). Often tumours can be viewed as aberrant organs due to tumours containing a hierarchical organisation which reflects a

healthy organ (Reya et al., 2001). However it should be made clear that CSC do not necessarily have to arise from an adult stem cell, an alternative source of CSC could be differentiated cells acquiring mutations allowing them to regress and gain stem cell properties (Figure 1.1) (Valent et al., 2012). Therefore, a CSC does not have to originate from a SC and has been defined as a cell within a cancer, which has the capacity to self-renew and give rise to heterogeneous lineages of cells that comprise a malignancy (Clarke et al., 2006). An important caveat of Clarke *et al* (2006) CSC definition proposes that a CSC may not be the original tumour initiating cell. A cell which initiates tumour formation may lack SC properties, which are acquired through additional mutations during cancer progression

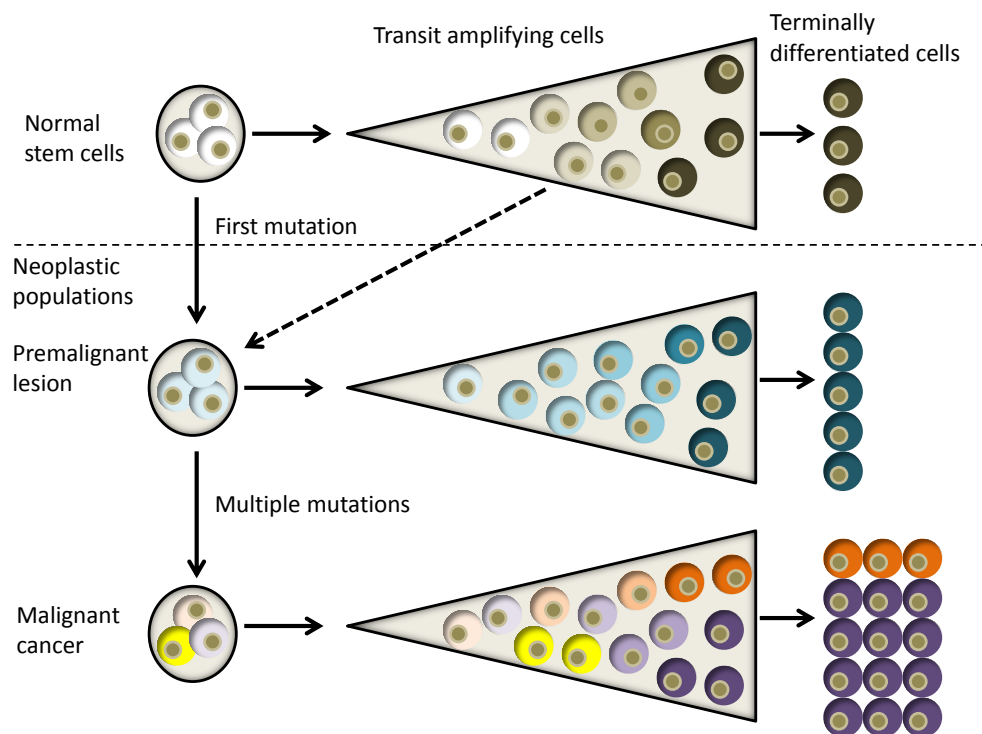


**Figure 1.1: Cancer stem cell evolution model.** As is found in normal stem cell populations within a healthy organ (top of figure) and cancer (middle and bottom of figure), stem cells can divide asymmetrically to produce transit amplifying cells, which will go through several rounds of division and differentiate to eventually become terminally differentiated cells, which can no longer divide. The evolution toward a malignant phenotype requires the acquisition of multiple mutations, in the middle of the figure either a stem cell or a de-differentiated transit amplifying cell has acquired a mutation which enhances its proliferation leading to clonal expansion of these cells and the formation of a premalignant lesion. The accumulation of further mutations in the CSC population leads to the formation of multiple CSC phenotypes (bottom of figure) indicated by different CSC colours, these cells not only have enhanced proliferation rates but also the ability to invade the surrounding tissue and metastasise. Adapted from Valent *et al.* (2012).

### 1.2.1 Evidence supporting the cancer stem cell theory

Observations that tumours contained a stem cell population date back to the 19<sup>th</sup> century when it was noted that cancers contain embryonic like cells (Askanazy, 1907). The first *in vitro* experiment proving the presence of CSC was achieved in murine myeloma cells (Park et al., 1971) and later in human cancers (Hamburger and Salmon, 1977). The experiments conducted from human myeloma patients found that only 0.001 – 0.1 % of myeloma cells had the ability to form colonies. Suggesting that not all cancer cells are capable of proliferating and only a small population of cells are responsible for myeloma growth (Hamburger and Salmon, 1977). An assay which was originally found to select multi-potent neuronal cells (Reynolds et al., 1992), allows the formation of spherical colonies in low attachment serum starved conditions. This assay is now commonly used to identify putative CSC and has been shown to harbour cells with increased murine tumourigenicity in breast cancer (Zhang et al., 2008), glioblastoma (Yuan et al., 2004) and osteosarcoma (Rainusso et al., 2011).

The assay now used to identify CSC is the serial transplantation of suspected CSC cells in to immunocompromised mice (Clarke et al., 2006), the ability of CSC to form tumours within a mouse model is now considered the gold standard. The first use of this *in vivo* technique was work carried out in leukaemia, separating cells according to the surface expression of CD34 and CD38. It was found that only cells expressing CD34 and lacking CD38 could recapitulate the original tumour heterogeneity in a xenotransplantation model (Lapidot et al., 1996, Bonnet and Dick, 1997).

Recent studies have used lineage tracing in mouse models to study tumour formation and the role CSC play in tumour maintenance. This model induces tumour formation through either the exposure to carcinogens or using a tumour susceptible mouse. The mouse model is also genetically modified with a cre-lox system (Sauer, 1987) which can be used to induce fluorescence in specific cells, allowing cells and their progeny to be monitored. Using this system benign papillomas and malignant carcinomas of the squamous tissue were compared. Interestingly the population of benign SC mirrored the SC hierarchy in healthy tissue and contained a population with limited proliferative potential and another with a longer lifespan and increased proliferation. In contrast the malignant counterpart was found to contain only one population of CSC which was solely responsible for tumour

formation and had a limited potential for terminal differentiation (Driessens et al., 2012). A study using a similar methodology in glioblastoma identified a quiescent population of CSC capable of recapitulating tumour heterogeneity after chemotherapy. Interestingly inhibiting the growth of these quiescent CSC eradicated tumour formation after chemotherapy treatment (Chen et al., 2012).

### 1.2.2 Markers of CSCs

Cancer therapy is often hindered because CSC have a reduced sensitivity to chemotherapy, making relapses possible even when the vast majority of the tumour mass is removed (Gong et al., 2010). The ability to identify and therapeutically target CSC is crucial for cancers to be effectively treated. Current research has focused on the identification of stem cell markers in healthy tissue with the expectation that these markers will also be found in CSC (McDonald et al., 2009). There is no consensus on the most suitable CSC marker, however, varying markers have been identified for each tissue type. The markers carry out a range of cellular functions including cell adhesion, cryoprotection and drug effluxing pumps (Alison et al., 2010b).

Xenotransplantation has also been used to prove the existence of CSC in solid tumours. Breast CSCs were the first to be identified based on the extracellular expression of CD44 (Al-Hajj et al., 2003). CD44 is a member of the cartilage link protein family (Stamenkovic et al., 1989), which is the principal extracellular receptor for hyaluronate (Aruffo et al., 1990). Hyaluronan is the most abundant component of the extracellular matrix and is vital for cell-cell and cell-matrix interactions (Almond, 2007). CD44 expression from CSC has so far been implicated in two roles; the activation of the transcription factor nanog which is important for self-renewal, pluripotency and chemo-resistance through increased expression of both apoptosis inhibitors and multi drug resistance proteins (Bourguignon et al., 2009). CD44 has been used as a CSC marker in a range of cancers (Table 1.2) and now *in vivo* studies suggest that it could also be used as a therapeutic target (Zoller, 2011). However, in somatic cells CD44 plays a role in maintaining homeostasis especially in the innate immune system. It has been found to be integral for leukocyte migration in early inflammation to non lymphoidal tissues (Veselska et al., 2008) and macrophage recognition and phagocytosis

(Vachon et al., 2006). This highlights the challenge of designing therapeutics that have the ability to differentiate between CD44 expression on healthy cells and CSC. One method which may provide some promise is the use of bispecific antibodies which bind CD44 in conjunction with a tumour specific surface protein. This method has been used in a murine model using an antibody able to bind both CD44 and a lymphoma specific marker. This antibody was found to reduce lymphoma metastasis and had no effect on immune responses unlike an antibody targeting only CD44 (Avin et al., 2004).

**Table 1.2:** CSC identified using a CD44 phenotype

Tumour	Antigenic phenotype	Reference
Breast carcinoma	CD44, CD24 <sup>-</sup>	Al-Hajj <i>et al.</i> , 2003
Squamous cell carcinoma	CD44, ESA	Biddle <i>et al.</i> , 2011
Head and neck, prostate and breast carcinomas	CD44	Harper <i>et al.</i> , 2010
Head and neck carcinomas	CD44	Prince <i>et al.</i> , 2007

The intracellular enzyme aldehyde dehydrogenase (ALDH) has been used to identify SC in a number of cancers including liver (Ma et al., 2008), colon (Huang et al., 2009), acute myeloid leukaemia (Pearce et al., 2005) and OS (Wang et al., 2011). ALDH comprises a family of enzymes which catalyse the pyridine-dependant oxidation of aldehydes to weak carboxylic acids (Sladek, 2003). In humans there are 19 ALDH genes which are organised into 11 groups, the largest is group 1 which comprises 6 members (Alison et al., 2010a). The cytosolic enzyme ALDH1 is found in higher quantities in stem cells because it enables the production of retinoids which are required for early differentiation (Chute et al., 2006). The presence of an elevated ALDH1 activity also provides resistance to chemotherapeutic agents such as cyclophosphamide (Magni et al., 1996), this resistance is achieved through the catalytic ability of ALDH to reduce the DNA cross-linking of alkylating agents (Bunting and Townsend, 1996). Inhibition of ALDH has been shown *in vitro* to sensitise breast CSC to chemotherapy (Croker and Allan, 2012), however, inhibition of ALDH in human haematopoietic stem cells and breast cancer cell lines suggest that this not a suitable

therapeutic strategy. The ALDH inhibitor diethylaminobenzaldehyde (DEAB) has been found to increase the spherical colony forming ability of breast cancer cell lines (Ginestier et al., 2009) and of the presence haematopoietic stem cells based on the phenotype CD34<sup>+</sup>CD38<sup>-</sup>Lin<sup>-</sup> (Chute et al., 2006). DEAB was proposed to increase the stem cell population through the inhibition of retinoic acid production which is required for stem cell differentiation.

The proto-oncogene c-kit expresses the transmembrane tyrosine kinase receptor CD117, which binds to the ligand stem cell factor (SCF). This signaling system plays a central role in normal cell differentiation, proliferation and maturation (Entz-Werle et al., 2005). The expression of CD117 has been identified in a number of solid cancers including melanoma (Berdel et al., 1992), testicular cancer (Strohmeier et al., 1991), OS (Adhikari et al., 2010, Entz-Werle et al., 2005) and breast cancer (Hines et al., 1995). In breast cancer CD117 was found to increase the growth of the breast cancer cell line MCF7 (Hines et al., 1995), whereas in OS CD117 expression correlates with poor chemotherapy response (Miiji et al., 2011). Work carried out by Adhikari *et al.* (2010) demonstrated that OS cells expressing both CD117 and the mesenchymal marker Stro-1, were found to produce xenotransplantable tumours which had elevated chemo-resistance properties. CD117 could provide a possible therapeutic mechanism for targeting CSC. The tyrosine kinase inhibitor imatinib mesylate is an antagonist of CD117 signaling and has been shown to decrease OS proliferation (Miiji et al., 2011), an alternative approach is the use of CD117 blocking antibodies, which has been shown to reduce breast carcinoma growth (Hines et al., 1995).

The expression of specific surface proteins and enzymes from CSC provide us with a means of isolating these highly tumourigenic cells. However, even cells lacking the expression of these markers can also produce tumours, suggesting a separate population of CSC exists (Adhikari et al., 2010). It has been suggested that these results are caused by differentiated cancer cells reverting to a CSC phenotype (Zapperi and La Porta, 2012). If true this would contradict the CSC hierarchy, so an alternative explanation could be the presence of multiple CSC phenotypes within a single tumour. An interesting study in squamous cell carcinoma identified two distinct CSC populations. The populations were identified via the expression of CD44 with either the presence or absence of epithelial specific antigen (ESA). Cells lacking ESA<sup>-</sup> had a migratory phenotype, whilst ESA<sup>+</sup> cells had proliferative phenotype,



it was found that only ALDH expressing cells could switch between the two phenotypes (Biddle et al., 2011). This finding highlights the complexity of CSC identification and importance of fully understanding the CSC population dynamics.

### 1.2.3 Cancer cell hierarchy

SC have the ability to divide either symmetrically to produce a daughter SC or asymmetrically to produce a cell that will mature, it has been proposed that in a healthy state each division will produce one SC and an asymmetric progeny. The maturing progeny are highly proliferative and will go through several rounds of division before maturing and terminally differentiating (Tudor et al., 2004). This hierarchy is fundamental to the maintenance of healthy organs and cellular systems within the body. In cancer this hierarchy is also present albeit in a dysfunctional manner, tumours have been proposed to behave like aberrant organs with a population of stem like cells driving growth (Reya et al., 2001).

The hierarchy which exists within healthy tissues has been examined by seeding cells *in vitro* at clonogenic (low) densities. The initial experiments carried out by Barrandon and Green (1987), demonstrated that when primary epithelial cells were grown as single colonies three different colony types were present; holoclones, meroclones and paraclones. Holoclones formed very tight colonies and possessed the greatest reproductive capacity, paraclones were made of loosely associated cells and were able to divide very few times before aborting and differentiating. Meroclones had features of both colonies and were considered to be a transitional stage between holoclone and paraclone (Barrandon and Green, 1987) (Figure 1.2). CSC have also been shown to reside only within the holoclones, a study using the prostate cancer cell line PC3 demonstrated that only holoclone cells could form xenotransplantable tumours (Li et al., 2008). In addition an OS study has demonstrated that holoclone cells isolated from the cell line MG63 display enhanced tumourigenic and drug resistance properties (Lou et al., 2010).

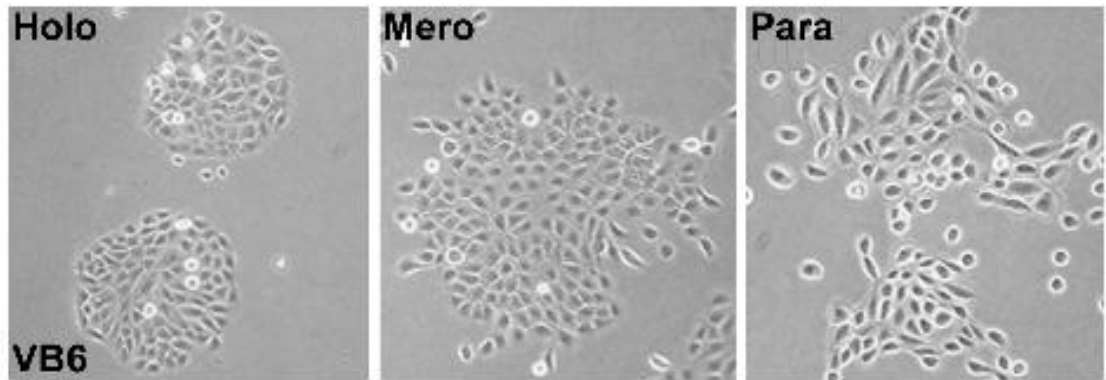


**Figure 1.2: Holoclone, meroclone and paraclone morphologies in the malignant cell line VB6 (Locke et al., 2005).**

The majority of studies examining the role of hierarchical organisation of cells within cancer utilise cell lines (Li et al., 2008, Wang et al., 2011), however, working with cells in an *in vitro* system has inherent limitations. Genomic comparison of over 50 breast cancer cell lines with primary breast cancer tissues has demonstrated that although the genomes were similar, the cell culture conditions were attributable for an increased number of high copy aberrations (Neve et al., 2006). Maintaining cells in an artificial environment alters cellular phenotypes but often the impracticalities of *in vivo* work make cell lines the most suitable option (Joseph and Morrison, 2005). Evidence suggests that cancer cell lines have the same hierarchical organisation (Locke et al., 2005) and include stem cells which express markers of stemness (Wang et al., 2009) as well as being able to induce tumour formation in NOD/SCID mice (Wang et al., 2011). In addition cell lines have been used to study CSC in a wide variety of cancers including breast (Hwang-Verslues *et al.*, 2009), liver (Ma *et al.*, 2008), colon (Deng *et al.*, 2010) and OS (Wang *et al.*, 2010); making them a useful alternative to circumvent the impracticalities of working *in vivo*.

#### 1.2.4 Epithelial to mesenchymal transition

The process of epithelial to mesenchymal transition (EMT) plays an integral role during embryo development with the most significant EMT event occurring when epithelial cells transition to mesenchyme and condense to become the mesoderm and endoderm (Hay, 2005). EMT is initiated by the disaggregation of epithelial cells followed by a change in

cellular morphology. Epithelial cells are defined as polarised because they have a basal surface which is bound to the underlying basement membrane and an apical membrane surface which is unattached (Hay, 2005). Upon initiation of EMT the polarised cell releases matrix metalloproteases which degrade the attachments to the basement membrane. This allows detachment of the cell followed by multiple biochemical changes including the expression of transcription factors, cytoskeletal rearrangement and changes in surface protein expression to acquire a motile mesenchymal phenotype (Kalluri and Weinberg, 2009).

EMT and the associated reverse process of mesenchymal to epithelial transition (MET) have been identified in three distinct biological settings. The first outlines the formation of mesenchymal cells required for embryogenesis, the second is in response to tissue damage or inflammation. In order to repair tissue mesenchymal cells are recruited to regenerate the tissue and this process is halted once inflammation ceases. The third setting is found only in neoplastic cells which have acquired specific genetic and epigenetic changes which allow them to undergo EMT. Once tumour cells acquire this ability to migrate and survive outside their cellular niche, an EMT cancer cell can enter the lymphatic or blood vessels in order to disseminate throughout the body (Friedl and Wolf, 2003). The transcription factor nuclear factor kappa-light-chain-enhancer of activated B cells (NFκB) has been shown to be integral for EMT. NFκB plays an important role in apoptosis resistance (Webster and Perkins, 1999) and acquisition of mesenchymal properties in mammary epithelial cells (Huber et al., 2004). Huber *et al* (2004) also demonstrated that inhibition of NFκB in human mesenchymal cells reverted them to an epithelial morphology, highlighting the requirement of NFκB for maintaining a mesenchymal morphology.

In order to protect somatic cells from neoplastic growth the aberrant activation of oncogenes results in senescence (Kalluri and Weinberg, 2009). Transcription factors over-expressed in cancer cells undergoing EMT have been implicated in escape from senescence, allowing tumour progression to continue (Ansieau et al., 2008). EMT associated transcription factors include twist 1 and 2 (Ansieau et al., 2008), slug (Thiery, 2002), snail (Ren et al., 2011) and zeb1 and 2 (Ahmad et al., 2011). The mechanism by which these transcription factors are up regulated is unclear, however the acquisition of mutations and epigenetic modifications as a tumour progresses is a likely mechanism (Kalluri and

Weinberg, 2009). Tumour associated stroma may also promote EMT through the expression of transforming growth factor  $\beta$  (TGF $\beta$ ) and epidermal growth factor (EGF). Both growth factors have been shown to increase the expression of EMT transcription factors and enhance tumour progression toward EMT (Thiery, 2002). Along with the up regulation of specific transcription factors there are several phenotypic changes which are indicative of EMT, with loss of e-cadherin arguably the most common marker of EMT. E-cadherin is a homophilic calcium dependent cell-cell adhesion protein (Takeichi, 1995), and loss of this protein allows cells to acquire a migratory phenotype (von Schlippe et al., 2000). Loss of e-cadherin has also been correlated with an increase in tumour grade and worse prognosis (Umbas et al., 1994).

An alternative marker which is gained as a result of a mesenchymal phenotype is the cytoskeletal protein vimentin. The presence of increased vimentin in cancer cell lines has been linked with enhanced invasiveness (Sommers et al., 1994, Salvatori et al., 2012). In order for a tumour cell to metastasise it must also undergo the reverse process of mesenchymal to epithelial transition (MET). The reason for a cell undergoing MET at a specific site is attributed to the favourable local environment provided by this secondary organ (Thiery, 2002, Kalluri and Weinberg, 2009). The exact mechanism by which MET occurs is not fully understood, however, bladder cancer studies have demonstrated that fibroblast growth receptor 2IIc (FGFR2IIc) is up regulated on metastatic cells and crucial for the reacquisition of an epithelial phenotype (Chaffer et al., 2006). This finding highlights the chemotactic effect particular organs may have on metastasising cells, and the potential therapeutic application of targeting these cellular receptors.

### **1.2.5 Cancer stem cells and epithelial mesenchymal transition**

In order for a cancer cell to metastasise to distant parts of the body it must not only acquire the ability to migrate but also to colonise and self-renew. Evidence now suggests that undergoing EMT may in fact transform a cell in to a stem cell. The transcription factors *Twist* and *Snail* have both been found to induce EMT (Yang et al., 2006, Cano et al., 2000). Mani *et al* (2008) has demonstrated that both the ectopic expression of both *Twist* and *Snail* in differentiated human mammary epithelial cells (HMEC) reverted epithelial cells to

a fibroblastic phenotype with enhanced self-renewal properties and increased expression of EMT markers. This effect was also observed in V12-HRas oncogene transformed HMECs and led to an increase in the presence of CSC and tumourigenic potential of the cells (Mani et al., 2008).

The homebox transcription factors *nanog* and *oct4* both play important roles in inducing pluripotency of differentiated cells (Okita et al., 2007) and have been shown to play a role in cancer EMT. Lung adenocarcinoma *in vitro* experiments demonstrated that expression of *oct4* and *nanog* enhanced the migration and expression of EMT associated proteins (Chiou et al., 2010). The ability of CSC to switch between proliferative and migratory phenotypes has been studied in oral squamous cell carcinoma. ALDH<sup>+</sup> CSC had the ability to switch from a migratory to a proliferative epithelial phenotype (Biddle et al., 2011).

### 1.3 Osteosarcoma chemotherapy treatment

OS chemotherapy strategies comprise a range of different chemotherapeutic combinations. Common treatment regimes include a combination of doxorubicin and cisplatin with or without the following agents: high dose methotrexate, ifosfamide or etoposide (Anninga et al., 2011). Radiotherapy is only used for patients with inoperable OS tumours (Jawad et al., 2011). The use of these drugs in pre and post-operative chemotherapy has improved OS long term survival to 66%, however this figure has not improved for 20 years (Jawad et al., 2011). The emergence of multi-drug resistant tumours is hindering improvement in long term survival (Bruland and Pihl, 1997) and highlights why tumour response to pre-operative chemotherapy is the most important prognostic factor (Bielack et al., 2002). Tumours often rapidly acquire resistance mechanisms to chemotherapeutics, which is highlighted by the majority of research focusing on resistance mechanisms following discovery of a new chemotherapeutic (Kelland, 2007). Recent OS research has identified a number of drug resistance mechanisms which vary depending upon the drug target. Understanding these mechanisms will be important in identifying the targets of future therapies as adjuvants which increase OS chemotherapy response will enable the toxicity of drugs regimes to be reduced and maximize the effectiveness of treatment strategies.

#### 1.3.1 Doxorubicin resistance

The anthracycline antibiotic doxorubicin has been used to treat osteosarcoma for the last 50 years (Singal and Iliskovic, 1998) and was first isolated from the bacteria *Streptomyces peucetius*. The cell killing action of anthracyclines is debatable but the following mechanisms have been suggested; DNA intercalation, generation of free radicals leading to DNA damage, DNA binding and alkylation, DNA crosslinking, inhibition of DNA unwinding or strand separation, a direct cell membrane effect and inhibition of topoisomerase II mediated DNA damage (Minotti et al., 2004).

When investigating doxorubicin resistance in OS, it has been found that seven genes were down regulated including *P53* (Rajkumar and Yamuna, 2008). The loss of the tumour

suppressor *P53* has previously been identified as a mechanism for OS doxorubicin resistance (Tsang et al., 2005). In response to DNA damage the wild type *P53* induces apoptosis through the activation of Bax homodimers resulting in outer membrane mitochondrial pore formation and release of cytochrome C which leads to the caspase cascade and apoptosis (Fan et al., 2005, Li et al., 1999). In OS loss of *P53* resulted in doxorubicin resistance due to an inability to activate caspase 3 in response to DNA damage (Tsang et al., 2005). Bcl-2 is commonly up-regulated in OS has been identified as a means of overcoming doxorubicin apoptosis by reducing the formation of Bax-Bax homodimers (Zhao et al., 2009). The nucleolar protein neuroguardin/CANu1 is also upregulated in tumour cells and provides OS cells (with a functional p53) a mechanism for doxorubicin resistance (Park et al., 2011a). Although the pathway through which neuroguardin/CANu1 signals is unclear it has been found to inhibit p21, which is activated by p53 in response to doxorubicin DNA damage and stabilize Bcl-2 (Figure 1.3).

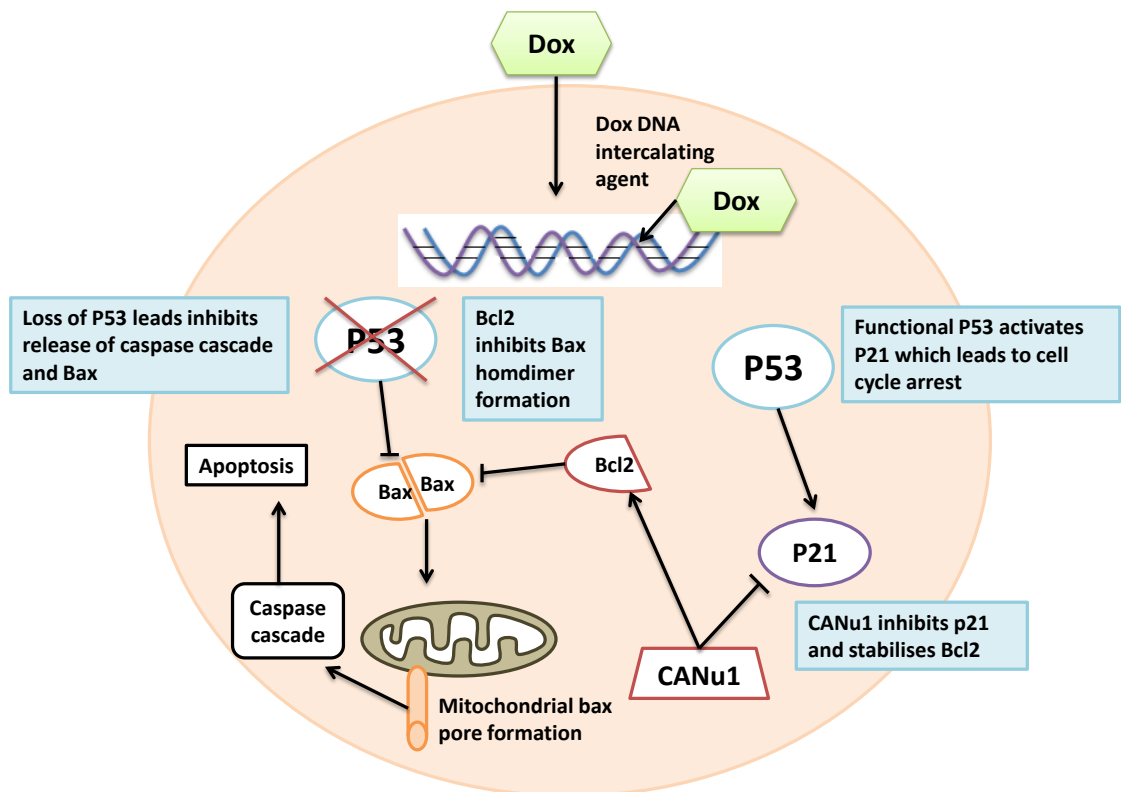


**Figure 1.3: Doxorubicin (Dox) resistance mechanisms.** Dox induces apoptosis through the action of p53 in response to DNA damage, however OS cells with mutated p53 are unable to activate the apoptotic caspase cascade or Bax homodimerisation which leads to outer mitochondrial membrane pore formation. OS cells with functional p53 have been found to resist dox DNA damage through the action of neuroguardin/CANu1 (CANu1). CANu1 inhibits p21 and stabilises Bcl2, inhibiting cell cycle arrest and Bax homodimerisation.

### 1.3.2 Platinum based by chemotherapy resistance

The platinum based chemotherapeutics include cisplatin and the less toxic alternative carboplatin, which exert tumour cell apoptosis by becoming intracellularly activated allowing them to covalently bind to DNA and form adducts (Kelland, 2007). The resistance of both cisplatin and carboplatin is based on three mechanisms: impeding the influx of drug in to a cell, improved DNA adduct repair (Kelland, 2007) and detoxification of the activated intracellular drug (Meijer et al., 1990).

In OS cell line research suggests tumour cells decrease the intracellular quantities of platinum based drugs not through efflux but by reducing membrane permeability (Martelli et al., 2007). The membrane changes in OS have yet to be identified, however rearrangements in membrane mobile lipids confer reduced permeability in breast cancer (Santini et al., 2001). Mutated *P53* has also been suggested as a means of cisplatin resistance, tumours with a wild type *P53* have increased sensitivity to cisplatin than mutated counterparts (Martelli et al., 2007). Tumour cells are able to overcome DNA adduct formation via mutations in genes involved with DNA mismatch repair. Loss of these proteins inhibits cells from identifying DNA damage and undergoing apoptosis (Aebi et al., 1996), in OS loss of the mismatch repair protein PMS2 has been found to induce cisplatin resistance in the cell line U2OS (Perego et al., 1999). The antioxidant glutathione and has been linked with intracellular cisplatin detoxification (Siddik, 2003). Activation of intracellular cisplatin through aquation allows cytosolic glutathione to carry out cisplatin detoxification in a reaction facilitated by glutathione S transferases. Clinical data shows that OS tumours expressing a high glutathione S-transferase P1 (GSTP1), had a significantly higher relapse rates and worse clinical outcome (Pasello et al., 2008).

### 1.3.3 Methotrexate resistance

The *de novo* synthesis of DNA relies on the reduction of folic acid via the enzyme dihydrofolate reductase (DHFR) to synthesise purine, pyrimidine and methionine (Hagner and Joerger, 2010). DNA synthesis is crucial for cell survival therefore targeting this process through the use of structural analogs of folate is a useful strategy in cancer therapy. One of the earliest antifolate drugs and still in use today is methotrexate (MTX). It was first used



to treat acute leukaemia over 60 years ago (Farber and Diamond, 1948) and causes cell death through inhibition of DHFR (Assaraf, 2007). Resistance to antifolate drugs has become a common problem in cancer treatment (Assaraf, 2007) with different tumours using alternative mechanisms (Bertino et al., 1996). Two common mechanisms of OS MTX resistance is the down-regulation of the folate receptor (FR), present in 65% of tumours, and over expression of the enzyme DHFR (Guo et al., 1999). Over expression of DHFR has been attributed to the gene *Rb* which is frequently altered in OS (Section 1.1.4). pRb negatively regulates the expression of E2F transcription factors which increase the expression of cell cycle proteins such as DHFR (Li et al., 1997). However OS cell line evidence contradicts this observation, DHFR expression was actually found to be increased in the *Rb* negative cell line SaOS-2. This *in vitro* study found MTX resistance to be independent of DHFR expression and instead relied on down regulation of FR (Serra et al., 2004).

The gene *C-MYC* is the only gene consistently gained in MTX resistant OS cell lines (Hattinger et al., 2003). Inhibition of *C-MYC* expression reduced resistance to MTX, (Scionti et al., 2008), the mechanism through which c-myc signals is unknown and appears to produce contradictory effects depending on the chemotherapeutic drug as elevated expression of *C-MYC* increased sensitivity to cisplatin (Xie et al., 2006).

A novel approach to investigating MTX resistance is to study the mRNA translational properties of micro RNAs (miRNA). Song and colleagues (2010) studied colon and OS cell lines and identified miR-215 conferred reduced MTX sensitivity through G2 cell cycle arrest. MTX can only target cells in the S phase so G2 arrest provides complete MTX resistance. It was hypothesized that miR-215 exerts its action by targeting the G2/M checkpoint regulator denticleless protein homolog (DTL) with inactivation of DTL preventing the ubiquitination of p53 allowing increased activation of p21 and consequently G2 cell cycle arrest occurs (Song et al., 2010).

#### **1.3.4 Cancer stem cells and chemotherapy resistance**

CSC have been found to have a reduced sensitivity to chemotherapy and have been attributed to relapses even when the vast majority of the tumour mass is removed (Gong

et al., 2010). In OS chemotherapy exposure has been found to enrich for CSC highlighting their ability to withstand higher drug concentrations (Tang et al., 2011). Several mechanisms have been identified which confer OS CSC chemotherapy resistance and include the expression of the ATP-binding cassette transporter ABCG2 which has been found on 60 – 90% of OS CSC (Adhikari et al., 2010). It is hypothesized that this transporter allows cells to efflux drugs reducing the opportunity of chemotherapies to interact with their intracellular targets. The enzyme aldehyde dehydrogenase (ALDH) which carries out the detoxification of aldehydes to weak carboxylic acids (Sladek, 2003), has also been suggested as a mechanism through which CSC detoxify chemotherapeutic agents (Honoki et al., 2010). Although not observed in OS, increased DNA repair could also be used to overcome drug induced apoptosis. Upon cisplatin exposure head and neck carcinoma stem cells have been found to increase time spent in the G2 phase of the cell cycle allowing an increase of cell cycle checkpoint proteins to be expressed, which aid in the repair of DNA damage (Harper et al., 2010). MTX resistance in colon CSC is linked with their 3 fold higher expression of miR-215, which enabled cells to spend an increased amount of time in G2, protecting against MTX apoptosis (Song et al., 2010).

### 1.4 Cell signaling networks

Cells within the body are tightly controlled by interaction with external stimuli during development and throughout the lifespan of an organism. This control is mediated via signaling molecules (ligands), which interact with extracellular receptors allowing intracellular signal transduction to proceed to the nucleus or cytoskeleton. The spatial location of a ligand releasing cell to the affected cell will determine the type of signaling, therefore there are four types of signaling; autocrine (acts on cell of origin), paracrine (secretion acts upon cells in close proximity) endocrine (ligand is released systemically), or juxtacrine, (ligand remains membrane bound and can interact with the receptor on an adjacent cell) (Singh and Harris, 2005) (Figure 1.4). The range of responses one receptor can activate is often diverse, for example the epidermal growth factor receptor has been found *in vitro* to play a role in cell proliferation, differentiation, de-differentiation and apoptosis depending upon the which signal transduction pathway is utilised (Fischer et al., 2003, Singh and Harris, 2005).

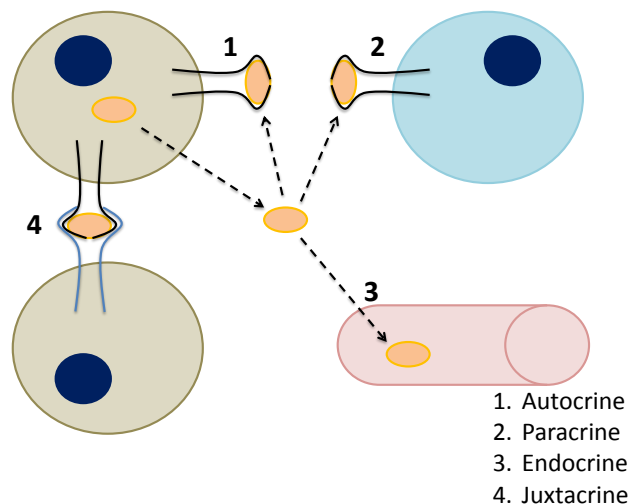


**Figure 1.4: Autocrine, paracrine, endocrine and juxtacrine signalling mechanisms.** A signaling molecule (orange oval) is produced from a cell and interact with a receptor in four possible mechanisms. Either autocrinally whereby it is released from a cell and binds to a receptor upon the same cell, alternatively it may bind paracrinely to a cell in the local environment. Endocrine signaling involves the signaling molecule being released systemically allowing it to reach a distant site in the body. Juxtacrine signaling does not involve the release of a growth factor, instead the molecule remains attached to the cell which presents it to a neighbouring cell.

### 1.4.1 Signalling networks in healthy bone

Bone is a rigid organ which is dynamic in terms of its ability to remodel and is required to do so during development, maintenance and repair (Boyle et al., 2003). The cells responsible for bone formation are the mesenchymal stem cells (MSC), these multipotent cells have the ability to differentiate in to the bone forming cells, osteoblasts which can secrete osteoid before fully differentiating to become osteocytes (Pittenger et al., 1999). MSCs reside within the bone marrow endosteal region (Mendez-Ferrer et al., 2010) and also the bone marrow perivascularity (Shi and Gronthos, 2003). Bone resorption is critical for maintaining bone mass and the osteoclast (a tissue specific macrophage) is able to degrade bone. To ensure that bone resorption is balanced with bone formation tight signaling controls are required (Friedenstein et al., 1966).

One signaling molecule which has been identified in the control of bone development and acts via an autocrine/paracrine signaling pathway is Wnt. Wnt ligands bind to the transmembrane domain frizzled receptor family and require LRP5/6 co-receptors for intracellular signal transduction (Guo et al., 2007, Tamai et al., 2000). Signals can lead to several different intracellular cascades: the canonical pathway leading to stabilization of  $\beta$ -catenin and activation of target gene genes; Wnt/ $\text{Ca}^2$  pathway activates  $\text{Ca}^2$  dependent enzymes (calmodulin-dependent protein kinase II and protein kinase C) (Kühl et al., 2000); and the JNK pathway (Thorpe et al., 2000). MSCs have been shown to differentiate in to osteoblasts after activation of Wnt10b and signal transduction via the canonical pathway (Bennett et al., 2007). Osteoblasts are reliant on Wnt signaling for proliferation, mice lacking *LRP5* have been shown to have decreased bone mass due to a reduced proliferation of osteoblast precursors (Kato et al., 2002), which is mirrored in humans lacking a functional *LRP5* gene (Gong et al., 2001). Control over Wnt signaling has also been shown to effect osteoblast apoptosis and differentiation. Loss of secreted Wnt inhibitor frizzled related protein 1 has been shown to increase bone mass, which was attributed to a decrease in osteoblast apoptosis and increase osteoblast differentiation to osteocytes. Interestingly this was only observed in mice after they had acquired a peak bone mass, suggesting that this control mechanism is activated to limit bone density in only differentiated bone forming cells (Bodine et al., 2004).

Osteoclast bone resorption is an essential process for bone remodeling during development and also for the release of important minerals during starvation. RANK (receptor activator of nuclear factor  $\kappa$  B) is an important receptor crucial for osteoclastogenesis and responds to the ligand RANKL which is secreted by osteoblasts (Yasuda et al., 1998b). Activation of osteoclast RANK leads to rapid actin cytoskeletal rearrangements and enhanced bone resorption (Burgess et al., 1999). In order to control osteoclast activity the receptor osteoprotegerin (OSP) inhibits osteoclastogenesis. Interestingly it is expressed by both osteoblasts and thyroid cells suggesting it acts via paracrine and endocrine pathways (Yasuda et al., 1998a). OSP mechanism of osteoclastogenesis inhibition is directly related to RANKL, OPG is a soluble decoy receptor which binds RANKL and competes with RANK. Therefore, reducing RANK ability to activate osteoclasts (Schoppet et al., 2002), which is highlighted by overexpression of OSP leading to decreased osteoclast differentiation and osteopetrosis (Simonet et al., 1997)

#### **1.4.2 Influence of the microenvironment upon cancer**

Tumours are unable to self-sustain and require external signals to maintain their malignant properties (Spaeth et al., 2009). The tumour microenvironment has been identified as the source of these stimuli and therefore plays an important role in tumour progression. A seminal study carried out in breast cancer identified that, when grown in 3D culture, reducing  $\beta$ 1 integrin activation was sufficient to revert malignant cells to a normal phenotype (Weaver et al., 1997). Cancer progression has also been found to heavily rely on a complex cytokine signaling network between both neighbouring tumour cells and supporting tissues (Mueller and Fusenig, 2004). Cytokine signaling in breast cancer has been observed to originate from distant sites in the body such as the bone marrow. One such pathway identified in breast cancer found tumour release of IL-6 recruited bone marrow derived MSCs to the tumour site. MSCs were found to enhance the growth of the breast cancer in response to IL-6 through the release of CXCL7, which created a positive feedback loop perpetuating tumour progression (Liu et al., 2011). Cytokines have also been secreted autocrinally to enhance tumour progression, one such factor secreted factor is the glycolytic enzyme phosphoglucose isomerase (PGI). In response to hypoxia tumour cells

secrete PGI which autocrinally acted upon breast cancer cells to increase cell motility (Funasaka et al., 2007).

#### **1.4.3 Osteosarcoma signaling networks**

Work carried out by Fawdar (2010) identified that holoclone cells from the OS cell line HOS secrete paracrine factors which supports holoclone formation and the growth and migration of paraclonal cells. In the absence of media conditioned by HOS holoclones the paraclone cells undergo several rounds of division before undergoing cell death. Conversely, in the presence of holoclone conditioned media the paraclonal cells proliferate and in the parental cell line an increase in holoclone formation was observed. In addition to these observations HOS paraclone cells were also found to migrate towards holoclone colonies, indicating that HOS holoclones secrete paracrine factors which are required for HOS paraclone growth, migration and also holoclone formation in the parental cell line. Although the paracrine factor responsible for these findings was never established OS cell lines have been found to secrete PGI which promotes migration. PGI is only released by cancer cells (Niinaka et al., 2010, Ahmad et al., 2011) and has been found to up regulate the expression of TGF- $\beta$  which has been implicated in the acquisition of a mesenchymal phenotype. Interestingly silencing of PGI in OS caused the cell line MG63 to differentiate and lose its malignant properties (Niinaka et al., 2010), highlighting a potential novel target for OS treatment.

#### **1.4.4 CCL2 expression in cancer**

The chemokine CCL2 (also known as monocyte chemoattractant protein MCP-1) is a 13 kDa protein, the gene maps to chromosome 17q11.2 and it has been found to signal via the G-protein coupled receptor CCR2 (Deshmane et al., 2009). It was initially of interest because of its potent monocyte chemoattractant properties (Matsushima et al., 1989) and has also been found to play an important role in bone development and in particular osseous metabolism (Graves et al., 1999). Osteolysis was found to occur through osteoblast

secretion of CCL2 which recruits monocytes, however, normal osteoblasts do not express CCL2 unless stimulated with IL-1 (Williams et al., 1992).

CCL2 expression has been implicated in cancer growth and progression. Breast cancer studies have demonstrated CCL2 expression from cancer associated fibroblasts, enhances the presence of breast cancer stem cells (CSC) (Tsuyada et al., 2012) and potential to metastasis (Nam et al., 2006, Youngs et al., 1997). Prostate cancer research has also demonstrated that tumour cells may migrate to the bone due to enhanced expression of CCL2, however in this case the CCL2 originates from bone marrow endothelial cells (Loberg et al., 2006). *In vivo* CCL2 neutralisation significantly reduces prostate tumour proliferation, and expression of the CCL2 receptor correlates with cancer progression and metastasis (Loberg et al., 2007). An autocrine response to CCL2 has also been observed, multiple myeloma cells were found to have an enhanced CCL2 expression in response to TNF $\alpha$ . This enhanced expression of CCL2 was proposed to increase metastasis to the bone via transendothelial migration (Johrer et al., 2004). Osteosarcoma studies have found that the cells do secrete CCL2 (Grigolo et al., 1999) and this expression was attributed to aid tumour progression through the recruitment of cancer associated macrophages (Graves et al., 1989).

CCR2 signal transduction is not fully understood, however, one pathway which seems to be indispensable for signaling is via phosphatidyl-inositol-3-kinase (PI3K). This pathway was found to be indispensable for both monocyte chemotaxis and prostate cancer proliferation (Terashima et al., 2005, Loberg et al., 2006). A downstream response of CCR2 signaling in breast cancer is up-regulation of notch, which has been found to play a pivotal role in renewing CSC (Tsuyada et al., 2012).

#### **1.4.5 IL-8 expression in cancer**

IL-8 is a member of the CXC chemokine family and was originally identified as a monocyte derived neutrophil chemotactic factor (Yoshimura et al., 1987). In humans IL-8 binds with high affinity to the G-protein coupled receptors CXCR1 and CXCR2 (Park et al., 2011b), and has been found to induce angiogenesis in endothelial cells by activation of the Rho and Rac

signaling pathways (Li et al., 2003). Due to IL-8 having a potent chemottractive effect on neutrophils it plays an important role in the initiation of acute inflammatory responses. Therefore its overexpression has been attributed as a causative agent in pathologies such as dermatitis, arthritis and immune complex type glomerulonephritis (Harada et al., 1994).

Aberrant IL-8 expression has been documented in tumours. Melanoma cells were the first neoplastic cells identified to express IL-8 and it was hypothesised to enhance tumour growth and progression (Zachariae et al., 1991). IL-8 has now been found to be expressed by a range of cancers including breast, colon, gastric, melanoma, pancreatic and B-cell chronic lymphocytic leukaemia (Lippitz, 2013). The expression of IL-8 from such a variety of cancers indicates it has profound role to play in tumour progression, colon cancer cells have been observed to increase proliferation in response to IL-8 (Lee et al., 2012), in breast cancer it has been found to not only enhance invasiveness (Freund et al., 2003) but also the presence of ALDH<sup>+</sup> CSC (Ginestier et al., 2010). CSC in breast cancer were found to have a significantly enhanced expression of CXCR1, when these cell lines were treated with recombinant IL-8 this was found to enhance the ALDH<sup>+</sup> population of cells and increase mammosphere formation (Charafe-Jauffret et al., 2009). This finding has been investigated further by Singh *et al* (2013) using patient derived tumours *ex vivo*, IL-8 concentration of metastatic fluid and pleural effusions correlated directly with mammosphere forming ability of tumours. IL-8 was found not to act in an autocrine loop, suggesting that surrounding stroma are responsible for the IL-8 secretion. IL-8 was found to signal via a pathway also utilized by human epidermal growth receptor 2 (HER2) (Singh et al., 2013). HER2 has been successfully targeted to treat breast cancers overexpressing HER2 using the humanised antibody trastuzumab (Piccart-Gebhart et al., 2005), therefore CXCR1/2 inhibitors (e.g. Repertaxin) may provide useful treatments in trastuzumab resistant tumours.

#### **1.4.6 Targeted cancer therapeutics**

The reliance of cancer cells upon particular growth factors and signaling pathways enables tumour cells to be specifically targeted with therapeutics. Many of these overactive pathways and signaling molecules are also present in healthy tissues often making some



treatments impractical due to high toxicity levels, however, this has not stopped the development of effective adjuvant therapies. One endocrine pathway which has been effectively targeted is the reliance of breast cancer cells on estrogen receptor activation (Howell et al., 1997). The pro-drug tamoxifen is an antagonist of the estrogen receptor. In patients with a high risk of breast cancer the long term administration of tamoxifen was found to reduce breast cancer incidence by 50 % (Fisher et al., 1998). Another receptor which is commonly targeted in breast cancer treatment is the epidermal growth receptor 2 (HER2). This receptor has been implicated in the evolution of breast and gastric cancers (Baselga and Swain, 2009), with 20 % of breast cancer patients over expressing the receptor (Owens et al., 2004). Treatment with trastuzumab inhibits signal transduction via HER2 and post chemotherapy was found to significantly enhance disease free survival (Piccart-Gebhart et al., 2005).

One of the most successful targeted therapies is imatinib mesylate which is a potent inhibitor of the tyrosine kinase ABL, platelet derived growth factor receptor and cKIT (CD117) (Ren, 2005). Imatinib has been successfully used to treat both chronic myeloid leukaemia (CML) and gastrointestinal stromal tumours (GIST) due to the presence of constitutively active mutant tyrosine kinases. The presence of the tyrosine kinase fusion protein BCR-ABL in CML and constitutively active CD117 in GIST allows imatinib to target these tumours and inhibit growth (Corless et al., 2011, Deininger et al., 1997). Currently no adjuvant therapies targeting OS signaling pathways exist, however, potential growth factors have been identified. Existing anticancer drugs may also provide some benefit for OS treatment, the expression of CD117 has been correlated with a poor chemotherapy response. In addition it was found that the use of imatinib could reduce the growth of the OS cell line MG63 and at high doses reduce migration (Mijji et al., 2011). Suggesting imatinib may provide some benefit in OS treatment, however further clinical trials will be required to prove this.

### 1.5 Thesis aims

OS CSC were recently described in OS cell lines (Adhikari et al., 2010, Wang et al., 2011). The main aim of this project is to extend their work by characterising the population of CSC which reside within a heterogeneous panel of OS cell lines. A more complete understanding of the OS CSC will enable the hierarchical organisation of OS cells to be further understood. The observation that OS CSC are more resistant to chemotherapeutics (Tang et al., 2011), will be utilised in an attempt to enrich CSC. Gaining an understanding of the phenotypic properties of these chemotherapy resistant cells could provide a mechanism for accurately determining an OS response to therapy. OS cell lines have been observed to secrete a factor which promoted growth of paraclonal colonies (Fawdar, 2010). An additional aim of this project will be to characterise this factor which will provide a significant insight in to the paracrine cell communication which occurs in OS. The ability to target this factor will also be investigated as possible means to inhibit OS growth.

In order to investigate these aims, the main objectives will be to:

- 1) Characterise putative CSC populations present within OS cell lines.** Using a panel of seven OS cell lines and one breast cancer cell line to act as a comparison to carcinoma, cell lines will be screened for a range of CSC markers. Cell lines will also be tested for the presence of the colony hierarchies identified by Locke *et al* (2005), and the ability of the cell lines to form sarcospheres will also be assessed.
- 2) Identify if CSC contribute to osteosarcoma chemotherapeutic drug resistance.** LD<sub>50</sub> for three chemotherapeutics (cisplatin, doxorubicin and methotrexate) will be determined for the panel of cell lines. Through exposure to a sub-lethal concentration of chemotherapy, CSC will be enriched due to their enhanced resistance to chemotherapeutics. These CSC enriched cell lines can then be tested for the presence of CSC markers and tumourigenic properties.

- 3) Characterise paracrine cell signalling used to control osteosarcoma growth.** The presence of secreted growth factors will be identified for the panel of cell lines. Cell lines can then be profiled for cytokine expression to identify candidate factors, which can then be further analysed via supplementation of the paracrine factor, gene expression knockdown and receptor inhibition.

# **Chapter 2**

## **Materials and Methods**

## 2.1 Materials

Unless otherwise stated all reagents, chemicals and stains were obtained from Sigma Aldrich® (Dorset, UK). Tissue culture reagents were obtained from Lonza® (Slough, UK) unless stated otherwise. Antibodies used for CSC marker expression assessment, identifying EMT status and analysing the receptors CXCR1, CXCR2 and CCR2 are listed in table 2.4. Primers used in the assessment of CCL-2 gene knockdown were purchased from Invitrogen (Paisley, UK).

## 2.2 Cell lines

The OS cell lines used within in this study include 143B, Cal72, G292, HOS, MG63, MNNG-HOS, OSS9-1, U2OS and SaOS-2 (Table 2.1). All these cell lines were derived from bone tumours and banked by ATCC (American Type culture collection); Cal72 (Rochet et al., 1999) and OS99-1 (Gillette et al., 2008) were the only exceptions which were generous gifts. Cal72 was obtained from Professor Adrienne Flanagan and Dr Nadege Presneau (The Cancer Institute, University College London). OS99-1 was obtained from Dr Sheila M. Nielsen-Preiss (Montana State University, US). The OS cell lines 143B and MNNG-HOS are derivatives of HOS via Ki-ras transformation for 143B (Hensler et al., 1994) and *N*-methyl-*N'*-nitro-*N*-nitrosoguanidine (MNNG) exposure (Rhim et al., 1977) (Table 2.1). The sarcoma cell lines HT1080 (Fibrosarcoma), SKLNS1 (Leiomyosarcoma) and RDES-1 were a kind gift from Dr Nadege Presneau (Cancer institute, UCL) and the adenocarcinoma cell line MCF7 was a kind gift for Dr Miriam Dwek (University of Westminster). HEK293T cells were used for lentivirus packaging and were a generous gift from Dr Alastair Barr (University of Westminster).

**Table 2.1: Osteosarcoma cell lines utilised within study.** \* Indicates cell line derived from HOS by either Ki-ras (\*<sup>1</sup>) or MNNG (\*<sup>2</sup>). # Indicates cell line not banked by ATCC<sup>®</sup>, cell line instead derived by #<sup>1</sup> (Rochet et al., 1999) or #<sup>2</sup> (Gillette et al., 2008).

Cell lines	Source	ATCC <sup>®</sup> number
143B* <sup>1</sup>	13 year old, female	CRL-8303
Cal72	10 year old, male	# <sup>1</sup>
G292	9 year old, female	CRL-1423
HOS	13 year old, female	CRL-1543
MG63	14 year old, male	CRL-1427
MNNG-HOS* <sup>2</sup>	13 year old, female	CRL-1547
OSS9-1	11 year old, female	# <sup>2</sup>
U2OS	15 year old, female	HTB-96
SaOS-2	11 year old, female	HTB-85

### 2.2.1 Cell culture

All cell lines were cultured in Dulbecco's modified eagles media (DMEM) (4.5 g/L glucose with ultraglutamine<sup>®</sup> and phenol red) supplemented with 10 % foetal bovine serum (FBS) (Biosera<sup>®</sup>, Sussex, UK) (Complete media). When thawing cells from liquid nitrogen, vials were quickly defrosted in a 37 °C water bath, washed in 5 ml of complete media and seeded in to suitable culture flask. Cells were maintained in a 37°C incubator (Binder APT.line™ C150) and media changes were made every 3 days. Antibiotics were used when specified using antibiotic-antimycotic (Invitrogen<sup>®</sup>: 100 x stock, 10000 units/ml penicillin G sodium. 10000 µg/ml streptomycin sulphate and 25 µg/ml amphotericin).

### 2.2.2 Passaging cell lines

Upon reaching the required confluency (70-90 %) cells were passaged or frozen for storage. When passaging, cells were washed once with Dulbecco's phosphate buffered saline (DPBS) (free from calcium and magnesium), detached by exposure to 0.25 % trypsin and 0.038 % EDTA (Invitrogen<sup>®</sup>) for 3 mins at 37 °C and the trypsin-EDTA neutralised with complete media. Cells were centrifuged at 1000 rpm for 3 mins (IEC CL30 centrifuge, Thermo

scientific®), cell pellet re-suspended in complete media and seeded into a fresh tissue culture flask. Depending upon the cell line, cells were passaged at a ratio of either at 1:3, 1:6 or 1:9. When freezing cells were re-suspended in FBS containing 10 % DMSO and kept at -80 °C for 24 hours prior to storage in liquid nitrogen.

### **2.2.3 Cell line trypsinisation and counting**

In order to prepare cells for seeding at specific densities cells were grown to 70 – 90 % confluency, complete media was removed and cells were washed once with DPBS (free from calcium and magnesium). Cells were detached from the culture vessel by exposure to 0.25 % trypsin and 0.038 % EDTA (Invitrogen®) for 3 mins at 37 °C and the enzyme neutralised with complete media. Cells were centrifuged at 1000 rpm for 3 mins (IEC CL30 Centrifuge, Thermo scientific®), cell pellet re-suspended in complete media and cell concentration was assessed using a minimum of four haemocytometer cell counts in duplicate.

### **2.2.4 Spherical colony assay**

OS cell lines and MCF7 were assessed for their ability to form primary and secondary spherical colonies in ultra-low attachment plates (Corning, Birmingham, UK). Growth media used was comprised of 2 ml serum free DMEM containing antibiotics/antimycotics, 20 ng/ml epidermal growth factor (EGF), 20 ng/ml basic fibroblast growth factor (bFGF) (PreproTech®, London, UK) and B27 supplement (Invitrogen®). In order to test the effect of recombinant IL-8 (BioLegend®, London, UK) and CCL-2 (BioLegend®) on sarcosphere formation 9 ng/ml of IL-8 or 36.4 mg/ml CCL-2 was supplemented in to the media and freshly added every 3 days throughout the experiment.

In order to assess colony formation, cell lines were trypsinised, counted (Section 2.2.3) and seeded at 1052 cells/cm<sup>2</sup> ultra low attachment plate. Fresh 20 ng/ml bFGF, EGF and B27 were added to cells every 3 days throughout the assay. After 7 days primary spherical colony images were captured and spherical colonies were collected and centrifuged at 1000 rpm for 3 mins. Washed with 2 ml DPBS and centrifuged (1000 rpm for 3 mins) and exposed to trypsin-EDTA for 5 mins at 37 °C. Prior to neutralising trypsin-EDTA with complete media trypsinised cells were aspirated and ejected 10 times with a 1000 µl pipette to dissociate cells, then centrifuged (1000 rpm for 3 mins). Media was removed and

in a volume of 200  $\mu\text{l}$  cells were re-suspended and counted using a haemocytometer. To ensure the majority of cells seeded were single cells, cells were only used if single cells comprised  $\geq 95\%$ . 210 cells/ $\text{cm}^2$  were seeded in to a low attachment plate and grown for 7 days to form secondary sarcospheres. Colony size was assessed using an eyepiece graticule and colonies  $\geq 40\ \mu\text{M}$  were counted. Colony size of primary sarcospheres was estimated using Imagej. Sarcosphere forming efficiency (SFE), was calculated using the following equation:

$$SFE (\%) = \left( \frac{\text{No. of secondary sarcospheres}}{\text{No. of cells seeded}} \right) \times 100$$

### 2.2.5 Soft agarose assay

OS cell line anchorage-independent growth has been previously assessed using the soft agarose assay (Fawdar, 2010), using the same methodology as Fawdar (2010) anchorage-independent growth has been assessed. A 2 % agarose solution was prepared by diluting 6 % autoclaved low melting point agarose (dissolved in DPBS) in complete media (containing antibiotic/antimycotic) and maintained as a liquid by incubating at 55 °C. The 2 % agarose was further diluted in complete media to make 0.6 % of which 2 ml was used as the base layer and set for 30 mins at 4 °C. Cells were trypsinised, counted (Section 2.2.3) and 10000 cells were seeded in 2 ml of 0.35 % agarose. This formed the middle layer of the assay, which was set for 30 mins at 4 °C and then incubated at 37 °C. The following day 2 ml of complete media (containing antibiotic/antimycotic) was added to wells and changed every 3 days for up to 15 days. Colony formation was monitored throughout the experiment and assessed after 12 or 15 days using an eye piece graticule. Due to the larger size of MG63 colonies, U2OS colonies  $\geq 85\ \mu\text{M}$  and MG63 colonies  $\geq 170\ \mu\text{M}$  were counted. For the assessment of CCL-2 and IL-8 upon soft agarose colony formation CCL-2 (36.4 ng/ml) or IL-8 (9 ng/ml) were added to the middle 0.6 % agarose layer and top media layer of the assay.



## 2.3 Chemotoxicity analysis

### 2.3.1 Assessment of median lethal doses in response to chemotherapeutics and DEAB

Cells were trypsinised and counted (Section 2.2.3), seeded at 15625 cells/cm<sup>2</sup> in a 96 well plate (BD falcon, Oxford, UK) and allowed to attach for 24 hours. After which media was removed and replaced with media containing either cisplatin (0 - 100 µM), doxorubicin (0 - 3 µM) or DEAB (0 - 800 µMol) for 48 hours. For methotrexate (0 - 3 µM) cells were exposed for 5 days. Cells were quantified by adding 100 µl of 1 mg/mL thiazolyl blue tetrazolium bromide (MTT) (dissolved in complete media) which was added directly to cells and incubated for 1 hour (except SaOS-2, where a 2 hour MTT incubation was used) at 37 °C. MTT containing media was removed and replaced with 50 µl of dimethyl sulfoxide (DMSO), absorbance was measured at 530 nm on a microplate reader (Sunrise, TECAN™) using softmax® pro. MTT reduction (% of control) was calculated using the following equation:

$$\left( \frac{\text{Absorbance (530 nm)}}{\text{Average blank (0µM) absorbance(530 nm)}} \right) \times 100$$

LD<sub>50</sub> values were calculated using a linear regression of drug concentration against cell viability.

### 2.3.2 Clonogenicity of chemotherapy treated cells

Cell lines were seeded at 15625 cells/cm<sup>2</sup> and allowed to attach and grow for 24 hours after which media was removed and replaced with media containing either cisplatin (0 - 100 µM) or doxorubicin (0 - 3 µM) for 48 hours. The incubation period was extended to 5 days for methotrexate (0 - 3 µM). After drug exposure cells were trypsinised and counted (Section 2.2.3) and re-seeded at low density (2 - 4 cells/cm<sup>2</sup>). Cells seeded at low density were grown for 14 days then washed with 5 ml DPBS, stained for 10 mins in 0.5 % crystal violet (dissolved in 100 % methanol) and washed 3 times with water. Prior to staining the first 30 colony hierarchies were randomly observed using an inverted microscope (Inverso 3650) and recorded. Colony size and number was assessed using the image processing software ImageJ, all colonies were measured.

### 2.3.3 Combined DEAB and chemotherapy exposure

Cells were trypsinised and counted (Section 2.2.3), seeded at 15625 cells/cm<sup>2</sup> in a 96 well plate (BD falcon, Oxford, UK) and allowed to attach for 24 hours with the cell line specific DEAB LD<sub>50</sub> concentration. DEAB media was removed and replaced with complete media containing a DEAB LD<sub>50</sub> and either cisplatin, doxorubicin or methotrexate LD<sub>50</sub>. Cisplatin and doxorubicin exposed cells were exposed for 48 hours and methotrexate for 5 days. Cells were quantified by adding 100 µl of 1 mg/mL thiazolyl blue tetrazolium bromide (MTT) (dissolved in complete media) which was added directly to cells and incubated for 1 hour at 37 °C. MTT containing media was removed and replaced with 50 µl of dimethyl sulfoxide (DMSO), absorbance was measured at 530 nm on a microplate reader (Sunrise, TECAN™)

## **2.4 Paracrine growth experiments**

### **2.4.1 Conditioned media collection**

For the collection of conditioned media each cell line was allowed to reach confluency in a cell culture dish (55 cm<sup>2</sup>). The media was replaced with 10 ml complete media which was harvested after either 24, 48 or 72 hours. Conditioned media was filtered using 0.2 µM filter (Millipore, Abingdon, UK) and stored at -20 °C. All conditioned media was diluted 1:1 in complete media when used as a growth media.

### **2.4.2 Conditioned media effect on colony formation**

In order to establish whether conditioned media effects cell growth each cell line was seeded in triplicate in 55 cm<sup>2</sup> growth area dishes at a cell density which produced approximately 100 colonies (2 - 4 cells/cm<sup>2</sup>) after 8 - 15 days. Cells were grown in either the presence of conditioned media or non-conditioned media (complete media). Media was changed every 3 days and growth examined by staining after 8 - 15 days depending upon the cell line. Cells were stained for 10 mins in 0.5 % crystal violet (dissolved in 100 % methanol) and washed 3 times with water. Prior to staining the first 30 colony hierarchies were randomly observed using an inverted microscope (Inverso 3650) and recorded. Colony size and number was assessed using the image processing software ImageJ, all colonies were measured.

### **2.4.3 96 well growth assay**

In order to assess the enhanced growth rates from exposure to conditioned media HOS and U2OS. Cells were seeded at either 125 cell/cm<sup>2</sup> (HOS) or 156 cell/cm<sup>2</sup> (U2OS) in to a 96 well plate in a volume of 100 µl, different cell densities were used to produce the same confluency of 80 % for both HOS and U2OS. After 8 – 9 days, 100 µl of 1 mg/ml MTT was added directly on to cells and incubated at 37 °C for 1 hour, after which, media was removed and replaced with 50 µl DMSO and plate absorbance was read at 530 nm on a microplate reader (Sunrise, TECAN™) using softmax® pro. Absorbances of a cell line tested in conditioned media or cytokine supplemented media was compared to the MCF7 conditioned media absorbances to assess statistically significant growth enhancement.

#### **2.4.4 CXCR1, CXCR2 and CCR2 receptor antagonist experiment**

Antagonising Antibodies for CXCR1 (Clone 42705) (R&D systems<sup>®</sup>, Abingdon, UK) CXCR2 (Clone 48311) (R&D systems<sup>®</sup>) and a small molecule CCR2 antagonist (RS 504393) (R&D systems<sup>®</sup>) were diluted in either complete media, U2OS or MG63 72 hour conditioned media. U2OS and HOS cells were trypsinised (Section 2.2.2) and seeded at either 125 cell/cm<sup>2</sup> (HOS) or 156 cell/cm<sup>2</sup> (U2OS) in to a 96 well plate and grown for 9 days. To assess cell growth 1 mg/ml MTT was added directly to cells and incubated at 37 °C for 1 hour, after which, media was removed and replaced with 50 µl DMSO, plate absorbance was read at 530 nm on a microplate reader (Sunrise, TECAN<sup>™</sup>) using the software softmax<sup>®</sup> pro.

## **2.5 Cytokine expression**

### **2.5.1 Cytokine array**

Assessment of the cytokine profile of 72 hour conditioned media was achieved using a cytokine array (R&D systems, Abingdon, UK). The array was tested according to the manufacturers instructions. To summarise, membranes were blocked with kit buffer for 1 hour whilst 700 µl of conditioned media was incubated with a cocktail of detection antibodies. Blocking buffer was removed from membranes and replaced with sample-antibody cocktail and incubated overnight on a rocking shaker. Membranes were washed with wash buffer 3 times for 10 mins each, incubated with streptavidin-HRP for 30 mins and washed with kit wash buffer. Chemiluminescence was analysed using an EZ-ECL kit (Geneflow, Lichfield, UK). Membranes were exposed for 10 mins before developing X-ray film (Kodak®, Hemel Hempstead, UK).

### **2.5.2 CCL-2 and IL-8 ELISA**

To determine the IL-8 and CCL-2 concentration of conditioned media, samples were analysed by antibody sandwich ELISAs (BioLegend®) following manufactures instructions. To briefly summarise the samples were diluted either 1:2, 1:10 or 1:40 in the provided assay buffer and 50 µl added to plates along with an equal volume of assay buffer. For all incubation periods plates were incubated shaking (185 rpm) at room temperature. Plates were washed using 300 µl wash solution per well 4 times and blotted dry on absorbent paper. To develop the assay 100 µl substrate solution was added to each well and incubated in the dark for 15 mins before the addition of 100 µl stop solution (1 M sulphuric acid). Once reaction was stopped plate absorbance was read at 450 nm and 570 nm on a microplate reader (Sunrise, TECAN™) using softmax® pro. Data analysed by subtracting absorbances at 570 nm from absorbances at 450 nm, all samples and standards were tested in triplicate and concentrations were calculated from the linear regression analysis of the standard curve.

## 2.6 CCL-2 RNA gene interference

In order to achieve stable CCL-2 knockdown the pLKO.1 vector was used which is a derivative of the third generation self-inactivating lentiviral vector pRRLSIN.cPPT.PGK/GFP/WPRE (Dull et al., 1998). This vector contains a human U6 promoter to drive expression of shRNA and human phosphoglycerate kinase promoter (hPGK promoter) for puromycin resistance (PuroR) gene expression for selection of transduced cells (Moffat et al., 2006) (Figure 2.1). Three separate plasmids were used for lentiviral packaging in HE293T cells which contained the packaging genes *Gag*, *Pol*, *Rev* and protein coat gene *Vsv-G* to minimise potential plasmid recombination and creation of replication competent viruses (Root et al., 2006). The RNAi consortium (TRC) was established to create shRNA libraries with multiple constructs for over 15,000 genes (Moffat et al., 2006). Using the TRC library five CCL-2 shRNA constructs were selected to identify potential shRNA with effective gene knockdown upon U2OS cells (Table 2.2)

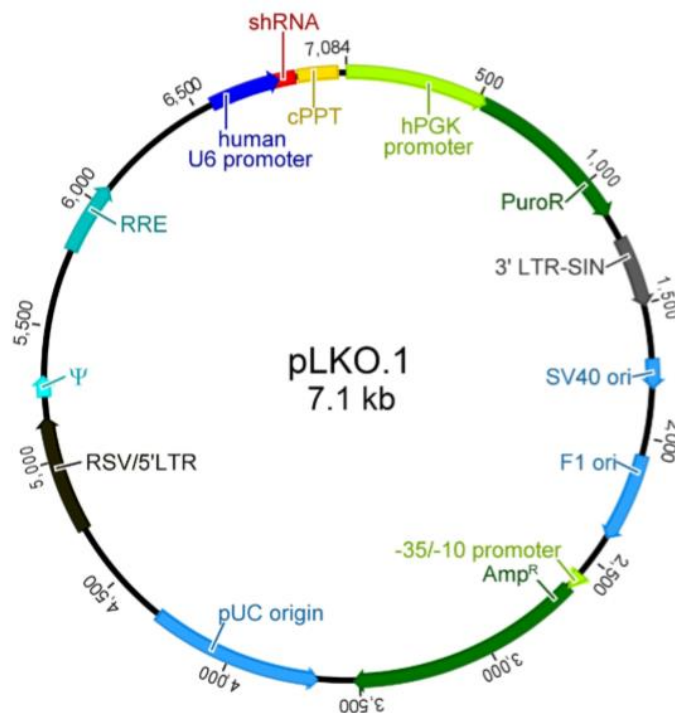


**Figure 2.1: Diagram of pLKO.1 vector map used for the RNA interference of CCL-2.** Image was taken from Thermo scientific TRC shRNA user manual (Dharmacon, 2014).

**Table 2.2: shRNA lentiviral sequences used to assess stable knockdown of CCL-2 in U2OS cells.** shRNA sequences were established by the RNAi consortium (TRC) and distributed by Thermo scientific®.

Thermo scientific® clone ID	Antisense sequence
RHS3979-201738552	TAAGGCATAATGTTTCACATC
RHS3979-201738553	TATTGGTGAAGTTATAACAGC
RHS3979-201738554	ATTCTTCTATAGCTCGCGAGC
RHS3979-201738555	AATGGTCTTGAAGATCACAGC
RHS3979-201738556	TTATAACAGCAGGTGACTGGG

### 2.6.1 Transforming bacterial competent cells

Packaging vectors were transformed into competent cells (XL1-blue competent cells) (Invitrogen®) by mixing 1 µl of plasmid DNA (packaging plasmids PL1, PL2 and pVSVG (Invitrogen®) with a vial of competent cells and incubated on ice for 5 mins. Competent cells were heat shocked at 42 °C for 1 min, incubated on ice for 5 mins followed by addition of 250 µl SOC buffer (2 % tryptone, 0.5 % yeast extract, 8.6 mM NaCl, 2.5 mM KCl and 10 mM MgCl<sub>2</sub>) and 1 hour shaking at 37 °C (200 rpm) to transform cells.

### 2.6.2 Plasmid preparation

TRC lentiviral shRNA (Thermo scientific®) constructs were received as bacterial stocks. Bacterial frozen stocks were streaked on to an agar plate containing 100 µg/ml carbenicillin, incubated overnight at 37 °C. 3 - 5 colonies were picked in to 6 ml of 2 x LB broth (LB-Lennox broth 20 g/L, peptone 10 g/L and yeast extract 5 g/L all from fisher) and incubated at 37 °C for 16 hours with shaking (200 rpm). Cultures were centrifuged at 3000 rpm for 10 mins, supernatant was discarded then plasmid extracted from the pellet using PureLink® quick plasmid miniprep kit (Invitrogen) according to the kit instructions. DNA was quantified using the nanodrop 1000 spectrophotometer (Thermo scientific) and stored at - 20 °C.

### 2.6.3 CCL-2 stable knockdown

U2OS CCL-2 knocked-down was achieved using lentiviral transduction, packaging of lentiviruses and U2OS transduction was carried out at St George's University (London, UK)

under their GM licence. HEK293T cells were used to package the vectors when grown to 80 % - 90 % confluency in a T25 flask. In a DNA free eppendorf 1.5 µg of pL1, pL3 and lentiviral construct were mixed with 1.09 µg pL2 and 23 µl polyethylenimine (PEI) along with 341 µl of 0.15 M NaCl. This mixture was vortexed and incubated at room temperature for 10 mins. The mixture was added to HEK293T cells at 80 - 90 % confluent in complete media and the media changed after 24 hours. After 48 hours of transfection the media contained packaged lentiviral particles at which point the media was collected, centrifuged at 4000 rpm for 10 mins and supernatant added to U2OS cells at 70 - 80 % confluency in a T25 flask. After 24 hours exposure the virus containing media was removed and cells were allowed to recover for 48 hours in fresh complete media. Transduced cells were transported back to the University of Westminster and exposed to 1.25 µg/ml puromycin (Fisher), to select for cells stably expressing the plasmid. Plasmids which conferred knockdown included the following the antisense sequence TTATAACAGCAGGTGACTGGG (RHS3979-201775815) and TAAGGCATAATGTTTCACATC (RHS3979-201738552) (Table 2.2).



## **2.7 Gene expression analysis**

### **2.7.1 RNA extraction**

Total RNA was extracted from cell lines using purelink RNA kit (Life technologies, Paisley, UK) following the manufacturers protocol. To summarise the procedure,  $1 \times 10^6$  cells were harvested from a 70 – 90 % confluent T25 flask (except for RNA extracted Illumina micro array gene analysis, U2OS cells were seeded at 36 cells/cm<sup>2</sup> in a 55cm<sup>2</sup> growth area and grown for 7 days before collecting RNA) and re-suspended in 600  $\mu$ l kit lysis buffer containing 1 % 2-mercaptoethanol. Cells were homogenised by passing 10 times through a 21 gauge needle. The homogenate was then centrifuged at 2600 x g for 5 mins, supernatant mixed with an equal volume of 70 % ethanol and transferred to a spin cartridge and centrifuged at 12000 x g for 15 seconds. Flow-through was discarded and the spin cartridge washed 3 times with kit washing buffers and membrane allowed to dry by centrifugation at 12000 x g for 15 seconds. RNA was eluted using 30  $\mu$ l RNAase free water which was incubated (on the column) at room temperature for 1 min, and eluted by centrifuging at 12000 x g to collect in an RNAase free eppendorf tube. RNA was quantified using a Nanodrop 1000 spectrophotometer (Thermo scientific) and stored at -80 °C.

### **2.7.2 Reverse transcription**

Reverse transcription (RT) was performed using the QuantiTect reverse transcription kit (Qiagen®, Crawley, UK). 1  $\mu$ g of the collected RNA was used in each reaction, which involved a 2 min incubation at 42 °C with the genomic DNA wipeout buffer. The RNA was then mixed with the kit buffers containing the reverse transcriptase and primers, incubated at 42 °C for 15 mins followed by 3 mins at 95 °C. DNA concentration was quantified using a Nanodrop 1000 spectrophotometer (Thermo scientific) and stored at -20 °C

### **2.7.3 Quantitative real time PCR**

Quantitative real time PCR was performed on the Qiagen rotor geneQ™ using the rotor gene kit SYBR green (Qiagen®). A typical 25  $\mu$ l reaction was set up using the following reagents: 100 ng of template DNA, 1  $\mu$ M of forward and reverse primers and 1x Qiagen rotor gene master mix containing DNA polymerase, dNTPs and MgCl<sub>2</sub>. The PCR conditions used were an initial activation of 95 °C for 5 mins followed by 35 cycles of 95 °C for 5 seconds and 60 °C for 10 seconds. A melt curve was also used to assess the primer annealing

temperatures. Reverse transcribed cDNA was tested in triplicate and normalised using 18s rRNA. Primer sets used: CCL2, 5' AAGATCTCAGTGCAGAGGCTCG 3' (forward primer) and 5'-TTGCTTGTCCAGGTGGTCCAT-3' (reverse primer); and 18S rRNA, 5'-CGCGTTCTATTTTGTGGT-3' (forward primer) and 5'-CCCTCTTAATCATGGCCTCA-3' (reverse primer).

#### **2.7.4 Gene microarray**

U2OS cells were seeded at 36 cells/cm<sup>2</sup> in a 55cm<sup>2</sup> growth area and grown for 7 days before collecting RNA (Section 2.7.1). RNA was prepared for microarray analysis using the Illumina Total prep-RNA amplification kit (Invitrogen®). To summarise briefly 500 ng mRNA was added to master mix (dNTPs, T7 oligo(dT) primer, RNase inhibitor and Array Script) and incubated at 42 °C for 2 hours for reverse transcription. Second strand cDNA was synthesised by incubating the reverse transcribed RNA with DNA polymerase, dNTPS and RNAase for 2 hours at 16 °C. Biotinylated cRNA was then produced by incubating with Biotin-NTP, T7 RNA polymerase and reaction buffer for 4 – 14 hours at 37°C. cRNA was then eluted and hybridised to the Illumina Sentrix array for analysis.

## 2.8 Flow cytometry

### 2.8.1 Extracellular antibody staining

Cells were trypsinised upon reaching 70 - 90 % confluency and stained using antibodies for the surface markers CD44-phycoerythrin (PE) (Miltenyl biotech®, Surrey, UK) or e-cadherin-fluorescein isothiocyanate (FITC) (BioLegend®, Cambridge, UK). Prior to staining cells were counted using a haemocytometer and diluted in ice cold DPBS and 1 % FBS to  $5 \times 10^5$  cells per sample. Centrifuged at 2000 rpm for 5 mins and re-suspended in 100  $\mu$ l 1% FBS and incubated with the appropriate concentration of primary antibody (1:100) on ice for 15 mins in the dark. Following antibody incubation cells were centrifuged at 1000 rpm for 3 mins and washed with 1 % FBS 3 times and re-suspended in 0.5 ml 1% FBS. For all antibodies tested a corresponding isotype control conjugated to the same fluorescent detector was used to assess non-specific binding with all cell lines tested in triplicate (Table 2.3).

**Table 2.3: Comparison of primary antibodies used for assessment of cell marker expression in flow cytometry.** Staining antibodies had specificity for protein marker and all control antibodies had no specificity to human proteins. All antibodies were either raised in mouse or rabbit. (Miltenyl biotech®, Surrey, UK), Santa cruz (Heidelberg, Germany), Abcam, R&D systems (Abingdon, UK), BioLegend (London, UK).

Protein marker	Staining antibody origin, isotype conjugate	Antibody supplier	Control antibody origin, isotype conjugate	Control antibody supplier
CD44	Mouse IgG2b (PE)	Miltenyl	Mouse IgG2bk (PE)	BioLegend
CD117	Mouse, IgG1k (APC)	BioLegend	Mouse, IgG1k (APC)	BioLegend
E-cadherin	Mouse, IgG1k (Alexa fluor® 488)	BioLegend	Mouse, IgG1k (Alexa fluor® 488)	BioLegend
Vimentin	Rabbit, IgG polyclonal (unconjugated)	Santa cruz	Rabbit, IgG polyclonal (unconjugated)	Santa cruz
CXCR1	Mouse, IgG2A (unconjugated)	R&D systems	Mouse, IgG2a (unconjugated)	BioLegend
CXCr2	Mouse, IgG2a (unconjugated)	R&D systems	Mouse, IgG2a (unconjugated)	BioLegend
CCR2	Mouse, IgG2a (unconjugated)	BioLegend	Mouse, IgG2a (unconjugated)	BioLegend

### 2.8.2 Intracellular antibody staining

Cells were trypsinised upon reaching 70 - 90 % confluency, then  $1 \times 10^6$  cells fixed in 100  $\mu$ l BD cell fix (BD Biosciences <sup>®</sup>, Oxford, UK) and incubated for 15 mins. 500  $\mu$ l of 1% BSA (diluted in DPBS) was added directly on to fixed cells then centrifuged at 2000 rpm for 5 mins and washed with a further 500  $\mu$ l of 1% BSA. Cell membranes were then permeabilised with 200  $\mu$ l 0.1% triton (diluted in DPBS) incubated in the dark for 10 mins followed by centrifugation (2000 rpm for 5 mins) and washed once with 500  $\mu$ l 1% BSA. Cells were re-suspended in 100  $\mu$ l 1% BSA FC blocker (Miltenyi Biotec, Surrey, UK) with appropriate antibody and incubated for 15 mins in the dark. Three 1 ml 1% BSA washes were used to remove any unbound antibody, followed by re-suspension in 100  $\mu$ l 1% BSA and incubation with secondary antibody (1:200) for 15 mins (Table 2.4). Finally cells were washed twice and re-suspended in 1 ml 1% FBS for flow cytometry analysis.

**Table 2.4: Antibodies used to stain for CSC markers, epithelial or mesenchymal status and expression of cytokine receptors.** \*Indicates co-incubation of antibody with Fc receptor blocker. All primary antibodies monoclonal and raised in mouse, except for the vimentin antibody which was polyclonal and raised in rabbit. Secondary antibodies were polyclonal and raised in goat. Dako (Cambridge, UK).

Antibody	Antibody conjugation		Dilution		Source	
	1 <sup>o</sup>	2 <sup>o</sup>	1 <sup>o</sup>	2 <sup>o</sup>	1 <sup>o</sup>	2 <sup>o</sup>
CD44	PE		1:100		Miltenyl	
CD117	APC		1:100		BioLegend	
E-cadherin	FITC		1:100		BioLegend	
Vimentin*		FITC	1:100	1:200	Santa Cruz	Dako
CXCR1*		FITC	1:100	1:200	R&D systems	Abcam
CXCR2*		FITC	1:100	1:200	R&D systems	Abcam
CCR2		FITC	1:100	1:200	BioLegend	Abcam

### 2.8.3 Aldehyde dehydrogenase staining (ALDH)

ALDH reconstitution was carried out according to manufacturer's instructions. Cells were stained for ALDH using the ALDEFLUOR kit (Stem cell technologies®, Genoble, France), after trypsinisation and counting (Section 2.2.3), cells were diluted in kit buffer to  $5 \times 10^5$  cells per 500  $\mu$ l sample. Next 2.5  $\mu$ l of the ALDH activated reagent was mixed with the sample and 250  $\mu$ l was immediately removed and mixed in a separate tube with 2.5  $\mu$ l of the ALDH inhibitor diethylaminobenzaldehyde (DEAB) to act as a negative control. Samples were incubated at 37 °C for 50 mins, centrifuged at 2000 rpm for 5 mins and re-suspended in 0.5 ml ALDH buffer and analysed using the flow cytometer.

### 2.8.4 Living cell discrimination

In order to distinguish between live and dead cells, propidium iodide (PI) or Live/dead staining kit (Invitrogen®) was used when PI conflicted with the emission spectra of the fluorescent detector. PI was used at 1  $\mu$ g/ $\mu$ l and incubated with a sample after antibody staining and 15 mins prior to flow cytometric analysis. PI can only interact with dead cell DNA producing an emission spectra detected by the PE channel, allowing cells positive for PE to be removed during data analysis.

The reconstitution of the live dead kit was carried out according to manufacturer's instructions. Briefly, live dead staining was undertaken either before fixation or after antibody staining of non-fixed, cells were centrifuged at 2000 rpm and re-suspended in 0.5 ml DPBS and stained with the activated reagent (1:1000) on ice in the dark for 30 mins. After staining cells were washed once in 0.5 ml DPBS and re-suspended in 1 % FBS (diluted in DPBS). The near IR channel live dead kit binds only to dead cell amines producing an emission spectra detected by the APC-cy7 channel, allowing these cells to be removed during analysis.

### 2.8.5 Flow cytometric analysis

For each sample a total of 10,000 cells were counted on a CyAn™ ADP flow cytometer (DakoCytomation) and data was analysed using the summit v4.3 software. Cell lines were gated according to an unstained sample and lasers were adjusted accordingly. Unstained cells were used to set gates for cell size and internal complexity, dead cells were removed along with doublets (two cells passing past the laser at once).

### **2.8.6 CSC marker expression of chemotherapy treated cells**

Cell lines were seeded at 15625 cells/cm<sup>2</sup> and allowed to attach and grow for 24 hours. After which media was removed and replaced with media containing either cisplatin (0 - 100 µM) or doxorubicin (0 - 3 µM) for 48 hours. Methotrexate (0 – 3 µM) was exposed to cells for 5 days, cells were then trypsinised and stained for either CD117 (Section 2.8.1) or ALDH (Section 2.8.3).

### **2.8.7 ALDH cell density expression**

Cell lines were seeded at 15625 cells/cm<sup>2</sup> and allowed to attach for 24 hours, after which, media was removed and replaced with complete media for 5 days, cells were then trypsinised and stained for ALDH (Section 2.8.3).

### 2.9 Confocal microscopy

Cells were seeded at 1050 cells/cm<sup>2</sup> on to 10 mm diameter circular cover slips (Fisher®) for 3 – 5 days. Upon colonies reaching a suitable size cover slips were washed once with 500 µl DPBS and for ALDH stained simultaneously using To-pro-3 (1:800) (Invitrogen), Aldefluor kit stain (1:400), and CD44 antibody (1:80) (BD sciences) diluted in ALDEFUOR kit buffer. Coverslips were stained for 37 °C for 50 mins, then washed 3 times in ALDEFUOR buffer and mounted with 50 % glycerol (diluted in ALDEFUOR buffer) and analysed immediately. For the ALDH control sample DEAB (1:50) was added in to the staining buffer to inhibit ALDH fluorescence.

CD117 and e-cadherin antibodies were used to stain colonies grown upon coverslips, prior to antibody staining cells were fixed in 400 µl 4 % paraformaldehyde. After fixation coverslips were washed with 400 µl DPBS, blocked in 7 % casein (diluted in DPBS) with RNAase (1:100) for 30 mins at 37 °C. Washed 3 times in DPBS and stained for 1 hour in the dark (antibodies diluted 1:50 in 7 % casein), then washed with 3 times with DPBS and stained with To-pro-3 (1:1000) for 30 mins at room temperature in the dark. Cells were washed 3 times with DPBS and mounted in 70 % glycerol (diluted in DPBS) and analysed using the confocal microscope (Leica).

# **Chapter 3**

## **Characterisation of putative osteosarcoma cancer stem cells**



### 3.1 Introduction

Osteosarcoma is defined as a cancer of the connective tissue origin which is characterised by the production of the bone matrix osteoid (Schajowicz et al., 1995). In most cases OS arises within the medullary cavity of the metaphysis of a growing long tubular bone, however rarer cases occur upon the bone surface, within the cortex or even in an extraskeletal site. High grade OS cancers are most commonly found within the medullary region of the bone, whilst surface OS lesions are often lower grade and occur in patients at least a decade later than common OS lesions (Klein and Siegal, 2006). OS primarily affects adolescents (Jawad et al., 2011) and it has been found that patients with OS are significantly taller, it was suggested that this observation may be linked to rapid growth of bones during puberty (Cotterill et al., 2004) (section 1.1.3).

Stem cells are responsible for the growth and maintenance of organs within the body (section 1.2). A similar hierarchical formation of cells has now been identified within many cancers including leukaemias (Bonnet and Dick, 1997) and solid tumours (Al-Hajj et al., 2003), through the identification of CSC which are attributable for the initiation and growth of tumours. Based on the expression of mesenchymal stem cells marker Stro-1 and the transmembrane tyrosine kinase receptor CD117, OS CSC have been identified using the gold standard technique of xenotransplantation (Section 1.2.2). Stro-1<sup>+</sup> CD117<sup>+</sup> positive cells sorted from cell lines (KHOS-NP and MNNG-HOS) and primary cells (BCOS) were able to serially form tumours and had an elevated resistance to chemotherapeutics (Adhikari et al., 2010). Based on the use of one OS cell line (OS99-1) CSC have also been identified using xenotransplantation of cells expressing the intracellular enzyme ALDH (Wang et al., 2011). These findings suggest that potentially even within one cancer type multiple CSC markers may exist, however, the studies undertaken by Adhikari *et al* 2010 and Wang *et al* 2011 utilised different procedures to assess the tumourigenicity of potential CSC. Therefore, the different markers of OS CSC identified by the groups may reflect differences in the methodologies used and not phenotypic differences, which highlight the need to utilise consistent protocols on a wide range of cell lines.

An alternative method to identify CSC, which is not based on the expression of surface proteins, is the identification of the colony hierarchies (Locke et al., 2005, Li et al., 2008)

(Section 1.2.3). In the OS cell line MG63 holoclonal cells have been found to have enhanced drug resistance and sarcosphere forming efficiency (Lou et al., 2010). Identifying the presence of holoclonal cells in a range of OS cell lines would provide further evidence that CSC reside within sarcomas. The ability to identify the expression of CSC markers within these colonies would provide further evidence of the proteins which distinguish OS CSC.

OS has a very poor prognosis which is often attributed to the presence of secondary tumours (Yen, 2009), 90% of OS metastatic tumours occur in the lungs (Jeffrey et al., 1975). Pulmonary secondary lesions pose a significant risk to patient health, halving long term survival (5 years) from 80% to 40% (Wu et al., 2009). In order for a cancer cell to colonise a distant site and form a secondary tumour it must first detach itself from surrounding cells, survive anoikis and transition through the circulatory system (Simpson et al., 2008). The role of the microenvironment has been found to play a crucial role in providing cells with suitable cues to evolve in to a metastatic cell (Glinskii et al., 2003). The acquisition of migratory properties is based upon epithelial to mesenchymal transition EMT which is integral in embryo development (Hay, 2005) and cancer progression (Thiery, 2002) (Section 1.2.4). The ability of a metastatic cell to colonise a new site and form a secondary tumour indicates this cell must have stem cell properties. Evidence now suggests that expression of EMT transcription factors converts cells to a CSC phenotype (Mani et al., 2008) (section 1.2.5). In OS the phenotype of metastatic cells is not well defined, understanding the EMT status of commonly used OS cell lines will help to further characterise this cancer.

## Aims

CSC from different cancer types often have unique markers which are specific to that cancer type, in OS ALDH and CD117 have been utilised to identify CSC, in contrast, in carcinoma CSC research CD44 is a commonly used marker. Published research using commercially available OS cell lines often focus on only a single CSC marker. Characterising a panel of 8 OS cell lines for a range of CSC markers will provide more robust evidence that putative CSC are present within these cell lines. In addition understanding whether these cell lines contain cells which have a mesenchymal or epithelial phenotype, will help to build up a picture of the nature of OS. The specific objectives of this study which will be tested using a panel of 8 OS cell lines (Table 1.1) and the breast cancer cell line MCF7 as a control, are as follows:

- Comparison of the CSC marker profiles of ALDH, CD44 and CD117.
- Analyse the expression of the epithelial marker e-cadherin and mesenchymal marker vimentin.
- Identification of the colony hierarchies based on the presence of holoclones, meroclones and paraclones.
- Use fluorescent microscopy to identify what colony hierarchies (holoclones, meroclones and paraclones) contain cells expressing CSC markers; ALDH, CD44 and CD117.
- Analyse the ability of cell lines to form spherical colonies in non-attachment conditions.
- Through immunostaining of spherical colonies formed in non-attachment conditions the presence of cells expressing CSC markers (ALDH, CD44 and CD117) will be assessed.

## 3.2 Expression of cancer stem cell markers

### 3.2.1 ALDH staining optimisation

The cancer stem cell marker ALDH was previously used to identify cancer stem cells in OS (Wang et al., 2011) using the ALDEFUOR kit (Stem cell technologies®, Grenoble, France) (section 1.2.2). To determine if ALDH activity varied in OS the enzyme activity was measured in seven OS cell lines and MCF7. In order to obtain accurate measurements of ALDH the flow cytometry assay (Section 2.8.3) was used along with the following analysis. Firstly data was collected from only single cells by gating the pulse width parameter (Figure 3.1), any cells above or below this were removed to exclude any doublets (two cells passing through the lasers at the same time) or debris. Cells were stained with propidium iodide (PI) so only living cells were analysed based on PE-texas red fluorescence. Due to the FITC fluorescence of ALDH stained cells interfering with the PE-texas channel of PI stained cells. A gate was used to include all the low expressing PE-Texas red cells and FITC expressing cells for both control (figure 3.2.A) and ALDH stained (Figure 3.2.B), this was used to identify all living and highly expressing ALDH cells. Finally, in order to identify the percentage of cells expressing ALDH the stained cells were compared to cells to which the ALDH inhibitor diethylaminobenzaldehyde (DEAB) was added (Figure 3.3). ALDH stained cells exceeding the FITC fluorescence of the DEAB inhibited cells were calculated as the ALDH positive population.

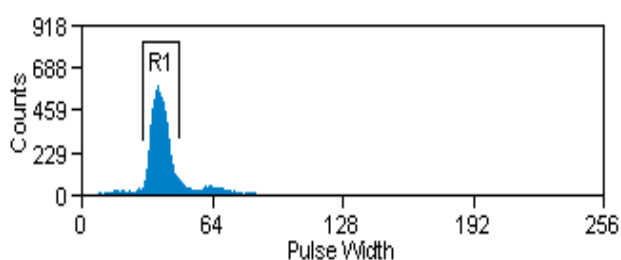


**Figure 3.1: Removal of two cells (duplets) passing through the flow cytometer laser at once.** A gate (R1) was placed over the majority of cells with the same pulse width (cell width), to ensure only cells of a similar size were included in the analysis. Image is an example of HOS pulse width analysis.

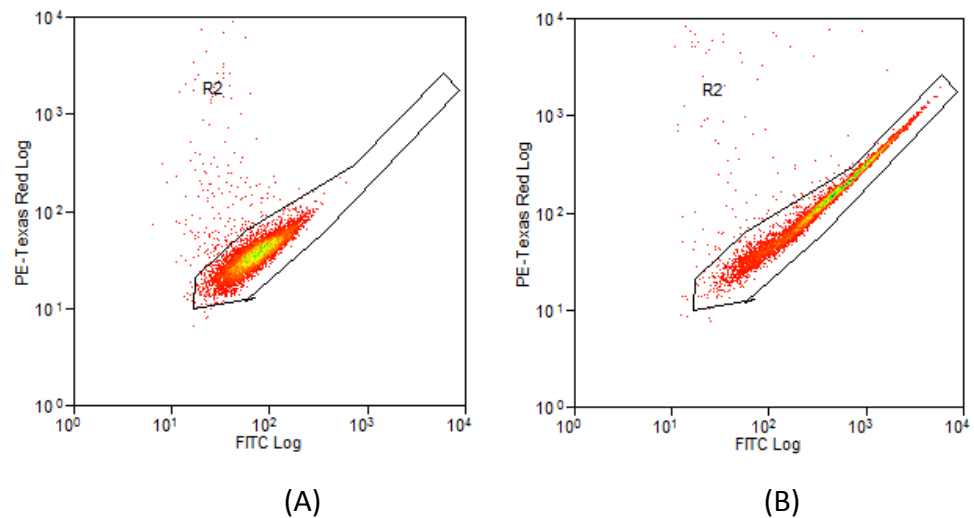


**Figure 3.2: Optimisation of live/dead cells in ALDH staining.** Propidium iodide was used to stain dead cells which could be detected using the PE channel. Due to FITC fluorescent cells (ALDH expressing cells) interfering with PE fluorescence detection, dead cells were removed by using a gate (R2) which would include all the cells expressing low levels of PE texas red for both DEAB control (A) and ALDH positive (B). Cells with a PE fluorescence corresponding to living cells were included in the gate (R2). Any cells outside this gate were considered dead and not included in the analysis. Image is an example of dead cell removal of HOS cells and is representative of 3 images.

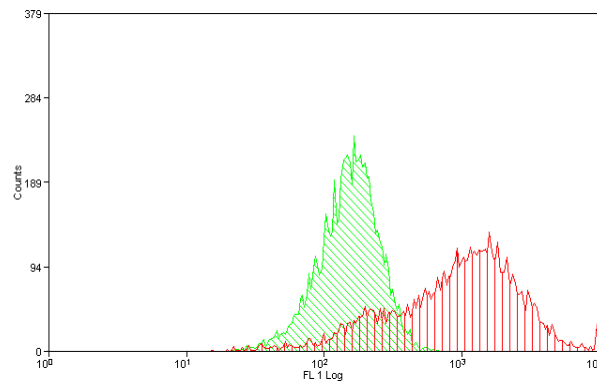


**Figure 3.3: Analysis of ALDH positive population.** The DEAB inhibited cells (green) were compared to the ALDH stained cells (red) (the example shows HOS stained cells (n=1)). Comparison of stained cells to non-stained cells was used to calculate the percentage of ALDH positive cells. Representative of 3 images.

### 3.2.2 Analysis of ALDH expression in OS cell lines and MCF7

The OS cell lines along with MCF7 were stained for ALDH to assess the percentage of cells expressing this putative CSC marker. The expression was heterogeneous ranging from 0.90 % in SaOS-2 to 60.60 % in HOS. The cell lines 143B and G292 also contained relatively large populations of 12.20 % and 9.60 % ALDH positive cells respectively. 143B contained a significantly larger ( $p < 0.05$ ) ALDH population than Cal72, MG63, MNNG-HOS and U2OS. The remaining cell lines all contained a similar sized population ranging from 2.13 % to 3.30 %, the epithelial breast cancer cell line containing 3.26 %.

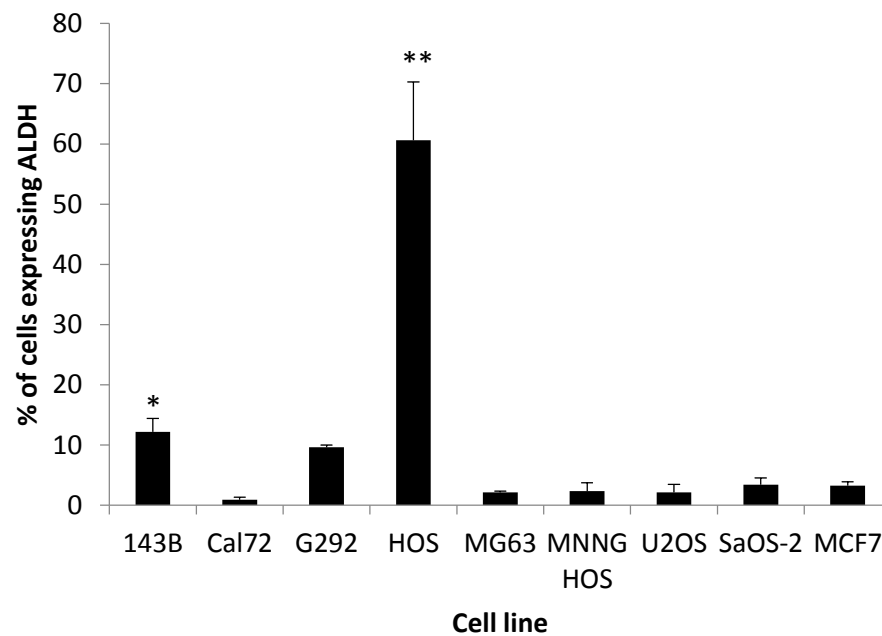


**Figure 3.4: Evaluation of the percentage of ALDH positive cells (ALDH<sup>+</sup>) in OS and MCF7 cell lines.** The HOS cell line contains a significantly larger population than all cell lines and 143B was significantly larger than Cal72, G292, MG63, MNNG-HOS and U2OS, and G292 (\* $p < 0.05$ , \*\* $p < 0.01$  Tukey's post hoc analysis) of ALDH positive cells, when compared to all other cell lines. Each cell line was tested in triplicate and data presented as mean and standard deviation.

### 3.2.3 CD117 staining optimisation

The CD117 tyrosine kinase receptor has been used to identify CSC in OS (Adhikari et al., 2010) and has been associated with poor chemotherapy response (Mijji et al., 2011). In order to accurately identify CD117 expression, the flow cytometry assay outlined in the methods section (Section 2.8.5) was used along with the following analysis. Duplets were removed from analysis as in the ALDH staining procedure (Figure 3.1), PI was used to stain for dead cells. Data from living cells was captured by gating the PE low stained cells to include only living cells (Figure 3.5). Evaluation of CD117 expressing cells was calculated by comparing the isotype control stained antibody fluorescence with the CD117 antibody stained cells (Figure 3.6). Stained cells exceeding the control cell fluorescence were calculated as the CD117 positive population.

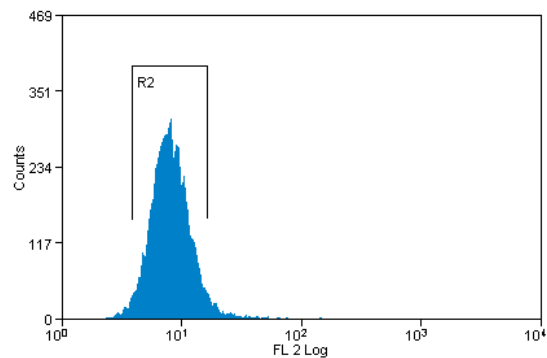


**Figure 3.5: Gating of dead cells using PE channel.** Cells were stained with PI, a gate (R2) was created to include only cells which had a low PE fluorescence and any cells outside of this gate were considered dead and excluded. Image is an example of dead cell removal in 143B cells.

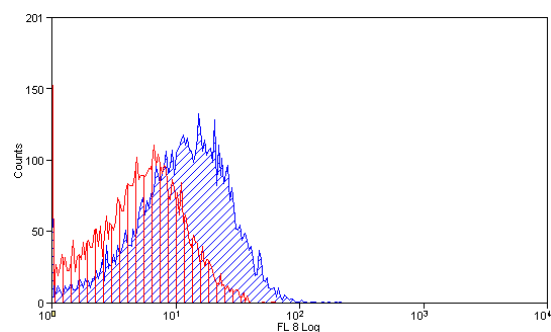


**Figure 3.6: Evaluation of the percentage of CD117 positive cells in the cell line 143B.** Cells stained for CD117 using a CD117 specific monoclonal antibody (IgG1, $\kappa$ ) conjugated to the fluorophore APC, isotype control IgG1, $\kappa$  APC conjugated antibody with no affinity for human cells. The isotype control stained cells (red), were compared to the CD117 stained cells (blue). Comparison of stained cells to isotype control cells was used to calculate the percentage of CD117 positive cells. Example shown is a representative of three images.

### 3.2.4 Analysis of CD117 expression in OS cell lines and MCF7

The presence of CD117 has only been tested in one commonly used OS cell line, U2OS which was found to contain 0.6 % CD117 positive cells (Tang et al., 2011). The majority (65 %) of clinical tumour samples are positive for CD117 (Entz-Werle et al., 2005) so identifying if this marker is also expressed in a panel of OS cell lines is of interest. Using the method outlined in 3.2.3 all cell lines except 143B (6.40 %) contained less than 1 % of cells expressing CD117, Cal72 and HOS contained populations of 0.93 % and 0.77 % respectively and the remaining low expressing cell lines contained negligible populations less than 0.1 %. U2OS contained 0.008 % CD117 expressing cells, which was smaller than population reported by Tang *et al.*, (2011). MG63 and MCF7 contained no CD117 positive cells and 143B contained a significantly larger population than all other cells lines of 6.40 % (Figure 3.7).

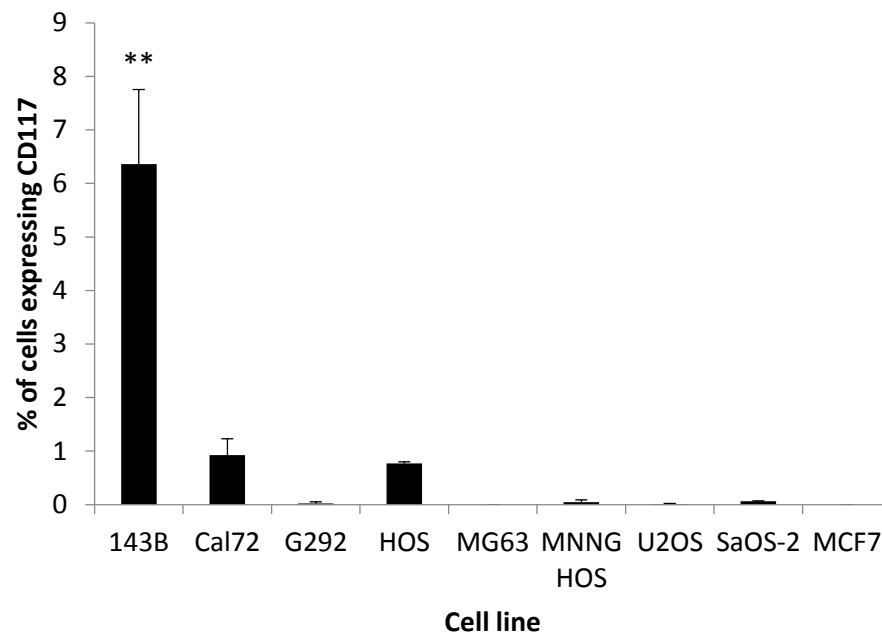


**Figure 3.7: Evaluation of the percentage of cells expressing CD117 in OS and MCF7 cell lines.** 143B contains a significantly larger population (\*\*p < 0.01 Tukey's post hoc analysis) of ALDH positive cells, when compared to all other cell lines. Results presented as mean and standard deviation. Each cell line tested in triplicate.



### 3.2.5 Analysis of CD44 expression in OS cell lines and MCF7

Carcinoma cells with increased expression of the adhesion protein CD44 have been shown to comprise putative CSC with enhanced tumourigenicity (Harper et al., 2010). Cells expressing CD44 and lacking CD24 have been identified as CSC in breast cancer using a xenotransplantation model (Al-Hajj et al., 2003). All cell lines were screened for CD44 using a PE labelled antibody and dead cells identified using live dead stain (Invitrogen). An isotype and fluorophore (PE) matched antibody was used as a control and used to identify the percentage of cells expressing CD44, using the same analysis approach as CD117 expression (Figure 3.5 and 3.6). OS cell lines tested express CD44, HOS cell lines contained the smallest population of 69 % whilst G292, MG63, MNNG-HOS and SaOS-2 all contained over 99% of cells CD44 positive. The epithelial breast cancer cell line MCF7 contained only 4.9 % of cells expressing CD44.

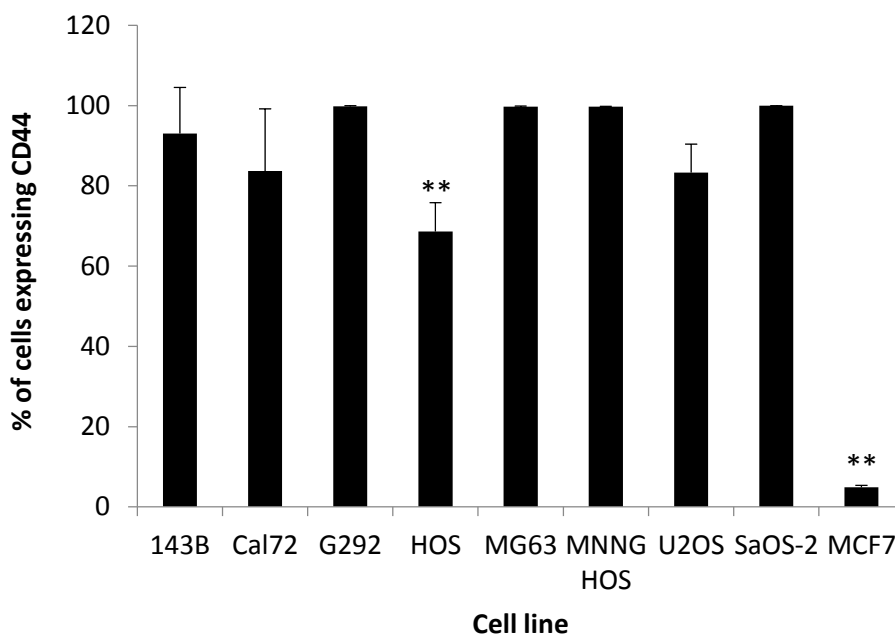


**Figure 3.8: Evaluation of the percentage of cells expressing CD44 in OS and MCF7 cell lines.** All cell OS cell lines contained a high proportion of CD44 positive cells in contrast MCF7 contained a significantly smaller population than all cell line and HOS was significantly smaller than 143B, G292, MG63, MNNG-HOS and SaOS-2 (\*\*P <0.01 Tukey's post hoc analysis). All results tested in triplicate. Results presented as mean and standard deviation.

### 3.3 Analysis of expression of mesenchymal and epithelial markers in OS cell lines and MCF7

The process of EMT has been found to play an integral role in cancer progression, once a cancer cell has acquired the ability to migrate and invade surrounding tissues this can lead to metastasis. The calcium dependant cell-cell adhesion protein e-cadherin (e-cad) is a marker of an epithelial phenotype. Loss of e-cad is characteristic of a cell adopting a migratory mesenchymal phenotype (von Schlippe et al., 2000), loss of e-cad is often associated with increased expression of the protein vimentin (vim), which is a type III intermediate filament protein highly expressed in mesenchymal cells (Steinert and Roop, 1988). In carcinoma the *de novo* expression of vimentin is associated with the acquisition of a mesenchymal phenotype and enhanced invasiveness (Sommers et al., 1994).

All cell lines were screened for both e-cad and vim using either a fluorescently labelled e-cad antibody or a primary vim antibody followed by a fluorescently labelled secondary antibody. Flow cytometry was used to detect cell fluorescence and analysis was carried out on  $1 \times 10^4$  cells, dead cells were removed by counter staining with PI for e-cad stained cells or live dead stain (Invitrogen®) for vim staining. Each labelled population was compared to an isotype control and where appropriate fluorescent label matched antibody. Overlay histograms were produced and the increase in fluorescence was determined using the same analysis approach as CD117 expression (Figure 3.5 and 3.6).

All OS cell lines contained low levels of e-cad expression ( $\leq 0.22\%$ ), U2OS was the only cell which contained no e-cad positive cells. 143B had the largest population of 0.22 %, whilst the remaining cell lines all contained negligible populations below 0.06%. MCF7 contained a significantly larger population of 66.9 % which reflects the epithelial phenotype of this cell line (Figure 3.9).

In the OS cell lines vim was highly expressed ranging from 90 % – 98 % of cells vim positive. MG63 and U2OS had the lowest average expression at 90 and 92 % respectively. SaOS-2 expressed it to the highest level at 98 %, whilst the remaining cell lines varied between 94 – 97 %. In accordance with the epithelial nature of MCF7 it contained a very low level of vim expression with only 0.15 % expressing the protein (Figure 3.10).

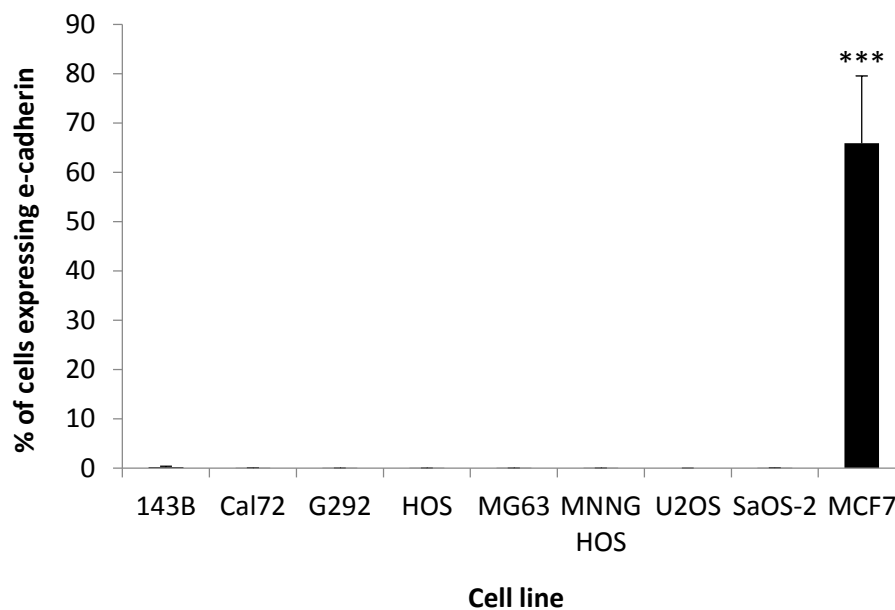


**Figure 3.9: Evaluation of cell lines expressing e-cadherin in OS and MCF7 cell lines.** All OS cell lines contained only a small population (< 0.22 %) of e-cadherin positive cells, in particular U2OS contained no e-cadherin expression. MCF7 contained a significantly larger population of e-cadherin expressing cells (\*\*p < 0.01 Tukey's post hoc analysis). Results tested in triplicate and presented as mean and standard deviation.

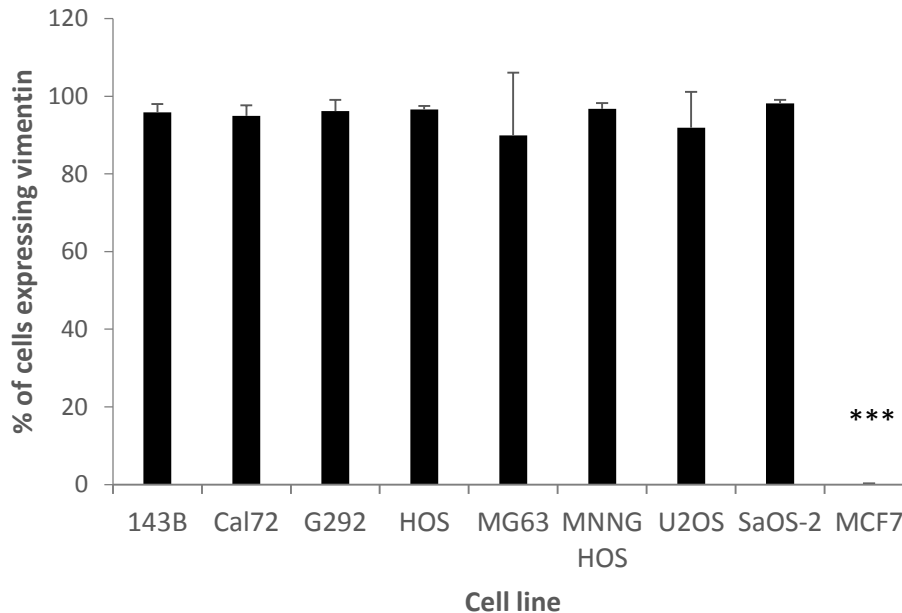
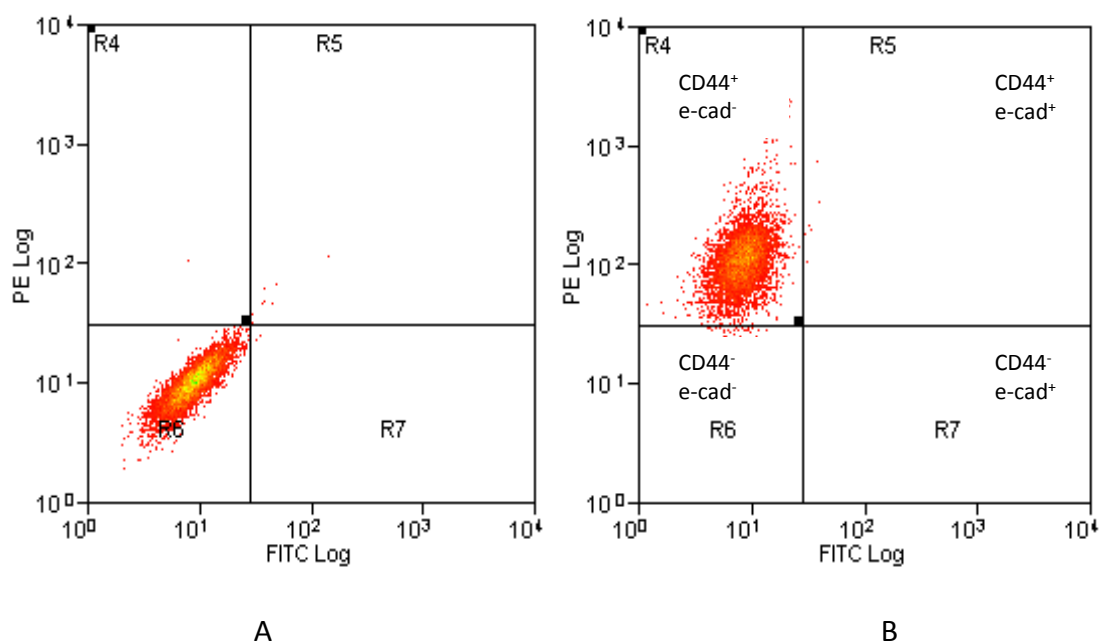


**Figure 3.10: Evaluation of cell lines expressing vimentin in OS and MCF7 cell lines.** All OS cell lines contained large populations vimentin positive cells, MG63 contained the smallest population of 90 % and SaOS-2 the highest at 98 %. MCF7 cells had a significantly smaller population of cells expressing vimentin. (\*\*p < 0.01 Tukey's post hoc analysis). Results tested in triplicate and presented as mean and standard deviation.

### **3.4 CD44 and epithelial and mesenchymal marker co-expression analysis**

#### **3.4.1 Optimisation of method used to assess CD44 and e-cadherin expression**

Using a system to detect both CD44 and either e-cad or vimentin allows the presence of a double positive population to be analysed according to their epithelial status. Further tests will be required to identify whether these double positive cells represent a CSC population. In order to identify cells positive for CD44 along with an epithelial marker, a PE labelled CD44 antibody was used simultaneously with either a FITC labelled e-cad antibody or primary vimentin antibody followed by a secondary FITC antibody. All cell lines were gated for live cells using live dead stain (Invitrogen®) and pulse width to remove doublets as stated in the ALDH analysis procedure (Figure 3.1). In order to identify the populations of cells expressing CD44 and e-cad control antibodies were used which matched according to antibody isotype and fluorescent label but have no specificity to human cells. Accurate measurement of CD44 and e-cad analysis was achieved by using quadrants to identify the population sizes. In order to have a consistent placement of the quadrant it was firstly placed on the control cells so the top two quadrants (R4 and R5) included between 0.5 % - 0.14 % (Figure 3.11 A) control cells. Once the quadrant placement had been fixed it was then overlaid on to the CD44 and epithelial marker stained cells and the populations quantified (Figure 3.11 B).

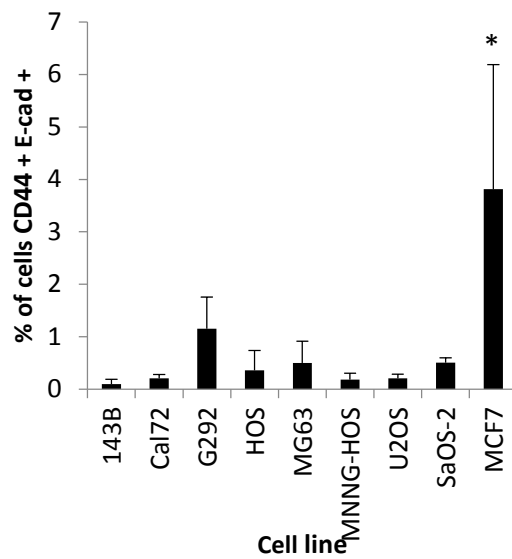
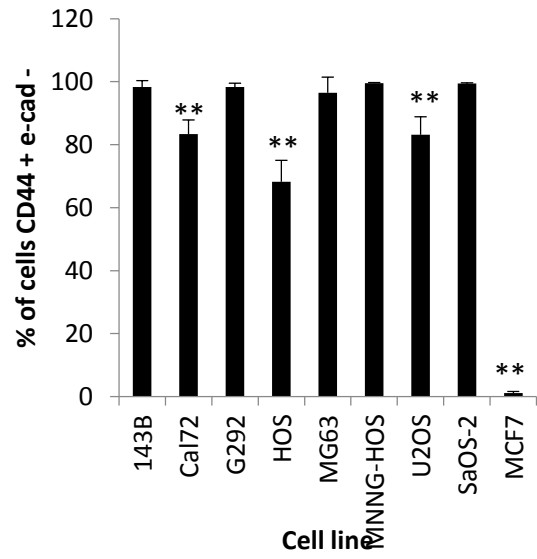
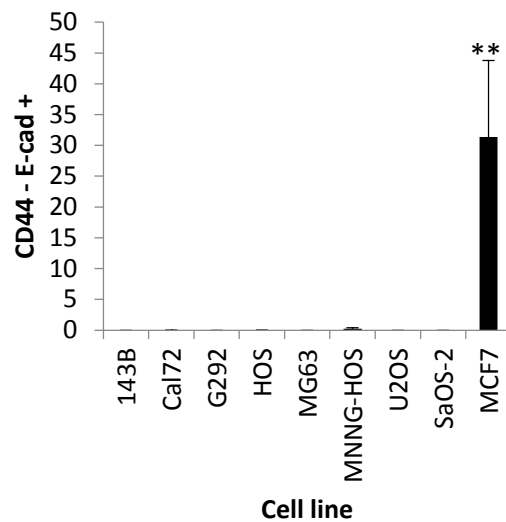
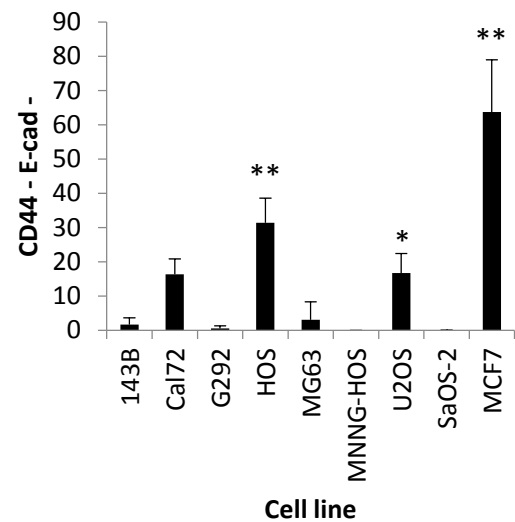


**Figure 3.11: Evaluation of CD44 and e-cadherin populations in OS and MCF7 cell lines.** A) U2OS control cells (stained with isotype control), quadrant placed so regions R4 and R5 include between 0.5 - 0.14 % of cells. The quadrant position obtained from A was then overlaid on to CD44 and e-cadherin U2OS stained cells (B). Y axis represent CD44 expression and x axis represents e-cadherin expression. Each quadrant is used to assess the frequency of the following populations; R4 = CD44<sup>+</sup> e-cad<sup>-</sup> stained cells; R5 = CD44<sup>+</sup> e-cad<sup>+</sup> stained cells; R7 = CD44<sup>-</sup> e-cad<sup>+</sup> stained cells and R6 CD44<sup>-</sup> e-cad<sup>-</sup>. Image representative of 3 images of HOS cells.

### 3.4.2 Characterisation of CD44/e-cadherin phenotypes in OS cell lines and MCF7

Four CD44/e-cad phenotypes were present based on cells either being double positive for both markers, single positive for a marker or double negative. In OS the CD44<sup>+</sup>/e-cad<sup>+</sup> double positive populations were relatively small and varied from 0.1 % (143B) to 1.2 % (G292) (Figure 3.12.A). In contrast the CD44<sup>+</sup>/e-cad<sup>-</sup> single positive cells comprised the largest populations ranging from 99 % (SaOS-2) to 68 % (HOS) (Figure 3.12.B). The CD44<sup>-</sup>/e-cad<sup>+</sup> single positive phenotype was the least common and present in only Cal72 (0.005 %), HOS (0.003 %) and MNNG-HOS (0.26 %) (Figure 3.12.C). Due to the small size of the Cal72 and HOS populations, these could in fact be an artefact caused by non-specific binding of antibodies to the cells. The presence of cells lacking both CD44 and e-cad (CD44<sup>-</sup>/e-cad<sup>-</sup>) forms the most variable population ranging from 0 % (MNNG-HOS) to 31 % (HOS) (Figure 3.12.D). As a consequence of MCF7 epithelial phenotype it has a large population of

CD44/e-cad<sup>+</sup> single positive cells which comprise 31 % (Figure 3.12.C) and also the largest population of CD44<sup>+</sup>/e-cad<sup>+</sup> double positive cells (3.8 %) found in all cell lines tested (Figure 3.12.A). In contrast to the OS cell lines, the smallest population of MCF7 was found within the CD44<sup>+</sup>/e-cad<sup>-</sup> population (1.1 %) (Figure 3.12.B) and largest within the double negative cells (CD44<sup>-</sup>/e-cad<sup>-</sup>) (63.7 %) (Figure 3.12.D). In order to clarify the markers expressed by each cell line, the CD44/e-cad phenotypes have been summarised within table 3.1.

(A) CD44<sup>+</sup>/e-cad<sup>+</sup>(B) CD44<sup>+</sup>/e-cad<sup>-</sup>(C) CD44<sup>-</sup>/e-cad<sup>+</sup>(D) CD44<sup>-</sup>/e-cad<sup>-</sup>

**Figure 3.12: Evaluation of CD44 and e-cadherin expression in OS and MCF7 cell lines.** A) frequency of cells positive for both CD44 and e-cad expression (CD44<sup>+</sup>/e-cad<sup>+</sup> cells) MCF7 contains a significantly smaller population than all cell lines. B) frequency of cells positive for CD44 expression and negative for e-cad (CD44<sup>+</sup>/e-cad<sup>-</sup>), MCF7 contains a significantly smaller population than all cell lines, HOS contains less than all OS cell lines, Cal72 and U2OS contain a smaller population than 143B, G292, MG63, MNNG-HOS and SaOS-2. C) frequency of cells negative for CD44 expression and positive for e-cad (CD44<sup>-</sup>/e-cad<sup>+</sup>), MCF7 contains a significantly larger population than all cell lines. D) frequency of cells negative for CD44 expression and negative for e-cad (CD44<sup>-</sup>/e-cad<sup>-</sup>), MCF7 contains a larger population than all cell lines, HOS contains a larger population than 143B, G292, MG63, MNNG-HOS and SaOS-2, U2OS contains a larger population than SaOS-2. All results tested in triplicate and presented as mean and standard deviation. \*p = <0.05, \*\*p = <0.01 (Tukey's post hoc analysis).

**Table 3.1. CD44/e-cadherin phenotypes in OS cell lines and MCF7.** Cell line CD44/e-cad populations presented tested in triplicate and presented as mean percentage values and standard deviation (S.D).

Cell line	CD44/e-cadherin populations (S.D)			
	% of cells expressing CD44 <sup>+</sup> /e-cad <sup>+</sup> ±S.D	% of cells expressing CD44 <sup>+</sup> /e-cad <sup>-</sup> ±S.D	% of cells expressing CD44 <sup>-</sup> /e-cad <sup>+</sup> ±S.D	% of cells expressing CD44 <sup>-</sup> /e-cad <sup>-</sup> ±S.D
143B	0.10 ± 0.09	98.30 ± 2.10	0.00 ± 0.00	1.60 ± 2.01
Cal72	0.21 ± 0.07	83.41 ± 4.40	0.005 ± 0.005	16.38 ± 4.41
G292	1.15 ± 0.61	98.30 ± 1.20	0.00 ± 0.00	0.55 ± 0.75
HOS	0.36 ± 0.31	68.26 ± 6.81	0.003 ± 0.005	31.38 ± 7.20
MG63	0.50 ± 0.42	96.43 ± 5.00	0.00 ± 0.00	3.06 ± 5.23
MNNG-HOS	0.18 ± 0.12	99.43 ± 0.21	0.26 ± 0.11	0.00 ± 0.00
U2OS	0.21 ± 0.08	83.14 ± 5.74	0.00 ± 0.00	16.66 ± 5.75
SaOS-2	0.50 ± 0.09	99.46 ± 0.13	0.00 ± 0.00	0.04 ± 0.03
MCF7	3.81 ± 2.37	3.81 ± 0.47	31.34 ± 12.46	63.72 ± 15.24



### 3.4.3 Characterisation of CD44/vimentin phenotypes in OS cell lines and MCF7

Four CD44/vim phenotypes were present based on cells either being double positive for both markers, single positive for a marker or double negative. In the OS cell lines tested the majority of cells were present within the CD44<sup>+</sup>/vim<sup>+</sup> double positive population with little very little variation present, population sizes ranged from 91 % (HOS) to 99 % (SaOS-2) (Figure 3.13.A). In contrast greater variability was observed in CD44<sup>+</sup>/vim<sup>-</sup> populations which ranged from 0.5 % (MNNG-HOS) to 4.7 % (143B) (Figure 3.13.B). Except for Cal72 which contained a population of 2.5 % of CD44<sup>-</sup>/vim<sup>+</sup> cells, the remaining OS cells lines contained a small percentage of CD44<sup>-</sup>/vim<sup>+</sup> cells ranging from 0.01 % (SaOS-2) to 0.9 % (U2OS) (Figure 3.13.C). The double negative CD44<sup>-</sup>/vim<sup>-</sup> phenotype was variable between OS cell lines. Ranging from 5.6 % (U2OS) to 0.09 % (SaOS-2) and making up a relatively small percentage of OS cells. In contrast MCF7 contained a large proportion (95.8 %) of these cells (Figure 3.14.D). The remaining MCF7 cells were mostly composed of CD44<sup>+</sup> vim<sup>-</sup>/cells (3.5 %) (Figure 3.14.B) and to a lesser extent CD44<sup>-</sup>/vim<sup>+</sup> (0.39 %) (Figure 3.13.C) and CD44<sup>+</sup>/vim<sup>+</sup> cells (0.27 %) (Figure 3.13.A). In order to clarify the markers expressed by each cell line, the CD44/vim phenotypes have been summarised within table 3.2.

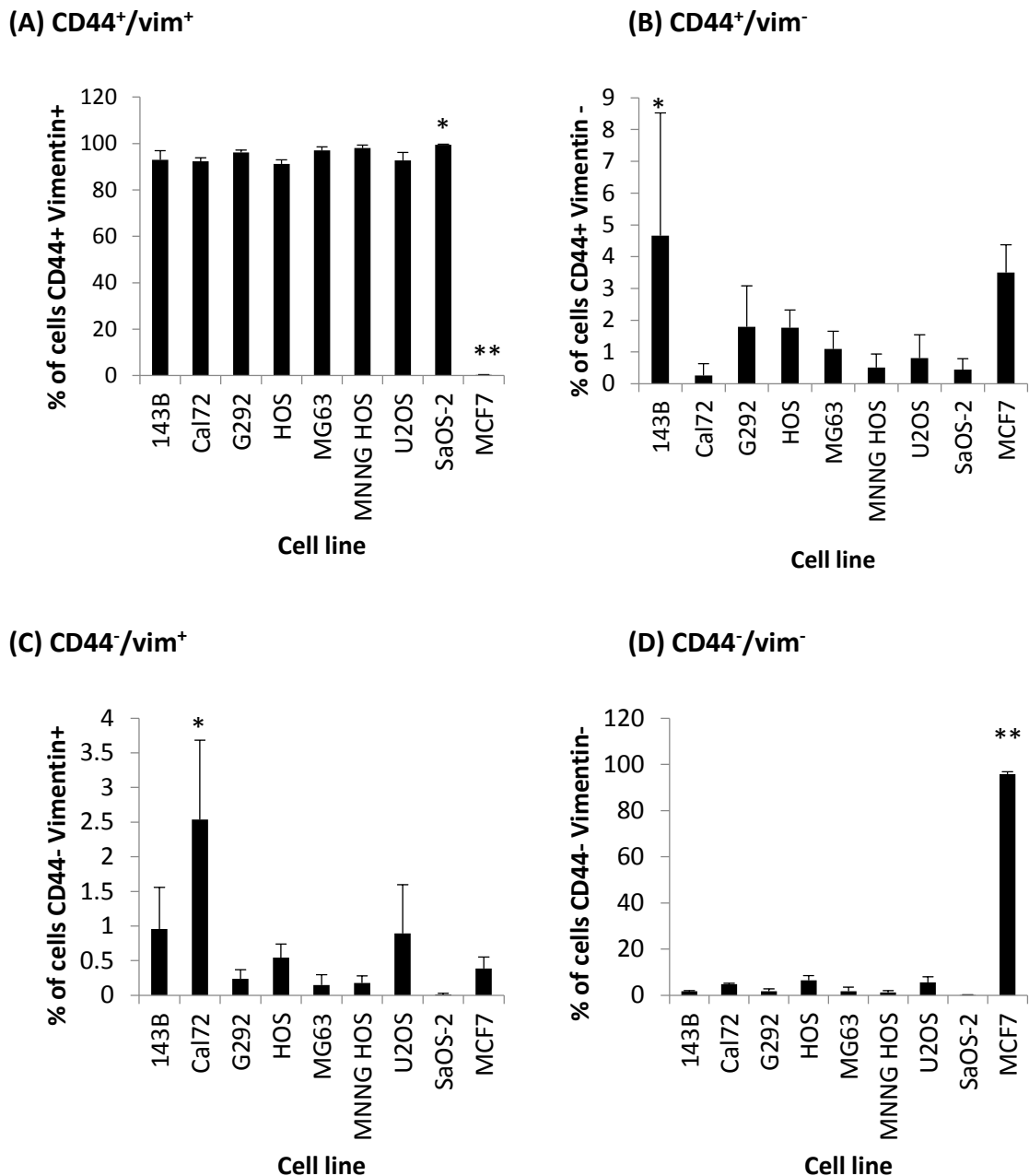


**Figure 3.13: Evaluation of CD44 and vimentin expression of OS cell lines and MCF7.** A) frequency of cells positive for both CD44 and vimentin expression (CD44<sup>+</sup> vim<sup>+</sup> cells), MCF7 contains a population smaller than all cell lines, SaOS-2 contains a larger population than 143B, Cal72, HOS and U2OS. B) frequency of cells positive for CD44 expression and negative for vimentin (CD44<sup>+</sup> vim<sup>-</sup>), 143B contains a significantly larger population than Cal72, MNNG-HOS and SaOS-2. C) frequency of cells negative for CD44 expression and positive for vimentin (CD44<sup>-</sup> vim<sup>+</sup>), Cal72 contains a significantly larger population than all cell lines. D) frequency of cells negative for CD44 expression and negative for vimentin (CD44<sup>-</sup> vim<sup>-</sup>), MCF7 contains a significantly larger population than all cell lines, HOS and U2OS contain larger populations than 143B, G292, MG63, MNNG-HOS and SaOS-2. All results tested in triplicate and presented as mean and standard deviation, \*p < 0.05, \*\*p < 0.01 (Tukey's post hoc analysis).

**Table 3.2: CD44/e-cadherin phenotypes in OS cell lines and MCF7.** Cell line CD44/e-cad populations presented tested in triplicate and presented as mean percentage values and standard deviation (S.D).

Cell line	CD44/vimentin populations (%)			
	% of cells expressing CD44 <sup>+</sup> /vim <sup>+</sup> ±S.D	% of cells expressing CD44 <sup>+</sup> /vim <sup>-</sup> ±S.D	% of cells expressing CD44 <sup>-</sup> /vim <sup>+</sup> ±S.D	% of cells expressing CD44 <sup>-</sup> /vim <sup>-</sup> ±S.D
143B	92.60 ± 4.02	4.66 ± 3.86	0.96 ± 0.60	1.71 ± 0.26
Cal72	92.38 ± 1.40	0.26 ± 0.37	2.54 ± 1.15	4.83 ± 0.27
G292	96.16 ± 1.03	1.79 ± 1.29	0.24 ± 0.14	1.82 ± 0.99
HOS	91.14 ± 1.85	1.76 ± 0.56	0.54 ± 0.20	6.56 ± 1.98
MG63	97.04 ± 1.54	1.09 ± 0.56	0.15 ± 0.15	1.72 ± 1.88
MNNG-HOS	98.03 ± 1.39	0.51 ± 0.49	0.18 ± 0.10	1.28 ± 0.72
U2OS	92.75 ± 3.43	0.81 ± 0.73	0.89 ± 0.70	5.55 ± 2.53
SaOS-2	99.45 ± 0.29	0.44 ± 0.34	0.01 ± 0.01	0.09 ± 0.09
MCF7	0.27 ± 0.12	3.50 ± 0.87	0.39 ± 0.17	95.84 ± 0.97

### 3.5 Identification of the colony hierarchies within OS cell lines and MCF7

The colony hierarchies identified by Locke *et al* (2005) represent the cellular heterogeneity present within both healthy tissues and tumours (Section 1.2.3). The identification of the tightly packed holoclones indicates the presence of putative CSC, meroclones (colonies containing features of both holoclones and paraclones) encompass a more mature population which will transiently divide before giving rise to the terminally differentiated paraclones (loose irregular colonies). All OS cell lines and MCF7 included in this study were able to recapitulate the three colony phenotypes (Figure 3.14) when seeded at low density (2 – 4 cells cm<sup>2</sup>) and cultured for 7 – 14 days. The appearance of the holoclones differed between each cell line, but all displayed tightly packed cells with a smooth boundary of cells encasing the colony. The holoclone shape was predominantly round or oval shape and was observed in the majority of cell lines (143B, HOS, MNNG-HOS, G292, U2OS, SaOS-2 and MCF7). In contrast Cal72 and MG63 displayed holoclones with a more angular shape with Cal72 holoclones almost square in shape, whilst MG63 had angular projections. Meroclones were a mixture of the holoclone morphology with cells beginning to migrate from the colony, OS paraclonal colonies were composed of a dispersed population of cells; often cells would become totally detached from one another. The only exception was U2OS and Cal72 which tended to contain clusters of cells still bound together. MCF7 paraclones were not as dispersed as the OS colonies and were composed of clusters of cells which had migrated a short distance.

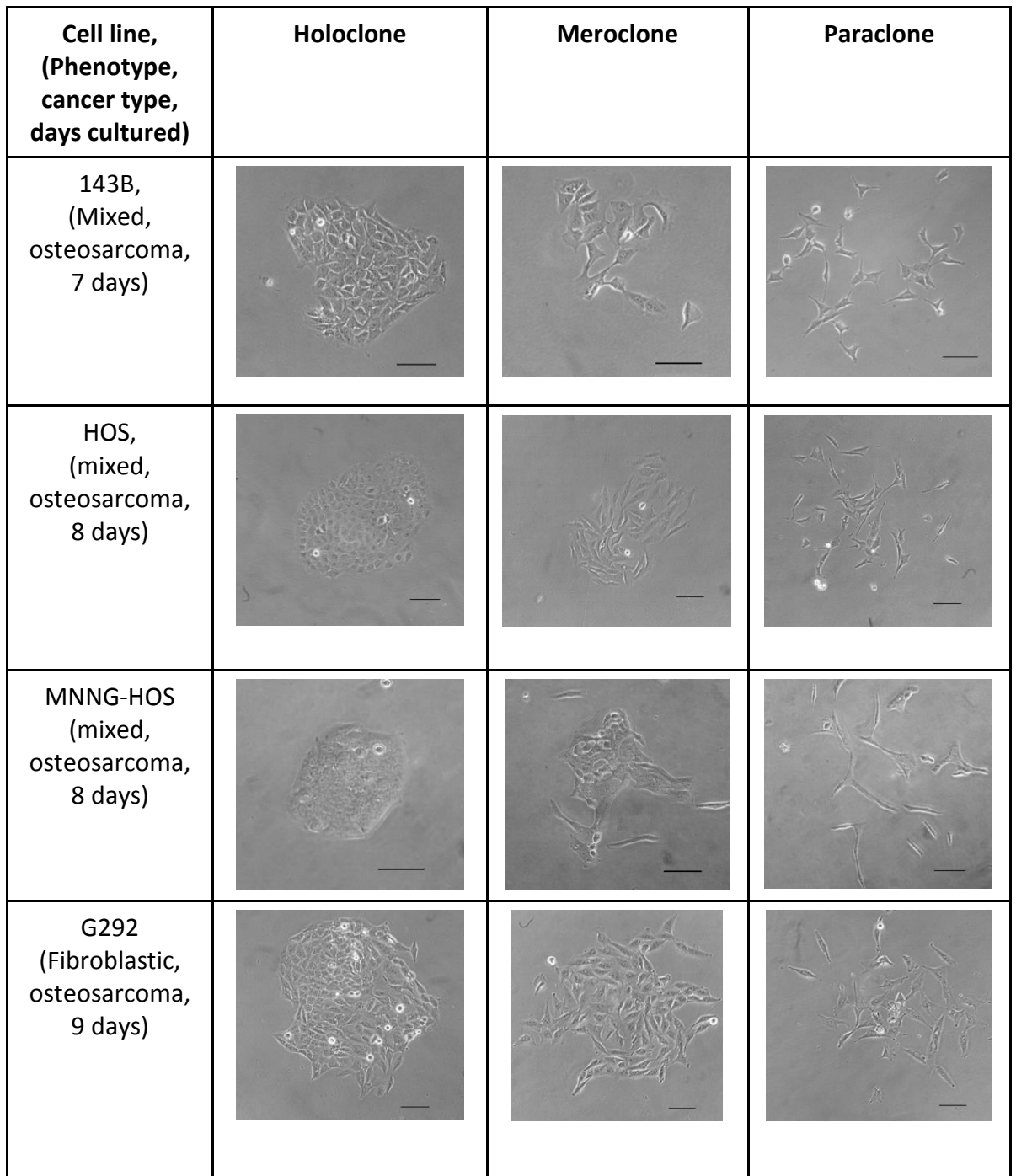
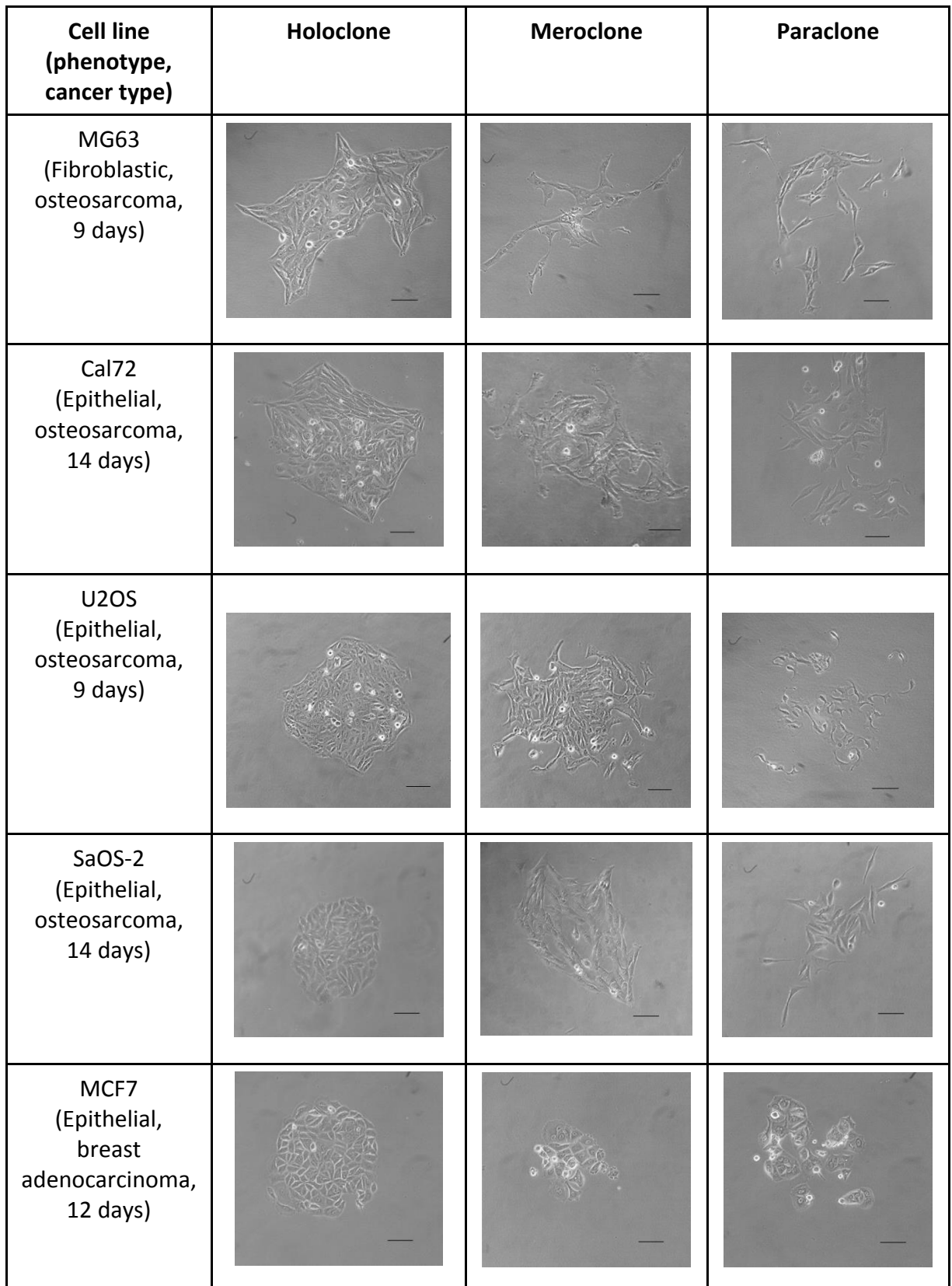


Figure 3.14: Continued overleaf



**Figure 3.14: Colony hierarchies present within each cell line.** Holoclone, meroclone and paraclone phenotypes from all cell lines when seeded at a density to produce 100 colonies per 55 cm<sup>2</sup> (seeding density varied from 2 - 4 cells per cm<sup>2</sup> depending upon the cell line) after 7 – 14 days of growth. Images representative of 4 images per hierarchy. Scale bar represents 100  $\mu$ M.

### 3.6 Presence of cells expressing CSC markers within colony hierarchies

Prostate cancer holoclones have been shown to contain CSC based on the expression of CSC markers (Li et al., 2008) providing a useful method of separating highly tumourigenic population of cells from their non tumourigenic counterparts. MG63 holoclones are reported to have enhanced clonogenicity and express elevated levels of CD133 (Lou et al., 2010). A similar observation has been observed in head and neck carcinoma holoclones which have increased levels of the putative CSC marker CD44 (Harper et al., 2010). The analysis of OS colony hierarchies for expression of the putative OS CSC markers (CD117 and ALDH) has not been determined, therefore identifying whether these cells are restricted to one hierarchy will give an indication of whether these cells function as CSC.

In order to investigate the location of CSC expressing cells within the colony hierarchies, cells were seeded at low density (26 cells/mm<sup>2</sup>) and grown on 12 mm circular coverslip for 3 - 4 days, allowing the colony morphologies to form. Cells were fixed with paraformaldehyde when staining for CD117 or CD44 and e-cad, however, due to ALDH being an intracellular enzyme, only living cells could be used for analysis. In this case an antibody ALDEFLUOR staining mixture was prepared and stained in a short time (50 mins) at 37 °C to minimise cell disruption. Upon mounting coverslips in 50 % glycerol (diluted in ALDEFLUOR buffer) slides were kept on ice and analysed immediately. Due to the high expression of CD44 within all OS cell lines this antibody was used as membrane marker to identify the location of membranes within the images. To ensure fluorescently labeled cells were not the result of non-specific antibody interactions, isotype and fluorescent labelled matched antibodies were also used to stain cell to assess antibody specificity, ALDH was also inhibited with DEAB (Appendix I).

#### 3.6.1 Location of ALDH expressing cells within OS cell lines and MCF7 colony hierarchies

According to flow cytometry the OS cell lines 143B, G292 and HOS all contain populations of ALDH expressing cells > 10 %, whilst the remaining OS cell lines all contained populations < 10 % (section 3.2.2). It was found that ALDH positive cells within the colony hierarchies are not restricted to holoclones in cell lines containing > 10 % ALDH<sup>+</sup> cells (as determined

by flow cytometry). The cell lines 143B, G292 and HOS all contained ALDH positive cells within the three colony morphologies. 143B colony hierarchies (Figure 3.15.1) contain ALDH positive cells in meroclones and paraclones, however the holoclone situated in the centre of the image contains no ALDH positive cells, a similar finding was also observed in G292 (figure 3.15.2) and HOS (figure 3.15.3). Cell lines with low ALDH expression MG63 (2.14 %) and SaOS-2 (3.4 %) contain ALDH positive cells which only reside within the holoclones, however, there are also holoclones present which lack any ALDH positive cells (figure 3.15.2 and figure 3.15.5). ALDH positive cells are present within MCF7 colonies but due to the low expression of CD44 it made identifying the colony morphologies difficult (figure 3.15.6), although, MCF7 ALDH cells appear restricted only to the densely packed holoclone like colonies.

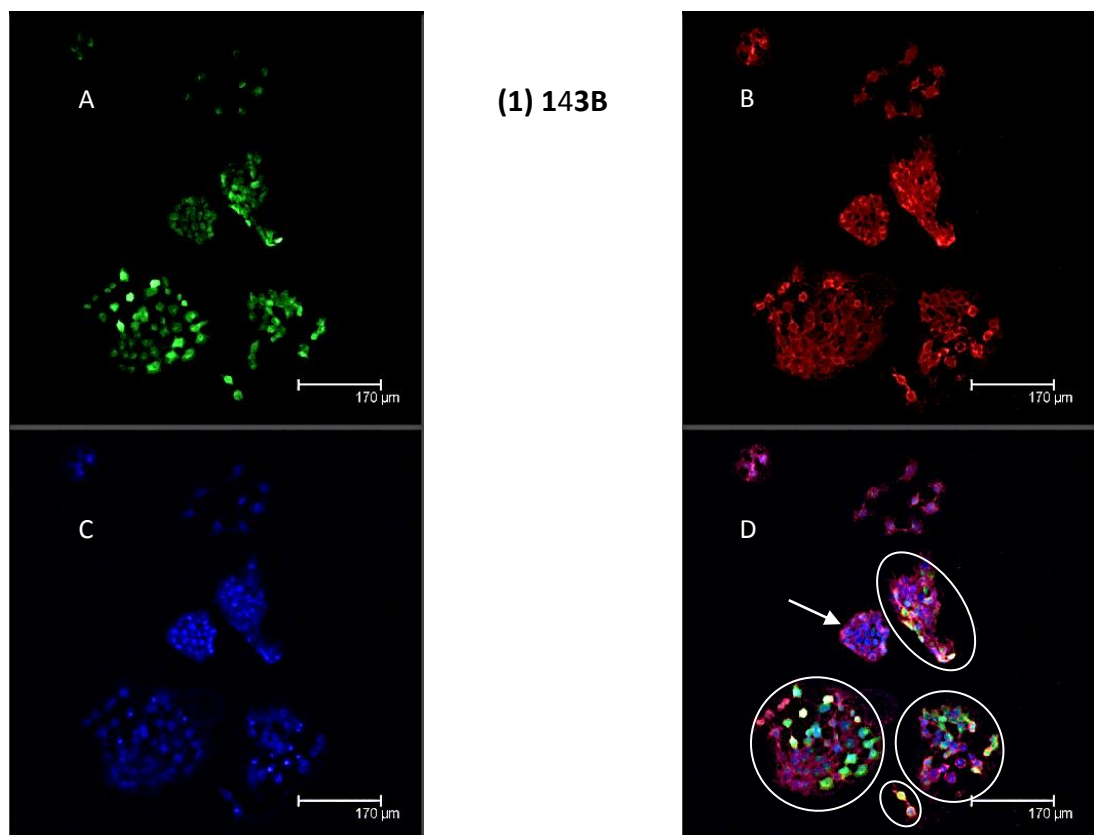
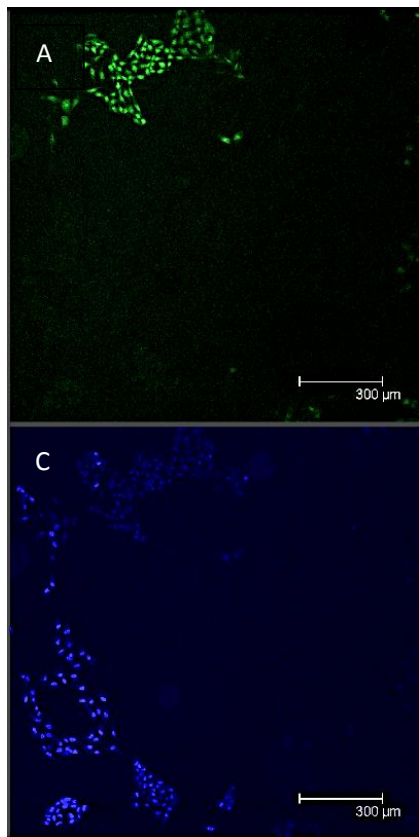
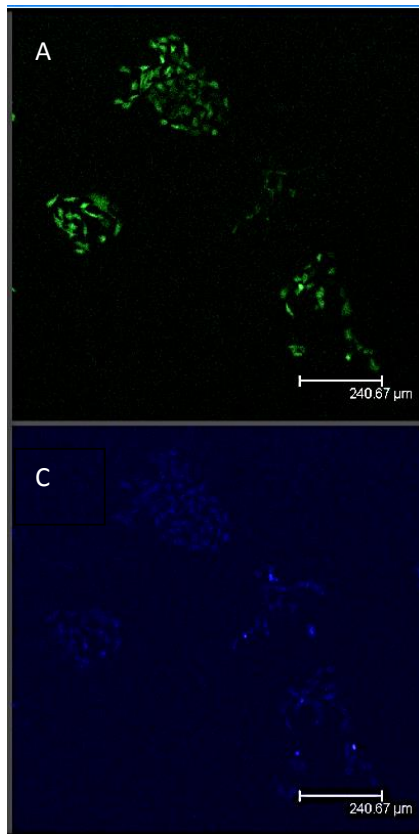
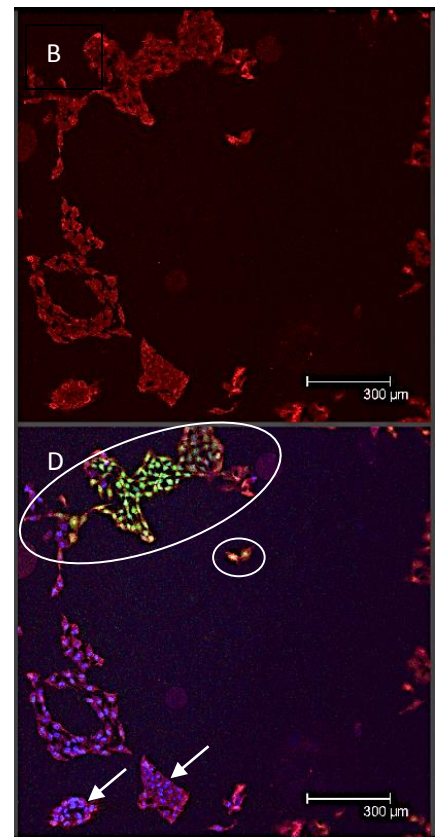


**Figure 3.15: Continued overleaf**





(2) G292



(3) HOS

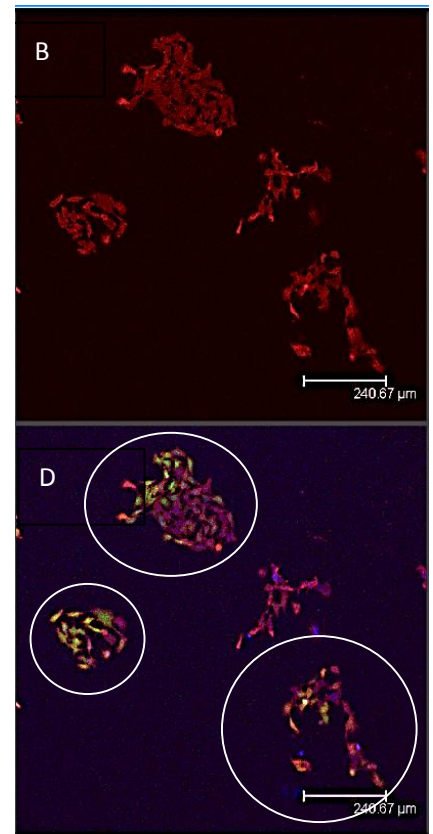
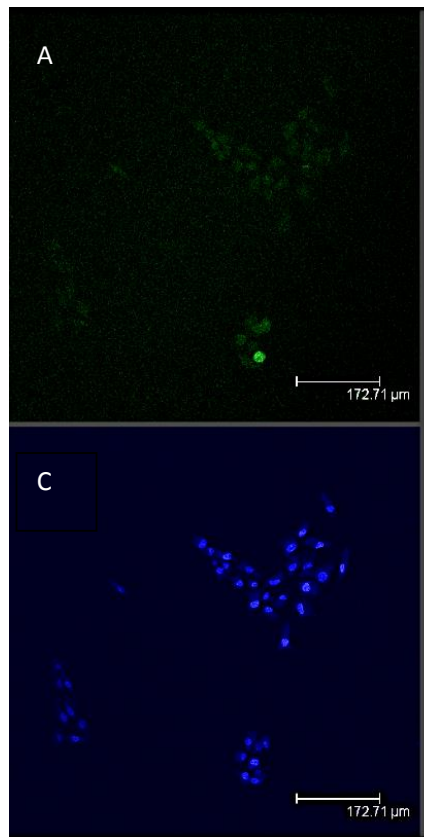
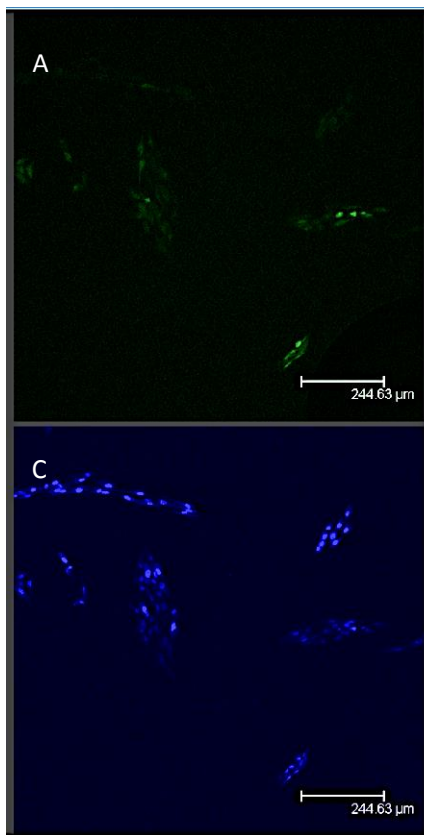
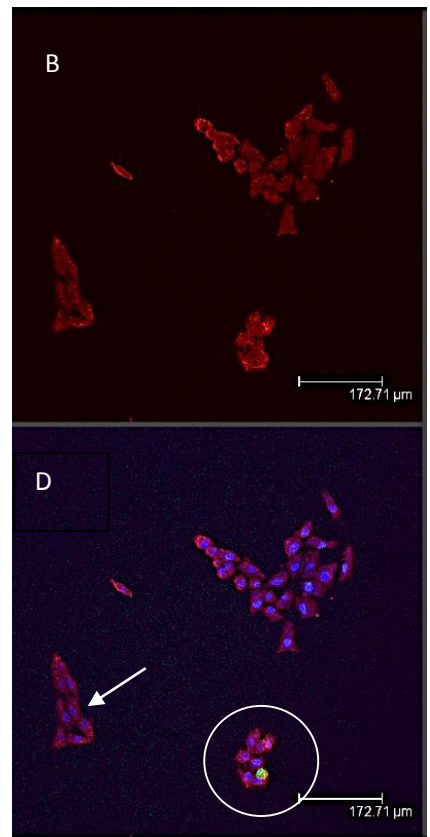


Figure 3.15: Continued overleaf



(4) MG63



(5) SaOS-2

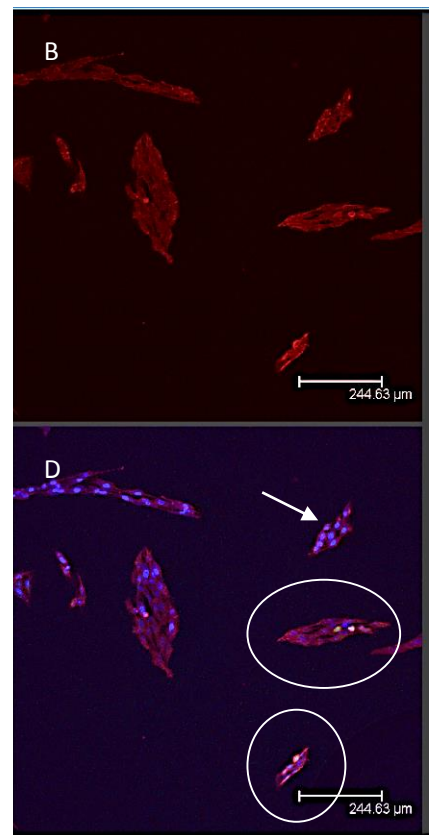
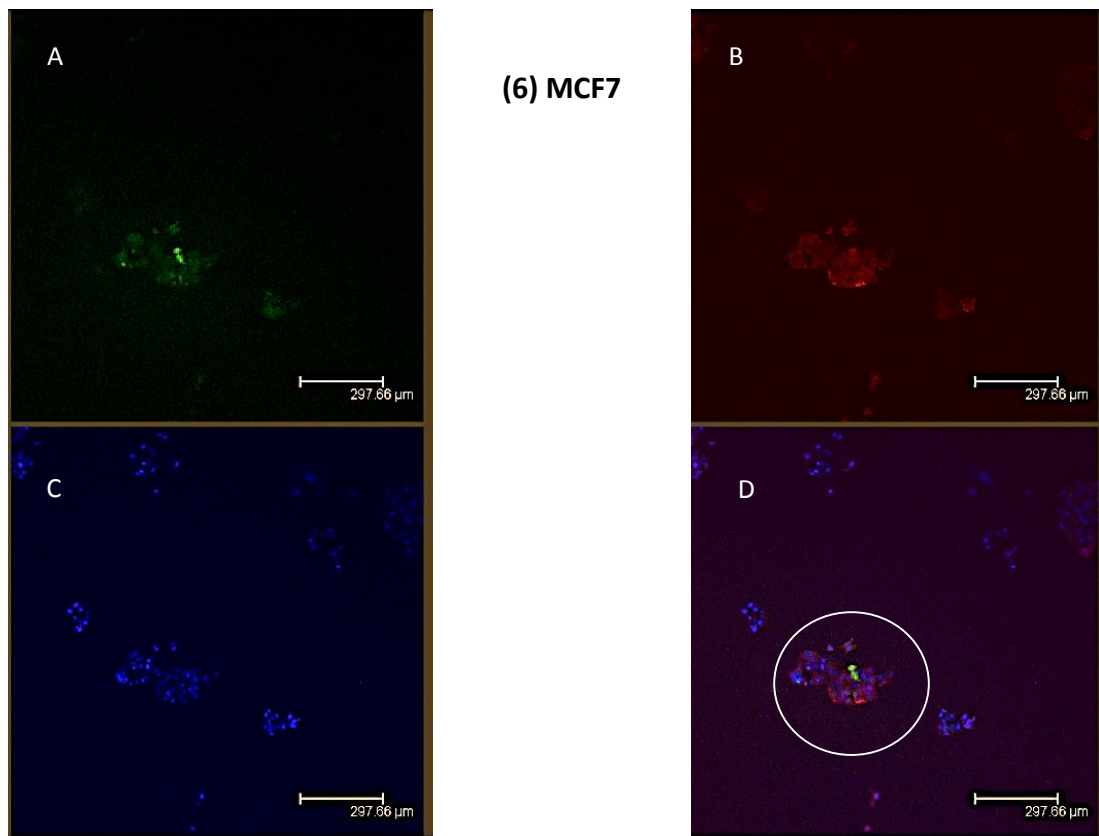


Figure 3.15: Continued overleaf



**Figure 3.15: Colony morphologies containing ALDH positive cells OS cell lines and MCF7.** Cell lines (143B (1), G292 (2), HOS (3), MG63 (4), SaOS-2 (5) and MCF7 (6) were seeded on coverslips (1050 cells/cm<sup>2</sup>) and grown for 3 - 5 days to form suitable sized colonies. ALDH expression was demonstrated by dual-colour fluorescence, coverslips were co-stained with To-pro-3 (blue nuclei), PE labelled CD44 antibody (red membrane) and ALDH using the ALDEFLUOR reagent (green putative CSC). (A) ALDH expressing cells, (B) CD44 expressing cells, (C) nuclei and (D) overlay of all 3 markers. ALDH positive colony circled. Image representative of at least 4 images.

### 3.6.2: Location of CD117 expressing cells within colony hierachy of 143B

According to the flow cyotmetry results 143B contained the largest population of CD117 cells (6.4 %) (Figure 3.7), therefore would make the most suitable cell line to identify where these cells reside within the colony hierachies. When tested at a low density (1050 cells/cm<sup>2</sup>) 143B contained very few cells expressing CD117, positive cells stained very weakly and were found around the outer the membranes of small holoclones (Figure 3.16). When 143B was allowed to reach a higher density (80 – 90 % confluency) the presence of CD117 increased. The high density meant colony hierachies were unidentifiable, however, CD117 expression was localised to very small sites on each cell and was present to the periphery of a colony, producing a speckled appearance around the colony edge (Figure 3.17).

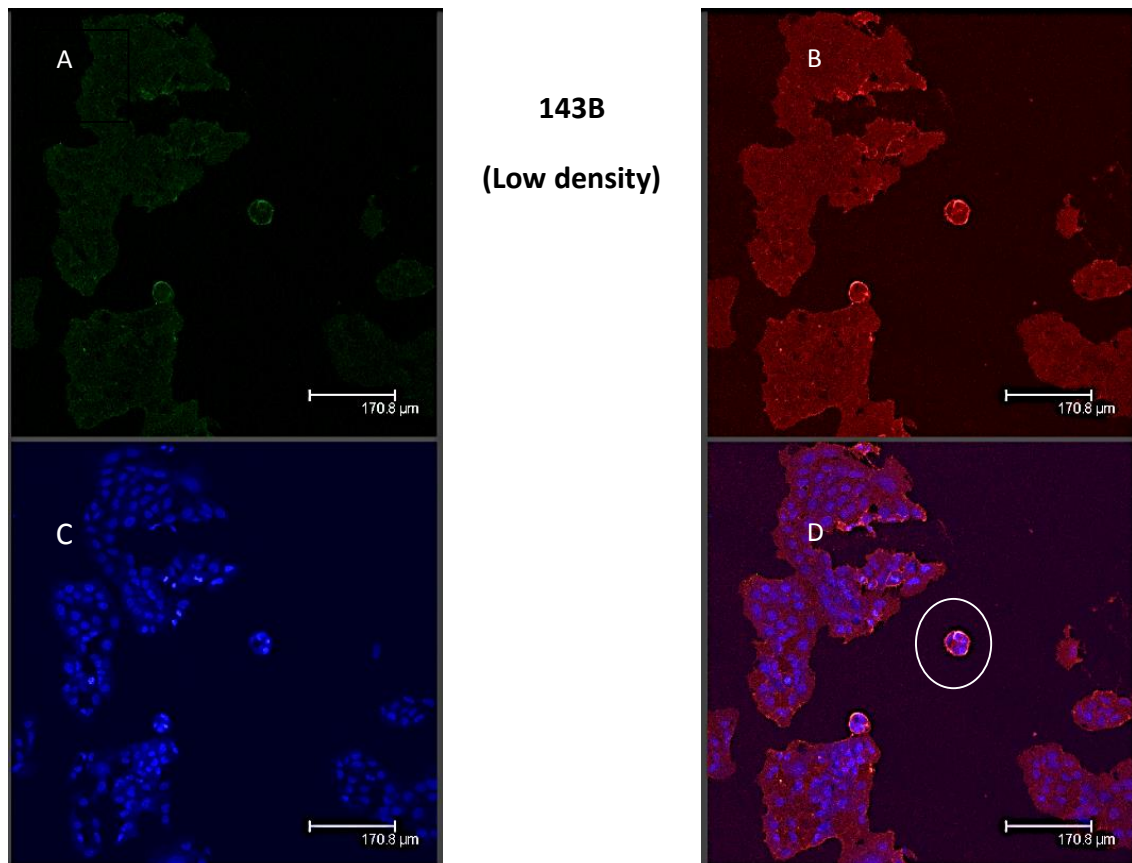


**Figure 3.16: Colony morphologies containing CD117 positive cells in 143B at low density.** Demonstrated by dual-colour fluorescence, 143B cells (1050 cells/cm<sup>2</sup>) were grown for 3 days then stained with To-pro-3 (blue nuclei), PE labelled CD44 antibody (red membrane) and FITC labelled CD117 antibody (green putative CSC). (A) CD117 expressing cells, (B) CD44 expressing cells, (C) nuclei and (D) overlay of all 3 markers. CD117 positive colony circled. Image representative of at least 4 images.

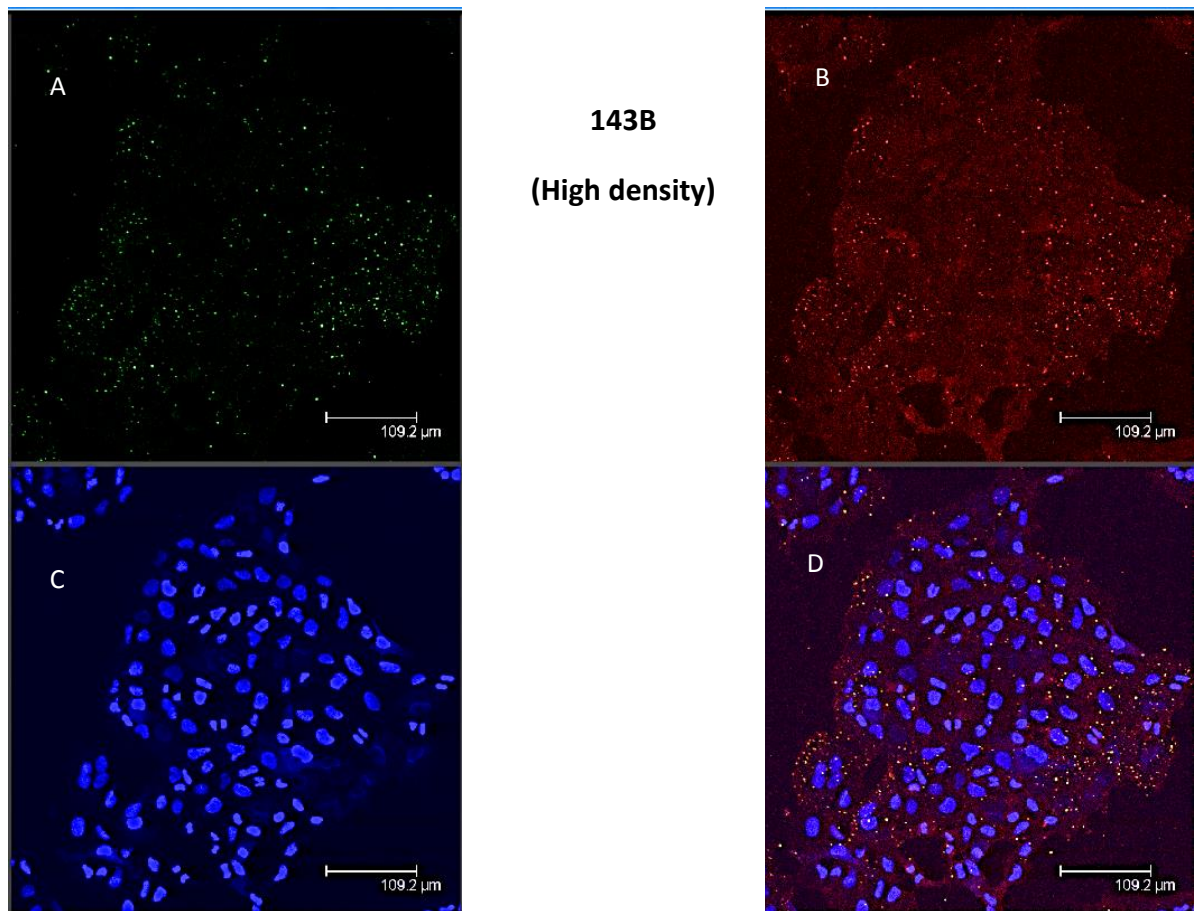


**Figure 3.17: Colony morphologies containing CD117 positive cells in 143B at high density.** Demonstrated by dual-colour fluorescence, 143B cells (2100 cells/cm<sup>2</sup>) were grown on coverslips for 3 days then stained with To-pro-3 (blue nuclei), PE labelled CD44 antibody (red membrane) and FITC labelled CD117 antibody (green putative CSC). (A) CD117 expressing cells, (B) CD44 expressing cells, (C) nuclei and (D) overlay of all 3 markers. Image representative of at least 4 images.

### **3.6.3: Location of CD44 and e-cadherin expressing cells within colony hierachy**

The presence of cells co-expressing CD44 and e-cad within the OS cell lines were rare. G292 had the largest population of co-expressing cells (1.15 %) when analysed using flow cytometry and was the only OS cell line found to contain cells expressing both markers. OS CD44<sup>+</sup> e-cad<sup>+</sup> cells were identified within paraclones (Figure 3.18.1) and meroclones (Figure 3.18.2) of G292. In contrast MCF7 contains heterogenous expression of both CD44 and e-cad in the colony hierarchies, cells which were highly expressing both CD44 and e-cad were found in the centre of holoclones, whilst cells only expressing CD44 were identified in paraclonal cells (Figure 3.18.3).

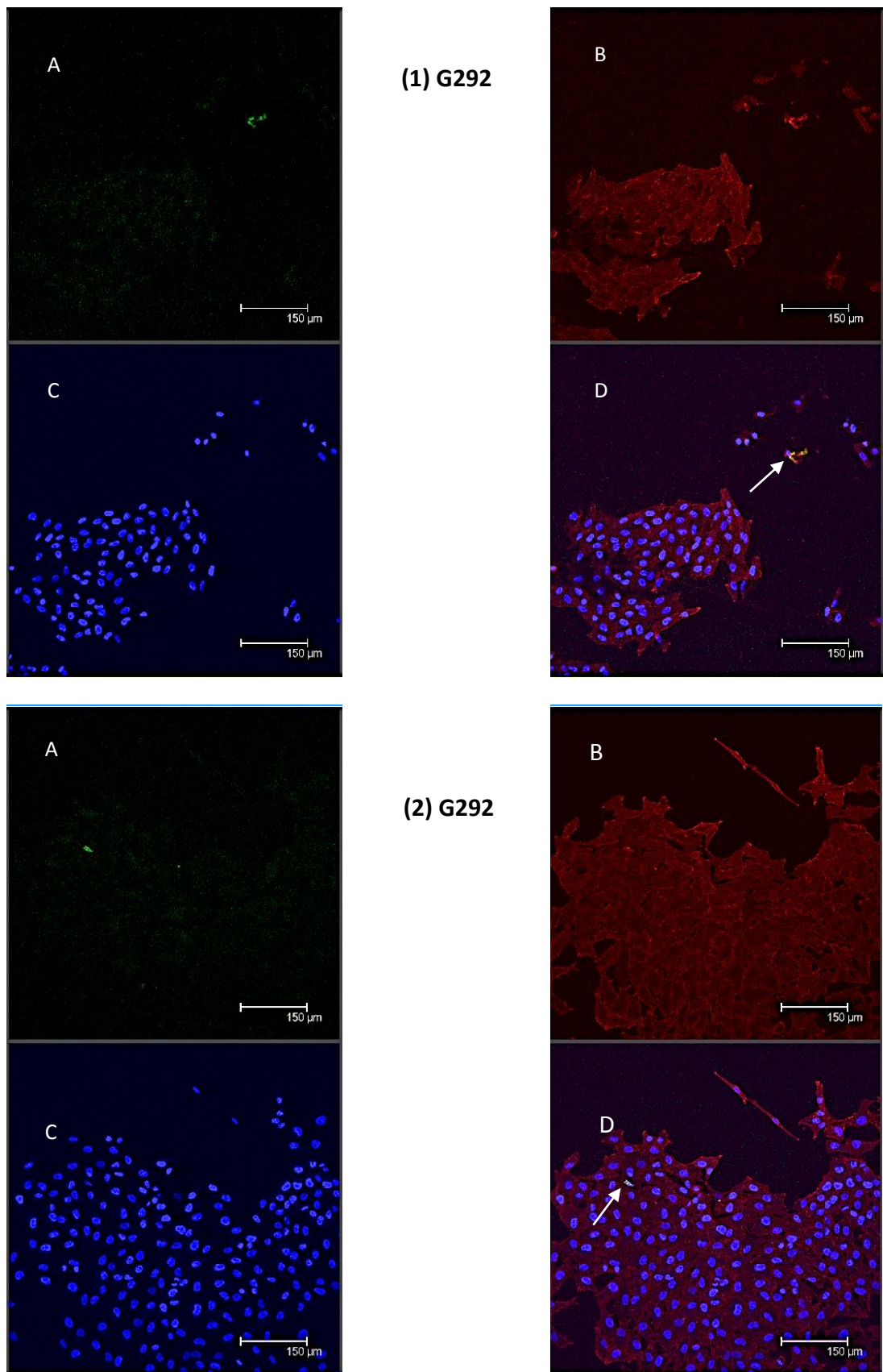
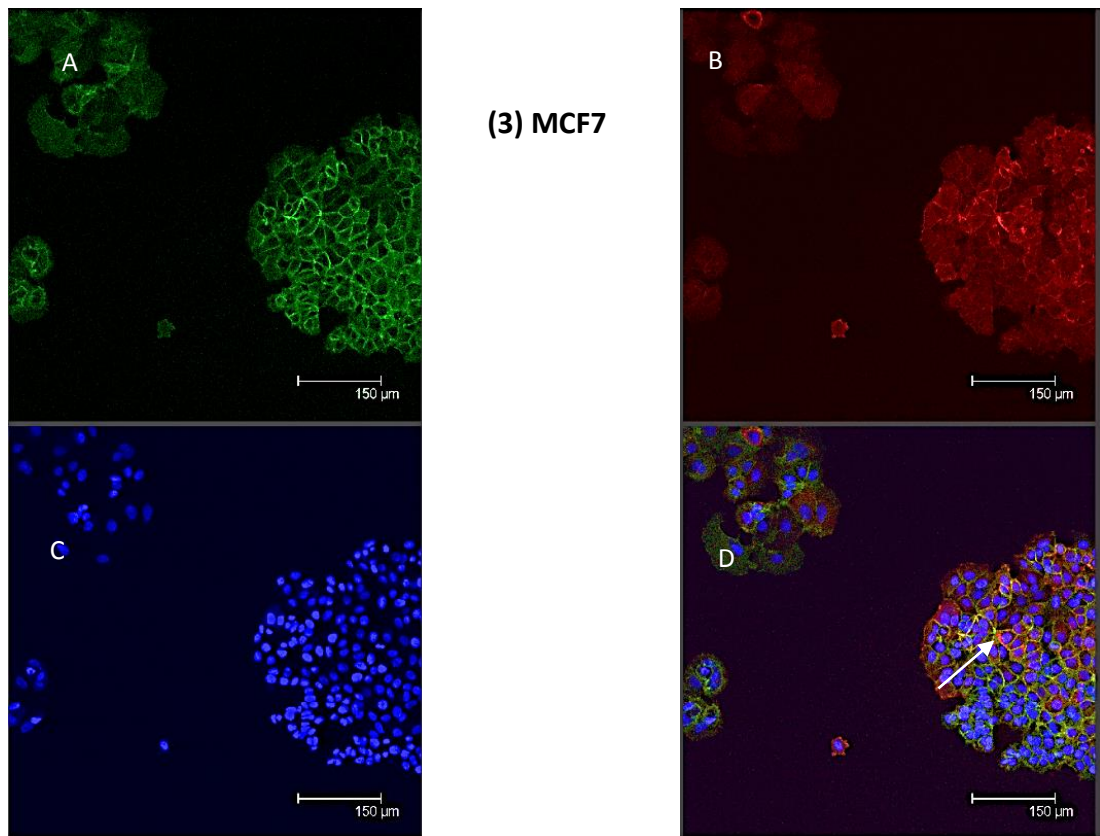


Figure 3.18: Continued overleaf



**Figure 3.18: Colony morphologies containing CD44 and e-cad positive cells in G292 and MCF7.** G292 (Images 1 and 2) and MCF7 (3) were grown on coverslips (1050 cells/cm<sup>2</sup>) for 4 days. CD44/e-cad expressing cell were demonstrated by dual-colour fluorescence, coverslips were stained with to-pro-3 (blue nuclei), PE labelled CD44 antibody (red membrane) and FITC labelled e-cadherin antibody (green). (A) E-cadherin expressing cells, (B) CD44 expressing cells, (C) nuclei and (D) overlay of all 3 markers. Arrow indicates a cell highly expressing both e-cadherin and CD44. Image representative of at least 4 images.



### 3.7 Evaluation of sarcosphere forming ability of OS cell lines and MCF7

Growing cells within serum starved low attachment conditions was originally used to select neuronal multipotent stem cells (Reynolds and Weiss, 1992). This technique has also been used to study stem cells within cancers. In osteosarcoma the spherical colonies produced in non-adherent conditions are termed sarcospheres, have increased expression of the stem cell transcription factors Nanog and Oct 3/4 as well as mesenchymal markers (Gibbs et al., 2005). In breast cancer spherical colonies were found to have enhanced ability to form xenotransplantable tumours, demonstrating the enrichment of CSC within these cell populations (Grimshaw et al., 2008).

In this study cell lines were tested by seeding cells single cells at 10,000 cells/non-adherent 6 well plate, and grown in the presence of 20 ng/ml bFGF and EGF along with B27 supplement, which was replenished every 3 days throughout the experiment (Section 2.2.4). After 7 days colony size was assessed before passaging sarcospheres and re-seeding at 210 cells/cm<sup>2</sup> and growing for a further 7 days after which colony size and number were assessed. When counting sarcospheres only colonies  $\geq 40 \mu\text{M}$  were included.

The appearance of the sarcospheres was markedly different to mammospheres produced by MCF7, which were produced under the same conditions as sarcospheres. In general OS primary sarcospheres did not have the classical spherical shape with smooth appearance. They were less uniform in shape and often visibly composed of clusters of cells, the uneven shape is most apparent in Cal72 and MG63 which are clearly composed of a colony of cells giving it a rougher appearance. In contrast MCF7 produced large spherical colonies with an almost smooth appearance making identifying individual clusters of cells challenging (Figure 3.19).

After the cells had been passaged and grown for a further 7 days to form secondary sarcospheres, the sarcospheres in all cell lines except 143B and MNNG-HOS were visibly smaller in size. Cal72, HOS and U2OS produced no colonies greater than 40  $\mu\text{M}$ , the only cells present were single cells, which had failed to divide. The secondary colonies produced by 143B and MNNG-HOS were more irregular in shape than the primary sarcospheres (Figure 3.9).

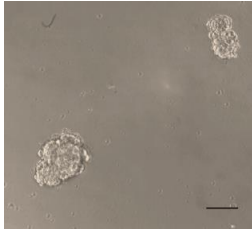
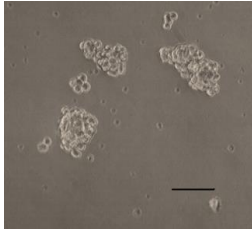
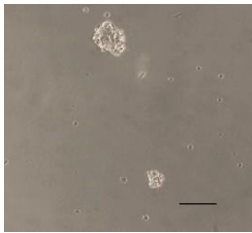
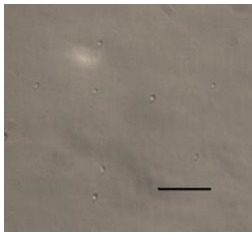
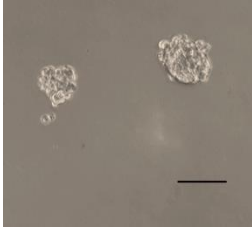
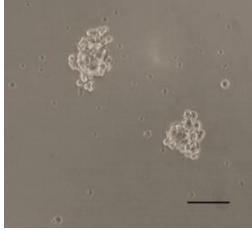
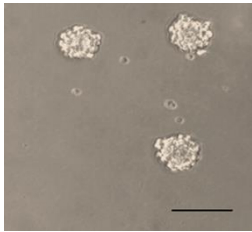
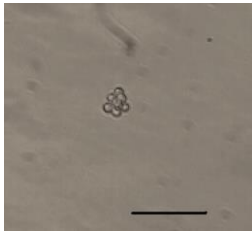
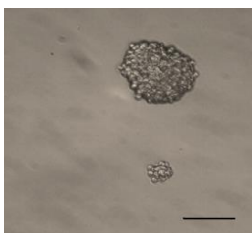
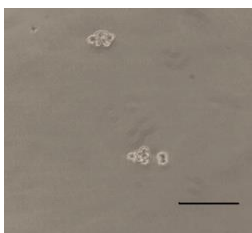
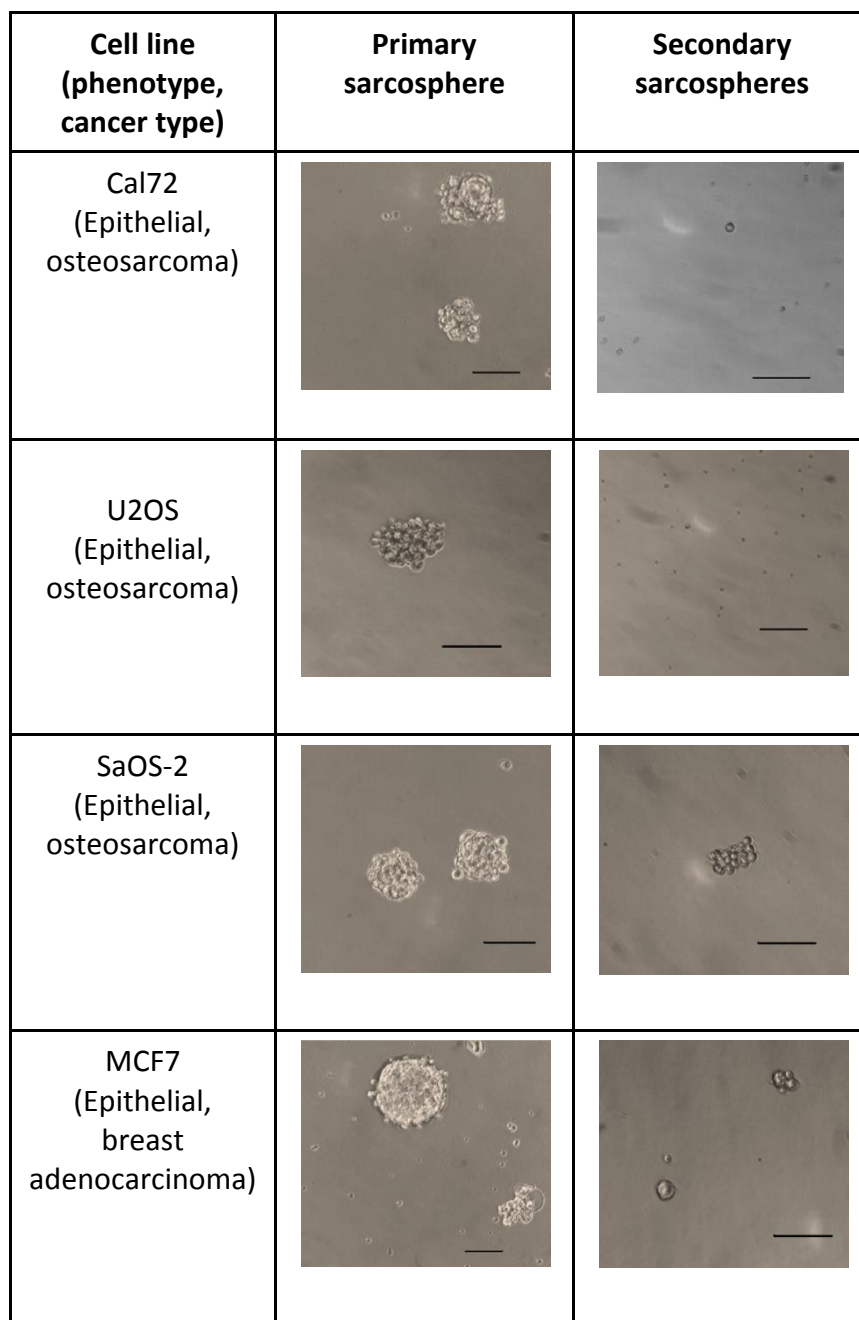
<b>Cell line (phenotype, cancer type)</b>	<b>Primary sarcospheres</b>	<b>Secondary sarcospheres</b>
143B (Mixed, osteosarcoma)		
HOS (Mixed, osteosarcoma)		
MNNG HOS (Mixed, osteosarcoma)		
G292 (Fibroblastic, osteosarcoma)		
MG63 (Fibroblastic osteosarcoma)		

Figure 3.19: Continued overleaf.

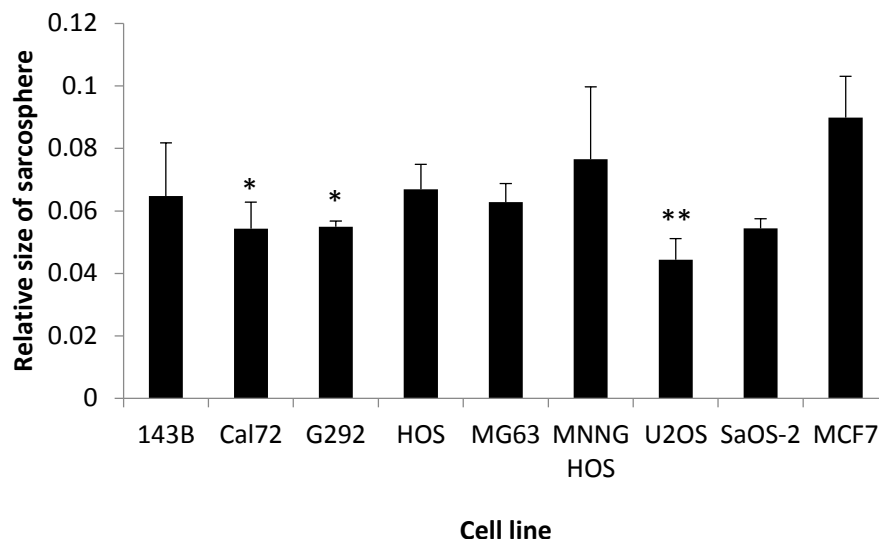


**Figure 3.19: Images of sarcospheres produced from OS cell lines and MCF7.** Primary sarcospheres grown for 7 days and secondary sarcosphere grown for a further 7 days post primary sarcosphere passage. Images representative of 12 images. Scale bar represents 100  $\mu$ M.

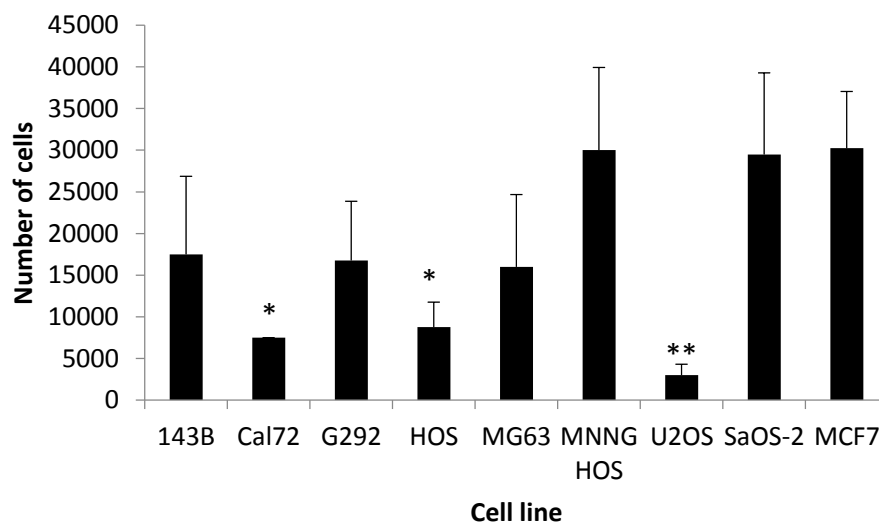
### 3.7.1 Evaluation of primary sarcosphere sizes in OS cell lines and MCF7

All cell lines tested were able to produce primary sarcospheres after the initial 7 days of growth and images were taken from four parts of each well, allowing sarcosphere size to be analysed (Section 2.2.4). Sarcosphere sizes present within each image could then be assessed using ImageJ. In addition during the passage of sarcospheres cell counts were made, making it possible to assess the number of living cells present within each cell line.

Comparison of primary spherical colony formation indicated that growth rates were variable across the cell lines. All cell lines were compared to one another and Cal72, G292 and U2OS produced significantly smaller colonies than MCF7 (Figure 3.20). When comparing the number of living cells present at this stage of the experiment U2OS had the lowest number of 3000 cells, which indicates that 70 % of the cells had died since seeding (Figure 3.21) and suggests that the majority of U2OS cells are undergoing cell death in response to the low-attachment conditions. All other cell lines had a significant increase in living cells when compared to U2OS. Although Cal72 and HOS had a significantly elevated number of cells compared to U2OS, they still contained less living cells than the 10000 seeded, suggesting they are also unsuited to the sarcosphere assay conditions. MNNG-HOS, SaOS-2 and MCF7 contained the most living cells with a total of 30000 cells (Figure 3.21).



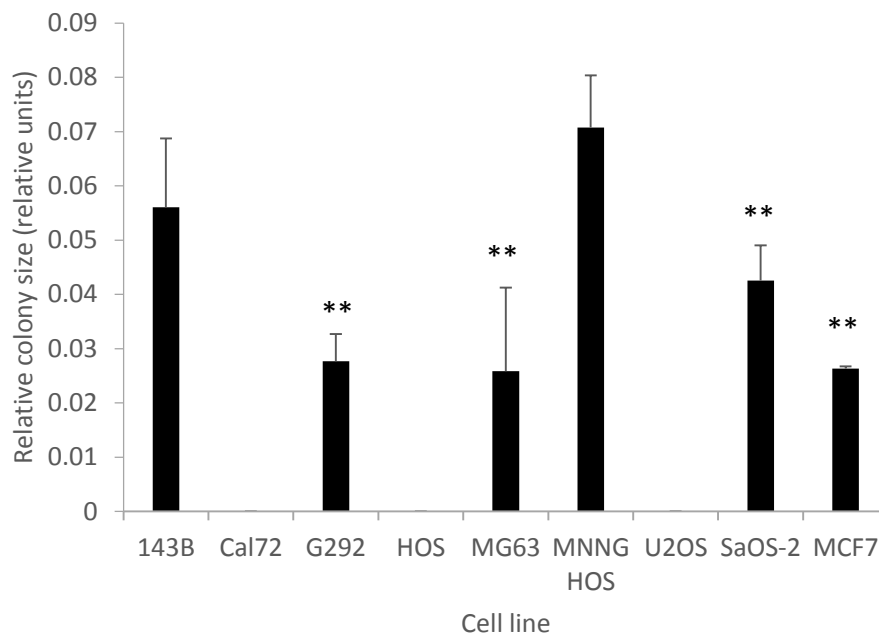
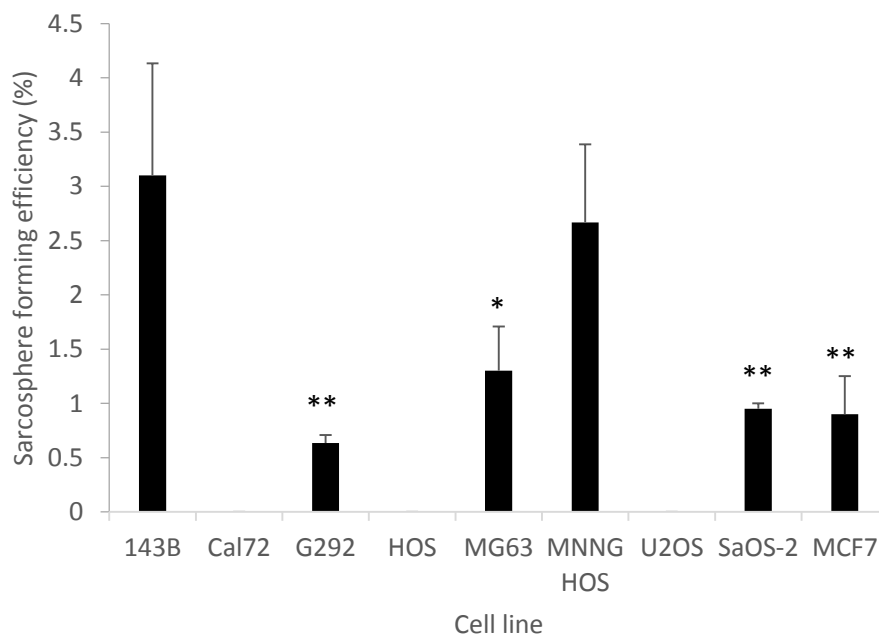
**Figure 3.20: Analysis of primary sarcosphere sizes in OS cell lines and MCF7.** Sarcosphere size assessed using ImageJ. Statistical significance calculated using Tukey's post hoc analysis, by comparing all samples to one another, Cal72, G292 and U2OS were found to be significantly different when compared to MCF7 (\*  $p < 0.05$ , \*\*  $p < 0.01$ ). Cell lines tested in triplicate and presented as mean and standard deviation.



**Figure 3.21: Analysis of number of cells present after passage of primary sarcospheres.** Statistical significance calculated using Tukey's post hoc analysis, all cell lines compared to one another, Cal72, HOS and U2OS contain significantly less cells than SaOS-2 and MCF7, U2OS also contains significantly less cells than MNNG-HOS (\*  $p < 0.05$ , \*\*  $p < 0.01$ ). Cell lines tested in triplicate and presented as mean and standard deviation.

### 3.7.2 Evaluation of secondary sarcospheres in OS cell lines and MCF7

After sarcospheres had been passaged and grown for a further 7 days (secondary sarcospheres), sarcosphere sizes were again analysed using ImageJ. In addition sarcosphere forming efficiency (SFE) was assessed using the equation outlined in the methods section (Section 2.2.4). Both SFE and colony size, although variable between cell lines, produced a similar result when comparing SFE (%) and colony size of the same cell line. Cal72, HOS and U2OS produced no spherical colonies, G292 produced the lowest SFE of 0.62 % and one of the lowest colony sizes of 0.27 (relative units) so was used for comparison with other cell lines to assess a statistical increase in colony formation (Figure 3.22.A). 143B and MNNG-HOS both had significantly larger colonies and enhanced SFE compared to G292, the remaining cell lines MG63, SaOS-2 and MCF7 had similar SFE of 1.3 %, 0.95 % and 0.9 % respectively (Figure 3.22.B).

**(A) Sarcosphere size****(B) Sarcosphere forming efficiency**

**Figure 3.22: Analysis of cell line relative sarcosphere sizes of and sarcosphere forming efficiency (SFE) of secondary sarcospheres.** A) Analysis of relative sarcosphere sizes, B) Analysis of SFE of secondary sarcospheres. Statistical significance calculated by using Tukey's post hoc analysis comparing all samples, G292, MG63, SaOS-2 and MCF7 were significantly smaller than 143B and MNNG-HOS (\* $p < 0.05$ , \*\* $p < 0.01$ ). All results repeated in triplicate and presented as mean and standard deviation.

### 3.7.3 Correlation of CSC marker expression with sarsosphere forming efficiency

Pearson's correlation coefficient was used to identify if the populations of cells expressing CSC markers analysed using flow cytometry (Section 3.2) correlated with increased spherical colony formation (Table 3.3). Analysis consisted of comparing either primary sarsosphere size against CSC marker expression or secondary sarsosphere forming efficiency compared to CSC marker expression. CD117 has been identified specifically as an OS CSC marker, therefore MCF7 was excluded from this analysis.

Primary sarsosphere forming ability correlated poorly with the expression of all CSC markers tested (ALDH, CD117 and CD44). CD44 expression when analysed as a sole marker produced a negative correlation of -0.66, CD44+/e-cad- cells produced a positive correlation of 0.67. CD117 had the closest relationship with formation of secondary sarsospheres, however this was a weak correlation of 0.58 (Table 3.3).

**Table 3.3: Pearson correlation coefficient analysis of primary or secondary spherical colony formation with CSC marker expression.** Cell lines included in analysis were 143B, Cal72, G292, HOS, MG63, MNNG-HOS, U2OS SaOS-2 and MCF7. Due to CD117 not being an established breast CSC marker, MCF7 was not included in CD117 analysis. No statistical significance was observed.

<b>Cancer stem cell marker</b>	<b>Primary sarsospheres</b>	<b>Secondary sarsospheres</b>
ALDH	0.10	-0.25
CD117	0.21	0.58
CD44	-0.66	0.40
CD44+ / e-cadherin+	0.67	-0.08
CD44+ / e-cadherin-	-0.08	0.44



### **3.8 Presence of ALDH and CD117 expressing cell within sarcosphere colonies**

To identify whether sarcospheres contained cells expressing OS CSC markers (ALDH and CD117) secondary sarcospheres from 143B were stained for these markers. 143B was selected because of the ability of this cell line to form robust sarcospheres. Cell membranes were identified using CD44 along with To-pro-3 for nuclei. The ALDH stain must be used on living cells so all sarcosphere staining procedures were conducted upon non-fixed cells.

#### **3.8.1 ALDH expression within 143B sarcosphere**

ALDH expressing cells were found within all sarcospheres analysed and the number of cells expressing ALDH increased in proportion with sarcosphere size. The smallest 143B sarcosphere analysed (Figure 3.23.1) contained several ALDH positive cells which were located mainly in the centre of the sarcosphere. The intermediate sized sarcosphere contained ALDH positive cells which were spread throughout the colony (Figure 3.23.2), whilst the sarcosphere largest in size contained regions either positive or negative for ALDH (Figure 3.23.3). The lower half of the largest sarcosphere contained the highest proportion of ALDH positive cells whilst the upper left side contained almost no ALDH positive cells, suggesting that ALDH cells may aggregate together as colonies grow larger.

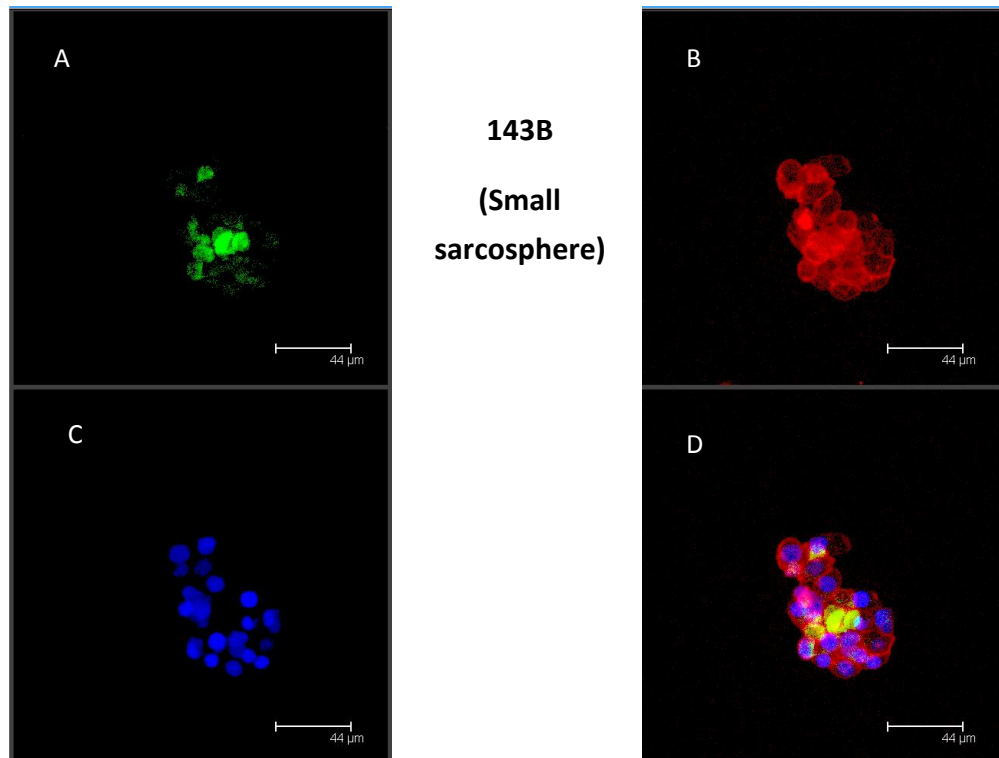


**Figure 3.23.1: Cells expressing ALDH within a small 143B sarcosphere.** Description below (3.22.3).

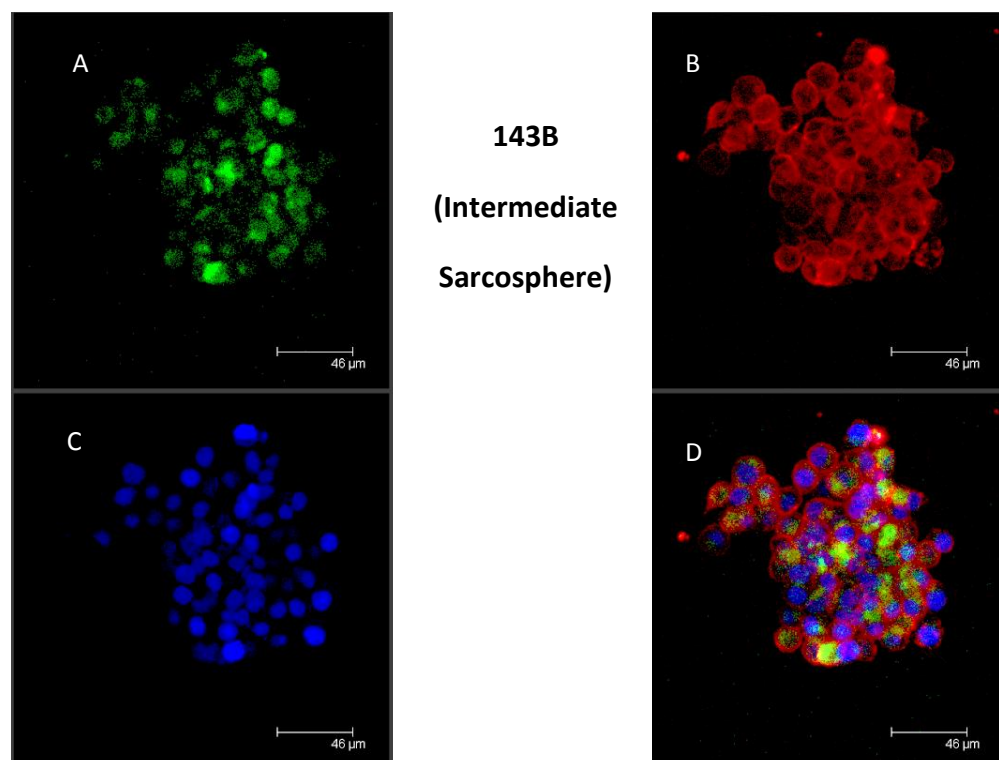


**Figure 3.23.2: Cells expressing ALDH within a intermediate sized 143B sarcosphere.** Description below (3.32.3).

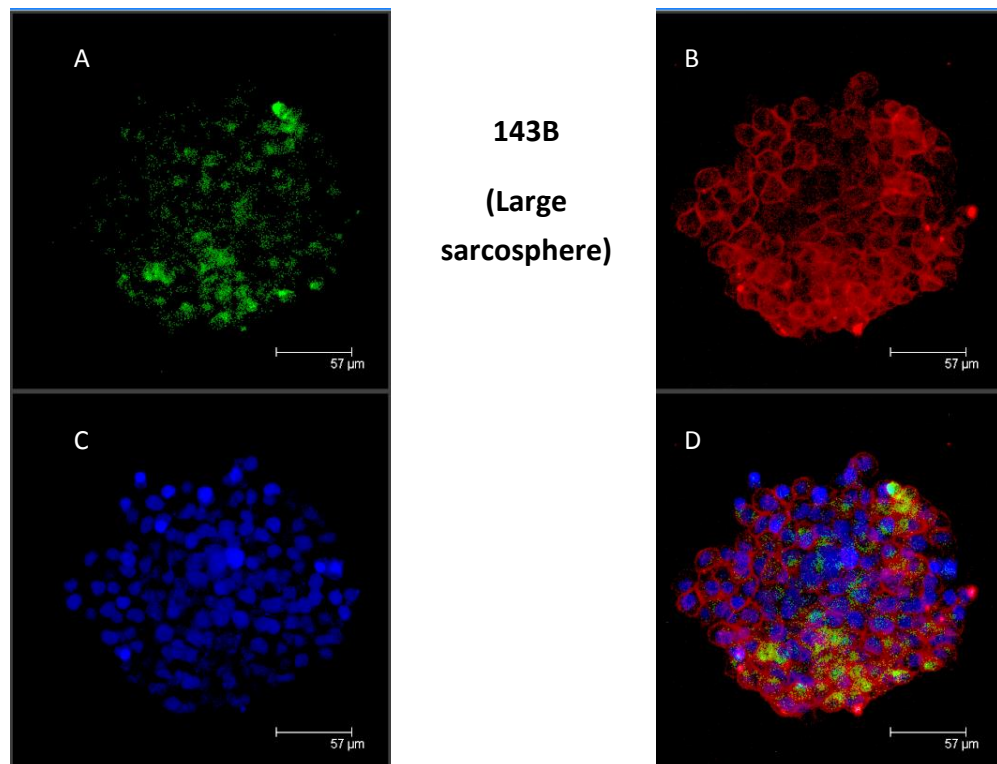


**Figure 3.23.3: Cells expressing ALDH within a large 143B sarcosphere.** Figures 3.30.(1,2 and 3) Demonstrated by dual-colour fluorescence, 143B sarcospheres were co-stained with to-pro-3 (blue nuclei), PE labelled CD44 antibody (red membrane) and ALDH using ALDEFUOR reagent (green). (A) ALDH expressing cells, (B) CD44 expressing cells, (C) nuclei and (D) overlay of all 3 markers. Each image representative of 2 images.

### 3.8.2 CD117 expression within 143B sarcosphere

143B sarcospheres were tested for the expression of the CSC marker CD117, when sarcospheres were co-stained with CD44 no cells CD117 cells were identified. To ensure that CD44 antibodies fluorescence were not masking the presence of CD117 positive cells, sarcospheres were tested without CD44. CD117 staining was identified in only two colonies, a single cell stained positively in a large colony (Figure 3.24.1) and the cell surface of a single cell in a small collection of cells (Figure 3.24.2) was also weakly stained for CD117. The rarity of CD117 cells sarcosphere is in stark contrast to monolayer 143B cells when analysed using flow cytometry contained a population of 6.4 % (Figure 3.7).

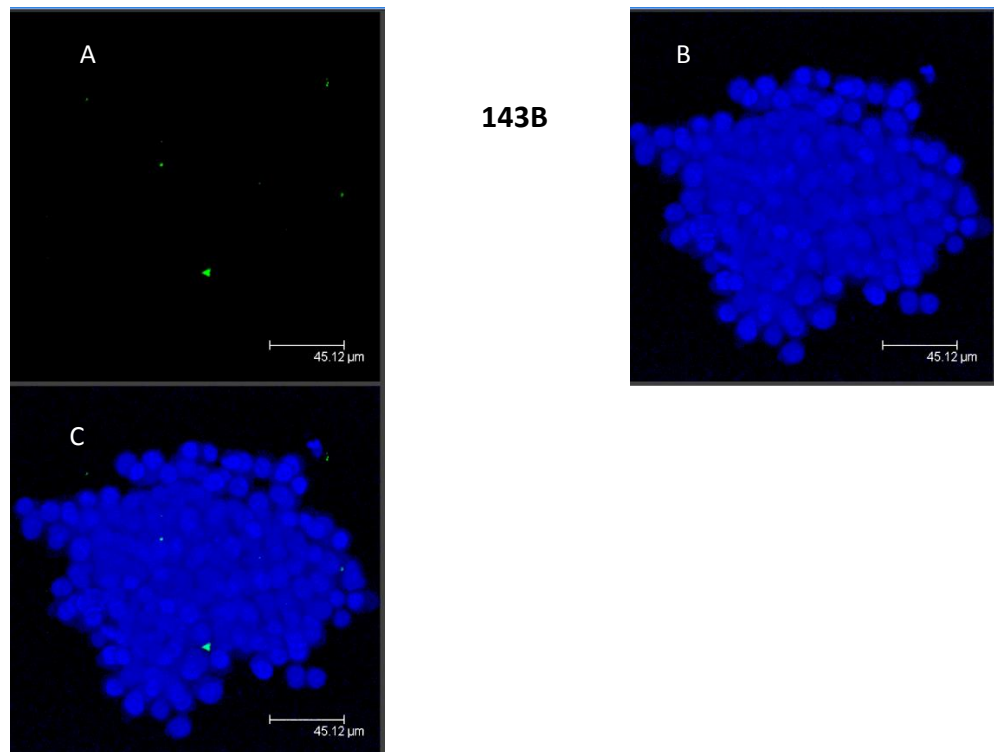


**Figure 3.24.1: Cells expressing CD117 within a 143B sarcosphere.** Description below 3.30.2.

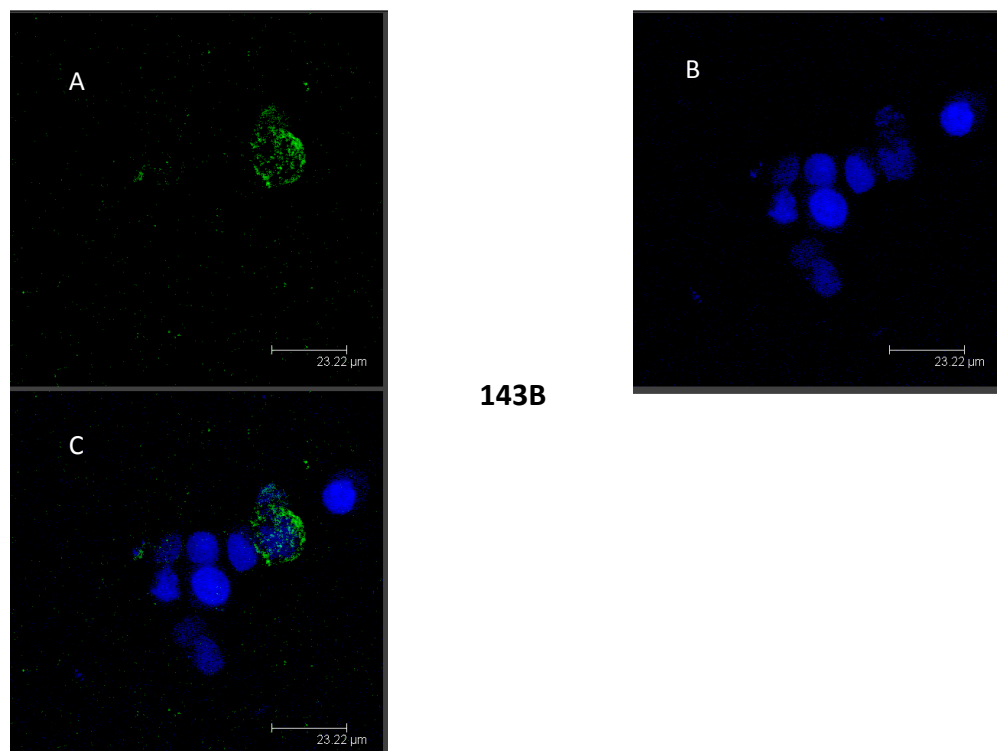


**Figure 3.24.2: Cells expressing CD117 within a 143B sarcosphere.** Demonstrated by dual-colour fluorescence, 143B sarcospheres were co-stained with to-pro-3 (blue nuclei) and FITC labelled CD117 antibody (green). (A) CD117 expressing cells, (B) nuclei and (C) overlay of the markers. Images representative of 1 image.

### 3.9 Discussion

CSC identification has been made possible through the isolation of cells expressing extracellular proteins such as CD44 (Al-Hajj et al., 2003), CD117 and the intracellular enzyme ALDH (Wang et al., 2011) (Section 1.2.2). Within breast carcinoma ALDH expressing cells have been found to have enhanced tumourigenic properties with the potential to self-renew and re-capitulate tumour heterogeneity (Ginestier et al., 2007). In this study ALDH was found to be heterogeneously expressed in OS cell lines (0.9 % – 61 %). The HOS cell line had 61 % of cells expressing ALDH and would therefore be predicted to have a high number of putative CSC and the greatest tumourigenic capabilities compared to other OS cell lines.

Although OS cells are notoriously difficult to grow via xenotransplantation and often fail to form tumours (Jia et al., 1999), HOS has been identified as non-tumourigenic in a mouse model, whereas 143B and MNNG-HOS were tumourigenic (Luu et al., 2005). This contradicts the predicted tumourigenicity of HOS based on ALDH expression, therefore, ALDH expression may not represent a CSC marker in OS. In breast cancer cell lines selecting ALDH expressing cells does not universally select for cells with enhanced clonogenicity (Hwang-Verslues et al., 2009). In melanoma ALDH positive and negative cells had an equal ability to form spherical colonies and xenograftable tumours. Interestingly ALDH negative cells could only self-renew, whilst ALDH positive cells could differentiate in to ALDH negative and recapitulate the original ALDH expression profile (Prasmickaite et al., 2010). Although the ability of a CSC to recapitulate the original tumour heterogeneity is a fundamental CSC property (1.2.1), melanoma mouse models now suggest that most tumourigenic CSC populations are only able to self-renew (Held et al., 2010).

The tyrosine kinase receptor CD117, has previously been found to be an OS CSC marker (Adhikari et al., 2010) and associated with a poor chemotherapy response (Miiji et al., 2011). Analysis of CD117 in the OS cell lines demonstrated that it was heterogeneously expressed. The majority of cell lines (G292, MNNG-HOS, U2OS and SaOS-2), all contained populations below 0.02 % and, due to the extremely small size of these populations it is possible that they are in fact just an artefact of cellular background fluorescence or non-specific antibody

binding. U2OS was found to have one of the smallest CD117 populations of 0.008 %, which is smaller than the 0.6 % observed by Tang *et al.*, (2011). Their study used a different CD117 detection method and co-stained with the mesenchymal marker STRO-1, which could account for the discrepancy between findings. MG63 was the only OS cell line with no CD117 expression. In contrast to MG63, 143B contained a significantly larger population of CD117 cells than all other cell lines. HOS contained the second largest CD117 population, interestingly 143B is derived from the HOS cell line via Ki-ras<sup>+</sup> transformation (Hensler *et al.*, 1994), which has thus resulted in the up-regulation of CD117.

Carcinomas with increased expression of the adhesion protein CD44 have been shown to comprise CSC with enhanced clonogenicity (Harper *et al.*, 2010). OS formation occurs in a genetically manipulated mouse model (APC<sup>+/min</sup> and P53<sup>+/tm1</sup>), in which the tumour suppressors APC and P53 are mutated. Knockout of CD44 in this mouse model did not affect tumour formation but did reduce OS metastasis when tested in a small sample of mice (24 mice) (Weber *et al.*, 2002). The reliance of cancer upon CD44 for migration is supported by the finding that a bi-specific anti-CD44 antibody reduced tumour growth and metastasis of the B cell lymphoma cell line 38C-13 in NOD/SCID mice (Avin *et al.*, 2004). Due to the importance of CD44 for non-malignant cellular functions (Camp *et al.*, 1993), bi-specific CD44 antibodies which also target tumour specific tumour antigens are important to circumvent any impact upon healthy cells. In this study the expression of CD44 across all OS cell lines was high with CD44 expressing cells ranging from 69 % (U2OS) to 99 % (SaOS). The high levels of CD44 indicate that the OS cell lines tested would have a propensity to migrate and metastasise, additionally, MSC also highly express CD44 (Lee *et al.*, 2004), therefore, the similar expression level of OS and MSC could indicate that OS arises from an MSC progenitor. The high expression of CD44 in cell lines is consistent with the findings in the literature, in which a high proportion of U2OS, MG63 and SaOS-2 cells were found to express CD44 when analysed using flow cytometry (Gillette *et al.*, 2004, Tirino and Desiderio, 2008). In contrast MCF7 had a significantly lower expression of CD44 (4.9 %), this small population may include an MCF7 population with enhanced tumourigenic properties. MCF7 CD44 expressing cells have been shown to have an increased tumourigenicity and migrative capabilities (Yan *et al.*, 2013), in addition, oncogene transformed human mammary epithelial cells and the breast cancer cell line MCF10A, contain a population of

cells with a mesenchymal phenotype and express CD44<sup>+</sup> (Morel et al., 2008). Therefore, the expression of CD44 in breast cancer, may be associated with the acquisition of a mesenchymal phenotype as malignant cells undergo EMT and acquire the ability to metastasise.

In addition to CD44, cells were simultaneously stained for the cell to cell adhesion protein e-cadherin (e-cad). E-cad has been used as a marker to identify cells with an epithelial phenotype and decreased expression has been linked to increased cancer aggressiveness (Siitonen et al., 1996). In all OS cell lines expression of e-cad was low or in the case of U2OS absent. In contrast the breast cancer cell line contained a large population of e-cad expressing cells (66.9 %). E-cad is expressed by epithelial cells (Damsky et al., 1983) and loss of this protein is associated with the acquisition of a mesenchymal phenotype (von Schlippe et al., 2000) (Section 1.2.5). Therefore, e-cad expression in MCF7 confirms the epithelial phenotype of this cell line and conversely its absence in OS cell lines is further evidence of their mesenchymal phenotype. Cell lines were also analysed for the mesenchymal marker vimentin (vim), all OS cell lines highly expressed the protein with over 90% of the population expressing this marker. This is consistent with a study staining SaOS-2 which found that this cell line highly express vim (Veselska et al., 2008). Interestingly OS cell lines with an epithelial morphology (Cal72 and SaOS-2) all highly expressed vim with SaOS-2 containing a larger population than the fibroblastic cell lines (G292 and MG63). Therefore OS cells with an epithelial morphology may have elevated expression of mesenchymal markers compared to the fibroblastic cells types. Vim is a marker associated with mesenchymal stem cells (Potapova et al., 2004), the high expression of vim in the OS cells lines is further suggestive evidence that they originate from a mesenchymal stem cell (MSC) progenitor. MSC have been identified as the cellular origin of alternative sarcomas such as Ewings's sarcoma (Riggi et al., 2005). Due to the potential of OS tumours to demonstrate multi-lineage differentiation (adipocyte, chondrocyte and osteoblast) (Klein and Siegal, 2006) the cellular origin of OS has been hypothesised as MSC (Tang et al., 2008), however no conclusive evidence is currently available. Human MSC have been found to initiate *in vivo* OS like tumours when genetically transformed with telomerase, simian virus 40 large T antigen and H-Ras. Although these tumours replicated the complex genomic rearrangements of OS they were devoid of bone matrix and failed to invade cortical bone,

which was possibly due to the genetic alterations used to manipulate the MSC (Li et al., 2009). Published data has found MCF7 cells to be negative for vim expression (Uchino et al., 2010), in this study MCF7 cells were found to contain a small population of vim expressing cells (0.15 %). This may represent a true population of vim positive cells, however the low expression level could also be attributed to non-specific antibody binding or due to Uchino *et al* (2010) using microscopy to analyse immunofluorescence.

To analyse the epithelial or mesenchymal characteristics of the CD44 populations, each cell line was co-stained for CD44 along with either e-cad or vim. Using this technique four different populations were identified. Using e-cad as an example, the populations included cells positive for both markers (CD44<sup>+</sup>/e-cad<sup>+</sup>), a population positive for CD44 only (CD44<sup>+</sup>/e-cad<sup>-</sup>), cells expressing e-cad only (CD44<sup>-</sup>/e-cad<sup>+</sup>) and negative for both markers (CD44<sup>-</sup>/e-cad<sup>-</sup>). The phenotype CD44<sup>-</sup>/e-cad<sup>+</sup> were rare in OS and observed in only Cal72, HOS and MNNG-HOS. This result was in contrast to MCF7 which contained 31 % of cells expressing e-cad (CD44<sup>-</sup>/e-cad<sup>+</sup>) and the largest population (3.8 %) of CD44<sup>+</sup>/e-cad<sup>+</sup> expressing cells. This is consistent with published data, where a large proportion (40 %) of MCF7 cells have been found to express e-cad (Vermeulen et al., 1995). Interestingly OS cells expressing e-cad were found mainly in the CD44 population, apart from G292 these CD44<sup>+</sup>/e-cad<sup>+</sup> expressing cells were rare comprising only 0.1 % – 0.5 % of cells. This phenotype could represent a more proliferative and less migratory CSC population than CD44<sup>+</sup>/e-cad<sup>-</sup> cells. Work carried out in squamous cell carcinoma found that there were in fact two separate CSC phenotypes present. One is migratory and associated with CD44 expression and reduced epithelial marker expression, the other is highly proliferative and associated with expression of CD44 and epithelial markers such as e-cad (Biddle et al., 2011). However, further tests will be required to confirm this in the migratory and proliferative properties of CD44<sup>+</sup>/e-cad<sup>+</sup> and CD44<sup>+</sup>/e-cad<sup>-</sup> cells.

The majority of OS CD44 cells also expressed vim (CD44<sup>+</sup>/vim<sup>+</sup>), OS cell lines contained a CD44<sup>+</sup>/vim<sup>+</sup> population between 91 – 99 %. Vim has been found to be up-regulated in primary OS compared to benign bone tumours (Li et al., 2010) and in breast cancer enhanced vim expression was found to correlate with enhanced occurrence of metastasis (Domagala et al., 1994). In addition sarcomas lacking CD44 are unable to metastasise



(Weber et al., 2002), therefore this population of CD44<sup>+</sup>/vim<sup>+</sup> could be hypothesised to have enhanced migratory capabilities to all other CD44/vim phenotypes.

The presence of the colony hierarchies within cell lines is further putative evidence of the presence of CSC. Holoclones have been found to contain CSC (Li et al., 2008) and were identified within all the cell lines along with meroclones which comprise an amplifying population of cells and the terminally differentiated paraclones. The OS holoclones displayed the classic densely packed arrangement of cells and excluding MG63 and Cal72 all holoclones were circular or oval in shape. Cal72 displayed more of an angular holoclone which was more rectangular in shape, whilst MG63 did display rectangular holoclones it also contained a unique holoclonal shape which contained pointed projections, making it form a star like shape. This unique MG63 holoclone still fulfilled all the holoclone criteria; tightly packed cells of a uniform size with a smooth layer of cells surrounding the colony (Locke et al., 2005). The paraclones formed by the OS cell lines were often composed of cells which were often highly dispersed and each cell would often independently migrate. This was especially true of the fibroblastic (MG63 and G292) and mixed (143B and HOS) OS cells lines, and suggests that these cell lines may be more prone to migration due to the ability of these cells to rapidly detach from one another and travel large distances apart. It has been shown that 143B which has a mixed morphology is able to migrate 2.7 times faster than the epithelial SaOS-2 (Rainusso et al., 2011), suggesting that OS cell lines containing fibroblastic cells may have enhanced migratory abilities. *In vitro* the OS cell lines are categorised in to either epithelial, fibroblastic or a mixture of both cell types, however, whether this morphology has any clinical relevance is unclear. Epithelioid osteosarcomas do occur and are characterised by poorly differentiated cancers, which demonstrate characteristics of carcinomas such as gland formation (Klein and Siegal, 2006), however, it has not been specified whether cell lines with a epithelial morphology were initiated from epithelioid OS tumours (Rochet et al., 1999). In carcinoma the acquisition of a fibroblastic morphology is indicative of a cancer cell undergoing EMT (Mani et al., 2008), an opposing process may occur in OS in which cells acquire an epithelial phenotype. In a case study of one epithelial OS tumour, OS cells were found to acquire an epithelial phenotype, which was attributed to tumour progression and increased intra-tumour heterogeneity (Kramer et al., 1993).

The presence of cells expressing the putative CSC markers (ALDH, CD117 and CD44) in the colony hierarchies were identified using confocal microscopy when cells were grown at low density. OS cell lines, which according to flow cytometry express high levels of ALDH ( $\geq 10\%$ ), were found to contain ALDH expressing cells not only in the holoclones. This contradicts the hypothesis that ALDH and holoclones represent the CSC populations. In G292, HOS and 143B the ALDH expressing cells were present in all the colony hierarchies. These highly expressing ALDH cell lines often contained clusters of cells all positioned adjacent to one another with high ALDH expression. Wang et al., (2011) found that the morphologically uncharacterised OS cell line OS99-1 contained a large population of ALDH expressing cells (45 %) and was able to form xenograftable tumours. However, the presence of ALDH positive cells in all hierarchies suggests either that ALDH or the colony hierarchies are not CSC identification methods in these highly expressing OS cell lines. Alternatively it is possible that ALDH expression is a dynamic state with cells switching between two phenotypes. Although a rare event, melanoma ALDH<sup>-</sup> cells taken from primary tumours, have been found to differentiate in to ALDH<sup>+</sup> cells when transplanted in to NOD/SCID mice (Prasmickaite et al., 2010).

In 143B, G292, MG63 and SaOS-2 holoclones were present which lacked the presence of any ALDH positive cells. These holoclones could represent the evolution of a holoclone to a meroclone, whereby cells go through a phase of transient amplification. Whether OS ALDH expressing cells initiate holoclone formation is unknown, the prostate cancer cell line PC3 is able to produce holoclones and the colony hierarchy replicates that observed by Locke *et al* (2005). However, PC3 cells either ALDH<sup>+</sup> or ALDH<sup>-</sup> can give rise to holoclones and ALDH expression could be switched on and off. Interestingly paraclones were found to contain the largest proportion of ALDH expressing cells with holoclones containing predominantly ALDH low expressing cells. It was hypothesised that although ALDH expressing cells have enhanced clonogenicity, ALDH expression may be transiently switched on and off accounting for ALDH<sup>-</sup> cells giving rise to ALDH<sup>+</sup> cells. In addition the high expression in paraclones may be unrelated to self-renewal, suggesting that based on proliferation two populations of ALDH expressing cells may be present (Doherty et al., 2011). The lack of ALDH expression in holoclones within all OS cell lines indicates that a

similar pattern of transient ALDH expression may also be occurring, therefore further research is required to investigate the ability of OS ALDH<sup>-</sup> cells to form holoclones.

Analysis of CD117 expression within the colony hierarchies at low density proved challenging, even 143B with the largest CD117 positive population (according to flow cytometry) contained very few CD117 expressing cells. When CD117 positive cells were identified the expression level was very low and it was restricted to cells from very small holoclones and small patches within large meroclones. A contrasting expression profile was observed when 143B was grown to a higher confluency (80%), at these higher cell densities CD117 expression was increased and could be identified throughout a colony but localised to small sites upon each cell membrane. This increase in CD117 expression suggests that cell density may play a role in protein expression. It has been found that high grade primary OS tumours which express CD117 have staining within a large number of cells throughout the tumour samples. In clinical samples of 20 OS tumours that were tested for CD117, expression ranged from 5% – 90% (Sulzbacher et al., 2007), which is much greater than the 0.075 – 6.36% observed in OS cell lines when tested at 70 – 90% confluency. Therefore, *in vitro* cell culture conditions may lead to a down-regulation of CD117, whereas the tumour environment may provide appropriate signals to enhance CD117 expression. The lack of this environment when growing cells *in vitro* could explain the rarity of these cells observed during confocal microscopy analysis. In order to identify if tumour environment does affect CD117 expression, the assessment of CD117 expression from tumours formed from OS cell lines *in vivo* would be an important experiment.

Colony hierarchies were also co-stained for CD44 and e-cad, these CD44<sup>+</sup>/e-cad<sup>+</sup> cells proved to be rare and were only identified in G292 colonies. According to flow cytometry analysis G292 contains the largest CD44<sup>+</sup>/e-cad<sup>+</sup> population, however, the lack of these cells in other OS cell lines suggests their presence may be affected by either the low cell density required for identification of the colony hierarchies or the fixation required for antibody staining. For cell fixation an optimum concentration for paraformaldehyde is recommended at 0.5 – 1% (Van Ewijk et al., 1980). Although 4% paraformaldehyde has been reported as a cell fixative of breast cancer and OS cell lines with no adverse effect on protein structure (Chambon et al., 2003, Fawdar, 2010). It is possible that the 4% used

within this study is damaging the CD44 and e-cad proteins which is attributing to the lack of cells positive for these markers.

OS holoclones have been identified as highly proliferative whereas paraclones will divide several times before undergoing cell death (Fawdar, 2010). G292, CD44<sup>+</sup>/e-cad<sup>+</sup> cells were found within large merclones and paraclonal colonies, suggesting it does not represent a CSC marker. The level of e-cad expression from both of these cell types was very low and contained one positive cell within each colony hierarchy. MCF7 cells produced heterogenous staining for CD44 and e-cad. MCF7 cells CD44<sup>+</sup>/e-cad<sup>+</sup> positive were found within holoclonal colonies, whilst CD44<sup>+</sup>/e-cad<sup>-</sup> cells were associated with paraclonal colonies. Cells expressing high levels of CD44 (CD44<sup>high</sup>) and low levels of CD24 (CD24<sup>low</sup>) have been identified as breast CSC (Al-Hajj et al., 2003). Further characterisation of these breast cancer CD44<sup>high</sup>/CD24<sup>low</sup> cells found they expressed low levels of e-cad and had undergone EMT (Mani et al., 2008). The presence of CD44<sup>+</sup>/e-cad<sup>-</sup> cells within paraclones is putative evidence that breast CSC which have undergone EMT have a paraclonal morphology. This finding contradicts the clonal hierarchy, however it is plausible if EMT CSC do exist *in vitro* they must acquire an ability to migrate. A migrating CSC must be detach itself from a colony which is indicative of a paraclone morphology.

Neuronal cells with the ability to form spherical colonies in low attachment serum starved conditions have been identified as multipotent stem cells (Reynolds et al., 1992). In general the appearance of OS sarcospheres is not a classic spherical colony as was produced in MCF7. Mammospheres are frequently spherical in shape with a smooth appearance, in contrast sarcospheres were irregular in shape and individual cells could be clearly defined. Primary sarcospheres were present in all cell lines, whereas secondary sarcospheres could not be grown in Cal72, HOS or U2OS. It has been found that mammospheres can be passaged only 5 times before growth was inhibited. This inhibition was attributed due to an increase in cell senescence (Dey et al., 2009). All OS cell lines had smaller sized secondary sarcospheres compared to primary sarcospheres, therefore, a senescence mechanism could also be occurring in OS cell lines but at a significantly quicker rate in Cal72, HOS and U2OS. 143B and MNNG-HOS both had a significantly greater sarcosphere forming efficiency and size than all other cell lines, which has been replicated in published data (Rainusso et

al., 2011). Rainusso *et al* 2011, found that 143B and MNNG-HOS produced significantly larger sarcospheres than MG63, SaOS-2 and U2OS. 143B and MNNG-HOS are both derived from the HOS cell line and have been transformed using N-methyl-N'-nitro-N-nitrosoguanidine (MNNG-HOS) and Ki-ras for 143B. These transformed cell lines were found to be highly tumourigenic and metastatic when grown within a mouse model, in contrast HOS was unable to form tumours (Luu et al., 2005). The ability of 143B and MNNG-HOS increased tumourigenicity and sarcosphere forming ability suggests that these cell lines harbour a larger population of CSC.

To identify whether CSC marker expression correlated with sarcosphere forming ability Pearson's correlation coefficient analysis was used. This analysis produced the strongest positive correlation (0.67) when correlating CD44<sup>+</sup>/e-cad<sup>+</sup> expression with primary sarcosphere size. However, cells CD44<sup>+</sup>/e-cad<sup>+</sup> correlated poorly with secondary sarcosphere size (-0.08), in which CD117 expression had the strongest correlation (0.58). CD117 has been demonstrated to be an OS CSC marker (Adhikari et al., 2010), therefore OS CD117 expressing cells may have enhanced sarcosphere forming abilities. Although the lack of a statistically significant correlation between these two factors makes this conclusion questionable.

Sarcospheres were stained for the presence of cells expressing CD44, ALDH and CD117 using confocal microscopy. All sarcospheres tested expressed CD44 on the membrane of all cells so was used to define cell membranes. ALDH positive cells were present within all sarcospheres tested, the number of cells expressing ALDH was found to increase as colonies grew larger. ALDH expressing MG63 cells are able to survive anoikis and have a higher sarcosphere forming ability than ALDH negative cells (Honoki et al., 2010), therefore, a CSC which is able to generate more ALDH expressing cells will be able to grow in to a larger sarcosphere. In the largest sarcosphere observed highly expressing ALDH cells were found to cluster in groups, CSC have been found to reside within a tumour niche which provides appropriate signals to maintain a stem cell phenotype (Iwasaki and Suda, 2009). It could be possible that as a sarcosphere grows larger the ALDH expressing cells cluster together and form a niche in order to maintain their ALDH positive phenotype.

As was observed with OS cells grown as a monolayer, CD117 cells in sarcospheres were very rare and not present within the majority of sarcospheres. CD117 has been identified as an OS CSC marker (Adhikari et al., 2010) and OS CSC have an enhanced ability to form sarcospheres (Rainusso et al., 2011). Therefore, the lack of CD117 expressing cells within the sarcospheres suggests that it may not be expressed by OS CSC within the panel of cell lines tested. CD117 has been found to be expressed in 20 % of OS cancers and over expression of CD117 has no impact on prognosis (Sulzbacher et al., 2007). This finding suggests that the use of CD117 as a CSC marker may be restricted to a small subset of OS tumours which are not included in the cell lines analysed within this study.

In order to further characterise OS cell lines for the presence of putative CSC, each cell line has been screened for the ability to form the colony hierarchies, expression of putative CSC markers, epithelial and mesenchymal markers and the ability to form sarcospheres in low attachment conditions. This study has demonstrated that the colony hierarchies identified by Locke *et al* (2005) are also replicated in all the OS cell lines tested, in contrast putative OS CSC markers (ALDH and CD117) are heterogeneously expressed across the cell lines. The expression of these markers did not correlate with an enhanced ability to form sarcospheres, suggesting that cells expressing these proteins are not CSC. This finding is supported by cells highly expressing ALDH (> 10 % subpopulation), containing ALDH positive cells within paraclones and meroclones. In addition holoclones were identified which lacked ALDH expressing cells, indicating that ALDH expression may be transient and could potentially be switched on and off as has been observed in the prostate cancer cell line PC3 (Doherty et al., 2011). Clinical OS tumours have a higher level of CD117 expression when compared to the cell lines tested in this study, an increase in CD117 expression was observed when increasing cell density *in vitro* therefore the tumour microenvironment may increase CD117 expression. The carcinoma CSC marker CD44 was highly expressed in all OS cell lines in addition to the mesenchymal marker vimentin, both markers are also highly expressed in mesenchymal stem cells, highlighting the mesenchymal phenotype of OS cells *in vitro*. Furthermore a population of CD44<sup>+</sup>/e-cad<sup>-</sup> cells were identified which produced a positive correlation with primary sarcosphere forming ability. This suggests that this population may be enriched in CSC, however, further evidence is required to confirm the tumourigenicity of these cells.

# **Chapter 4**

## **The role of putative osteosarcoma cancer stem cells in chemotherapy resistance**

## 4.1 Introduction

In the last 30 years improvements have been made in the treatment and management of OS tumours. Despite the toxic nature of chemotherapeutics they form the core therapeutics of any OS treatment strategy. A standard treatment program utilises the DNA intercalating agents cisplatin and doxorubicin with either the dihydrofolate reductase antagonist methotrexate, alkylating agent ifosfamide or the topoisomerase inhibitor etoposide (Anninga et al., 2011) (Section 1.3). In addition to chemotherapy, surgery also provides an invaluable tool for improving relapse free survival. It has been reported that 36 % of patients who had surgical removal of metastatic OS tumours were relapse free after 3 years, compared to 0 % of patients who did not have surgery (Ferrari et al., 2003). The poor survival rate of metastatic OS is often due to the chemo-resistant nature of secondary tumours (Yen, 2009), which is highlighted by prognoses being largely based upon pre-operative response to chemotherapy (Bielack et al., 2002).

The platinum based chemotherapeutics which include cisplatin (cis), were discovered by accident 40 years ago when platinum electrodes were being used to subject cells to electromagnetic radiation (Rosenberg et al., 1965). The products identified were used to treat sarcoma growth within mice, which resulted in marked tumour regression (Rosenberg and Vancamp, 1969). The mechanism by which OS resists the toxic effect of chemotherapeutics varies depending upon the mode of action. Platinum based chemotherapeutics cause cell apoptosis upon intracellular activation, they covalently bind to purine DNA bases forming DNA adducts resulting in the activation of a number of signal transduction pathways including DNA repair, cell cycle arrest and apoptosis (Kelland, 2007). Some cancers are intrinsically resistant to cis (Perego et al., 1999) due to a number of different mechanisms including reduced membrane permeability (Santini et al., 2001), mutated P53 (Martelli et al., 2007) and loss of DNA mismatch repair proteins (Perego et al., 1999) (Section 1.3.2).

The dihydrofolate reductase (DHFR) inhibitor methotrexate (MTX) was one of the earliest chemotherapeutic agents to be identified as a result of work carried out by Sidney Farber, who initially trialed folic acid as a possible leukaemic treatment. This led to an acceleration of disease progression and the first realisation that a folic acid antagonist may be of use,



the subsequent use of MTX led to temporary leukaemia remission (Farber et al., 1948). Resistance to MTX can occur via different mechanisms, which include acquisition of enhanced DHFR expression or decreased expression of folate acid receptors, which reduces the ability of MTX to enter the cell (Guo et al., 1999) (Section 1.3.4).

Doxorubicin (dox) represents the anthracycline class of chemotherapeutics which is commonly used to treat OS (Singal and Iliskovic, 1998). Anthracyclines have the widest spectrum of activity against human cancers, only a few tumour types are unresponsive (Weiss, 1992). Dox intercalates with the DNA, however the mechanism by which it evokes cell death is debatable. Resistance to dox has been observed in cells with the loss of the cell cycle regulator P53 or enhanced expression of the protein Bcl2 which forms Bcl2-Bax homodimers. This stabilisation of Bax increased apoptosis through Bax induced cytochrome c release in to the cytoplasm (Zhao et al., 2009) (Section 1.3.1).

In breast cancer CSC pose a specific therapeutic challenge based on their enhanced resistance to chemotherapy allowing tumours to re-grow even when the majority of differentiated cells are removed (Gong et al., 2010) (Section 1.3.4). Putative CSC within OS cell lines have been found to have an enhanced cisplatin and doxorubicin resistance (Honoki et al., 2010). These cells had elevated expression of ALDH, which was suggested as a mechanism for the observed resistance due to due to the detoxification capabilities of ALDH (Honoki et al., 2010). OS cells expressing the CSC marker CD117 have also been found to have enhanced doxorubicin resistance due to drug efflux through enhanced expression of ATP binding cassette transporters (Adhikari et al., 2010). The elevated resistance of OS CSC to chemotherapeutics therefore represents a possible mechanism of enriching a CSC population. In breast cancer this has been found to occur during patient chemotherapy programs, in which CSC are enriched within tumours post chemotherapy treatment (Creighton et al., 2009). *In vitro* data now suggests that OS putative CSC can also be enriched using MTX in the U2OS cell line (Tang et al., 2011). This approach provides a method for isolating CSC without having to sort cells based on the expression of specific markers thus enabling the phenotype of drug resistant cells to be characterised within a heterogenous population of cells.

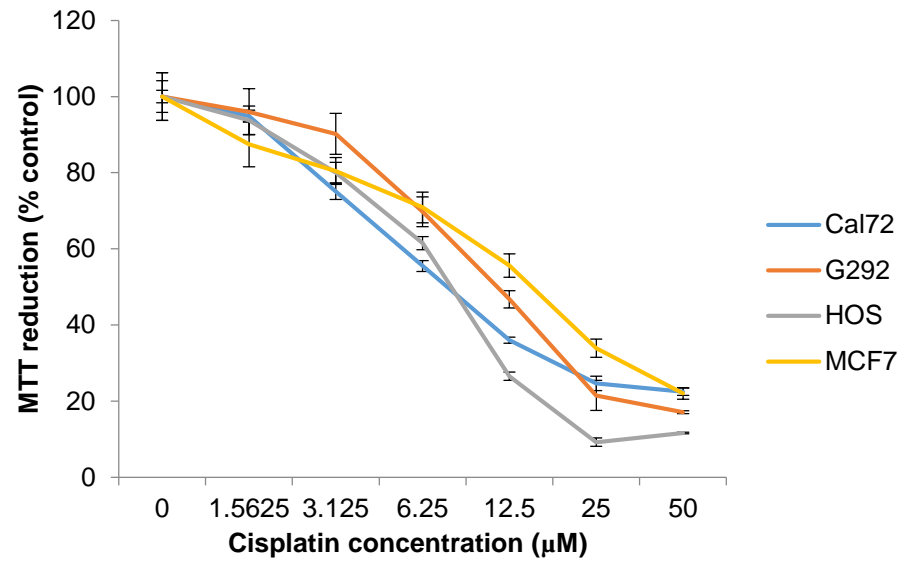
## Aims

To test the sensitivity of a range of OS cell lines to three chemotherapeutics (cisplatin, doxorubicin and methotrexate). Based on the median lethal doses ( $LD_{50}$ ) of each cell line, a short exposure to the chemotherapeutic will be used to enrich a drug resistant population of cells. The expression of CSC markers, clonogenicity and stem cell properties will be tested in the drug treated populations. The contribution of ALDH to chemo-resistance in the OS cell lines will be assessed using the ALDH inhibitor diethylaminobenzaldehyde (DEAB). The specific objectives which will be tested on a panel of OS cell lines and MCF7 are as follows:

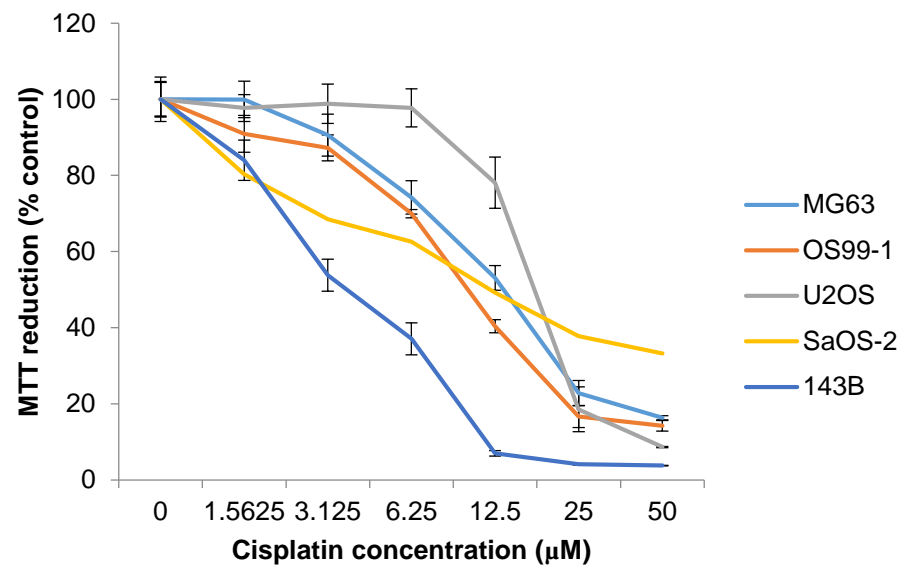
- Establish the  $LD_{50}$  for cisplatin, doxorubicin and methotrexate.
- Select a population of drug treated cells using methotrexate, cisplatin and doxorubicin at sub-lethal doses.
- Analyse the expression of OS CSC markers (ALDH and CD117) in drug treated cells.
- Test the growth rates of methotrexate treated cells.
- Test the sarcosphere forming efficiency of MG63 methotrexate treated cells.
- Establish the  $LD_{50}$  of the ALDH inhibitor diethylaminobenzaldehyde (DEAB)
- Analyse if DEAB exposure enhances chemotherapeutic sensitivity of selected cell lines in response to methotrexate, cisplatin and doxorubicin.

## 4.2 Chemotherapy sensitivity of OS cell lines and MCF7

Commonly used OS treatment regimes incorporate the chemotherapeutics cis, dox and MTX (Anninga et al., 2011) (Section 1.3). To analyse the sensitivity to these chemotherapeutic agents, cell lines were grown in increasing concentrations of the drugs and cell viability assessed using an MTT assay (Section 2.3.1). Cis and dox were exposed to cells for two days, MTX which took longer for cell death to be observed was exposed for five days. In order to establish the median lethal dose ( $LD_{50}$ ) for a chemotherapeutic agent, linear regression analysis of each dose response curve was used to identify the drug concentration which killed 50 % of cells (Table 4.1). All cell lines exhibited varying sensitivities to the chemotherapeutic agents (Figure 4.1. A, B, C, D, E and F), in response to cisplatin (Figure 4.1B). U2OS demonstrated the greatest resistance to cis with the highest  $LD_{50}$  of 18  $\mu\text{M}$  and 143B the lowest (0.38  $\mu\text{M}$ ) (Figure 4.1B). Cell lines with the greatest  $LD_{50}$  to doxorubicin (Figure 4.1 C and D) did not correlate with the highest  $LD_{50}$  for cisplatin. For example MG63 had the largest dox  $LD_{50}$  of 0.76  $\mu\text{M}$  and SaOS-2 with the lowest of 0.15  $\mu\text{M}$  (Figure 4.1D). Interestingly SaOS-2 had an opposing resistance to MTX with the largest  $LD_{50}$  (0.09  $\mu\text{M}$ ) and HOS the lowest (0.02  $\mu\text{M}$ ) (Figure 4.1 E and F).

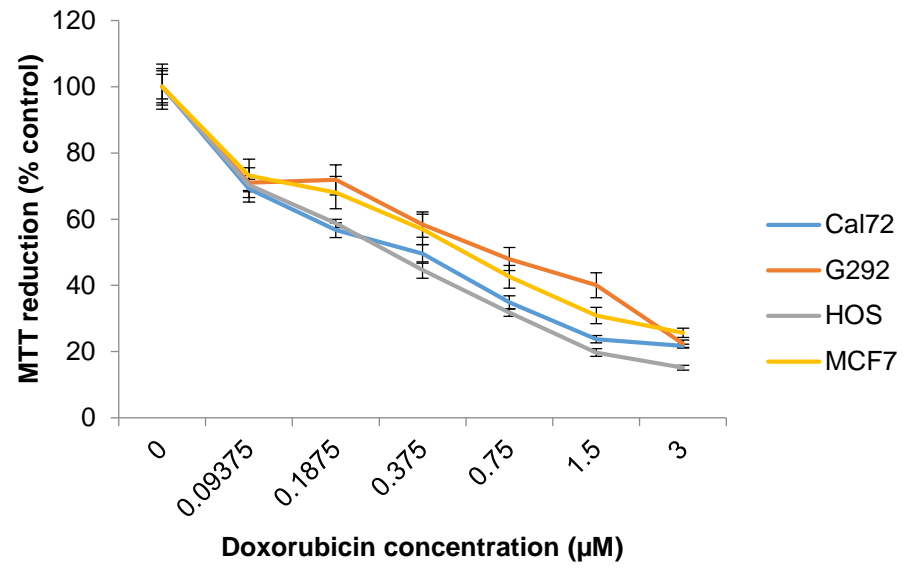


(A) Cal72 – MCF7

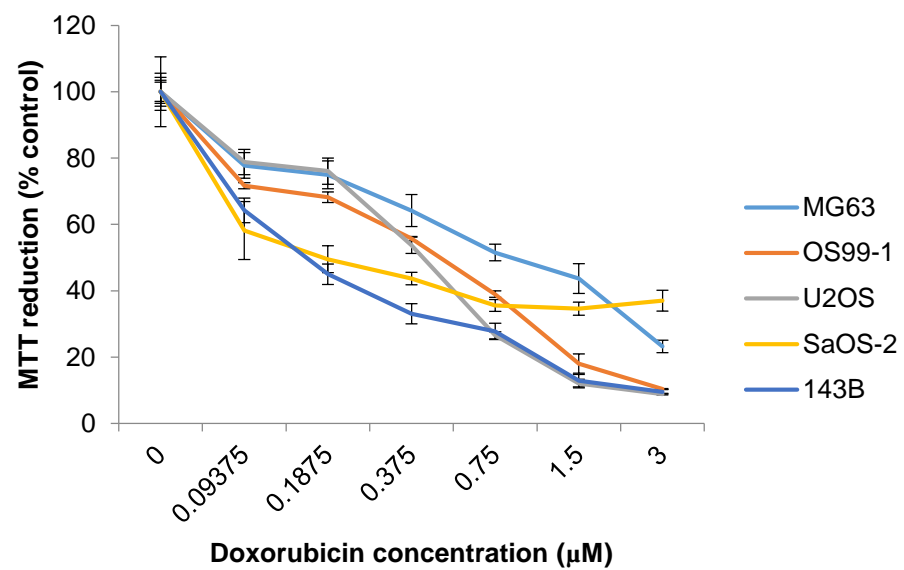


(B) MG63 – 143B

Figure 4.1: Continued overleaf

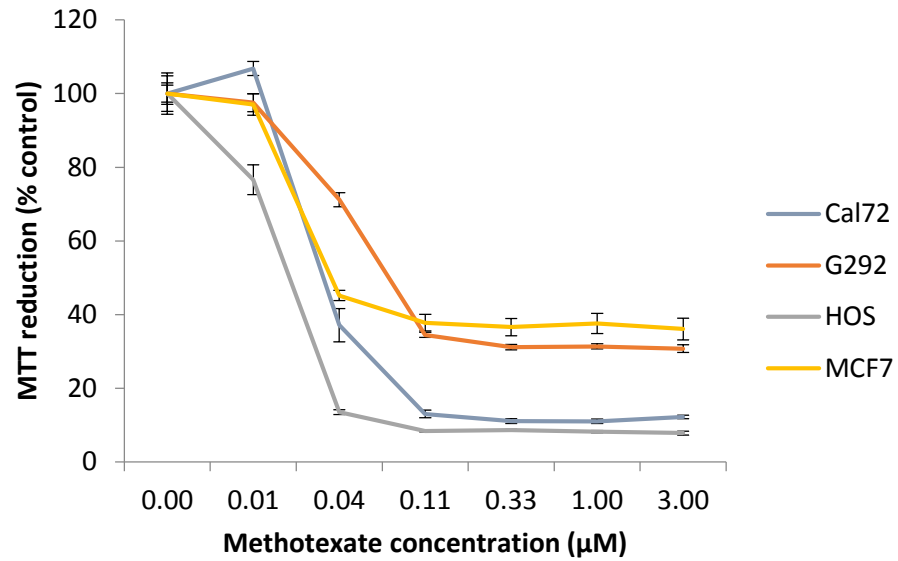


(C) Cal72 – MCF7

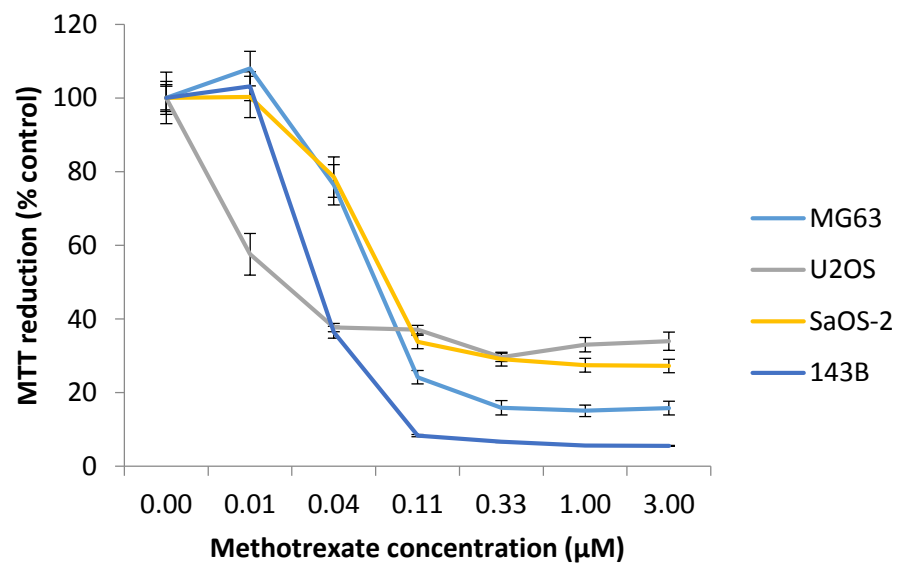


(D) MG63 – 143B

Figure 4.1: Continued overleaf



(E) Cal72 – MCF7



(F) MG63 – 143B

**Figure 4.1: Dose response curves for Cisplatin (A and B) and Doxorubicin (C and D) and methotrexate (D and E) dose response curves for OS cell lines and MCF7.** Concentration range of 0 -50 µM was used for cisplatin, 0 - 3 µM for doxorubicin and methotrexate 0 - 3 µM. Cisplatin and doxorubicin were incubated with cells for 48 hours and methotrexate for 5 days. Each experiment was repeated in triplicate in 3 separate experiments (n=3 independent replicates), results are presented as mean and standard error.

**Table 4.1: Comparison of cisplatin, doxorubicin and methotrexate median lethal doses (LD<sub>50</sub>) in OS cell lines and MCF7.** Statistical significance calculated by comparing to MCF7, \*p = <0.05, \*\*p = <0.01 (Tukey's post hoc analysis). LD<sub>50</sub> presented as average concentration and standard error (Std error)

Cell line	Cisplatin LD <sub>50</sub> (μM) ± Std error	Doxorubicin LD <sub>50</sub> (μM) ± Std error	Methotrexate LD <sub>50</sub> (μM) ± Std error
143B	3.8 ± 0.73 **	0.47 ± 0.06	0.05 ± 0.004
Cal72	8.6 ± 0.37 *	0.36 ± 0.09	0.06 ± 0.004 *
G292	13.0 ± 1.80	0.65 ± 0.15	0.08 ± 0.004 **
HOS	10.1 ± 1.05 *	0.34 ± 0.01	0.02 ± 0.001
MG63	15.0 ± 1.89	0.76 ± 0.42	0.08 ± 0.006 **
OS99-1	10.5 ± 0.67	0.59 ± 0.04	N/A
U2OS	18.0 ± 1.53	0.46 ± 0.02	0.03 ± 0.003
SaOS-2	14.0 ± 3.61	0.15 ± 0.11	0.09 ± 0.007 **
MCF7	16.5 ± 2.20	0.57 ± 0.18	0.03 ± 0.001

### 4.3 Clonogenicity assessment of cisplatin and doxorubicin treated cells in selected OS cell lines and MCF7

To identify if cis and dox exposure enriches for a CSC population with enhanced clonogenic properties. The following cell lines, U2OS, MG63, MCF7 and HOS were chosen because each OS cell line represents one of the different OS morphologies (U2OS is epithelial, MG63 is fibroblastic and HOS is mixed). MCF7 was included for comparison to a commonly used epithelial carcinoma cell line. Each cell line was exposed to a concentration equivalent to their LD<sub>50</sub> (Table 4.1), after exposure to these drugs for 2 days cells were seeded at a low density (2.4 – 3.8 cells/cm<sup>2</sup>) and grown for up to 12 days. No colonies were present, suggesting that the exposure to these drugs at an LD<sub>50</sub> concentration caused all the cells to undergo cell death. The LD<sub>50</sub> concentration of cis and dox was halved to equal the LD<sub>25</sub> concentration, again cells were exposed for two days and seeded at a clonal density but no colonies formed. After being exposed for 48 hours to cis and dox LD<sub>25</sub> the appearance of each cell line was consistent with the cell morphology prior to drug addition. Except for MCF7 each OS cell line had undergone some growth in the presence of cis and dox, which was apparent with the increased cell density after 48 hours (Figure 4.2).

To establish if cell communication is important for cell line recovery post drug treatment, U2OS and MG63 cells were seeded cells at a higher density (1 in 4 passage) post 48 hour drug treatment. Interestingly both cell lines when re-seeded at high density the drug treated cells had a fibroblastic appearance (Table 4.3 and table 4.4). In the case of U2OS (Figure 4.3) and MG63 (Table 4.4), after cis exposure these cells would undergo some growth but growing colonies were characterised with dendrite-like structures connecting cells to one another. These colonies stopped growing after 9 days. U2OS (Figure 4.3) and MG63 cells (Figure 4.4), did not form any colonies after dox exposure. Surviving cells were very large in size and had a fibroblastic morphology, often with long dendrite-like structures extending from the cells but would not form colonies.



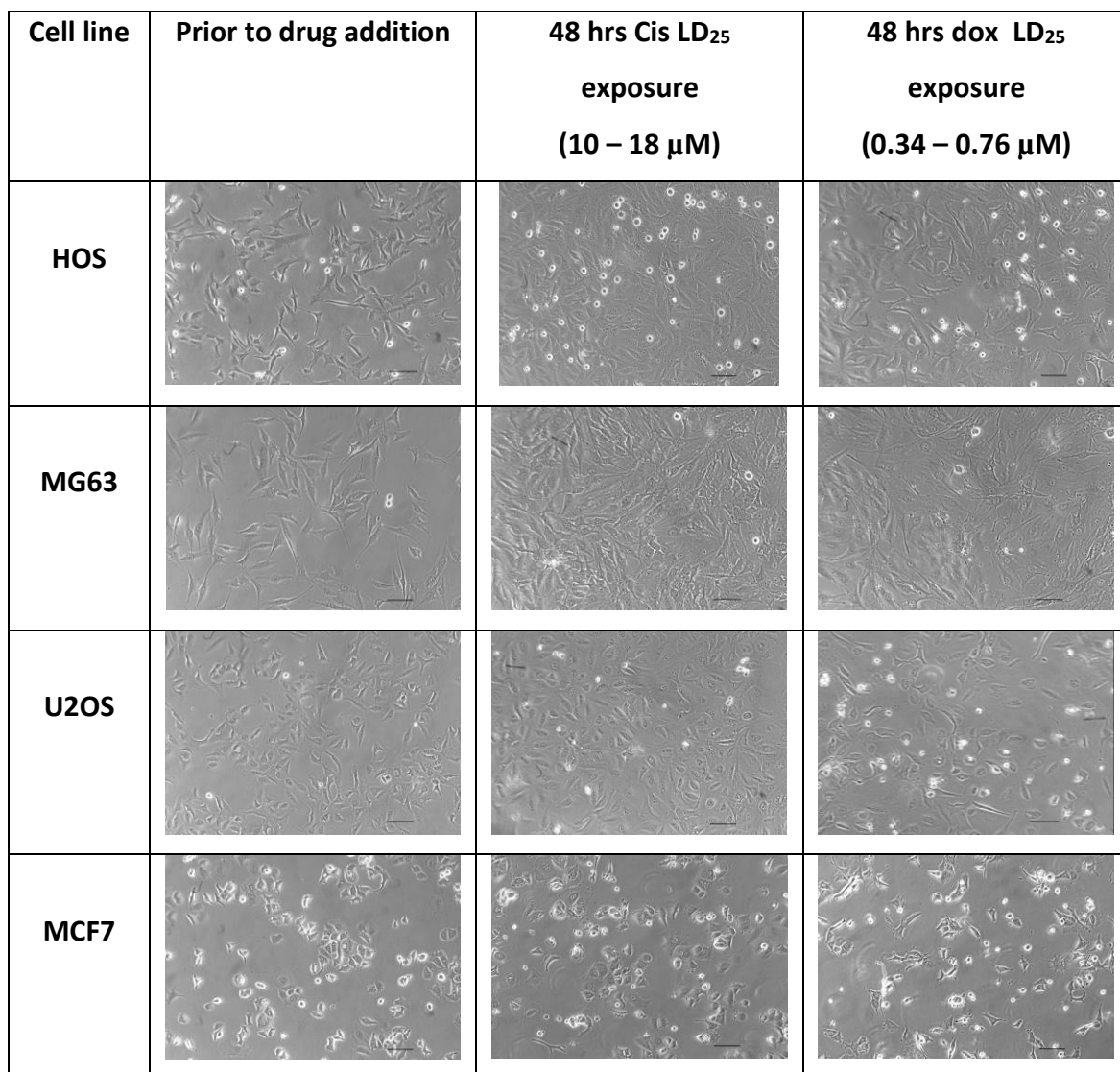


**Figure 4.2: Appearance of OS cell lines and MCF7 after 48 hours of cisplatin or doxorubicin LD<sub>25</sub> exposure.** Representative of 4 images, scale bars represent 100  $\mu$ m.

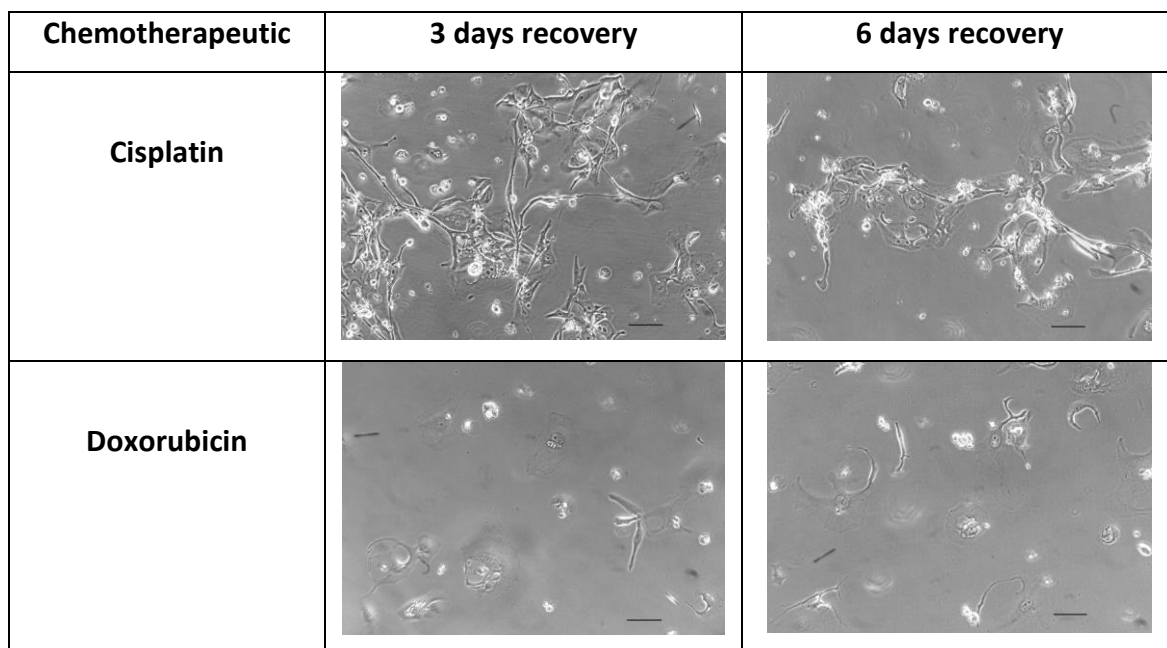


**Figure 4.3: U2OS cells exposed to LD25 of either cisplatin or doxorubicin.** Cells exposed to drugs for 48 hours then passaged and re-seeded at high density (1 in 4) and allowed to recover in the absence of drug. Representative of 4 images, scale bar represents 100  $\mu\text{m}$ .

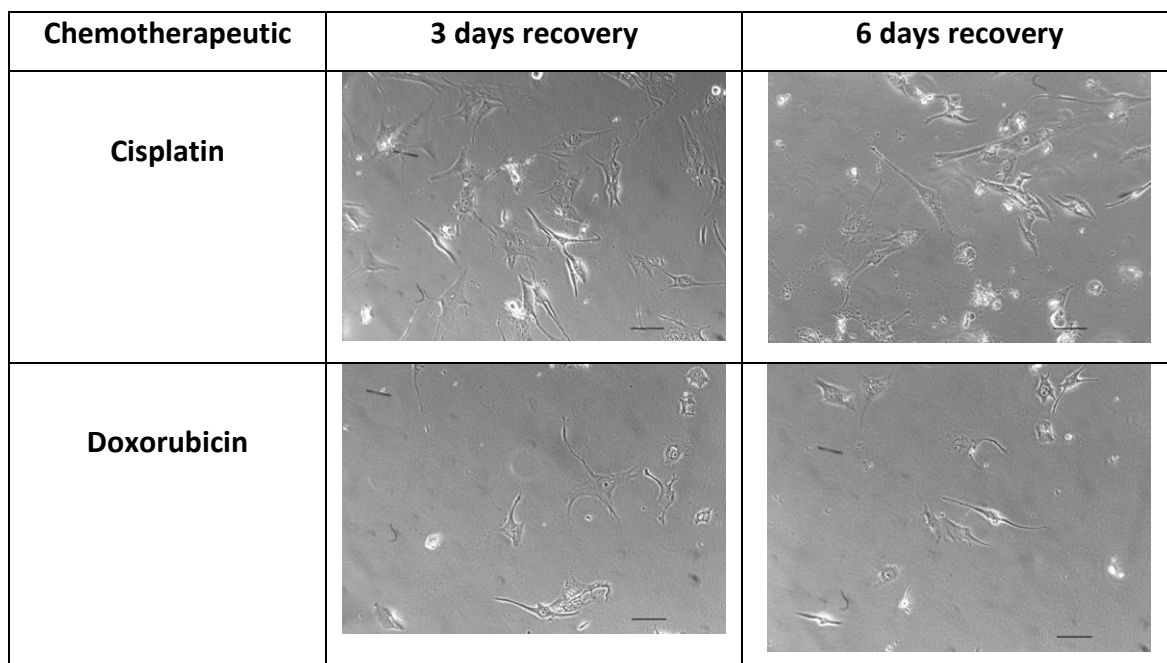


**Figure 4.4: MG63 cells exposed to LD25 of either cisplatin or doxorubicin.** Cells exposed to drugs for 48 hours then passaged and re-seeded at high density (1 in 4) and allowed to recover in the absence of drug. Representative of 4 images, scale bar represents 100  $\mu\text{m}$ .

#### **4.4 Analysis of putative CSC marker expression in cisplatin and doxorubicin treated cells in selected OS cell lines and MCF7**

To identify if 48 hour exposure of cis and dox led to enhanced expression of cancer stem cell markers (ALDH, CD117 and CD44). Cells were exposed for 48 hour to LD<sub>25</sub> drug concentration, after which cells were labelled with CSC marker antibodies (CD117 or CD44) or substrates (ALDH) and analysed using flow cytometry (Section 2.8).

Both cis and dox possessed auto-fluorescence which interfered with the phycoerythrin (PE) channel of the flow cytometer, this made the analysis of these markers utilising PE fluorescence inaccurate. Uptake of both cis and dox by all cell lines tested resulted in an increase in the PE fluorescence of the cells. In order to set a baseline PE fluorescence which can be used to identify the increase in PE fluorescence, an unstained population was compared to a stained population to identify an increase (Section 3.2). However due to the increased fluorescence of cis and dox treated cells this led to the baseline PE fluorescence of the unstained cells to be increased (Figure 4.5.B), which is evident when comparing to a normal population of non-drug treated cells (Figure 4.5.A). This increased PE background fluorescence is important for either PI staining (when distinguishing live from dead cells) or identifying CD44 positive cells, hence making analysis of these markers inaccurate. This masking effect is evident when comparing CD44 populations observed in untreated cells (68.6 %), which was reduced in cis treated (6.4 %) and dox treated cells (2.64 %) (Table 4.2).

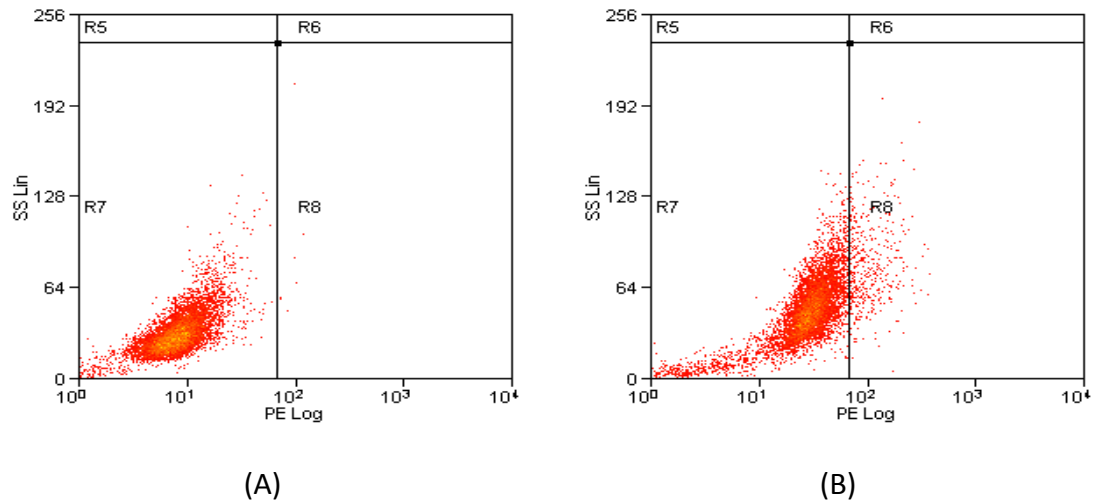


**Figure 4.5: Auto-fluorescence of doxorubicin and cisplatin exposed cells detected by flow cytometry analysis in HOS cell line.** HOS cells untreated (A) or treated with LD<sub>50</sub> concentration of doxorubicin (B). This experiment was tested in once in for both cis and dox exposure.

**Table 4.2: Identification of CD44 positive populations of HOS cells when comparing untreated cells with cis and dox exposed cells.** Untreated cells tested in triplicate, cis and dox LD<sub>50</sub> treated cells tested once.

Marker	Untreated	Cis LD <sub>50</sub> (10.1μM)	Dox LD <sub>50</sub> (0.34μM)
CD44 (%)	68.6 ± 6.8	6.4	2.64

#### 4.5 Growth rates of methotrexate exposed cell in selected OS cell lines and MCF7

The dihydrofolate reductase inhibitor MTX, has been previously used to enrich putative CSC in the OS cell lines U2OS and MG63 (Tang et al., 2011). Tang *et al* (2011) was able to enrich putative OS CSC based upon exposure to 100 ng/ml and 300 ng/ml MTX for 5 days with surviving cells having increased clonogenicity and spheroid forming ability compared to untreated cells. The LD<sub>50</sub> of the OS cell lines tested ranged from 20 nM to 80 nM (Table 4.1), based on the cell MTX sensitivities two concentrations were chosen, 5 nM was selected because all cell lines could form colonies after 5 days exposure and also 50 nM to identify if an increased MTX concentration would more efficiently enrich drug resistant cells. The concentrations utilised by Tang *et al* (2011) equated to 220 nM (100 ng/ml) and 660 nM (300 ng/ml), these concentrations were tested but no cells survived after 5 days of MTX exposure.

Images taken of the cells after 5 days of MTX exposure (Figure 4.6) show that at 5 nM MTX all cell lines (HOS, MG63, U2OS and MCF7) grew at a similar rate to the untreated cells (0 nM) and had reached 100 % confluency after 5 days. At 50 nM MTX cell growth was reduced in HOS, MCF7 and U2OS which all displayed below 30 % confluency, in contrast MG63 growth rate was least effected reaching approximately 95 % confluency. Interestingly a common feature of cells which had grown in 50 nM MTX was the acquisition of a fibroblastic appearance with the presence of dendrite-like structures connecting cells together.

After the cells had been exposed to 5 nM and 50 nM MTX concentrations they were passaged and seeded at a clonal density (2.4 – 3.8 cells/cm<sup>2</sup>). Colonies were allowed to form in the absence of MTX for 14 days (media was changed every 3 days), after which colonies were stained using crystal violet and size assessed using ImageJ® (Figure 4.7). Growing HOS and U2OS in 50 nM MTX resulted in no colony formation, whilst the MG63 and MCF7 formed colonies in both MTX concentrations. Interestingly no significant change in colony size was observed in response to 5 nM and 50 nM MTX, suggesting that the cell lines (HOS, MG63, U2OS and MCF) treated with MTX have the same growth rates as the untreated cells (Figure 4.7).

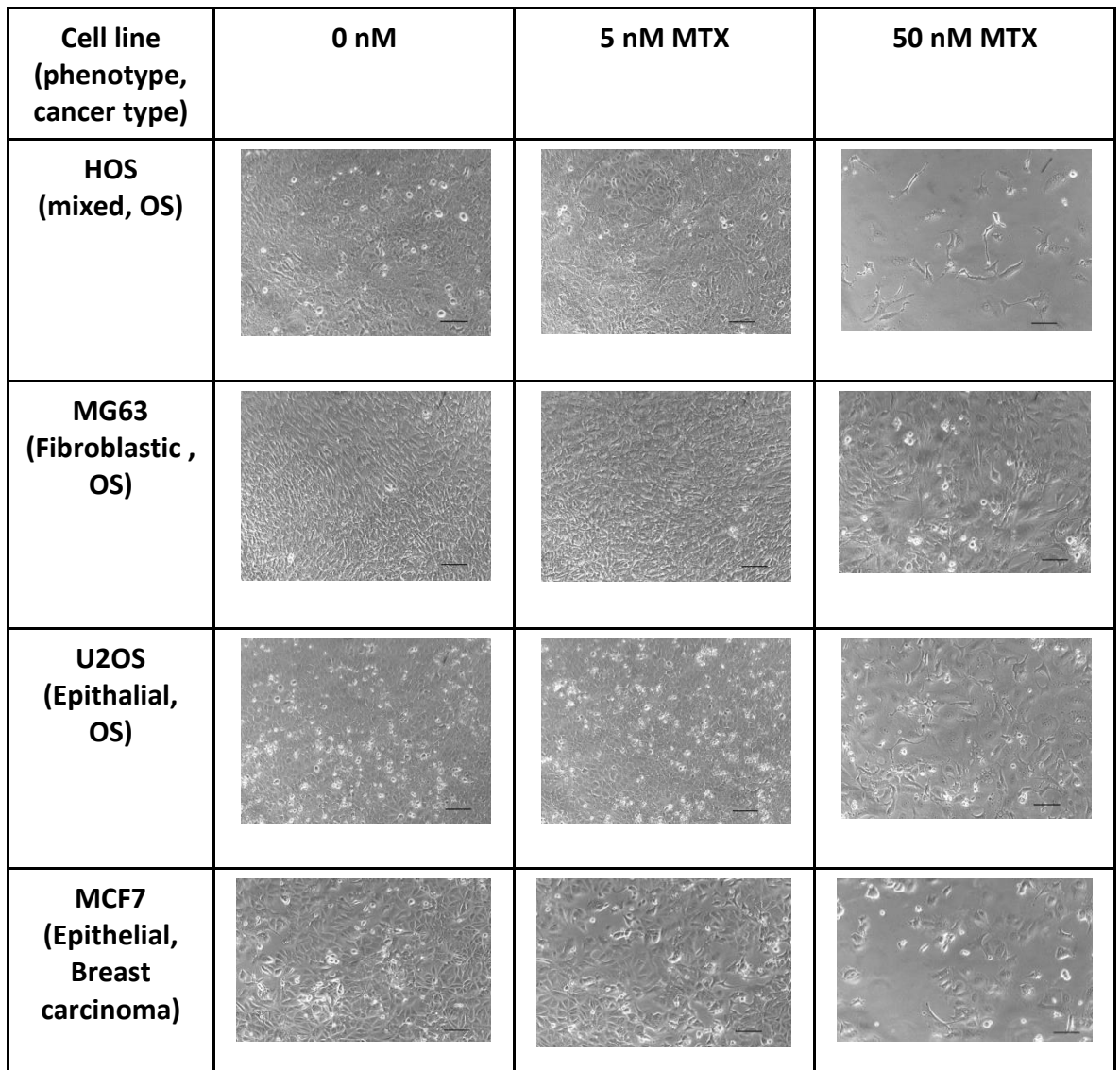


**Figure 4.6: Images of OS cell lines (HOS, MG63 and U2OS) and MCF7 in response to methotrexate exposure at 0, 5 and 50 nM. 15625 cells/cm<sup>2</sup> were seeded images taken after 5 days of MTX exposure. Representative of 4 images, scale bar represents 100  $\mu$ m.**

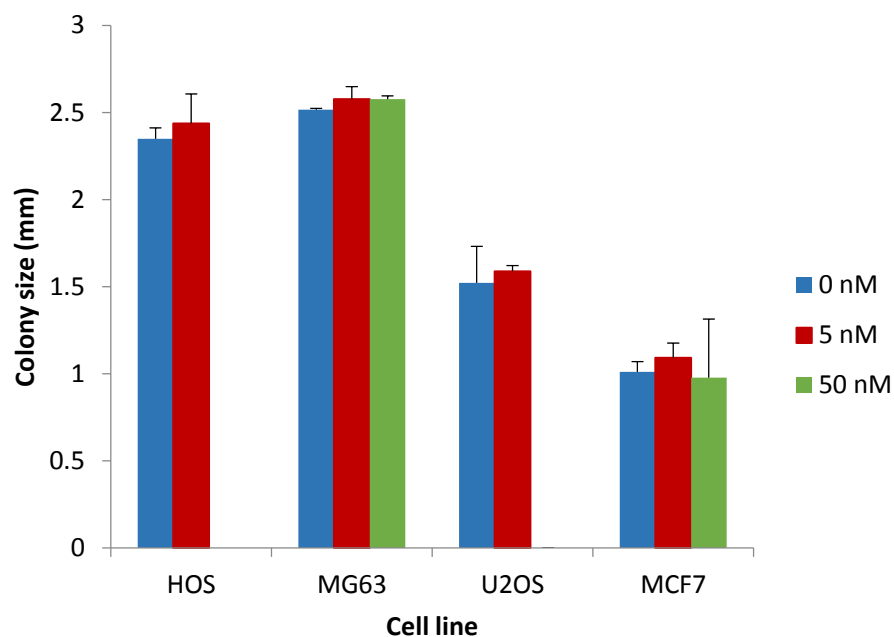


**Figure 4.7: Assessment of colony size of HOS, MG63, U2OS and MCF7 exposed to MTX concentrations (0, 5 and 50 nM).** Cells were seeded at 15625 cells/cm<sup>2</sup> and grown in the presence of methotrexate for 5 days before seeding at a clonal density (2.4 – 3.8 cells/cm<sup>2</sup>) and growing for a further 14 days (Section 2.3.2). Colony size assessed using ImageJ. Results tested in triplicate and data presented as mean and standard deviation. Statistical significance assessed using Tukey's post hoc analysis for 0, 5 and 50 nM treated cells for each cell line. No statistical significance observed.

#### **4.6 Presence of putative cancer stem cells in methotrexate treated OS and MCF7 cells lines**

OS CSC have been found to have an enhanced resistance to chemotherapeutics (Adhikari et al., 2010) (Section 1.3), and the colony hierarchies (holoclones, meroclones and paraclone) have been shown to contain CSC within the holoclones from a prostate cancer cell line (Li et al., 2008). Holoclones are therefore at the base of this cellular hierarchy and can give rise to rapidly amplifying meroclones which will eventually terminally differentiate and become paraclones (Section 1.2.3). The identification of holoclones, therefore provides a method for identifying putative CSC without the requirement for analysis of surface or intracellular CSC protein markers. Although in chapter 3 of this thesis, it was shown that OS cell lines highly expressing ALDH contain these ALDH<sup>+</sup> cells within all three colony hierarchies (Section 3.6.1), which could indicate that CSC may reside within all colony hierarchies.

The colony hierarchy frequency present after MTX treatment was assessed by exposing cells to MTX for 5 days. Cells were then re-seeded at a clonal density and grown for 14 days in the absence of MTX, after which colony hierarchies were assessed (Section 2.3.2). Due to the sensitivity of HOS and U2OS to MTX no colonies survived at 50 nM MTX in HOS and less than 10 colonies were present in MCF7. HOS was the only cell line to have a statistically significant change, which resulted in a reduction in holoclones present in 5 nM MTX compared to 0 nM MTX (Figure 4.4). No change in colony hierarchy frequency was observed in response to MTX in the cell lines MG63 (Figure 4.8.B), U2OS (Figure 4.8.C) and MCF7 (Figure 4.8.D). MCF7 50 nM MTX exposed colonies were not included in the analysis due to less than 30 colonies being present (Figure 4.8.D).

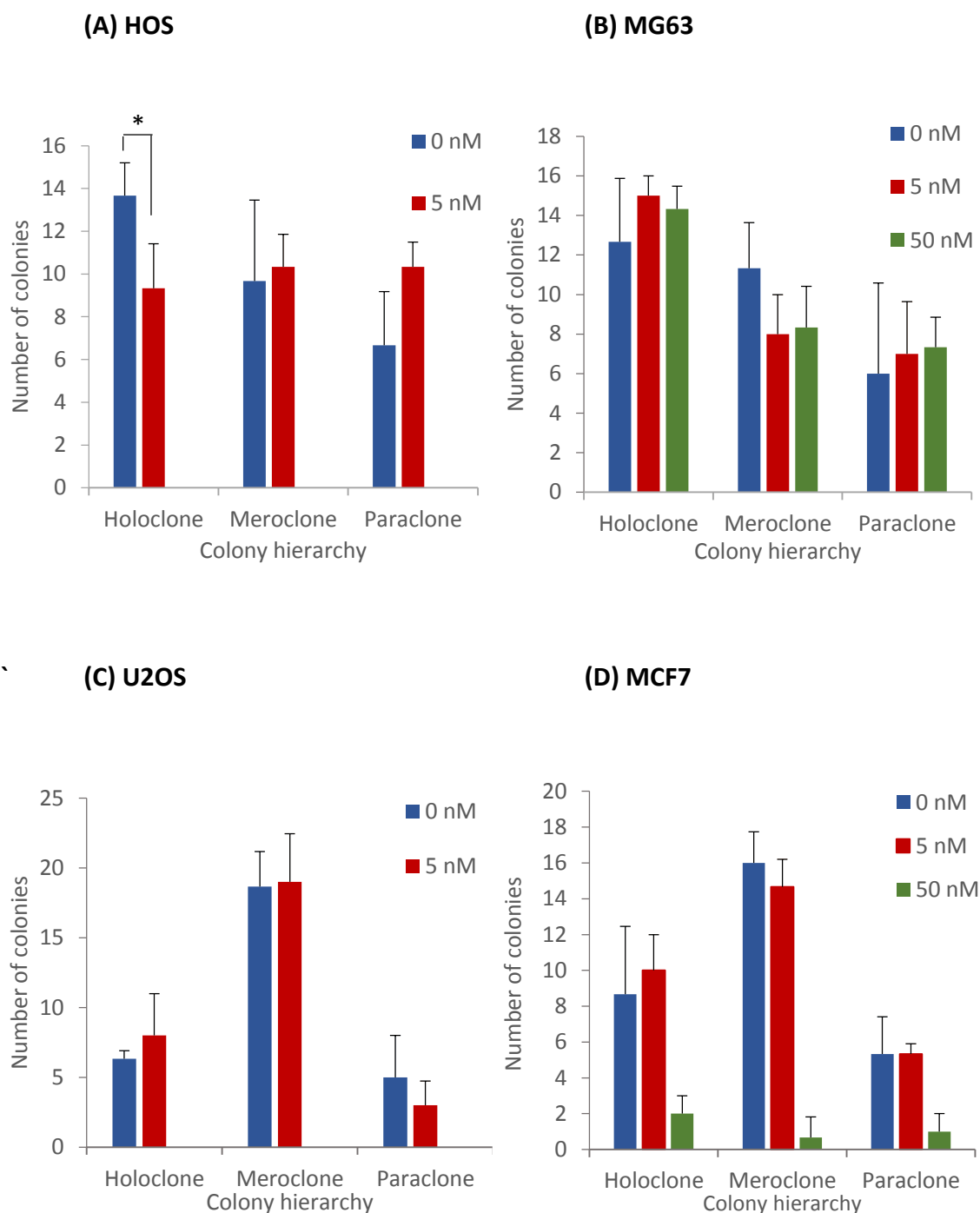
##### **4.6.1 Cancer stem markers expressed by methotrexate treated cells**

MTX treated cells were also analysed for the expression of CSC markers (ALDH and CD117). Cells (15625 cells/cm<sup>2</sup>) were seeded and allowed to attach for 24 before addition of MTX. After short term exposure to MTX (5 days) cells were harvested and stained for the markers and analysed by flow cytometry (Section 2.8.6). HOS which contains the largest population of ALDH cells (60.6 %) according to flow cytometry (Section 3.2.2), had a significantly

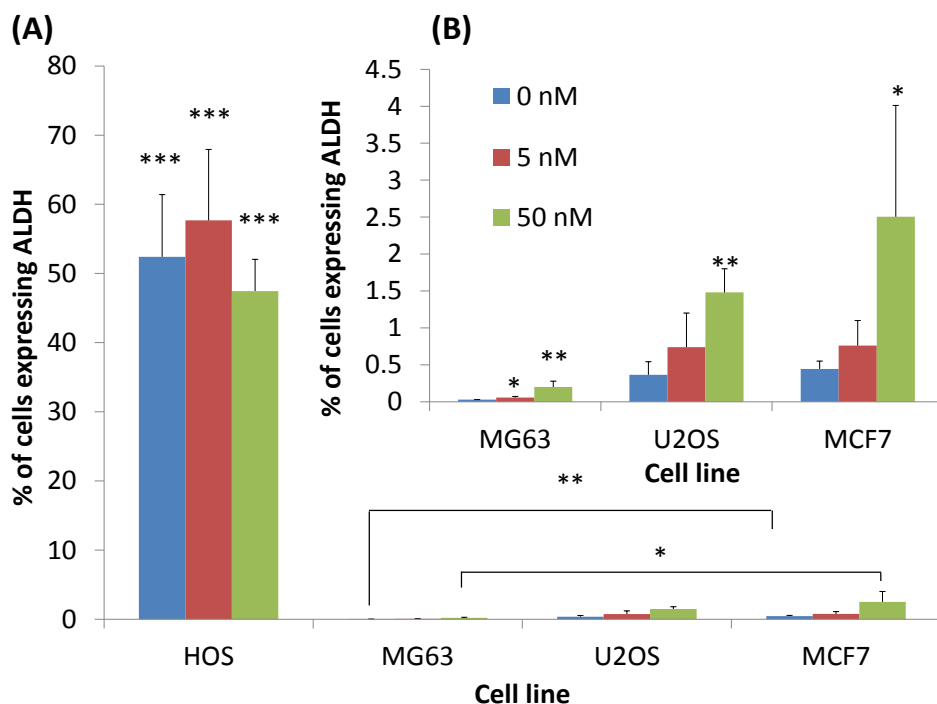


greater population of ALDH cells at all MTX concentrations compared to the other cell lines tested (Figure 4.9.A). However, HOS was the only cell line which did not have an increase in ALDH expression in response to 5 nM MTX, suggesting that the ALDH positive cells in HOS are not MTX resistant. In contrast MG63, U2OS and MCF7 had an increase in the percentage of ALDH positive cells in response to 50 nM MTX (figure 4.9.B). MG63 was the only cell line to have a significant enrichment in ALDH expressing cells at 5 nM MTX, suggesting that ALDH positive cells have enhanced MTX resistance compared to cells lacking ALDH expression in MG63 and to a lesser extent U2OS and MCF7.

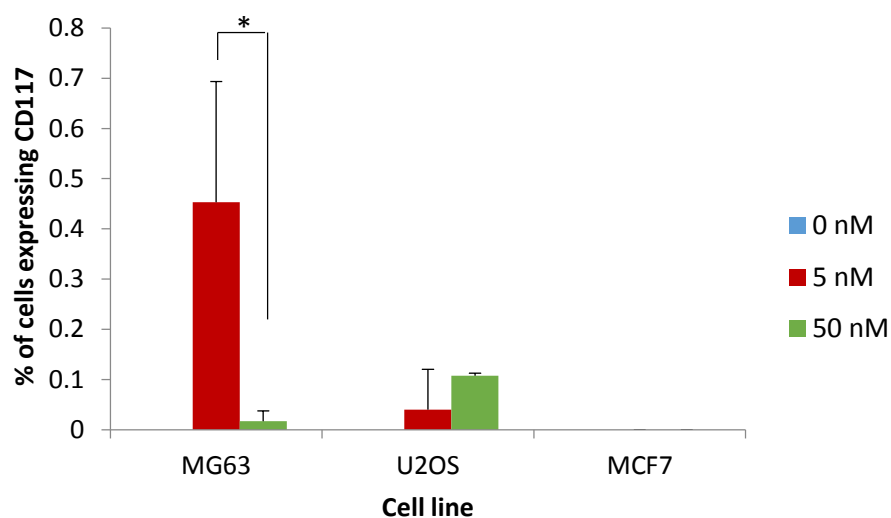
MTX exposure altered the expression of CD117 in both MG63 and U2OS, in the absence of MTX neither cell line expressed CD117, however, in response to MTX both cells were found to express the cell surface receptor (Figure 4.10). Exposure to 5 nM MTX resulted in MG63 cells containing a CD117 population of 0.45 %, whereas U2OS contained 0.05 %. Increasing the concentration to 50 nM led to an increase in CD117 expression in U2OS, whilst in MG63 a decrease of cells expressing CD117 was observed (Figure 4.10).



**Figure 4.8: Analysis of the frequency of the colony hierarchies in methotrexate treated HOS, MG63, U2OS and MCF7 cells.** HOS (A), MG63 (B), U2OS (C) and MCF7 (D) cells were seeded at 156 cells/mm<sup>2</sup> and grown in the presence of methotrexate (0, 5 or 50 nM) for 5 days before seeding at a clonal density (2.4 – 3.8 cells/cm<sup>2</sup>) and growing for a further 14 days. Colony hierarchy was assessed by counting the first 30 colonies prior to crystal violet staining. No colonies were present in 50 nM MTX of HOS or U2OS cells. Results tested in triplicate. Significance calculated using Tukey's post hoc analysis ( $p < 0.05$ ), MCF7 50 nM treated cells not included because less than 30 colonies were present.



**Figure 4.9: Presence of ALDH expressing cells in MG63, U2OS and MCF7 MTX treated cells.** A) ALDH expression of HOS, MG63, U2OS and MCF7 after 5 days exposure to MTX (0, 5 and 50 nM). HOS had a significantly larger proportion of ALDH cells at all concentrations. Tukey’s post hoc analysis \*\*\* = <0.0001. B) ALDH expression of MG63, U2OS and MCF7 in response to MTX (0, 5 and 50 nM). Significance calculated using Tukey’s post hoc analysis, \* = <0.05, \*\* = <0.01 and \*\*\* < 0.001 . Analysis compared to 0 nM MTX ALDH populations. Samples tested in triplicate.

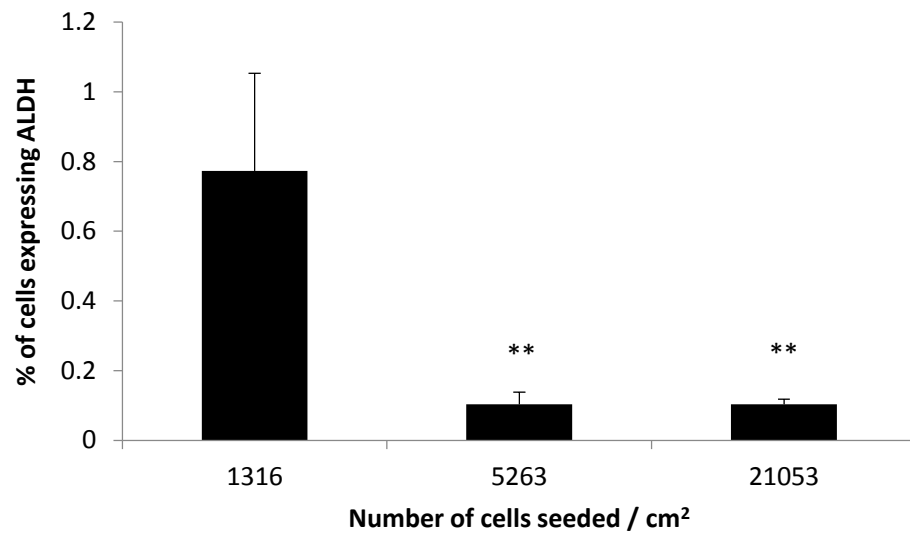
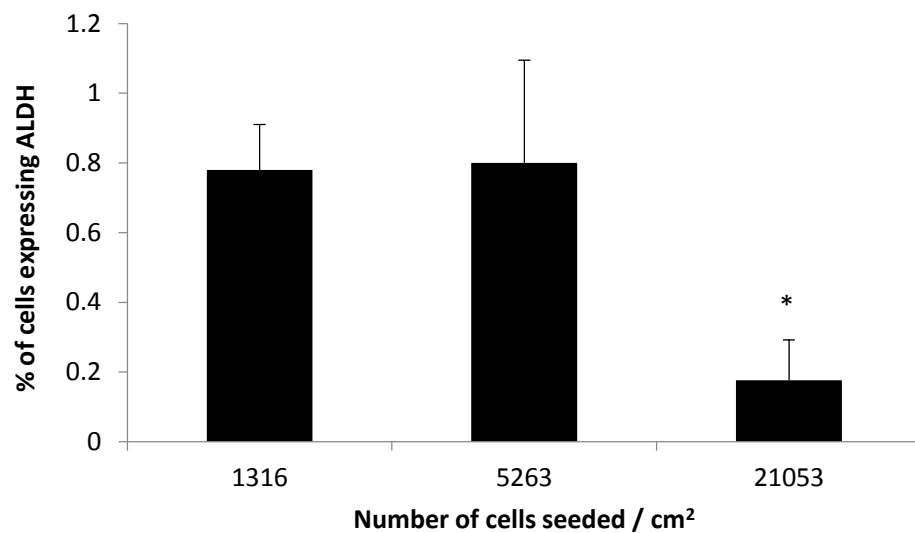


**Figure 4.10: Presence of CD117 expressing cells in MG63, U2OS and MCF7 MTX treated cells.** CD117 expression of MG63, U2OS and MCF7 after 5 days exposure to MTX (0, 5 and 50 nM). Significance calculated using Tukey’s post hoc analysis, \* = <0.05. Experiment tested in triplicate.

#### 4.7 Effect of cell density on ALDH expression in selected OS cell lines and MCF7

Exposure to 50 nM MTX enriched ALDH expressing cells in the following cells lines; MG63, U2OS and MCF7 (figure 4.5.B). To obtain this result cells were seeded at high density (15600 cells/cm<sup>2</sup>), allowed to attach for 24 hours before adding the MTX for 5 days and then analysing ALDH expression. At MTX concentrations of 0 nM and 5 nM, cells would have reached 100 % confluency at the time of ALDH analysis, however, the 50 nM MTX treated cells had a reduced growth rate so confluency would be 90 % in MG63 and < 30 % in the remaining cell lines (HOS, U2OS and MCF7). Therefore an important experiment is to ensure that cell density is not affecting the expression of the CSC markers. To test this MG63 and MCF7 cells were seeded at 1310, 5240 and 21000 cells/cm<sup>2</sup> so that cells grown for 6 days at different densities could be compared for ALDH expression. ALDH was monitored after 6 days because this reflected the incubation time utilised in the MTX treated ALDH expression experiment (Section 2.8.7).

In both MG63 and MCF7 ALDH expression was found to be significantly lower ( $p = <0.01$ ) in the highest seeding densities (21053 cells/cm<sup>2</sup>) (figure 4.11A and B), MG63 was found to have a reduced expression at 5263 cells cm<sup>2</sup> (figure 4.11.A). Therefore at higher cell densities the presence of ALDH positive cells is reduced. Suggesting that the increase in ALDH expression observed in response to 50 nM MTX may be a result of the MTX decreasing growth, which decreases cell density leading to enhanced ALDH expression.

**(A) MG63****(B) MCF7**

**Figure 4.11: Analysis of effect of cell density upon ALDH expression.** A) MG63 or B) MCF7 cells were seeded at either 1316, 5263 or 21053 cells/cm<sup>2</sup>, grown for 5 days and the tested for ALDH expression. Significance calculated by comparing to 12500 cells using Tukeys post hoc analysis, \* $p < 0.05$  \*\*  $p < 0.01$ . Results tested in triplicate. Data presented as mean and standard deviation.

#### **4.8 Correlation of cancer stem cell marker expression with chemotherapeutic resistance in osteosarcoma cell lines and MCF7**

OS cells expressing either CD117 or ALDH, have been sorted using flow cytometry and were reported to have an enhanced chemotherapeutic resistance (Honoki et al., 2010, Adhikari et al., 2010). However, whether the expression of these markers in an unsorted population of cells correlates with *in vitro* chemotherapy resistance is absent within the literature. In order to identify if the expression of the CSC markers ALDH and CD117 correlates with an enhanced chemotherapeutic resistance, the LD<sub>50</sub> from OS cells lines (except OS99-1) and MCF7 were compared with the population sizes expressing the CSC markers identified using flow cytometry to see if a correlation existed (section 3.2). Both linear regression and Pearson's correlation coefficient were used to assess the correlation between the two variables.

Correlating CSC marker expression with LD<sub>50</sub> concentrations for all chemotherapeutics tested produced a negative correlation (Figures 4.12 – 4.17). Pearson's correlation coefficient analysis confirmed that increased putative CSC marker expression is related to increased sensitivity to chemotherapeutic treatment, in particular CD117 expression produced a strong negative correlation with cisplatin (-0.70) (Figure 4.11), which was supported by producing a statistically significant negative Pearson's correlation of -0.84 (Table 4.3). ALDH expression produced weak negative correlations with all drugs tested (cis, dox and MTX), however, according to Pearson's correlation none were statistically significant.

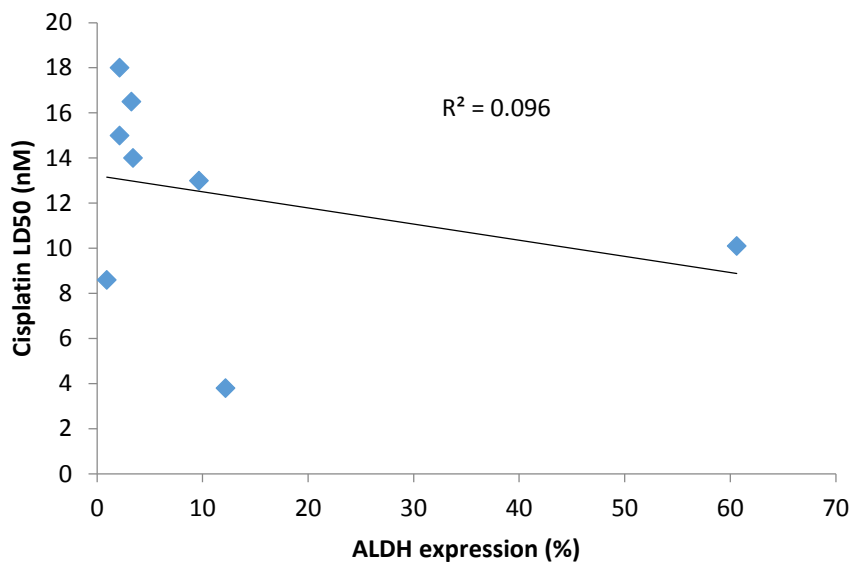


**Figure 4.12:** Linear regression analysis of cell line (143B, Cal72, G292, HOS, MG63, U2OS, SaOS-2 and MCF7) cisplatin LD<sub>50</sub> concentration against ALDH expression. The correlation coefficient ( $R^2$ ) is 0.01 and Pearson's correlation coefficient of -0.31.

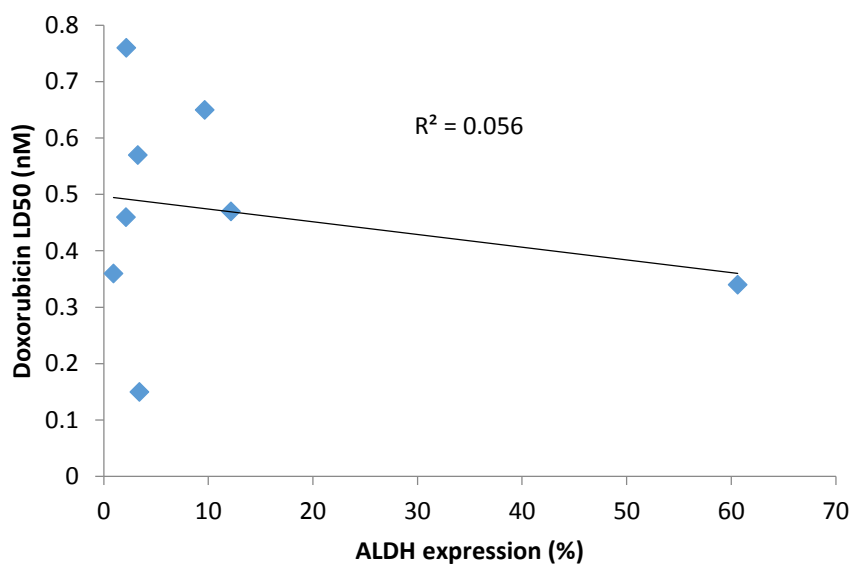


**Figure 4.13:** Linear regression analysis of cell line (143B, Cal72, G292, HOS, MG63, U2OS, SaOS-2 and MCF7) doxorubicin LD<sub>50</sub> concentration against ALDH expression. The correlation coefficient ( $R^2$ ) is 0.06 and Pearson's correlation coefficient of -0.24.

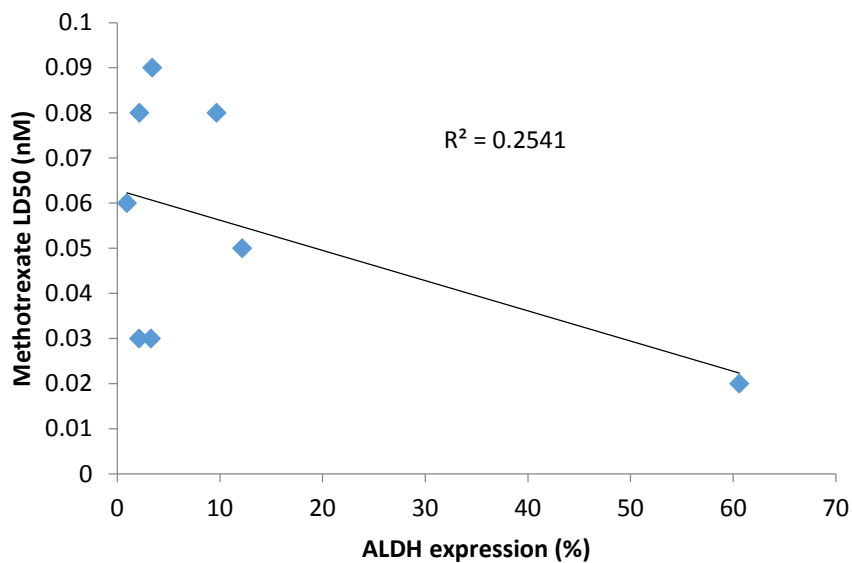


**Figure 4.14:** Linear regression analysis of cell line (143B, Cal72, G292, HOS, MG63, U2OS, SaOS-2 and MCF7) methotrexate LD<sub>50</sub> concentration against ALDH expression. The correlation coefficient ( $R^2$ ) is 0.25 Pearson's correlation coefficient of -0.50.

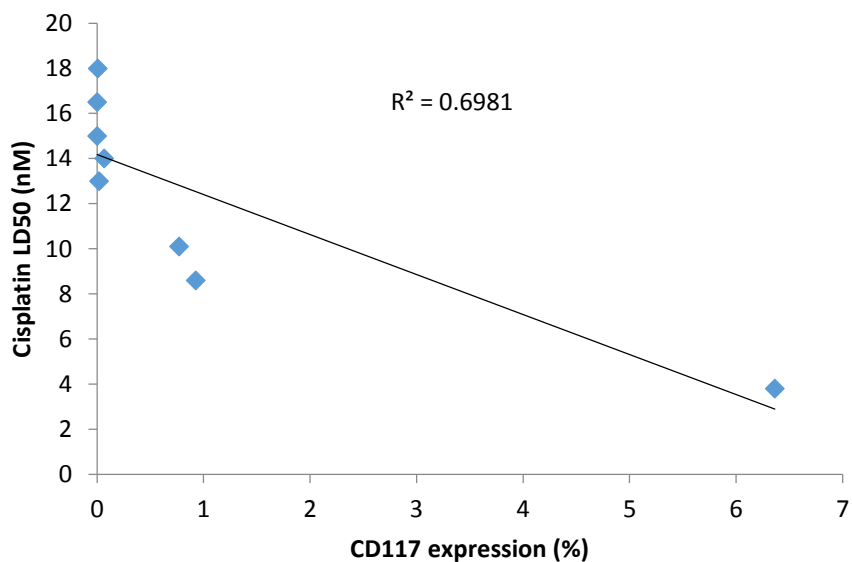


**Figure 4.15:** Linear regression analysis of cell line (143B, Cal72, G292, HOS, MG63, U2OS, SaOS-2 and MCF7) cisplatin LD<sub>50</sub> concentration against CD117 expression. The correlation coefficient ( $R^2$ ) is 0.69 and a spearmanns rank correlation coefficient of -0.84.



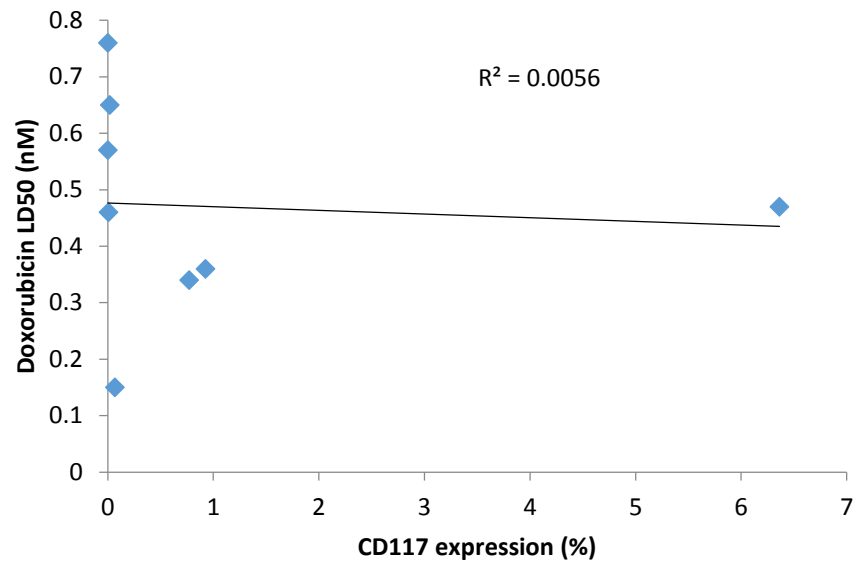


**Figure 4.16: Linear regression analysis of cell line (143B, Cal72, G292, HOS, MG63, U2OS, SaOS-2 and MCF7) doxorubicin LD<sub>50</sub> concentration against CD117 expression. The correlation coefficient ( $R^2$ ) is 0.006 and Pearson's correlation coefficient of -0.07.**

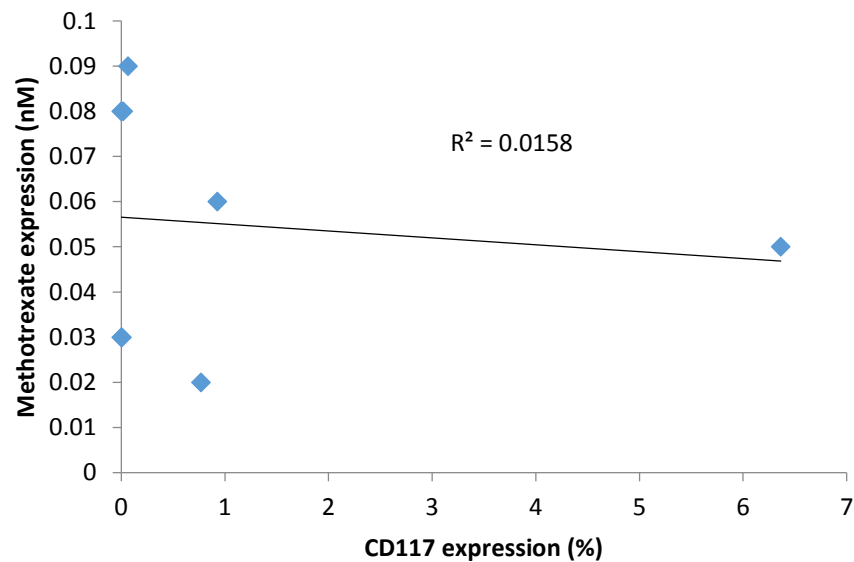


**Figure 4.17: Linear regression analysis of cell line (143B, Cal72, G292, HOS, MG63, U2OS, SaOS-2 and MCF7) methotrexate LD<sub>50</sub> concentration against CD117 expression. The correlation coefficient ( $R^2$ ) is 0.016 and Pearson's correlation coefficient of -0.013.**

**Table 4.3: Pearson's correlation coefficient of cell lines CSC marker expression and chemotherapy LD<sub>50</sub>.** The cell lines 143B, Cal72, G292, HOS, MG63, U2OS, SaOS-2 and MCF7 were correlated for the expression of cancer stem cell markers (ALDH and CD117) against the LD<sub>50</sub> concentrations of the chemotherapeutic agents cisplatin, doxorubicin and methotrexate (\*\* =  $p < 0.01$ ).

<b>Chemotherapeutic</b>	<b>ALDH</b>	<b>CD117</b>
Cisplatin	-0.31	-0.84**
Doxorubicin	-0.24	-0.07
Methotrexate	-0.50	-0.13

#### 4.9 Sarcosphere forming ability of MG63 methotrexate exposed cells

Growing cells in serum starved low attachment conditions allows spherical suspension colonies to form which are enriched in stem cells (Reynolds et al., 1992). This technique was used by Rainusso *et al.*, (2011) to study OS CSC and it and they reported that cells with an enhanced sphere forming ability also have enhanced tumourigenicity.

If MTX treatment enriches for CSC we would predict to see an increase in enhanced sarcosphere formation. To test this, the cell line MG63 was chosen for its ability to form secondary sarcospheres (Section 3.7) and the enrichment of ALDH and CD117 expressing cells in response to MTX (figure 4.9 and 4.10). MG63 cells were seeded at a high density (15600 cells/cm<sup>2</sup>), allowed to attach for 24 hours before being treated with MTX for 5 days, after which cells were passaged and seeded (1052 cells/cm<sup>2</sup>) in to the serum starved low attachment conditions. After 7 days primary sarcosphere size was assessed from 5 images of each well using ImageJ, passaged and seeded (210 cells/cm<sup>2</sup>) and grown for a further 7 days to form the secondary sarcospheres. Secondary sarcospheres were assessed by counting all sarcospheres  $\geq 40 \mu\text{m}$  and calculating the sarcosphere forming efficiency (%) (MG63 MTX treated sarcosphere assay procedure summarized in figure 4.18).

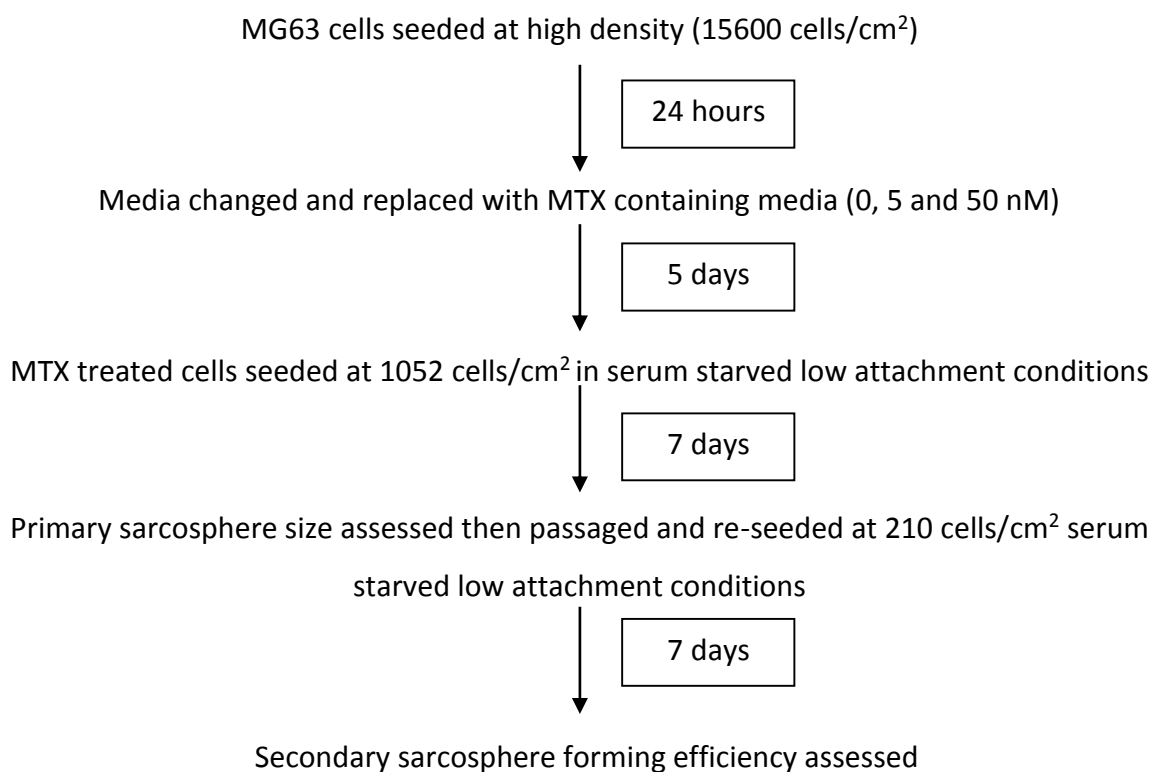


**Figure 4.18: MG63 methotrexate treated sarcosphere assay procedure.**

The appearance of primary sarcospheres when treated with 5nM was similar to untreated cells, the colonies were of an oval shape with a rough appearance. Cells treated with 50 nM MTX also formed primary sarcospheres and also had a rough appearance but more irregular in shape. These cells did not produce the oval shape observed in the lower concentrations. Secondary sarcospheres across all the concentrations had the same appearance, they were observed to be smaller in size than the primary sarcospheres and had an irregular shape (Figure 4.19).

MG63 cells treated with 5nM MTX were found to have an increased primary sarcosphere size compared to untreated sarcospheres (Figure 4.20). This increase in sarcosphere size suggests that exposing OS cells to 5 nM MTX enriches a population of cells with a higher growth rate in low attachment conditions. In contrast cells exposed to 50 nM MTX had no change in colony size, suggesting that the increased concentration negates the effects caused by 5 nM. Analysis of secondary sarcospheres demonstrated that no change in sarcosphere size was observed in either 5 nM or 50 nM MTX (Figure 4.21). The lack of any

change suggests that the effect of 5 nM MTX upon primary sarcospheres may be a transient effect which is lost upon passage. The cell line U2OS was also assessed for sarcosphere forming efficiency in response to 0 nM, 5 nM and 50 nM MTX, however, no secondary sarcospheres were present in all concentrations suggesting that MTX exposure does not enrich U2OS cells with the ability to grow in low attachment conditions.

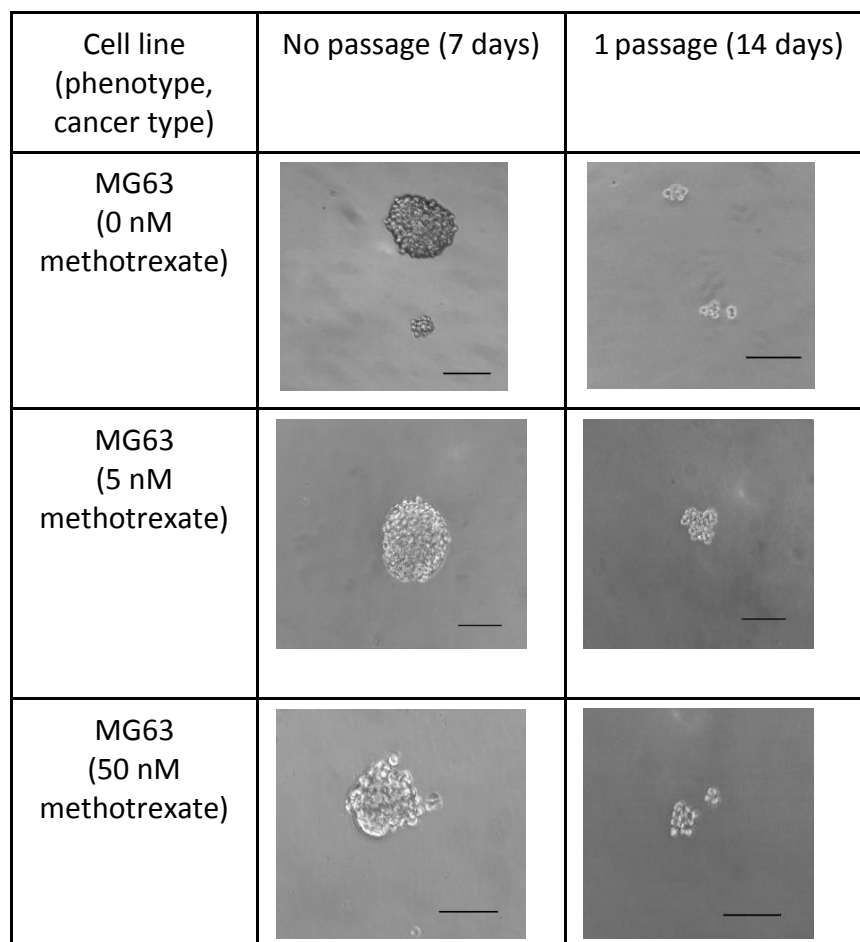


**Figure 4.19: Images of MG63 sarcospheres in response to methotrexate exposure (bar = 100  $\mu$ M). Images representative of 4 images.**

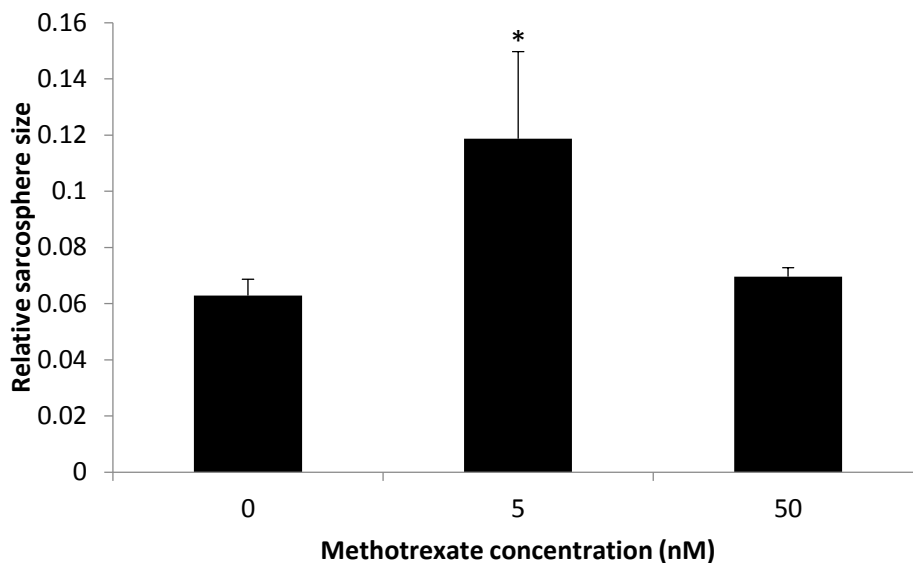


**Figure 4.20: Analysis of primary sarcosphere size in MG63.** Five images per well were analysed using ImageJ. 5 nM MTX treated cells contained significantly larger colonies. Significance calculated by comparing each treatment sarcosphere size using Tukey's post hoc analysis (\* $p < 0.05$ ), 5 nM sarcospheres significantly larger than 0 nM and 50 nM. Results tested in triplicate and presented as mean and standard deviation.

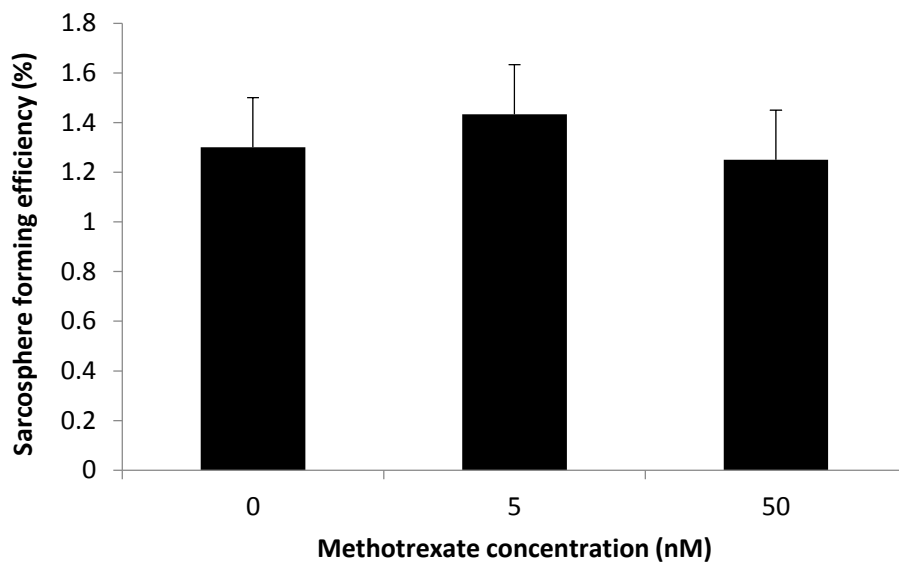


**Figure 4.21: Analysis of secondary sarcosphere forming efficiency.** Sarcosphere forming efficiency was calculated by counting all spheres  $\geq 40 \mu\text{M}$  and dividing this by the number of cells seeded. No significant difference was observed (Tukey's post hoc analysis). Results tested in triplicate and presented as mean and standard deviation.

#### 4.10 Effect of ALDH inhibition on methotrexate sensitivity upon selected OS cell lines and MCF7

ALDH has been identified as not only a OS CSC marker (Wang et al., 2011) but also as a mechanism to enhance chemo-resistance (Honoki et al., 2010) (Section 1.3.4). The ALDH specific inhibitor diethylaminobenzaldehyde (DEAB) has been used *in vitro* to sensitise breast cancer cells to chemotherapeutics (doxorubicin and paclitaxel) and radiation (Croker and Allan, 2012). To identify if DEAB also sensitises OS cell lines to chemotherapeutics the toxicity of DEAB was first assessed to obtain LD<sub>50</sub> concentrations for each cell line. The cell lines HOS, MG63, U2OS and MCF7 were selected because the OS cell lines represent each morphology (fibroblastic, epithelial and mixed) and MCF7 for comparison to a commonly used epithelial breast cancer cell line. DEAB LD<sub>50</sub> were assessed by exposing cells seeded at high density (15600 cells/cm<sup>2</sup>) to DEAB for 2 days then assessing cell death using an MTT assay (Section 2.3.1).

MG63 had the highest DEAB LD<sub>50</sub> whilst MCF7 had the lowest (Table 4.4). Interestingly sensitivity to DEAB did not correlate with the level of ALDH expression in each cell line (Table 4.9) as HOS which had the highest ALDH expression was not the most effected by DEAB. This suggests that the ALDH population size does not dictate DEAB sensitivity. No enhancement in drug sensitivity upon HOS, U2OS and MCF7 was observed when a DEAB concentration equivalent to the LD<sub>50</sub> for each cell line was combined with MTX at an LD<sub>25</sub>. In contrast, a reduction in MG63 cell viability was observed when comparing exposure to DEAB and MTX against MTX and a vehicle control (ethanol) (Figure 4.23). This observation suggests that the ALDH cells in MG63 may have an elevated MTX resistance, however the reduction is small and extending the length of time exposed to MTX and DEAB may enhance this effect. Cisplatin and doxorubicin co-exposure with DEAB experiments were only tested in HOS and U2OS, however, each drug effected cell lines in different ways. Cis and DEAB co-exposure caused a reduction in U2OS cell viability (figure 4.24), whilst dox co-exposure reduced HOS cell viability. This indicates that the ALDH cells from U2OS are attributing to cis resistance, whilst HOS ALDH are dox resistant (figure 4.25). This finding implies that ALDH populations within different OS cell lines are resistant to different drugs.

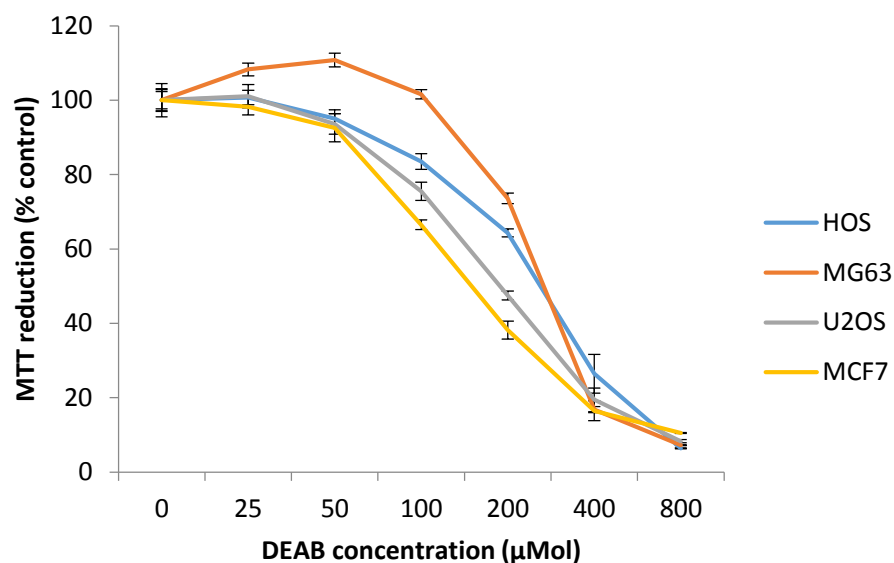


**Figure 4.22: DEAB dose response curve of HOS, MG63, U2OS and MCF7.** Cell lines were grown for 2 days in DEAB, before assessing cell number using an MTT assay. Linear regression was used to DEAB LD<sub>50</sub> for each cell line. Results tested in triplicate in three separate experiments (n = 3 independent replicates). Data presented as mean and standard error.

**Table 4.4: DEAB LD<sub>50</sub> concentrations and percentage of cells expressing ALDH HOS, MG63, U2OS and MCF7.** Percentage of cells expressing ALDH was assessed in section 3.2.2. Statistical significance calculated using Tukey's post hoc analysis (\*\*p = <0.01) and comparing all cell lines to one another. HOS has statistically larger ALDH expressing population than MCF7, MG63 and U2OS. No significant difference was observed when comparing DEAB LD<sub>50</sub> concentrations.

Cell line	DEAB LD <sub>50</sub> µMol ± Std error	% of cells expressing ALDH ± Std deviation
HOS	94.03 ± 19.14	60.60 ± 9.67 **
MG63	115.83 ± 63.56	2.14 ± 0.14
U2OS	87.25 ± 12.58	2.13 ± 0.78
MCF7	81.30 ± 7.78	2.36 ± 0.35



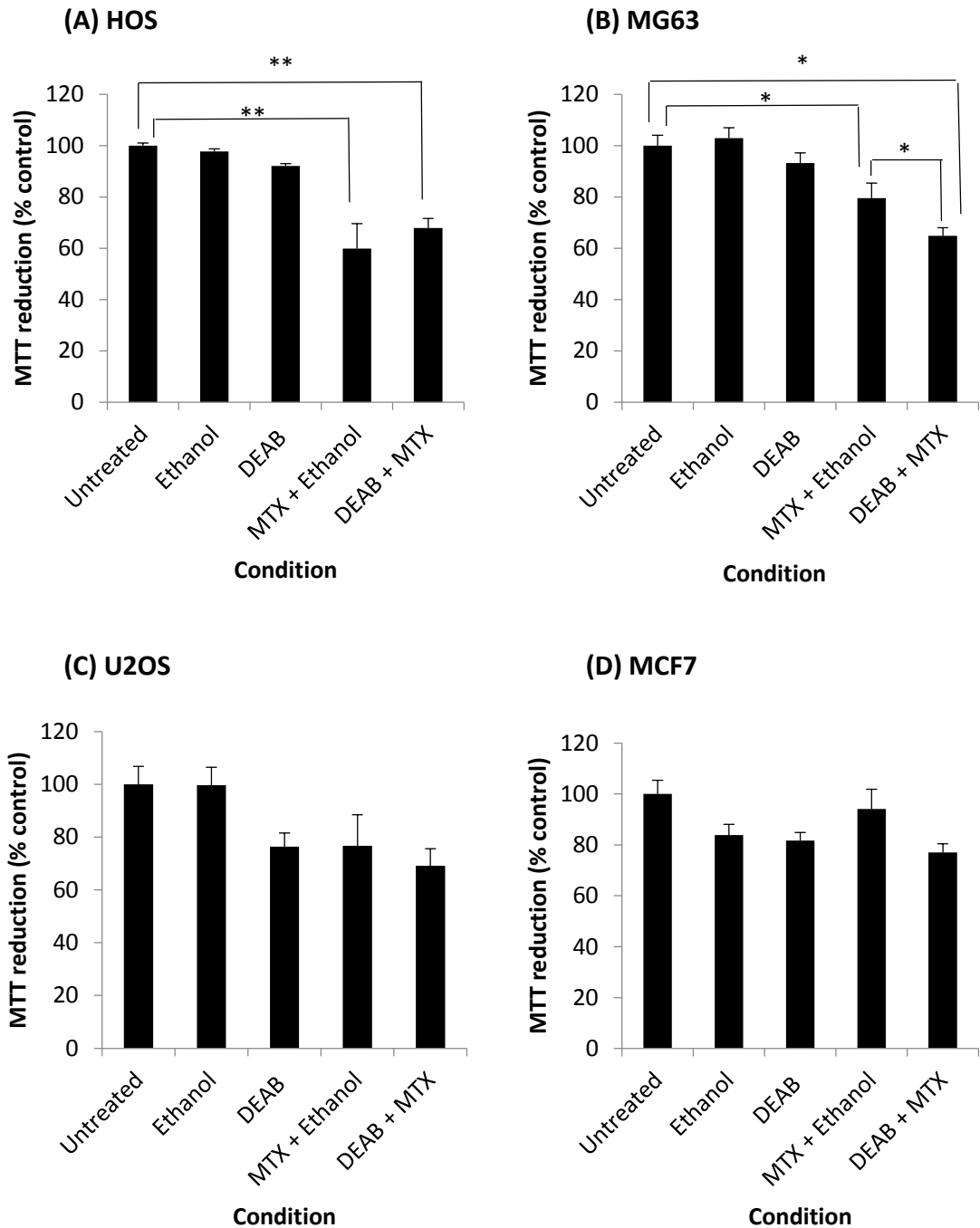


**Figure 4.23: Cell sensitivity to MTX LD<sub>25</sub> and DEAB LD<sub>50</sub> in HOS, MG63, U2OS and MCF7.** The cell lines A) HOS, B) MG63, C) U2OS and D) MCF7 were exposed to their specific DEAB LD<sub>50</sub> concentration and MTX LD<sub>25</sub> concentration. Ethanol was used to as a vehicle control for the DEAB. Significance calculated using Tukey's post hoc analysis (\*p = 0.05 and \*\*p = < 0.01). Each result was tested in triplicate in three separate experiments (n = 3), data presented as mean and standard error.

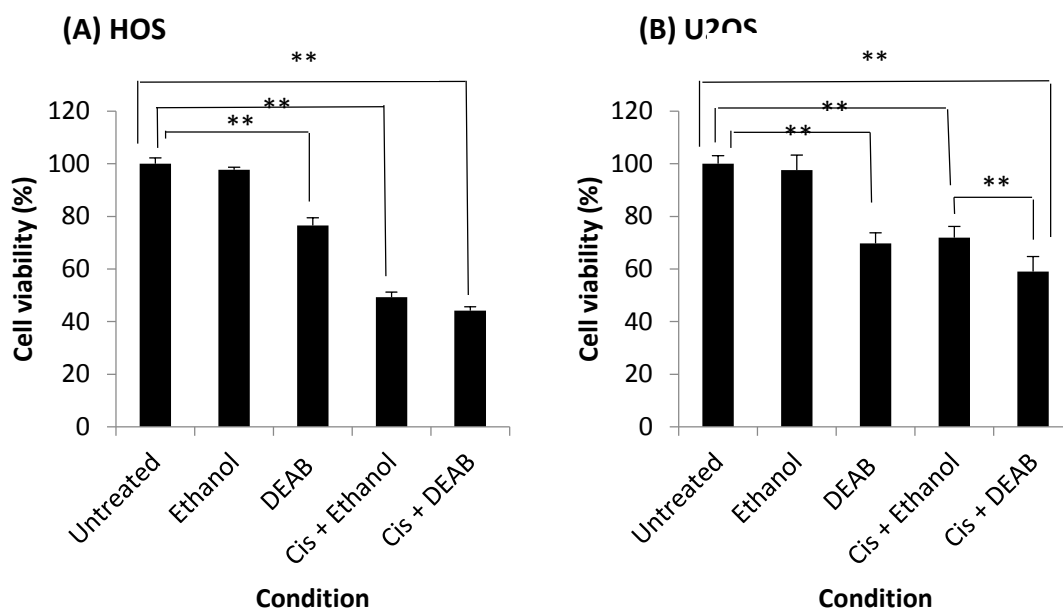


**Figure 4.24: Cell sensitivity to cis LD<sub>25</sub> and DEAB LD<sub>50</sub> in HOS and U2OS.** The cell lines A) HOS and B) U2OS were exposed to their specific DEAB LD<sub>50</sub> concentration and cis LD<sub>25</sub> concentration. Ethanol was used as a vehicle control for DEAB. Significance calculated using Tukey's post hoc analysis (\*p = <0.05, \*\*p = <0.01). Each result was tested in triplicate, data presented as mean and standard deviation.

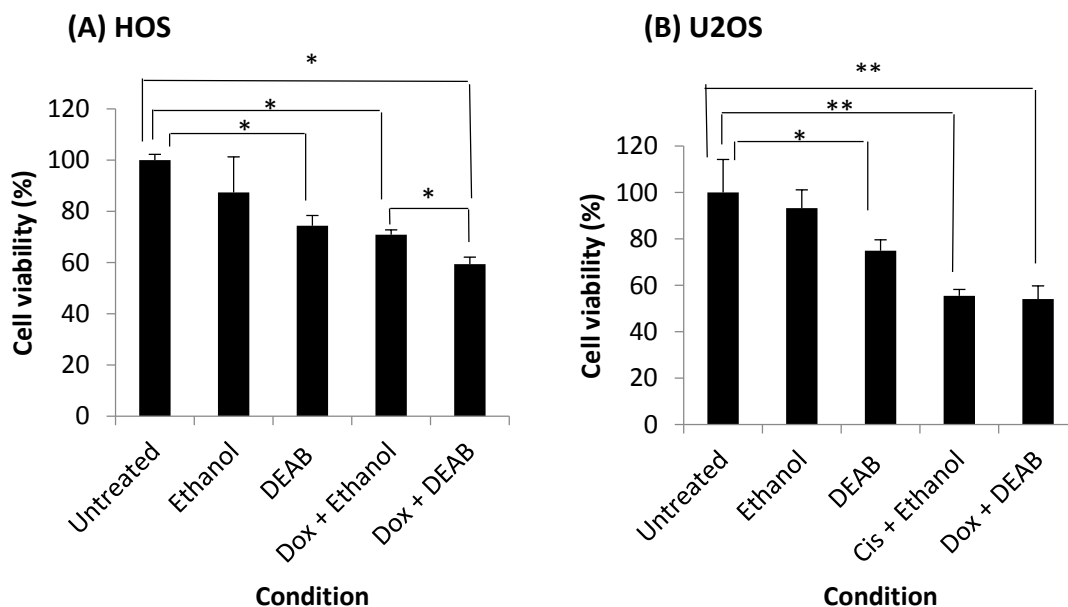


**Figure 4.25: Cell sensitivity to dox LD<sub>25</sub> and DEAB LD<sub>50</sub> in HOS and U2OS.** The cell lines A) HOS and B) U2OS were exposed to their specific DEAB LD<sub>50</sub> concentration and cis LD<sub>25</sub> concentration. Ethanol was used as a vehicle control for DEAB. Significance calculated using Tukey's post hoc analysis (\*p = <0.05, \*\*p = <0.01). Each result was tested in triplicate, data presented as mean and standard deviation.

### 4.11 Discussion

OS cell lines were tested for their sensitivity to three commonly used OS chemotherapeutics, the drugs cisplatin (cis), doxorubicin (dos) and methotrexate (MTX). Cell lines demonstrated differing sensitivities depending upon the drug used, which is attributed to the mechanism of toxicity utilised by the drug and mutations present within each cell line, conferring either resistance or susceptibility (Holohan et al., 2013). In response to the DNA intercalating agent cis U2OS had the highest LD<sub>50</sub> of 18 µM, which is consistent with published data in which U2OS was found to have a cis LD<sub>50</sub> of 17.6 µM (Martelli et al., 2007). Interestingly Martelli *et al* (2007) also found that having a wild type *p53* conferred greater resistance than a mutant copy. *p53* status may be relevant as MCF7 (Fan et al., 1995) and U2OS with the largest cis LD<sub>50</sub> were the only cell lines with wild type *p53*, the remaining cell lines contain a mutant copy and in particular, G292, MG63 and SaOS-2 completely lack endogenous P53 (Chen et al., 1990, Chandar et al., 1992). Functional P53 has been found to protect against cis cell death by repairing cis induced DNA lesions (Fan et al., 1995). Interestingly Fan *et al* (1995), identified that an operational G2 checkpoint compensates for loss of *p53* by providing a mechanism to repair drug induced DNA lesions. 143B has the lowest cis LD<sub>50</sub> of 3.8 µM it expresses a mutant P53 (Mohseny et al., 2011, Ottaviano et al., 2010) and is also the most rapidly dividing OS cell line (Fawdar, 2010), therefore, loss of P53 function and decreased G2 checkpoint may be accounting for its elevated sensitivity to cis.

*p53* status may also contribute to resistance to the DNA intercalating agent Dox but using an opposing mechanism to cis resistance. Dox DNA damage in cells with wild type *p53* induces apoptosis through activation of the caspase cascade with activation of Bax leading to outer membrane pore formation and release of cytochrome C (Katiyar et al., 2005). In OS, loss of *p53* leads to doxorubicin resistance due to an inability to activate caspase 3 in response to DNA damage (Tsang et al., 2005). Results presented in this chapter showed that MG63 had the highest dox LD<sub>50</sub> and lacking endogenous *p53* (Chandar et al., 1992) supports this finding, however, MCF7 and U2OS with the third and fifth highest dox LD<sub>50</sub> and functional *P53* do not support this hypothesis. The protein Bcl-2 is commonly up-regulated in OS and has been identified as a means of overcoming doxorubicin apoptosis.

This occurs through inhibition of cytochrome C release and reducing the formation of Bax-Bax homodimers which insert in the outer mitochondrial membrane which leads to pore formation in response to DNA damage. Inhibiting Bcl-2 in MG63 has been found to sensitise cells to dox treatment (Zhao et al., 2009). The nucleolar protein neuroguidin/CANu1 is upregulated in U2OS and provides increased doxorubicin resistance (Park et al., 2011a). Although the pathway through which neuroguidin/CANu1 signals is unclear it has been hypothesised to inhibit p21 and stabilize Bcl-2, therefore up-regulation of Bcl-2 maybe one mechanism through which U2OS can resist dox even with the presence of a wild type *P53* gene.

SaOS-2 was the most resistant to the dihydrofolate reductase (DHFR) inhibitor MTX, producing a MTX LD<sub>50</sub> of 0.09 µM and HOS had the lowest LD<sub>50</sub> of 0.02 µM. Two common mechanisms of OS MTX resistance is the down regulation of the folate receptor (FC) present in 65% of tumours and over expression of the enzyme DHFR (Guo et al., 1999). Over expression of DHFR has been attributed to a gene frequently altered in OS, retinoblastoma (*Rb*). *Rb* negatively regulates the expression of E2F transcription factors which increase the expression of cell cycle proteins such as DHFR (Li et al., 1997). SaOS-2 has a defective copy of *Rb* (Ory et al., 2007), whilst in contrast HOS and U2OS with the lowest MTX LD<sub>50</sub> both have functional *Rb* (Serra et al., 2004), therefore, loss of *Rb* and up-regulation of DHFR could be one mechanism for enhancing OS MTX resistance. However, other factors such as down regulation of the folate receptor in *Rb* negative cells have also been found to be important in MTX resistance (Serra et al., 2004).

Following chemotherapy treatment breast cancers have been shown to be enriched in cells expressing CSC markers (Creighton et al., 2009), which suggests that CSC have enhanced resistance to chemotherapeutics. In order to identify if cis or dox exposure led to an enrichment of cells with enhanced clonogenicity, the colony formation of U2OS, MG63, U2OS and MCF7 in response to cis or dox LD<sub>50</sub> exposure was assessed. Due to the toxicity of the LD<sub>50</sub> concentrations no colonies formed, reducing the concentration to an LD<sub>25</sub> also produced no colonies due to cell death. The reason for this observation may be related to cis and dox causing cell death via DNA intercalation. Therefore, cell death is delayed until cell division occurs and the LD<sub>50</sub> concentrations obtained from the dose response curves

overestimate the number of living cells. Allowing cells to recover from cis and dox exposure before assessing the cell death could have been used to minimise this effect. Another factor which may be important for cell resistance to chemotherapeutics is interaction with surrounding cells. It was found that after cells were exposed to cis and dox and re-seeded at high density, colonies would survive for a short period (9 days) if they made contact with surrounding cells. Surviving cells had a fibroblastic morphology with dendrites connecting cells to one another. A similar observation has been observed OS cell lines in response to MTX treatment, whereby the surviving cells had a fibroblastic appearance and were characterised by the presence of dendrite-like structures (Tang et al., 2011).

Cis and dox exposure enhanced the PE auto-fluorescence of treated cells, making analysis of CSC markers impractical because this change in cell appearance would mask that of cells stained with fluorophores and dyes utilising the PE channel. Flow cytometry analysis of either CD44 expression or the presence of dead cells (based on propidium iodide staining) was inaccurate, as both the CD44 PE conjugated antibody and propidium iodide required the PE channel for analysis. As a consequence the flow cytometry analysis of cis and dox treated cells was abandoned.

MTX has been successfully used to enrich a population of putative OS CSC with enhanced clonogenicity and CD117 expression in U2OS and MG63 cell lines (Tang et al., 2011). The same experimental design was used in section 4.4, where cells were exposed to MTX and then re-seeded at low density. The concentration of MTX used by Tang *et al* (2011) of 660 nM and 220 nM, formed no colonies so a concentration of 5 nM and 50 nM was used instead. The reason for this discrepancy is unknown, MTX was sourced from the same supplier, therefore, MTX batch variation could be contributing to this observation although unlikely. The appearance of cells which survived in 50 nM MTX had a fibroblastic appearance as observed by Tang *et al* (2011) in response to high (220 nM and 660 nM) MTX concentrations. However, only MCF7 and MG63 produced colonies in the 50 nM MTX, and no difference in colony size was observed across the MTX concentrations. This suggests that the MTX treated cells have the same growth rates as untreated cells. The colony hierarchies can be used to assess the presence of putative CSC through the identification of holoclones (Li et al., 2008). Using this method MTX treated cells were compared to

identify if exposure increased the presence of putative CSC. Across all cell lines tested no significant increase in holoclones or any other hierarchy was observed suggesting that MTX is not selecting for a specific colony hierarchy. Within HOS a decrease in holoclones was observed in response to 5 nM MTX, this indicates that HOS holoclones have an enhanced sensitivity to MTX. Holoclones have been identified to contain CSC in the prostate cancer cell line PC3 (Li et al., 2008), if CSC also reside in HOS holoclones, this could account for this cell line having the lowest MTX LD<sub>50</sub> because MTX induced loss of CSC would inhibit HOS growth and survival. If this hypothesis is correct it would indicate that ALDH is not a CSC marker in HOS, because ALDH<sup>+</sup> cells were present in all three colony hierarchies (Section 3.6.1).

The study by Tang *et al* (2011) found that MTX treated U2OS cells had an increased expression of CD117 and stro-1 and additionally ALDH expression has been found to confer MTX resistance (Takebe et al., 2001). To identify if exposure to MTX enriched for expression of these putative CSC markers after MTX treatment, cells were stained for CSC marker expression and analysed using flow cytometry. CD117 expression was enhanced in both U2OS and MG63 as neither cell line expressed the protein without MTX, whereas both 5 nM and 50 nM MTX treatment led to the emergence of a CD117 population. In MG63 the CD117 population was largest at 5 nM with 0.45 % of cells expressing the marker and then significantly decreased at 50 nM to 0.02 %. U2OS contained a CD117 population of approximately 0.1 % at both 5 and 50 nM. Possible mechanisms through which OS CD117 expressing cells resist chemotherapeutics is via increased expression of ATP binding cassette transporters. This has been identified in OS and has been implicated in the efflux of chemotherapeutics and development of tumours with multi-drug resistance in CD117 expressing cells (Adhikari et al., 2010).

ALDH expression was increased 20 fold in HOS at all concentrations of MTX compared to other cell lines, which reflects the large population of ALDH expressing cells present within HOS (section 3.2.2). HOS was the only cell line which did not have an increase in ALDH expressing cells in response to MTX. This suggests that either HOS ALDH expressing cells do not have enhanced MTX resistance or alternatively the high ALDH expression observed in HOS (Section 3.2.2) may be due to its deregulated expression, therefore, is unable to be

elevated in response to chemotherapeutics. In contrast MG63, U2OS and MCF7 all had an increase in ALDH expression at 50 nM MTX, with MG63 also presenting an increase at 5 nM MTX. Therefore ALDH expression in these cell lines appears to be related to MTX resistance. ALDH has been proposed to confer chemotherapeutic resistance in OS via drug detoxification, enhanced DNA repair mechanisms and overexpression of cell membrane drug efflux transporters (Honoki et al., 2010).

The observed increase in ALDH expression in response to MTX appears to be a result of the experimental design. Cells were seeded at a high density (15600 cells/cm<sup>2</sup>) allowed to attach for 24 hours before MTX was added to cells and exposed for 5 days, cells at low concentrations of MTX would become over confluent, to test whether this over confluency effects ALDH expression cells were seeded at a range of densities and then grown for 6 days before analysing ALDH expression. In both MG63 and MCF7 cell lines increasing density was found to decrease ALDH expression. Interestingly MG63 had lower expression at 5263 cells/cm<sup>2</sup>, whilst MCF7 did not, which may represent the faster rate of MG63 division which allows it to become confluent at the lower cell density. This observation also occurs when OS cell lines are murine xenotransplanted, as a dramatic reduction in ALDH expression is observed in the resulting *in vivo* derived tumours than the original cell line (Wang et al., 2011). The decrease in ALDH expression was attributed to the change in growth conditions during xenotransplantation, however, the results in this chapter suggest that cell density is also a contributing factor. At high cell density ALDH expression is decreased, the mechanism by which ALDH expression is controlled could be via a cytokine network. In breast cancer IL-8 signaling via phosphoinositide 3-kinase has been found to enhance the presence of ALDH expressing CSC (Singh et al., 2013). Targeting IL-8 could therefore provide a mechanism to target CSC (Ginestier et al., 2007).

To assess whether MTX exposure could increase the presence of putative CSC, a sarcosphere assay was used to test the sphere forming ability of MG63 after MTX exposure. MG63 was selected because of its ability to form secondary sarcospheres (section 3.7.2) and the enrichment of both ALDH and CD117 expressing cells in response to MTX. In OS cell lines increased sarcosphere forming ability correlated with enhanced tumourigenic capabilities *in vivo* (Rainusso et al., 2011). The sarcosphere assay therefore provides a

method for identifying if the increased expression of CSC markers is related to an increased presence of putative CSC. Results from the previous chapter demonstrate that large sarcospheres contained a higher proportion of cells expressing the putative CSC marker ALDH (Section 3.8.1), which indicates that ALDH expressing cells may drive sarcosphere growth. Images taken of primary sarcospheres from cells treated without MTX and 5 nM MTX, demonstrated both conditions produced sarcospheres with the same spherical rough appearance, however 50 nM treated cells produced less regular sarcosphere shapes which were not spherical. MG63 has been found to contain a heterogenous population of cells all with varying tumorigenicities, drug resistance and holoclonal morphologies (Lou et al., 2010). Therefore, the change in shape of 50 nM MTX sarcospheres could reflect the selection of a particular MG63 drug resistant subpopulation. MTX 5 nM treated MG63 cells produced larger primary sarcospheres than 0 nM and 50 nM MTX treated cells. This observation suggests that exposure at 5 nM MTX enriches spherical colony forming cells, however the same effect is not observed at 50 nM MTX. Upon passage of these sarcospheres and subsequent growth of secondary sarcospheres, the presence of increased spherical colony formation was lost and both 5 nM and 50 nM MTX treatments resulted in similar sarcosphere formation. Tang *et al* (2011) found that 220 nM and 660 nM MTX treatment also led to increased sarcosphere formation of MG63 cells, however, only primary colony formation was assessed. Therefore, MTX may transiently increase the presence of sarcosphere forming cells, which is lost upon passage and growth of secondary sarcospheres. OS cell lines have been demonstrated to contain putative CSC which are quiescent (Rainusso et al., 2011), in breast cancer mammospheres can only be passaged 5 times before growth is inhibited through quiescence (Dey et al., 2009). Passaging of MG63 sarcospheres, therefore, may lead to CSC cells undergoing quiescence which could account the reduction in sarcosphere forming efficiency in 5 nM MTX treated secondary sarcospheres.

MTX 5 nM treated MG63 cells not only had enhanced primary sarcosphere formation but also increased expression of CD117 and ALDH. Both CD117 and ALDH have been implicated in OS CSC and enhanced drug resistance (Adhikari et al., 2010, Wang et al., 2011, Honoki et al., 2010), therefore the expression of these markers within the cell lines may correlate with drug resistance. This hypothesis was tested using Pearson's correlation coefficient cell



line LD<sub>50</sub> concentrations were correlated with CSC marker expression (ALDH and CD117) (section 3.2). CD117 expression correlated weakly with dox and MTX, but produced a strong negative correlation with cis, suggesting that CD117 expression is not related to drug resistance. This poor correlation may be related to highly expressing CD117 cell lines such as 143B not displaying resistance to these drugs. To explore this hypothesis 143B with the highest CD117 according to flow cytometry analysis expression (6.36 %) (Section 3.2.3) was removed from analysis, which produced weaker correlations and produced Pearson's correlations closer to 0 for all chemotherapeutics. CD117 expressing cells from this cell line appeared to be more sensitive to the drug exposure, therefore producing low LD<sub>50</sub> values. CD117 expression correlated weakly with dox and MTX LD<sub>50</sub>, therefore, CD117 expressing cells are susceptible to cis but not dox or MTX, indicating that CSC could be targeted using specific drugs. Cell line ALDH expression correlated with a weak negative correlation with cell line LD<sub>50</sub> for all drugs tested, no statistical significance was observed for any of the correlations, suggesting increased cell line ALDH expression has no impact upon chemotherapeutic resistance.

ALDH expression has been demonstrated to enhance chemotherapeutic resistance (Honoki et al., 2010), the mechanism by which ALDH isoenzymes provide chemoresistance has not been fully elucidated for all ALDH isoenzymes. ALDH enzymes detoxify aldehyde compounds, which may be common drug resistance mechanism to all ALDH enzymes (Moreb et al., 2012). In the human corneal cell ALDH3A1 is also localised to the nucleus and in response to DNA damage has been found to inhibit cell division and promote cell survival (Pappa et al., 2005). It is unclear if all ALDH enzymes are involved with cell cycle control, however, if so this may indicate that ALDH enzymes are intricately involved with chemoresistance. The hypothesis that ALDH positive cells are more resistant to chemotherapy can be tested using the specific ALDH inhibitor DEAB, which has been identified as a competitive inhibitor of ALDH1 and ALDH2 enzymes (Moreb et al., 2012). This procedure has been successfully used by Crocker and Allan (2012), they exposed ALDH<sup>+</sup>/CD44<sup>+</sup> breast cancer cells and found that this sensitised them to dox and the mitosis inhibitor paclitaxel (Crocker and Allan, 2012). To analyse whether DEAB has the same effect in OS cell lines the toxicity of DEAB for the selected cell lines (HSO, MG63, U2OS and MCF7) was identified. The LD<sub>50</sub> for DEAB identified MG63 as the most resistant with an LD<sub>50</sub> of

115.83  $\mu\text{Mol}$  and MCF7 as the least with an  $\text{LD}_{50}$  of 81.30  $\mu\text{Mol}$ . Interestingly ALDH population size did not reflect sensitivity to DEAB, HOS with the largest population of ALDH positive cells > 60 % (Section 3.2.2) was not the most susceptible to DEAB with the second largest DEAB  $\text{LD}_{50}$  of 94.03  $\mu\text{Mol}$ . In comparison MG63 with one of the smallest ALDH populations (2.14 %), was most resistant to DEAB. The Aldefluor kit is a pan ALDH detection kit. Therefore, the specific ALDH detected is not known, however, it would be of interest to analyse if OS cell lines express the same ALDH isoforms and whether different isoforms are responsible for OS chemotherapy resistance.

To identify if ALDH expression through DEAB sensitised cell lines to chemotherapeutics, OS cell lines and MCF7 were exposed to their DEAB  $\text{LD}_{50}$  concentration in combination with the chemotherapeutic  $\text{LD}_{25}$ . When combining DEAB with MTX an increase in cell death was only observed in MG63, no increase in cell death was observed in the remaining cell lines (HOS, U2OS and MCF7). Suggesting that only MG63 ALDH cells comprise a MTX resistant population of cells. When co-incubating DEAB with cis or dox (DEAB + cis/dox) the OS cell lines responded differently. HOS ALDH cells were sensitive to dox, whilst U2OS to cis, suggesting that the ALDH cells present within each OS cell line may be sensitive to a different drug. The CSC phenotype within cancer subtypes or even the same subtype is not uniform (Visvader and Lindeman, 2008), within breast cancer cell lines ALDH was not found to be a marker of increased tumorigenicity in all cell lines tested (Hwang-Versluis et al., 2009). Breast CSC have also been found to be more sensitive than the bulk population of cells to cyclophosphamide, treatment with this drug reduced the ALDH population of cells and led to reduced tumour formation (Zielske et al., 2010). These findings highlight the highly variable nature of CSC within the same cancer types and different responses they can have to specific drugs.

A limitation of DEAB exposure as a mechanism for reducing the presence of putative CSC, is the affect DEAB has upon the balance between CSC division and differentiation. Assuming ALDH expressing cells are CSC, treating them with DEAB may not be an efficient mechanism for reducing the CSC population. Breast cancer studies have demonstrated that treating cell lines with DEAB actually increases the CSC population, this finding appears counterintuitive but could be explained due to ALDH being a requirement for early

differentiation. Therefore inhibition of this enzyme results in the inhibition of differentiation and an increase in the size of the CSC population (Ginestier et al., 2009).

To summarise the findings of this chapter OS cell lines display heterogeneous sensitivities to the chemotherapeutic agents (cis, dox and MTX) and P53 status may be a determining factor. Functional P53 may protect against cis conversely P53 loss may contribute to dox resistance. Previous studies have demonstrated that MTX exposure enriches cells with CSC properties (Tang et al., 2011), results from this chapter show that MG63 cells treated with 5 nM MTX have an increased primary spheroid proliferation rate. In response to MTX treatment both U2OS and MG63 increased expression of the putative CSC markers CD117 and ALDH. The increased ALDH expression was found to be attributed to increased cell density and not MTX in MG63 and MCF7. To further examine the role ALDH plays in chemotherapeutic resistance the ALDH inhibitor DEAB was combined with LD<sub>25</sub> concentrations of cis, dox and MTX. In response to DEAB MG63 was sensitised to MTX, U2OS to cis and HOS to dox. This finding highlights that the ALDH expressing cells within different OS tumours are sensitive to different classes of chemotherapeutics.

# **Chapter 5**

## **Characterisation of paracrine growth signalling utilised by osteosarcoma cells**

## 5.1 Introduction

The development and maintenance of all cells within every organ of the body is tightly regulated by a complex network of protein signaling molecules (ligands) (Orsi and Tribe, 2008). These ligands are recognised by cell membrane spanning receptors, which allow signal transduction to occur upon ligand receptor interaction. The location of the cell which releases the ligand will dictate the type of cell signaling, therefore four types of signaling can occur; autocrine, juxtacrine, paracrine and endocrine (Singh and Harris, 2005) (Section 1.4).

Bone is a highly specialised tissue which plays a crucial role in internal support and maintaining calcium homeostasis (Weiner et al., 1999). Bone is composed of three cell types; osteoblasts which can regulate the mineralisation of bone and are found near the bone surface along with osteoclasts which are responsible for bone resorption. Osteoblasts can differentiate to become osteocytes which are found within the bone interior, these cells are responsible for the synthesis of the bone matrix and to a lesser extent bone resorption (Bilezikian et al., 2008). Therefore, signaling networks within bone are focused on ensuring bone resorption and synthesis is balanced. For example Wnt ligands have been found to affect bone density in mice through their effect on osteoblasts (Bodine et al., 2004), whereas osteoblasts have been found to release RANK which increases osteoclast bone resorption (Burgess et al., 1999) and osteoprotegerin which inhibits this process (Schoppet et al., 2002) (Section 1.4.1).

Cell signaling that stimulates cell proliferation is a common mechanism by which cancer cells promote growth. Cancer cells have been found to utilise a variety of signaling mechanisms (section 1.4.2). Holoclones from the OS cell line HOS have been found to secrete a paracrine factor which helps support the growth of paraclonal cells, which suggests that differentiated OS cells are reliant upon progenitor cells for survival, however the identity of this factor was never established (Fawdar, 2010). A number of cytokines involved in tumour progression have been identified in OS including phosphoglucoisomerase (PGI), which has been found to enhance migration and growth of the cell line MG63 (Niinaka et al., 2010) (Section 1.4.3). Hepatocyte growth

factor, which is released by several OS cell lines (Cal72, MG63 and SaOS-2) has been hypothesised as a mechanism to promote the aggressive nature of OS tumours (Rochet et al., 1999).

### **Aims**

HOS holoclonal cells have been shown to secrete a paracrine factor which supports the growth and survival of paraclones (Fawdar, 2010), however, the cytokine network responsible for this observation was not established. In order to elucidate the cytokines responsible for OS growth a panel of OS cell lines will be used to analyse media conditioned by the cell lines (cell line conditioned media) for the presence of growth factors. Conditioned media with growth enhancing properties will be screened for the presence of candidate proteins. The specific objectives of this study which will be tested upon a panel of 8 OS cell lines and the breast cancer cell line MCF7 as a control, are as follows:

- Assessment of OS cell lines and MCF7 proliferation rates in response to conditioned media taken from the same or different cell lines.
- Identification of candidate growth factors through the cytokine expression analysis of growth enhancing conditioned media.
- Analysis of the expression profile of candidate growth factors from cell lines.

## 5.2 Paracrine signaling in OS cell lines and MCF7 in response to 24 hour conditioned media

To assess whether the OS cell lines utilised paracrine signalling to enhance growth, each cell line was grown at low cell density in the absence and presence of its own conditioned media (conditioned media was collected after 24 hours exposure to confluent cells) (Section 2.4.1). Upon reaching a suitable colony size (approximately 1 - 2 mm) colonies were fixed and stained with crystal violet and colony size was assessed using ImageJ (Section 2.4.2). The majority of OS cell lines produced a significant increase in colony size in response to conditioned media (Figure 5.1), however, 143B, HOS, and MCF7 did not respond to their conditioned media whereas MG63 produced the largest increase in colony size in response to its own conditioned media.

To determine if the paracrine effect is unique to each cell line the conditioned media from a selected cell line was tested upon another. The media from two cell lines which responded with an increase in colony size (U2OS and MG63) were compared with a non-growth enhancing conditioned media (HOS and MCF7) in the following cell lines; MG63, U2OS, HOS and MCF7. U2OS and MG63 conditioned media produced equal growth enhancement in responsive cell lines (MG63 Figure 5.2.A and U2OS Figure 5.2.B). U2OS media was found to evoke a significant increase in growth of the previously unresponsive HOS cell line (Figure 5.2.C) and also in MCF7 (Figure 5.2.D), suggesting that U2OS secretes a growth factor which is common to other OS cell lines and also the unrelated MCF7 cells. In all OS cell lines tested MCF7 conditioned media had no effect on colony formation, suggesting that it lacks the expression of a growth enhancing factor. Interestingly, HOS conditioned media, which did not enhance growth of HOS and MCF7, produced an increase in growth in MG63 and U2OS (Figure 5.2.A and 5.2.B). This indicates that HOS may produce low levels of a growth factor which may only be detected by MG63 and U2OS.

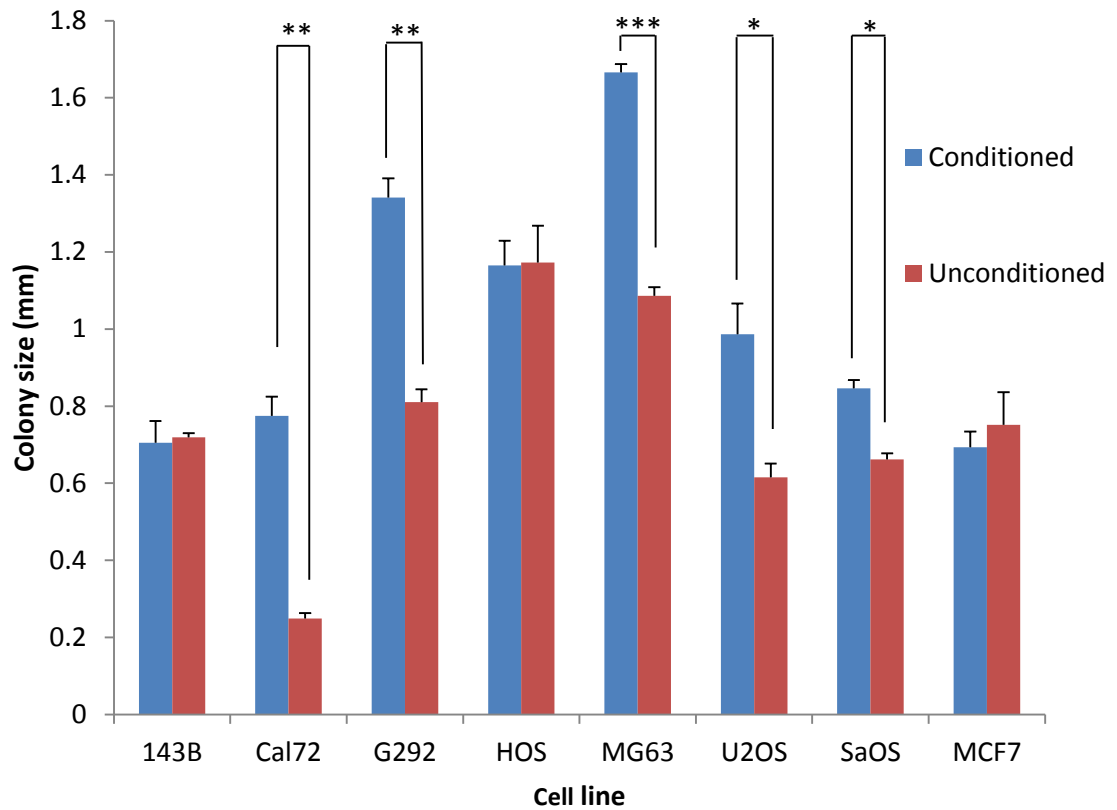


**Figure 5.1: Average colony size of OS cell lines and MCF7 exposed to either conditioned (collected after 24 hours exposure to confluent cells) or unconditioned media.** Only 143B, HOS and MCF7 did not respond to their conditioned media and had no significant increase in colony size. All OS cell lines and MCF7 tested have been analysed by measuring colony size using ImageJ®. Data presented as mean and standard deviation, n=3 (\* = 0.05, \*\* = 0.005 \*\*\*= 0.0005; unpaired T-test).



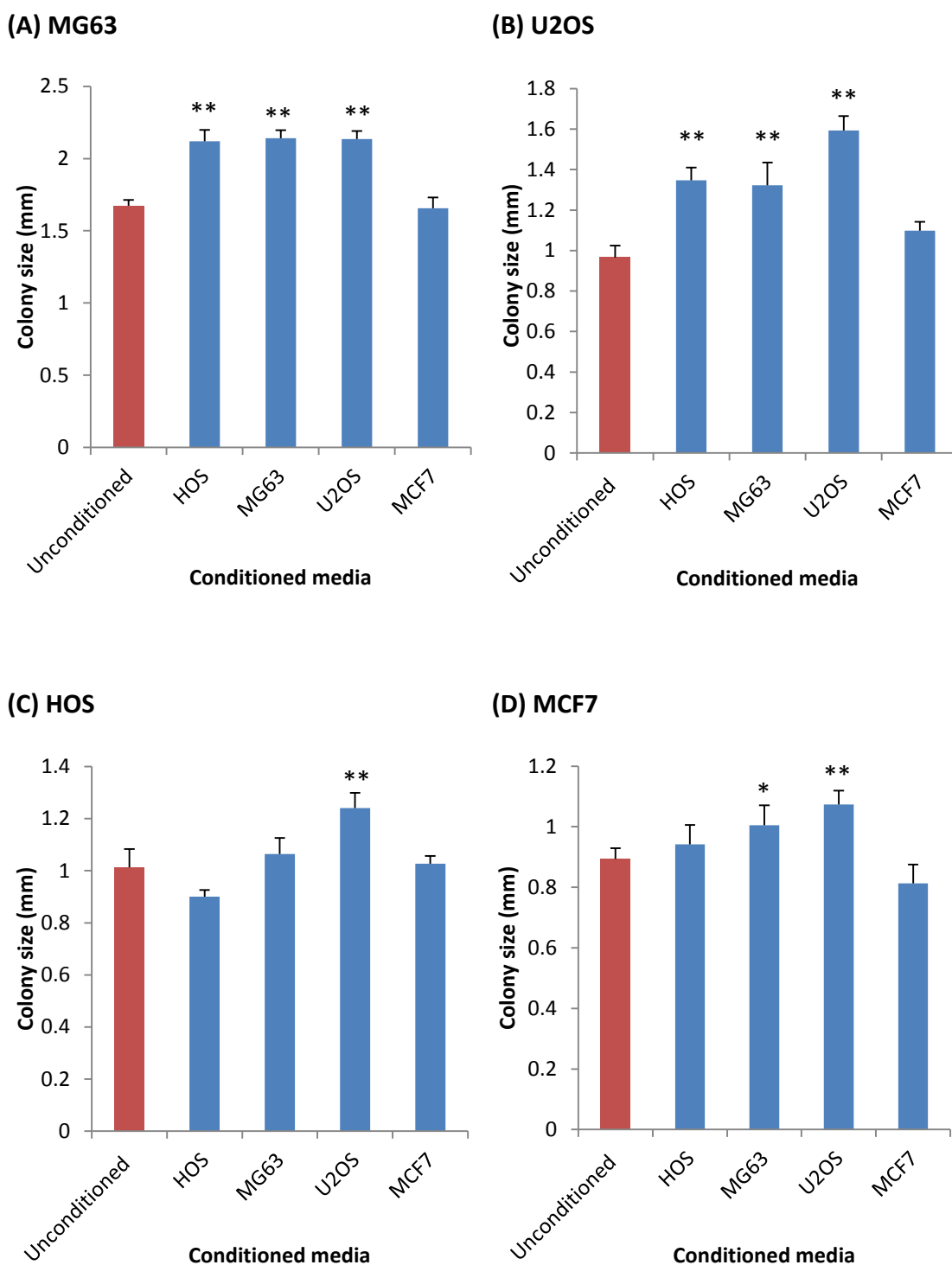


**Figure 5.2: Response of HOS, MG63, U2OS and MCF7 cells to 24 hour conditioned media from growth increasing and non-growth responsive conditioned media.** MG63 (A), U2OS (B), HOS (C) and MCF7 (D) cell lines tested using unconditioned and conditioned media from each cell line to assess the growth enhancement of each cell line. Colony size was assessed using ImageJ. Data presented as mean and standard deviation (n=3), significance calculated by comparing to MCF7 conditioned colony size (\* = <0.05, \*\* = <0.01; Tukey's post hoc analysis).

### 5.3 Assessment cell density during 24 hour media conditioning for HOS, MG63, U2OS and MCF7 cells

The cell density during the conditioning of the media was assessed in order to determine if the growth enhancement of conditioned media from MG63 and U2OS (Figure 5.2) was related to an increased number of cells at confluency. After 24 hours of conditioned media collection (Section 2.4.1) HOS, MG63, U2OS and MCF7 cells density was assessed through cell trypsinisation and counting using a haemocytometer. It was found that MCF7 contained a higher density of cells compared to the OS cell lines (Figure 5.3). The OS cell lines all contained similar cell densities, suggesting that the number of cells present is not responsible for the variation in growth enhancing properties of conditioned media.

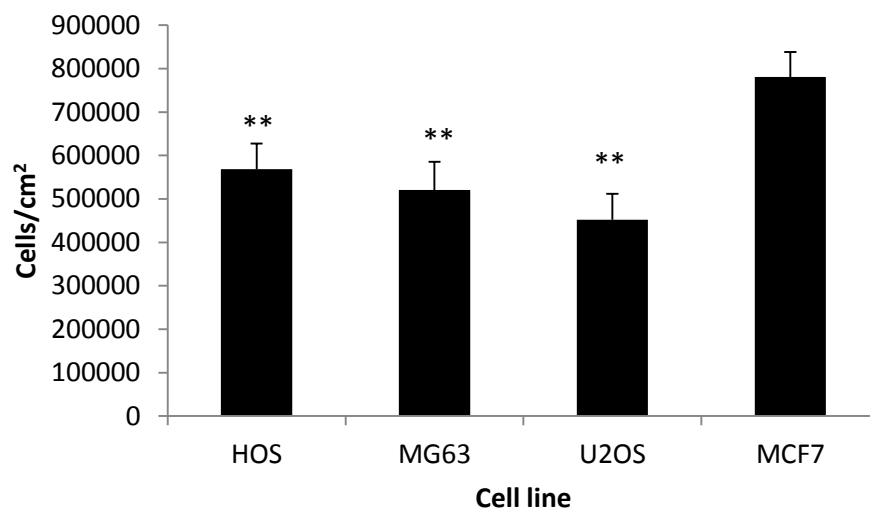


**Figure 5.3: Cell density of HOS, MG63, U2OS and MCF7 for 24 hour conditioned media collection.** Cell lines were grown under the same conditions as used for conditioned media collection. After reaching confluency media was changed and after 24 hours cell density was assessed. Data presented as mean and standard deviation (n=3), significance calculated by using Tukey's post hoc analysis and comparing OS cell lines to MCF7 (p \*\* = < 0.01).

#### 5.4 Analysis of paracrine growth signaling in sarcoma cell lines

To identify if non-osteosarcoma sarcoma cell lines express and respond to paracrine growth factors, conditioned media from three different sarcoma cell lines was compared to U2OS conditioned media (which enhanced growth in all cell lines tested (Figure 5.2)). The sarcoma cell lines selected were HT1080 (fibrosarcoma), SKLNS1 (leiomyosarcoma) and RDES-1 (Ewing's sarcoma). Each was tested with its own conditioned media and U2OS conditioned media, however, RDES-1 cells detached from the growth surface making colony size assessment impractical due to absence of colony formation. HT1080 cell conditioned media was found to produce a greater increase in its own colony size compared to U2OS conditioned media (Figure 5.4.A) indicating that it also expressed a growth factor, therefore, media from this cell line was also used to test on SKLNS1. Interestingly no significant increase in colony size was observed in SKLNS1 cells in response to U2OS or HT1080 but its own conditioned media increased colony size (Figure 5.4.B). RDES-1 conditioned media did not produce an increase in growth in U2OS cells suggesting it does not produce a paracrine growth factor, however HT1080 and SKLNS1 produced an equivalent increase in colony size when compared to U2OS conditioned media (Figure 5.4.C).

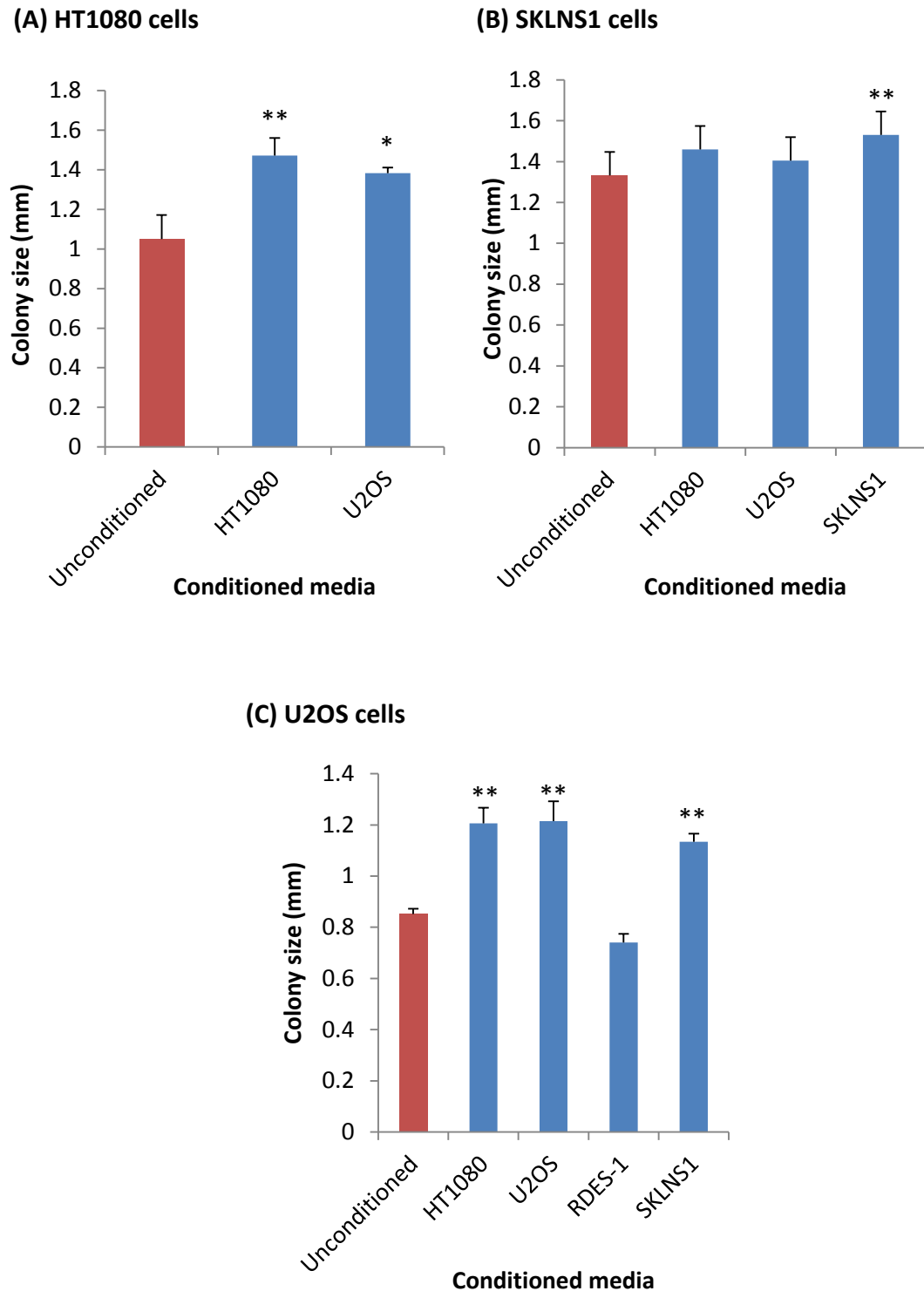


**Figure 5.4: Growth response of sarcoma cell lines (HT1080 and SKLNS1) and U2OS to conditioned media from U2OS and sarcoma cell lines.** HT1080 cells (A), SKLNS1 cells (B) and U2OS cells (C) were tested with conditioned media from the same cell line and alternate cell lines to identify growth effected by the conditioned media. All sarcoma cell lines tested have been analysed by measuring colony size using ImageJ. Results tested in triplicate (n=3), data presented as mean and standard deviation. Statistical significance calculated by comparing to unconditioned colony size (\* = <math><0.05</math>, \*\* = <math><0.01</math> Tukey's post hoc analysis).

### **5.5 Analysis of U2OS cell confluency and cell exposure time upon the growth enhancing properties of conditioned media**

Conditioned media was collected from U2OS cells once they reached approximately 100 % confluency (Section 2.4.1), however, this method does not take in to consideration exact cell densities. Therefore, to identify if cell density may contribute to variation in the growth potential of the conditioned media, media was collected from confluent cells and lower confluencies (70 and 90 %). U2OS cells were selected because this cell line produces a robust paracrine growth response in previous experiments (Figure 5.2 and 5.4). Results show that conditioned media from U2OS cells at 70 % and 90 % did not significantly alter the colony size compared to 100 % conditioned media, indicating that although a lower concentration of paracrine growth factors may be present in the lower confluencies this has no discernible impact on growth rates (Figure 5.5). The length of time in which the media was exposed to confluent U2OS cells was also tested to identify if increased time of conditioned media cell exposure affected colony growth rates. Media which had been exposed to U2OS cells for longer periods was found to produce significantly larger colonies (Figure 5.6).

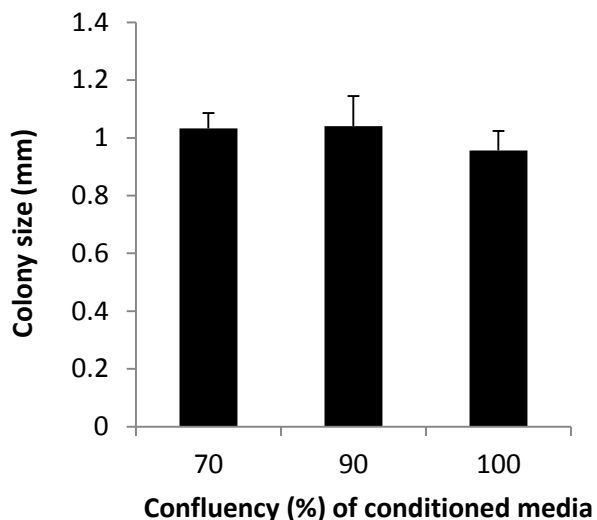


**Figure 5.5: Growth effect of U2OS conditioned media taken after 24 hours exposure to U2OS cells at 70, 90 and 100 % confluency.** Conditioned media collected from U2OS cells at 70, 90 and 100 % produced colonies of an equivalent size. U2OS colony size analysed using ImageJ®. Results tested in triplicate, data presented as mean and standard deviation. No significant difference observed (Tukey's post hoc analysis).

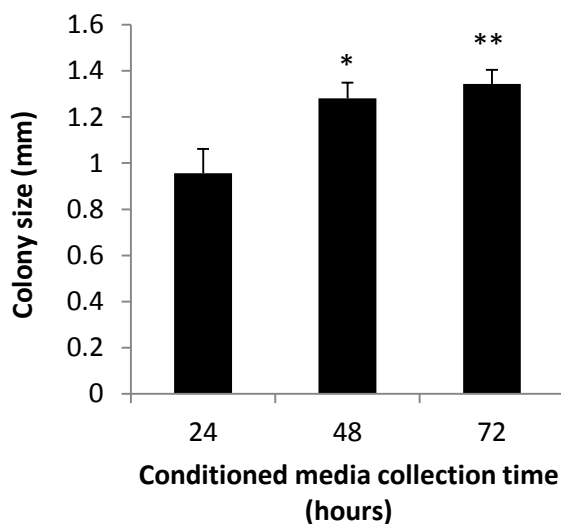


**Figure 5.6: Growth effect of U2OS conditioned media collected from confluent U2OS cells after 24, 48 and 72 hours.** Compared to 24 hour U2OS conditioned media, media taken from cells after 24 and 72 hours produced significantly larger colonies. U2OS colony size has been assessed using ImageJ®. Results tested in triplicate, data presented as mean and standard deviation, significance calculated by comparing to unconditioned colony size (\* = <math><0.05</math>, \*\* = <math><0.01</math> Tukey's post hoc analysis).

### **5.6 Paracrine signaling in OS cell lines and MCF7 in response to 24 hour and 72 hour conditioned media**

Conditioned media taken from U2OS cells after 72 hours produced a greater enhancement of colony size compared to 24 hour conditioned media (Figure 5.6), therefore, 72 hour conditioned media from the cell lines HOS, MG63, U2OS and MCF7 was analysed to identify if it also had altered growth enhancing properties compared to 24 hour conditioned media. Compared to MCF7 conditioning both MG63 and U2OS cells responded with increased colony size in response to MG63 and U2OS conditioned media at 24 and 72 hours (Figure 5.7.A and figure 5.7.B), HOS conditioned media increased MG63 colony size to the same size at 24 and 72 hours of conditioning and U2OS cells only responded to 24 hour HOS conditioned media. As was observed in 24 hour media HOS and MCF7 cells had increased colony size in response to U2OS 72 hour conditioned media, however, this was not a significant increase for U2OS 72 hour conditioned media due to 72 hour MCF7 conditioned media also increasing HOS and MCF7 cell growth (Figure 5.7.C and 5.7.D). In contrast to 24 hour conditioned media, 72 hour MG63 conditioned media resulted in the largest colony sizes in HOS cells. This suggested that after 72 hours of MG63 media conditioning the concentration of a particular growth factor, had increased to a level which was capable of enhancing the colony size of HOS.

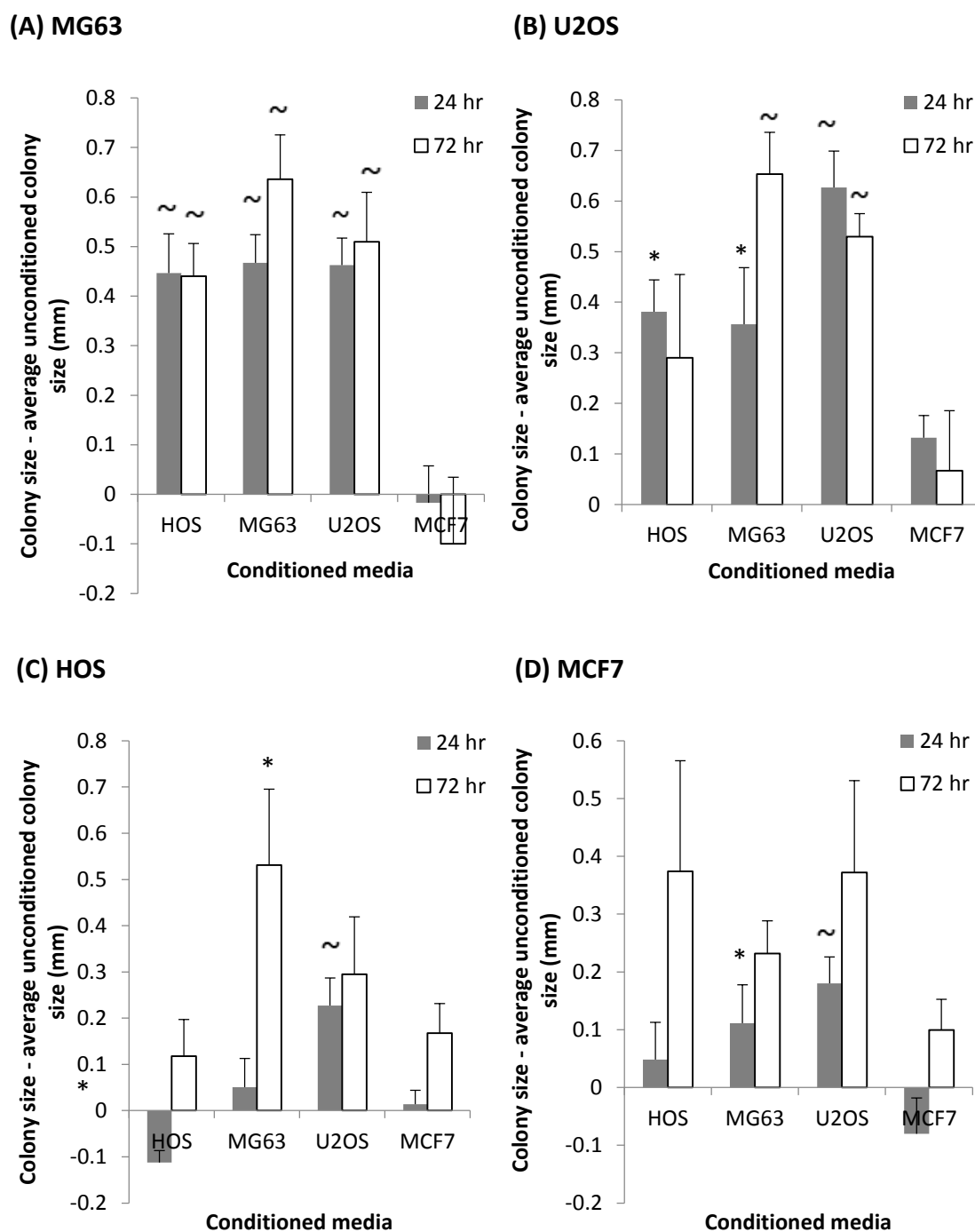


**Figure 5.7: Response of HOS, MG63, U2OS and MCF7 cells to 24 hour and 72 hour conditioned media.** MG63 (A), U2OS (B), HOS (C) and MCF7 (D) tested using unconditioned and conditioned media from each cell line to assess the growth enhancement of each cell line. All cell lines tested (MG63, U2OS, HOS and MCF7) have been analysed by measuring colony size using ImageJ®. Average unconditioned colony size was subtracted from conditioned colony size. Data presented as mean and standard deviation, n=3, significance calculated by comparing to MCF7 colony size (\* = <0.05, ~ = <0.01; Tukey's post hoc analysis).



### **5.7 Analysis of the growth response of U2OS and HOS cells to 72 hour conditioned media within a 96 well assay**

A 96 well growth assay was developed due to the large quantities of media required for the colony formation assays (55 cm<sup>2</sup> growth area) and to minimise any inaccuracies associated with manually measuring colonies to assess growth. This assay used minimal volumes of media (100 µl), which allowed the number of replicates for each condition to be increased and cell growth to be assessed by measuring the well absorbance following staining with MTT (Section 2.4.3). To analyse the growth response in a 96 well assay, 72 hour conditioned media from MG63, U2OS, HOS and MCF7 was tested upon U2OS and HOS cells. As was observed in the colony formation assay (Figure 5.7) U2OS and MG63 conditioned media increased the growth rate of U2OS cells using the 96 well assay, however, HOS conditioned media had no impact upon growth (Figure 5.8.A). HOS cells only responded with increased growth to U2OS conditioned media (Figure 5.8.B) using the 96 well assay, which is in contrast to the colony formation assay, where it was observed that MG63 conditioned media also increased HOS growth (Figure 5.7.C). These results demonstrate that although a 96 well assay format may be less sensitive to growth responses, it provides an efficient assay for the assessment of growth in response to conditioned media.

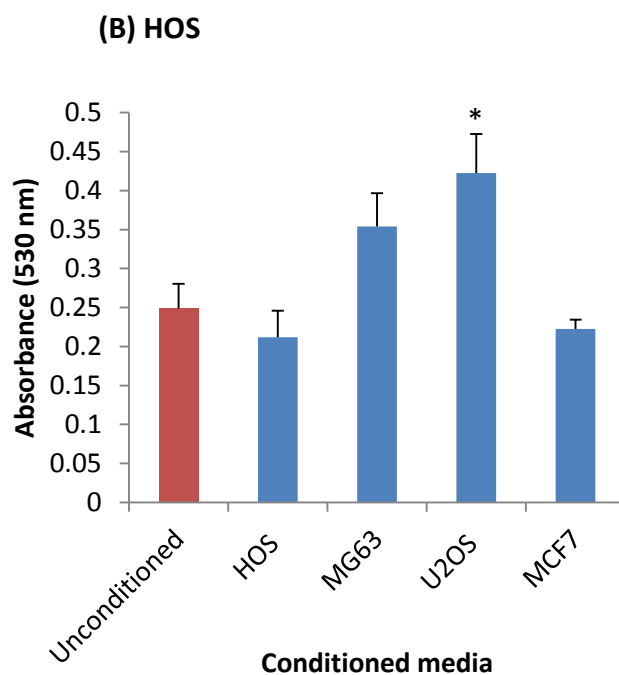
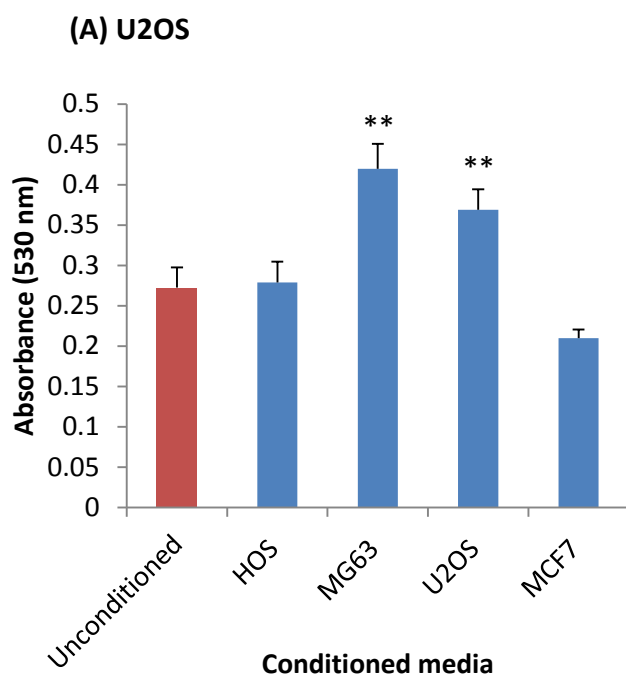


**Figure 5.8: Response of HOS and U2OS cells to 72 hour conditioned media from HOS, MG63, U2OS and MCF7 in a 96 well assay.** To assess the practicality of a 96 well conditioned media assay U2OS (A), and HOS (B) cells were tested using unconditioned (complete media) and 72 hour conditioned media from HOS, MG63, U2OS and MCF7 to assess the growth of each cell line. All cell lines tested (MG63, U2OS, HOS and MCF7) have been analysed by staining cells with MTT and measuring absorbance at 530 nm. Data presented as mean and standard error, each sample tested 16 times in three separate experiments ( $n=3$  independent replicates), significance calculated by comparing to MCF7 conditioned colony size (\* =  $<0.05$ , \*\* =  $<0.01$  Tukey's post hoc analysis).

### 5.8 Assessment of colony hierarchy frequency in response to conditioned media in HOS, U2OS and MCF7 cells

The colony hierarchies identified by Locke *et al.*, (2005) have been used to identify prostate CSC in the cell line PC3, through the isolation of cells from the holoclone morphology (Li *et al.*, 2008) (Section 1.2.3). In OS MG63 holoclones possess enhanced clonogenicity and proliferated more rapidly (Lou *et al.*, 2010). Based on these findings it could be hypothesised that the increased colony size in response to U2OS conditioned media (Figure 5.7), could be due to a paracrine factor which is maintaining cells in a holoclone morphology. To test this hypothesis cell lines (HOS, U2OS and MCF7) were seeded at a clonal density ( $2 - 4 \text{ cells cm}^2$ ) and exposed to 24 hour conditioned media (from HOS, MG63, U2OS and MCF7 cells) for 9 – 14 days (approximately 100 colonies would form per plate), after which the first 30 colony hierarchies from each plate were recorded using an inverted microscope (Section 2.4.2).

An observation which was consistent in all three cell lines tested (HOS, U2OS and MCF7) was an increased paraclone frequency in response to MCF7 conditioned media (Figure 5.9). MCF7 conditioned media also caused a decrease in meroclone formation in both HOS and MCF7 (Figure 5.9). In response to MG63 conditioned media HOS cells responded with a decrease in holoclone frequency (Figure 5.9.A), the same response was not observed in U2OS, which contained an enhanced frequency of holoclones and meroclones in response to its own conditioned media as well as HOS and MG63 conditioned media (Figure 5.9.B). In addition, these same conditioned media (HOS, MG63 and U2OS) also produced enhanced colony formation in U2OS (Figure 5.7), therefore, U2OS appears to respond to paracrine factors from these cell lines which enhance the presence of holoclone and meroclone colonies.

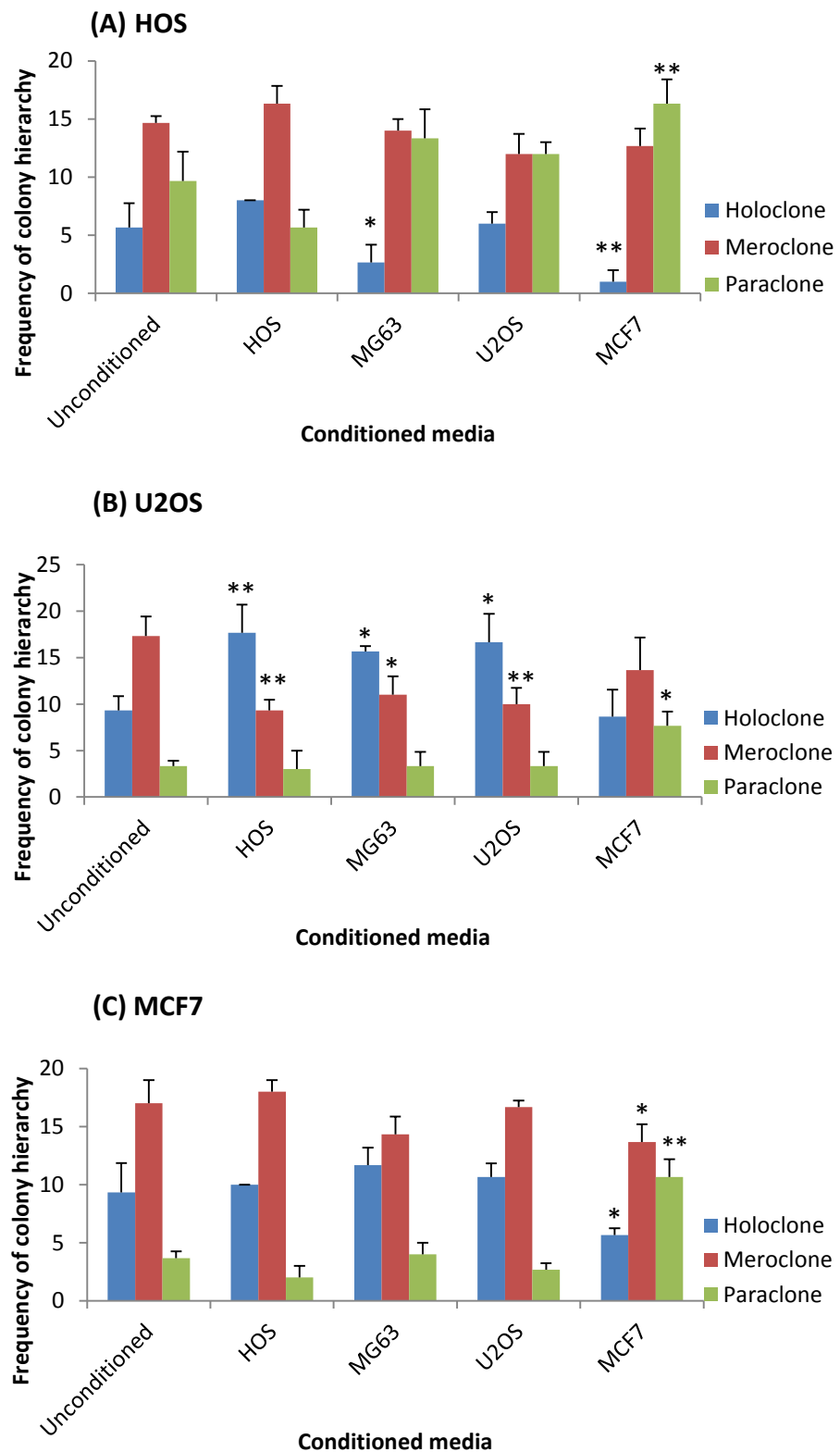


**Figure 5.9: Colony hierarchy frequency in response to 24 hour conditioned media in HOS, U2OS and MCF7 cell lines.** After exposure to conditioned media 30 colony hierarchies were recorded in HOS (A), U2OS (B) and MCF7 (C) cell lines. Data presented as mean and

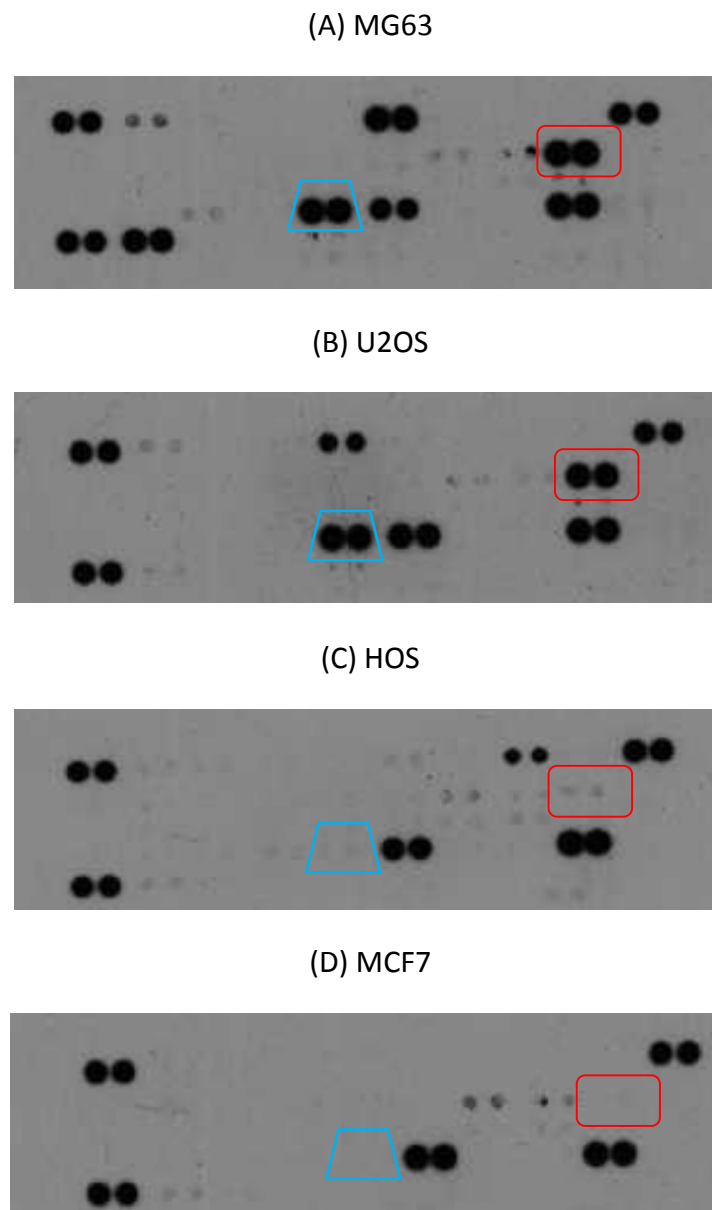
standard deviation,  $n=3$ , significance calculated by comparing to unconditioned colony frequency (\* =  $<0.05$ , \*\* =  $<0.01$  Tukey's post hoc analysis).

### 5.9 Cytokine profiling of HOS, MG63, U2OS and MCF7 72 hour conditioned media

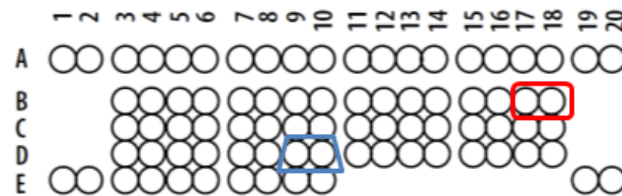
Cytokines have been found to increase proliferation in carcinomas (Westley and Rochefort, 1980, Loberg et al., 2007), sarcomas (Li et al., 2011), leukaemia (Digel et al., 1989) and neuroblastoma (Airoldi et al., 2004). In order to identify candidate cytokines proteins which may confer enhanced growth in OS cell lines and MCF7, 72 hour conditioned media from HOS, MG63, U2OS and HOS were analysed using a human cytokine profiler (Section 2.5.1). The array detects 36 different cytokines which are commonly used in cell signaling networks. U2OS and MG63 conditioned media were selected because U2OS consistently produced increased growth in all cell lines tested and MG63 media enhanced growth in U2OS and MG63 cells (Figures 5.7). It was predicted therefore that the conditioned media from both of these cell lines will contain a growth factor that is not present in MCF7 conditioned media (as this did not produce growth enhancement). The response to HOS conditioned media consistently produced growth enhancement in U2OS and MG63, never in HOS and inconsistently in MCF7 (Figures 5.7). These findings suggest that although HOS may express a growth factor it may be at a lower concentration than MG63 and U2OS.

Based on the observed growth promoting effects of the conditioned media, cytokines which could be considered candidate growth factors must be present within MG63 and U2OS, absent within MCF7 and weakly expressed in HOS. The cytokine array identified two proteins which fulfilled this criteria. Both IL-8 and CCL-2 were expressed in U2OS and MG63 media, weakly in HOS and absent in MCF7 (Figure 5.10). Analysis of the pixel density of the each spot identified in the cytokine array confirmed the expression profile of CCL-2 and IL-8, with MG63 producing a pixel density above 6000 for IL-8 and CCL-2 and U2OS produced pixel densities of 4977 for IL-8 and 5637 for CCL-2 (Figure 5.11). HOS conditioned media contained lower concentrations and produced pixel densities of 336 for IL-8 and 263 for CCL-2 and neither proteins were detected in MCF7 conditioned media (5.11). MCF7 conditioned media was found to contain less proteins within its conditioned media compared to the OS cell lines (Figure 5.11). All cell lines expressed IL-5, IL-23, macrophage inhibitory factor (MIF), serpin E1 and RANTES (also known as CCL-5). HOS was found to

secrete the greatest number of cytokines, but the majority were only present at low concentrations which is evident because of the low relative pixel density ( $< 500$ ) of each spot (Figure 5.11).



**Figure 5.10: Images of the cytokine array of HOS, MG63, U2OS and MCF7 72 hour conditioned media.** Using R&D systems human cytokine profiler (Cat no. ARY005), 72 hour conditioned media from MG63 (A), U2OS (B), HOS (C) and MCF7 (D) was tested and exposed on to X-ray film for 10 mins before developing. Red rectangle denotes IL-8 location and blue trapezium denotes CCL-2 location, all cytokines are spotted on to the array in duplicate.

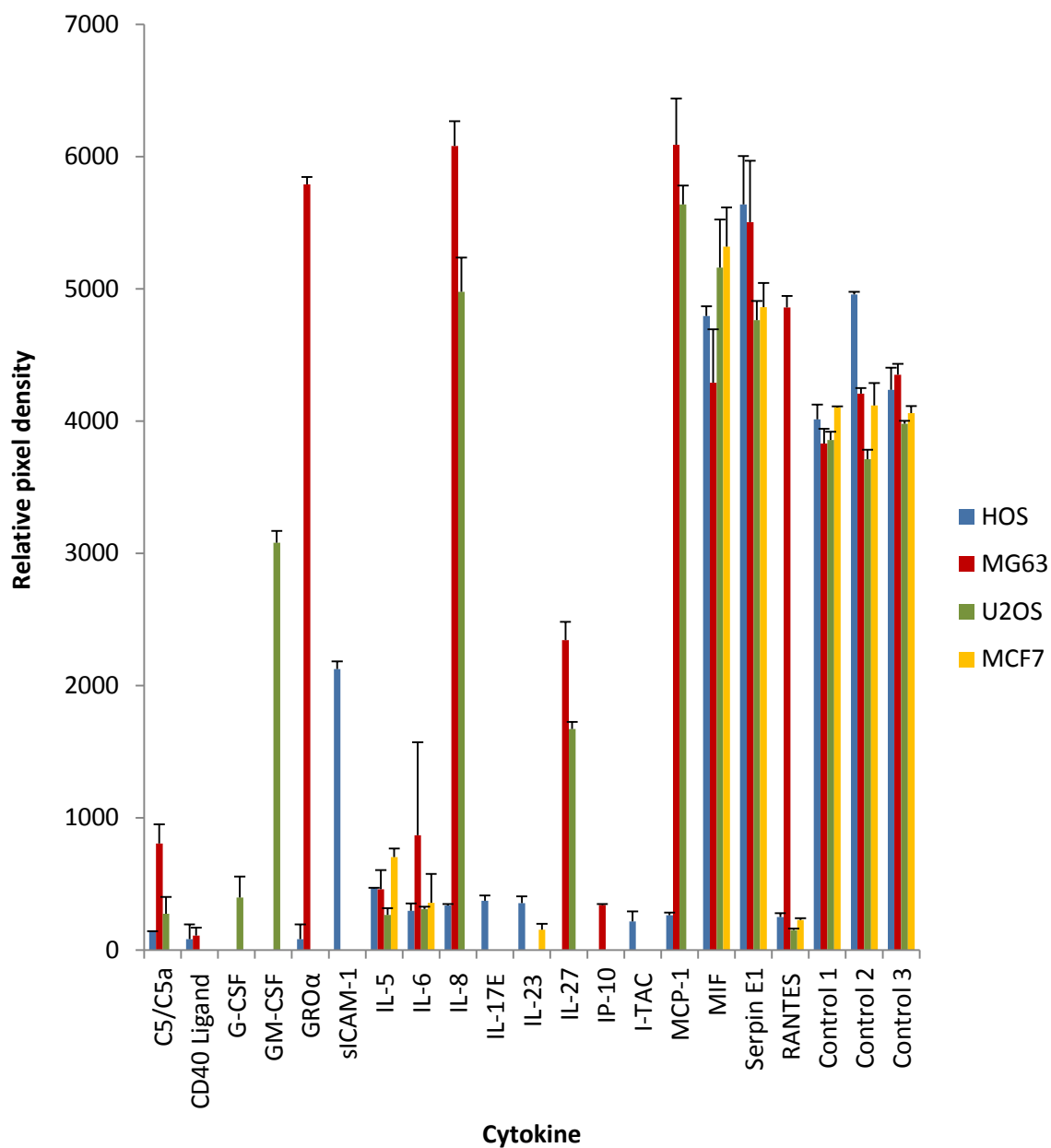
**Table 5.1: Position of cytokines in cytokine array used in figure 5.10.**

Coordinate	Target/Control	Alternate Nomenclature
A1, A2	Reference Spot	—
A3, A4	C5/C5a	Complement Component 5/5a
A5, A6	CD40 Ligand	CD154
A7, A8	G-CSF	CSF $\beta$ , CSF-3
A9, A10	GM-CSF	CSF $\alpha$ , CSF-2
A11, A12	GRO $\alpha$	CXCL1
A13, A14	I-309	CCL1
A15, A16	sICAM-1	CD54
A17, A18	IFN- $\gamma$	Type II IFN
A19, A20	Reference Spot	—
B3, B4	IL-1 $\alpha$	IL-1F1
B5, B6	IL-1 $\beta$	IL-1F2
B7, B8	IL-1ra	IL-1F3
B9, B10	IL-2	—
B11, B12	IL-4	—
B13, B14	IL-5	—
B15, B16	IL-6	—
B17, B18	IL-8	CXCL8
C3, C4	IL-10	—
C5, C6	IL-12 p70	—
C7, C8	IL-13	—
C9, C10	IL-16	LCF
C11, C12	IL-17	—
C13, C14	IL-17E	—
C15, C16	IL-23	—
C17, C18	IL-27	—

Table 5.1: Continued overleaf

Coordinate	Target/Control	Alternate Nomenclature
D3, D4	IL-32 $\alpha$	—
D5, D6	IP-10	CXCL10
D7, D8	I-TAC	CXCL11
D9, D10	MCP-1	CCL2
D11, D12	MIF	GIF, DER6
D13, D14	MIP-1 $\alpha$	CCL3
D15, D16	MIP-1 $\beta$	CCL4
D17, D18	Serpin E1	PAI-1
E1, E2	Reference Spot	—
E3, E4	RANTES	CCL5
E5, E6	SDF-1	CXCL12
E7, E8	TNF- $\alpha$	TNFSF1A
E9, E10	sTREM-1	—
E19, E20	Negative Control	—





**Figures 5.11: Densitometry analysis of cytokines present on the cytokine array of HOS, MG63, U2OS and MCF7 72 hour conditioned media.** Cytokines which were present in the cytokine array from MG63, U2OS, HOS and MCF7 72 hour conditioned media were tested for pixel density using ImageJ. In order to normalise all cytokine spots with background staining, the pixel density of the blot around each spot was analysed and the total background pixel density was averaged and subtracted from each positive result, to calculate the relative pixel density. Data presented as mean and standard deviation, n=2.

### 5.10 Expression profile of CCL-2 and IL-8 from sarcoma cell lines and MCF7

The cytokine array (Figure 5.10) identified the proteins IL-8 and CCL-2 as candidate growth promoting factors in OS conditioned media. Commercially available ELISA kits for IL-8 and CCL-2 (BioLegend®) (Section 2.5.2) were used in order to establish the concentration of the cytokines within 24 hour and 72 hour conditioned media (Appendix II).

The pattern of IL-8 expression as measured by ELISA did not correlate with the conditioned media growth enhancement observations (Figure 5.12.B). 143B cells which was found not to produce an enhanced colony sizes in response to its own conditioned media was found to secrete more IL-8 than HT1080, SKLNS1 and U2OS (Figure 5.13), which all produced conditioned media which increased colony size (Figure 5.12.B). Both 24 hour and 72 hour conditioned media from MG63, U2OS, HOS and MCF7 were reciprocally tested upon each cell line to identify if the growth enhancing properties of each conditioned media were observed in the other cell lines (Figure 5.7). U2OS 24 hour conditioned media was found to be the most growth enhancing media when compared to MG63 and enhanced the growth of all cell lines tested, whereas MG63 conditioned media had no effect on HOS or MCF7 (Figure 5.7). U2OS 24 hour and 72 hour conditioned media IL-8 concentration is statistically lower than MG63, which would therefore indicate that IL-8 is not a growth factor (Figure 5.14). This is supported by Pearson's correlation coefficient analysis of IL-8 concentration with the change in colony size in response to a cell lines conditioned media. This produced a positive correlation of 0.6, however, this correlation was not statistically significant (Table 5.2).

CCL-2 expression was found to more closely resemble the observed growth responses to conditioned media. When comparing 24 hour conditioned media to the non-growth responsive media from 143B, it was found that all cell lines which responded with increased growth to their media (Figure 5.12.A) (Cal72, G292, MG63, HT1080, SKLNS1, U2OS and SaOS-2) contained elevated concentrations of CCL-2 compared to non-growth enhancing media (Figure 5.15). When analysing the 24 hour and 72 hour conditioned media of MG63 and U2OS 24 hour conditioned media was found to contain an elevated concentration compared to MG63 media (Figure 5.16). As U2OS 24 hour conditioned media was found to enhance colony growth in all cell lines tested, whereas MG63 was unable to in HOS and

MCF7 (Figure 5.7), this is consistent with the growth responses observed. Interestingly 72 hour MG63 media contained elevated quantities of CCL-2 compared to U2OS (Figure 5.16), HOS and MCF7 conditioned media contained a significantly lower concentration of CCL-2 than MG63 conditioned media at 24 and 72 hours. Correlating colony growth increases with CCL-2 24 hour conditioned media concentration also supports CCL-2 as a candidate growth factor, producing a statistically significant positive correlation of 0.67 (Table 5.2).

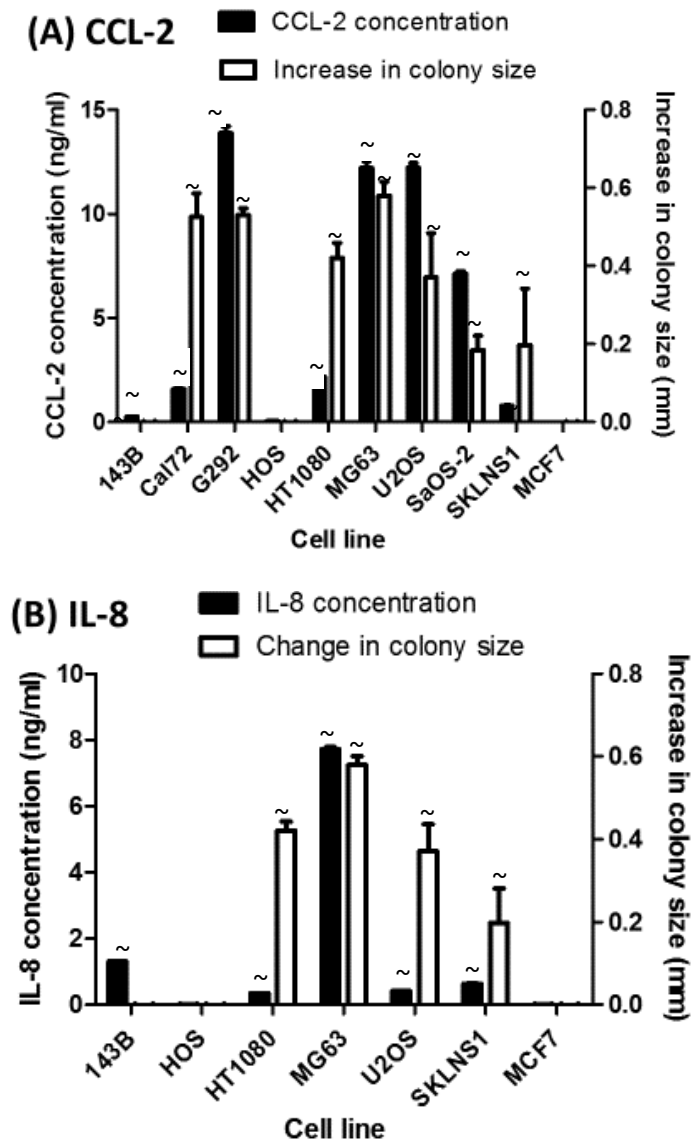


**Figure 5.12: Analysis of CCL-2 and IL-8 concentration of conditioned media from sarcoma cell lines and MCF7 and the growth response of each cell line to its conditioned media.** The concentration of CCL-2 (A) and IL-8 (B) was assessed upon 24 hour conditioned media using a commercially available ELISA. The change in growth rate was assessed by identifying the change in colony size of unconditioned colonies compared to conditioned colonies. Data presented as mean and standard deviation ( $n = 3$ ). Statistical significance calculated by comparing to MCF7 IL-8, CCL-2 concentration or change in colony size (Tukey's post hoc analysis,  $\sim p = <0.01$ )

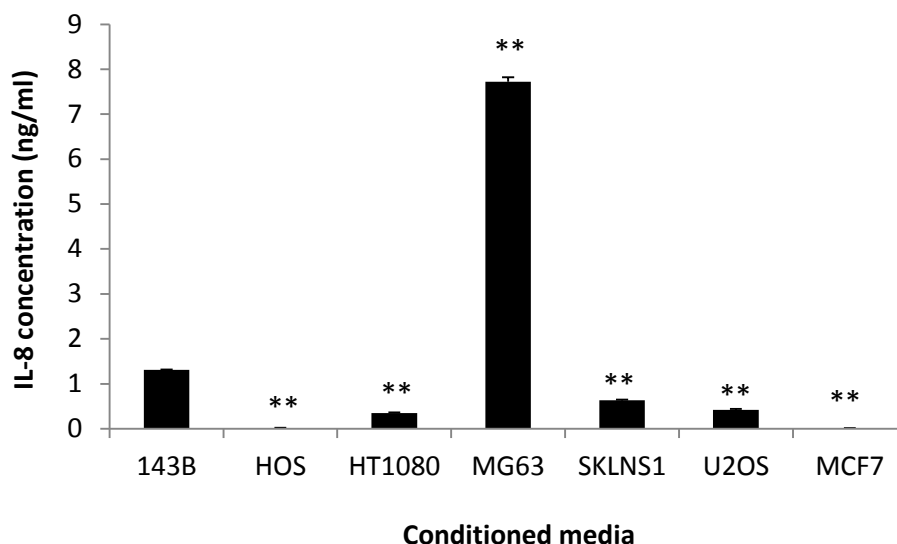


**Figure 5.13: Concentration of IL-8 in 24 hour conditioned media from sarcoma cell lines and MCF7.** A commercially available IL-8 ELISA was used to assess IL-8 concentration. 143B conditioned media had no growth enhancing effect (Figure 5.1), therefore was used for comparison to identify statistically significant changes in IL-8 expression. Data presented as mean and standard deviation, n=3, significance calculated by comparing to 143B IL-8 concentration (\* = <0.05, \*\* = <0.01 Tukey's post hoc analysis).

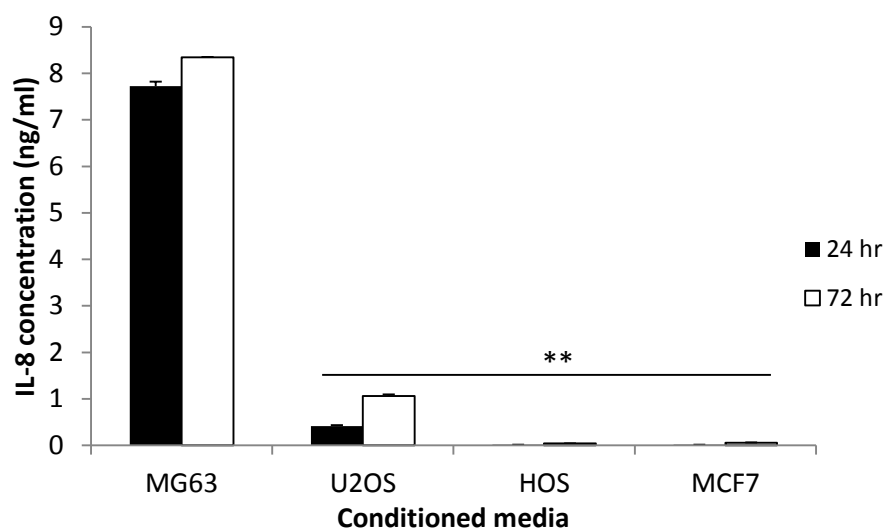


**Figure 5.14: Comparison of IL-8 concentration of 24 hour and 72 hour conditioned media from MG63, U2OS, HOS and MCF7.** A commercially available IL-8 ELISA was used to assess IL-8 concentration. Statistical significance was calculated by comparing to MG63 24 and 72 hour IL-8 concentration. Data presented as mean and standard deviation, n=3, significance calculated by comparing to MG63 IL-8 concentration (\*\* = <0.01 Tukey's post hoc analysis).

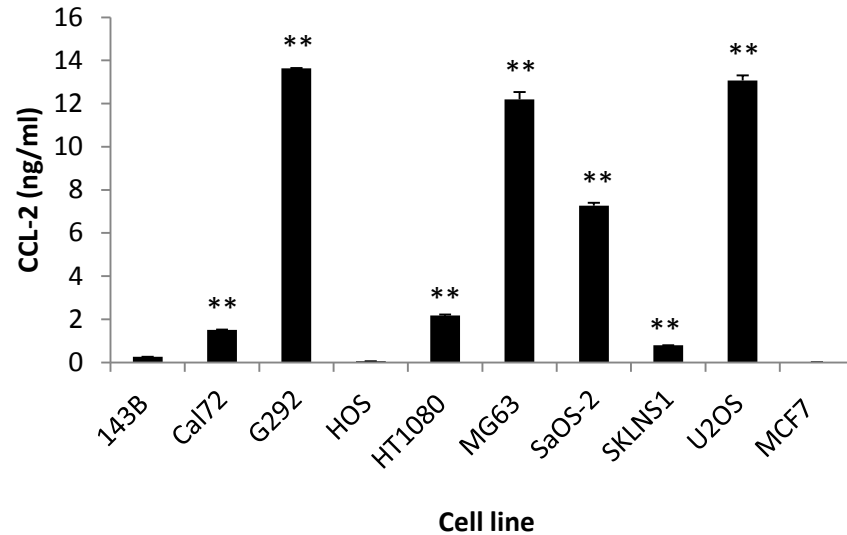


**Figure 5.15: Concentration of CCL-2 in 24 hour conditioned media from sarcoma cell lines and MCF7.** A commercially available CCL-2 ELISA was used to assess CCL-2 concentration. 143B conditioned media had no growth enhancing effect (Figure 5.12.A), therefore was used for comparison to identify statistically significant changes in CCL-2 expression. Data presented as mean and standard deviation, n=3, significance calculated by comparing to 143B CCL-2 concentration (\* = <0.05, \*\* = <0.01 Tukey's post hoc analysis).

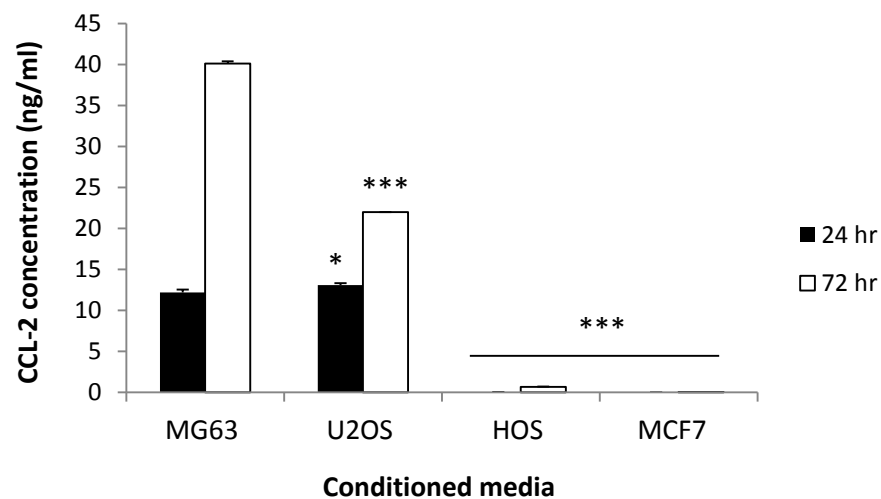


**Figure 5.16: Comparison of CCL-2 concentration of 24 hour and 72 hour conditioned media from MG63, U2OS, HOS and MCF7.** A commercially available CCL-2 ELISA was used to assess CCL-2 concentration. Statistical significance was calculated by comparing 24 hour CCL-2 concentration to MG63 24 hour and 72 hour concentration. Data presented as mean and standard deviation, n=3, significance calculated by comparing to MG63 CCL-2 concentration (\* = <0.05, \*\*\* = <0.0005 Unpaired T-test).

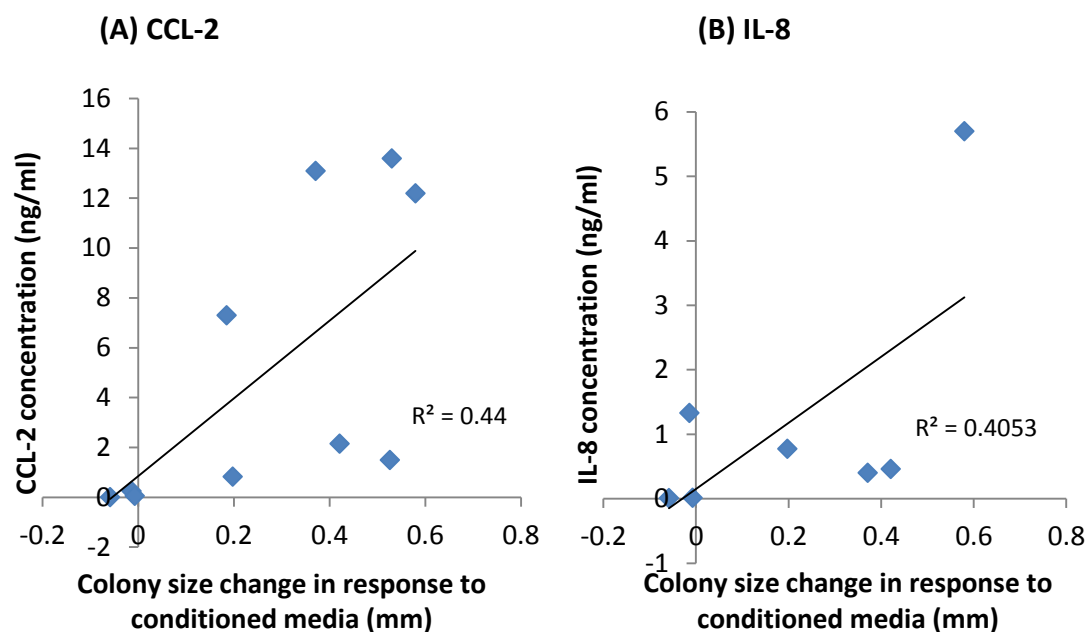


**Figure 5.17: Linear regression analysis of CCL-2 or IL-8 concentration of OS cell lines and MCF7 24 hour conditioned media against colony size change in response to growth in conditioned media. CCL-2 (A) and IL-8 (B) data presented as mean values, all conditions tested in triplicate.**

**Table 5.2: Pearson's correlation coefficient of sarcoma cell lines and MCF7 colony size change in response to auto conditioning with either CCL-2 or IL-8 24 hour conditioned media concentration. Pearson's correlation coefficient was calculated using graph pad (\* =  $p < 0.05$ ).**

	<b>CCL-2 (P value)</b>	<b>IL-8 (P value)</b>
<b>Pearson's correlation coefficient</b>	0.67 (0.04)*	0.60 (0.15)

### 5.11 Discussion

In order to identify if OS cell lines and MCF7 secrete a paracrine growth factor, conditioned media from each cell line was used to assess its impact on colony formation. The OS cell lines Cal72, G292, MG63, U2OS and SaOS-2 all responded with increased colony size in response to their conditioned media, indicating that these OS cell lines secrete a paracrine factor which increases growth. Although this factor may enhance cell proliferation, its role in protection against apoptosis has not been established. Therefore, the paracrine factor can only be described as increasing growth, which is the net cellular gain after cell death and proliferation. 143B, HOS and MCF7 do not release or respond to a paracrine signalling molecule. In the subsequent experiment two cell lines which responded with increased growth (U2OS and MG63) were compared with two cell lines which did not respond (MCF7 and HOS). The results indicate that the unresponsive cell line HOS could be encouraged grow in the presence of U2OS and MG63 conditioned media, this increase was statistically significant in response to U2OS conditioned media indicating it has a greater ability to enhance growth. This finding demonstrates that OS shares a common paracrine signalling factor, which is supported by the finding that HOS enhanced the growth of MG63 and U2OS cells. The inability of HOS conditioned media to enhance its own proliferation suggests that it may be less responsive to the growth factor in comparison to MG63 and U2OS.

In this chapter OS conditioned media (U2OS) was found to evoke a significant increase in the growth of the breast cancer cell line MCF7, which suggests that the paracrine signalling factor released by U2OS may have an effect on multiple cancer types. MCF7 cellular proliferation has been demonstrated to increase in response to SDF-1 which is released by cancer associated fibroblasts (Orimo et al., 2005). No cell line tested responded with increased growth to MCF7 conditioned media, therefore, this cell line does not secrete a growth factor and *in vivo* may obtain growth signals from surrounding fibroblasts in a paracrine fashion. MCF7 had the highest cell density when conditioned media was collected as compared to MG63, U2OS, HOS and MCF7. This indicates that the growth enhancing properties of conditioned media are independent of cell density.

To further characterise the growth enhancing potential of U2OS conditioned media, conditioned media collected at different cell densities and cell exposure times was compared. It was found that a confluency ranging from 70 % – 100 % did not alter the growth properties of the conditioned media but increasing the exposure time did. Conditioned media exposed to cells for 72 hours was found to increase growth more than 24 and 48 hour conditioned media. Analysis of the growth enhancing properties of 72 hour conditioned media using reciprocal analysis of MG63, U2OS, HOS and MCF7 cells, demonstrated that U2OS and MG63 cells produced the same response as was observed in 24 hour conditioned media (MG63, U2OS and HOS conditioned media increased growth of both cell lines). HOS and MCF7 cells responded with increased growth to U2OS media which was also observed in response to 24 hour media. MCF7 cells also responded with increased growth to HOS conditioned media and HOS cells responded to MG63 conditioned media at 72 hours. This finding suggests that MG63 cells do secrete growth factors which can influence multiple cell lines, however, the concentration at 24 hours is too low to achieve this.

In order to increase the volume of reagents required for the growth assessment of conditioned media, 72 hour conditioned media from the same four cells lines (HOS, MG63, U2OS and MCF7) was tested in a 96 well format upon HOS and U2OS cells. This assay may present a less sensitive assay to measure growth than assessing colony size as HOS conditioned media had no effect upon on U2OS. In addition HOS cells did not respond with enhanced growth to MG63 conditioned media, which had been observed to increase colony size. Therefore, although the 96 well format does not exactly mirror the results of the colony size assay it does present a more efficient method to assess growth in response to conditioned media.

In order to assess whether the growth enhancing properties of OS is common to other types of sarcoma, conditioned media from a Ewing's sarcoma (RDES-1), fibrosarcoma (HT1080) and leiomyosarcoma (SKLNS1) was tested upon the same cell line and upon U2OS cells. RDES-1 cells were loosely attached so would not form colonies making this cell line inappropriate for testing growth enhancement. HT1080 and SKLNS1 both produced growth factors which increased growth upon the same cell line and also U2OS cells. This finding



suggests that these cell lines may share a common growth factor with U2OS, to further elucidate this hypothesis SKLNS1 proliferation was tested using its own conditioned media and also HT1080 and U2OS conditioned media. SKLNS1 was found to respond only to its own conditioned media but not in response to HT1080 or U2OS media. Two explanations could explain this observation, either SKLNS1 utilise an alternative growth factor to HT1080 and U2OS. Alternatively, SKLNS1 conditioned media may contain higher concentrations of the same cytokine and SKLNS1 cells have a reduced sensitivity.

Isolated holoclones from the MG63 cell line have been shown to have enhanced clonogenicity and proliferate more rapidly *in vitro* than non-holoclones (Lou et al., 2010). In order to assess whether growth enhancing conditioned media also enhances the presence of holoclones. The colony hierarchy frequencies were assessed in the presence of 24 hour conditioned media, by the reciprocal testing of the cell lines HOS, U2OS and MCF7 with each of their conditioned media along with MG63 conditioned media. U2OS cells which responded with increased growth in response to U2OS, HOS and MG63 conditioned media also responded with an elevated presence of holoclones and meroclones. Therefore, the enhanced growth in U2OS cells in response to paracrine factors could be linked to enhancing the maintenance of holoclones. Assessment of putative CSC based on mammosphere forming ability has demonstrated that IL-8 signalling inhibition can decrease putative CSC in breast cancer cells *ex vivo* (Singh et al., 2013) and also decreases tumour growth *in vivo* (Ginestier et al., 2010). A cytokine present in OS conditioned media could therefore be promoting the growth of holoclones by maintaining the CSC phenotype in U2OS. The same increase in holoclones was not observed in HOS or MCF7, suggesting that holoclone increase is not attributing to their enhanced growth in response to conditioned media. One observation common to all cell lines tested was in response to MCF7 conditioned media, which resulted in an increase in paraclones in all cell lines tested. Additionally HOS and MCF7 also had a reduced frequency of holoclones and meroclones. This reduction in amplifying colony types and shift toward the differentiated paraclonal colonies with limited proliferative properties could be attributed to MCF7 conditioned media inability to enhance growth. MCF7 has been identified to display characteristics of differentiated mammary epithelial tissue (Soule et al., 1973), therefore, may release a cytokine which enhanced differentiation in not only MCF7 but also OS cell lines.

In order to identify candidate growth factors responsible for the paracrine effects conditioned media cells from cell lines that enhanced growth (MG63 and U2OS) was compared to conditioned media which did not enhance growth (MCF7). In addition HOS conditioned media was also tested which enhanced growth but only upon MG63 and U2OS. These cell lines had an increased sensitivity to growth enhancing conditioned media, therefore HOS conditioned media is predicted to contain a lower growth factor concentration. Based on these findings any candidate growth factor must be highly expressed by U2OS and MG63, absent in MCF7 and weakly expressed by HOS. IL-8 and CCL-2 were two cytokines to fit these criteria so were hypothesised to act as growth factors in OS conditioned media. The complement component 5 (C5) was also expressed by all three cell lines, however was not further tested due to its established role in innate immunity (Gerard and Gerard, 1991).

Interestingly, all of the cell lines tested expressed the following cytokines; MIF, IL-5, IL-23, serpinE1 and RANTES. MIF was originally identified because it could inhibit monocyte migration *in vitro* (George and Vaughan, 1962), its expression has been associated with poor prognosis in soft cell sarcomas (Takahashi et al., 2013) and it has been found to act as a growth factor in esophageal squamous cell carcinoma *in vivo* (Wang et al., 2014). IL-5 recruits and differentiates eosinophils (Dubucquoi et al., 1994), IL-23 has been found to play a role in the suppression of innate immune responses against cancer cells, through the induction of murine tumours after exposure to carcinogens (3-methylcholanthrene). Mice lacking IL-23 have reduced fibrosarcoma formation and metastasis, however, this protection was lost if natural killer cells were absent, suggesting it suppresses immune response to cancer cells (Teng et al., 2010). SerpinE1 is a serine protease inhibitor which is important for blood clot breakdown, fibrinolysis and tissue repair (Bauman et al., 2002). Its role in cancer progression may seem contradictory, as metastasis relies upon tissue breakdown and dissemination of cancer cells, however, serpinE1 has been found as a marker of poor oral carcinoma prognosis (Gao et al., 2010). siRNA inhibition of serpinE1 in cell lines of fibrosarcoma (HT1080) and breast cancer (MDA-MB-231) has been shown to decrease *in vivo* tumour formation of these cell lines, which was attributed to increased cancer cell apoptosis (Fang et al., 2012). RANTES is a chemotractant for a variety of

leukocytes including eosinophils (Kameyoshi et al., 1992) and plasma and tissue levels correlate with breast and cervical cancer stage (Niwa et al., 2001). The cytokines with shared expression from the cell lines have a common role in inflammation and tissue repair, tumours have been shown to arise from sites of chronic inflammation (Anderson and Wong, 2010). Therefore the cytokine expression profile from these cell lines indicates that maintaining the expression of inflammatory cytokines is important for continual cancer growth *in vitro*.

In order to further characterise the IL-8 and CCL-2 expression profile from sarcoma cell lines and MCF7, the concentration of IL-8 and CCL-2 was quantified in conditioned media (collected after 24 hours growth) using an ELISA. No correlation was observed between IL-8 expression and the enhanced growth rates observed in response to conditioned media. This was particularly evident in the U2OS conditioned media which consistently increased growth and was found to contain less IL-8 than 143B conditioned media which had no growth enhancing effect. This finding was supported when correlating IL-8 concentration with increase in colony size observed in response to conditioned media from the same cell line, which was not found to produce a statistically significant Pearson's correlation. In contrast, CCL-2 conditioned media concentration closely resembled the growth enhancement observed. Cell lines which produced conditioned media with an elevated concentration of CCL-2 were correlated with increased cell line growth at low density.

CCL-2 has been shown to increase the proliferation and migration of prostate cancer cells *in vitro*. Interestingly the CCL-2 was hypothesised to originate not from tumour cells but bone marrow endothelial cells (Loberg et al., 2006). Media taken at 24 hours from U2OS cells was found to secrete a higher concentration than MG63, however, at 72 hours the conditioned media from MG63 contained an elevated concentration compared to U2OS. This finding indicates that U2OS CCL-2 expression although rapid after 24 hours may decrease over time, whereas MG63 cells continually secrete CCL-2 at a consistently high rate. In response to the glycoprotein oncostatin U2OS cells have been found to express CCL-2, interestingly the CCL-2 mRNA levels peaked after 8 hours, which led to rapid CCL-2 secretion over 24 hours and the rate of secretion decreased after 48 hours and 72 hours (Kok et al., 2009), which could explain the reduction in U2OS CCL-2 expression over time.

The growth enhancing properties of conditioned media from the cell lines MG63 and in particular U2OS has been established. The growth factors secreted from U2OS are able to enhance growth in not only alternative OS cell lines but sarcoma cell lines and MCF7 as well, indicating the presence of a common cancer growth factor. The growth enhancement in response to conditioned media was not found to be related to an increase in holoclones, however, the conditioned media from MCF7 which did not increase proliferation was found to increase the presence of paraclones, suggesting that this media may enhance the differentiation of these cell lines. The cytokine profiles of the cell lines tested, indicates that inflammatory cytokines are closely related to cancer progression in OS cell lines. IL-8 and CCL-2 were identified as candidate growth factors in growth enhancing conditioned media, which have both been identified in carcinoma proliferation. IL-8 has been demonstrated to enhance the symmetrical division of breast CSC (Singh et al., 2013, Ginestier et al., 2010), CCL-2 has been shown to increase prostate cancer proliferation and migration (Loberg et al., 2006, Loberg et al., 2007). Therefore, further investigation will be important to further understand the role these cytokines play in OS *in vitro* cell growth.

# **Chapter 6**

## **Assessment of IL-8 and CCL-2 in osteosarcoma proliferation**

## 6.1 Introduction

OS cell lines have been demonstrated to secrete a paracrine factor which enhances both OS and MCF7 growth (Section 5.2), the proteins IL-8 and CCL-2 were identified as candidate OS growth factors which may be responsible for this growth (Section 5.10). In response to tumour necrosis factor  $\alpha$  (TNF $\alpha$ ) the OS cell lines HOS, MG63, U2OS and SaOS-2 have been found to alter their expression profile with increased expression of the cytokines CCL-2 and IL-8 (Grigolo et al., 1999). CCL-2 and IL-8 are two cytokines which have been implicated in cancer progression, CCL-2 was originally identified for its role in inflammation and is a potent chemotractant factor for monocytes (Matsushima et al., 1989) and is utilised by osteoblasts for recruitment of monocytes to aid with osteolysis (Williams et al., 1992) (Section 1.4.4). CCL2 signals via the G-protein coupled receptor CCR2 and has been found reliant upon phosphatidylinositol-3-kinase (PI3K) for intracellular signal transduction in both monocyte chemotaxis and *in vitro* prostate cancer growth (Terashima et al., 2005, Loberg et al., 2006) (Section 1.4.4). In OS CCL2 secreted from the cell line MG63 has been attributed to cancer progression through the recruitment of tumour associated macrophages (TAM) (Graves et al., 1989). Solid tumours contain not only cancer cells but a large number of non-malignant cells (Pollard, 2004), these non-malignant cells frequently include TAM. In breast cancer TAM have been found to promote tumour progression by expressing TNF $\alpha$ , vascular endothelial growth factor and basic fibroblast growth factor, which have been implicated in angiogenesis (Lewis et al., 1995). The chemokine IL-8 signals via the CXCR1 and CXCR2 receptors (Park et al., 2011b) it has a potent chemottractive effect upon neutrophils (Yoshimura et al., 1987), therefore plays an important role in acute inflammatory responses. IL-8 is expressed by a wide range of cancer types including cancers including breast, colon, gastric, melanoma, pancreatic and B-cell chronic lymphocytic leukaemia (Lippitz, 2013), in breast cancer IL-8 has been demonstrated to not only increase cancer invasiveness (Freund et al., 2003) but also the presence of putative CSC based on the expression of ALDH and mammosphere formation (Charafe-Jauffret et al., 2009) (Section 1.4.5).

The reliance of cancer cells upon growth factors and signaling molecules provides a therapeutic target to inhibit their growth or progression. These treatments often provide treatment strategies with decreased toxicity and high affinity for cancer cells (Heinrich et

al., 2003, Fisher et al., 1998, Fisher et al., 1994). Two successful examples of this targeted treatment strategy in breast cancer include the estrogen receptor antagonist tamoxifen, which has been found to reduce breast cancer incidence by 50 % in high risk patients (Fisher et al., 1998) and humanized monoclonal antibody trastuzumab which inhibits signal transduction via HER2 (Owens et al., 2004) (Section 1.4.6).

## **Aims**

In order to establish the role CCL-2 and IL-8 play in OS proliferation, recombinant CCL-2 and IL-8 will be supplemented in to unconditioned media to assess changes in proliferation. In addition IL-8 and CCL-2 receptor anatagonism and gene knockdown through RNA interference (RNAi) will be analysed to assess the impact upon cell line growth. This study will use OS cell lines HOS and U2OS. MG63 will also be used to replace HOS for low attachment assays in which HOS is unsuited. The specific objectives within this chapter are as follows:

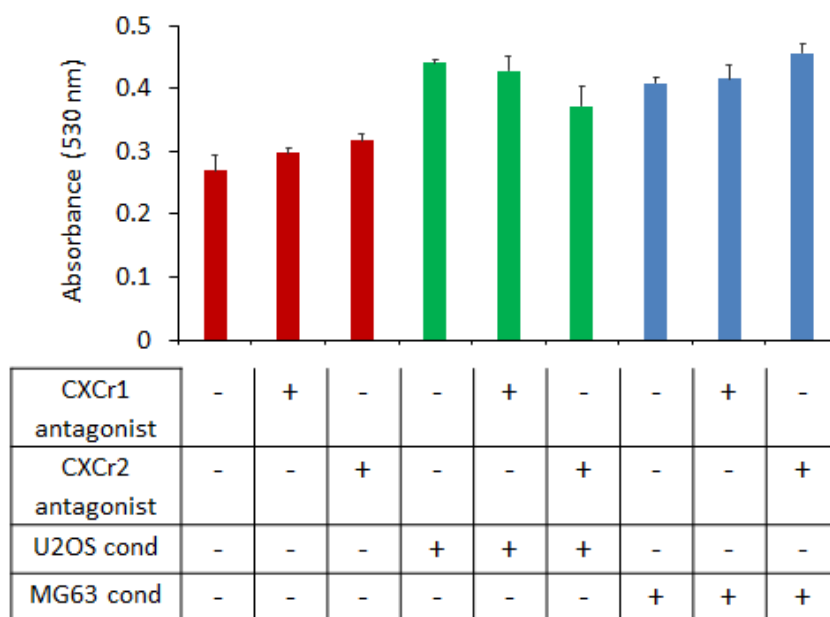
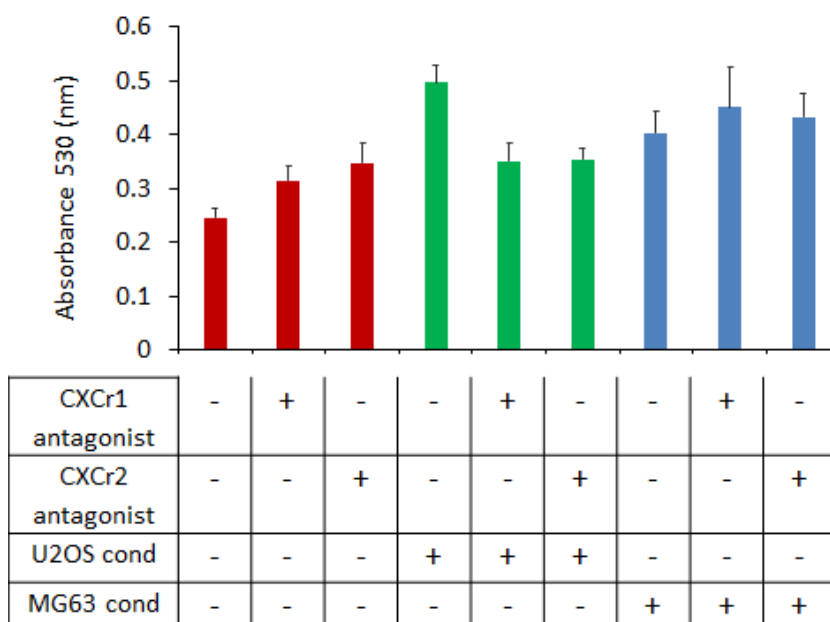
- Assessment of the *in vitro* role of candidate growth factors in OS growth through receptor inhibition, gene expression knockdown and cytokine supplementation.
- Assessment of low attachment colony formation (sarcosphere assay and soft agarose assay) in response to recombinant CCL-2.
- Analysis of gene expression in response to candidate cytokine and growth enhancing conditioned media to identify genes associated with enhanced proliferation.

## 6.2 Effect of IL-8 and CCL-2 receptor antagonism on HOS and U2OS growth rates

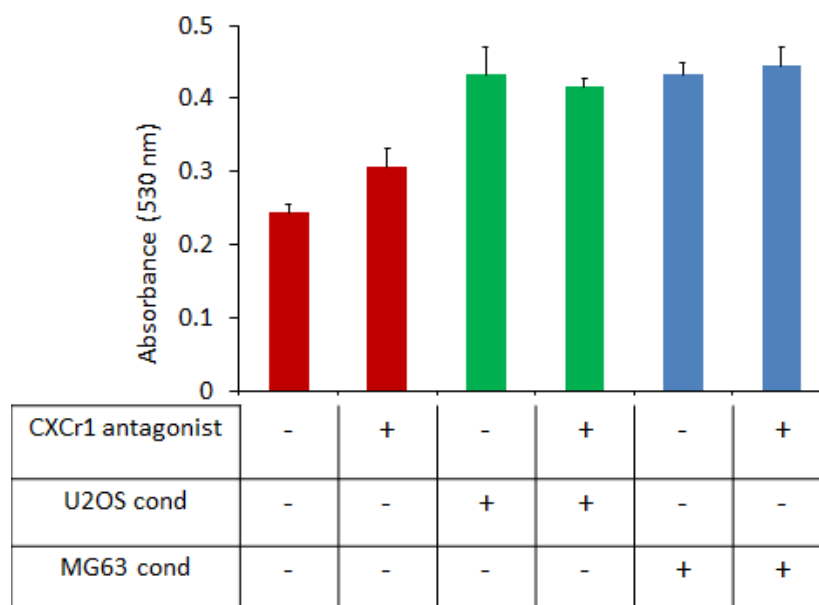
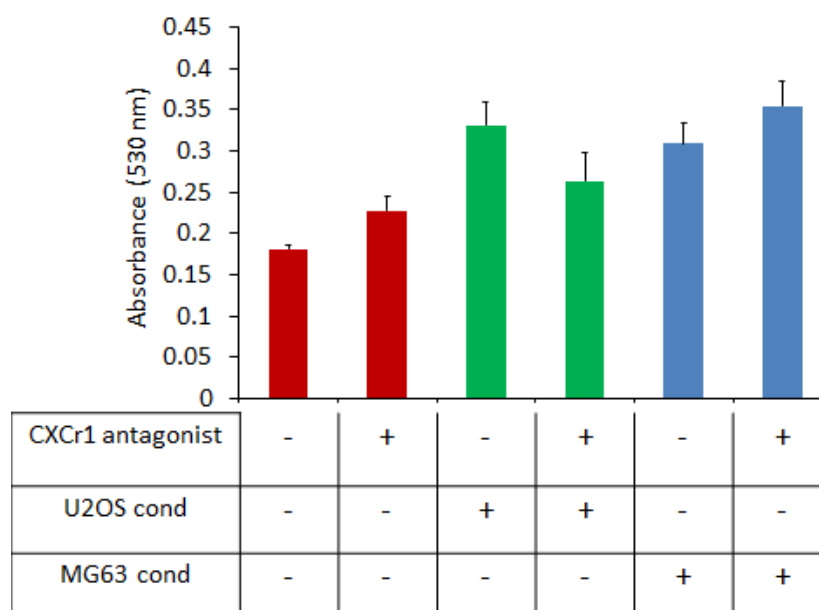
The cytokines IL-8 and CCL-2 have been identified as potential growth enhancing factors produced in OS conditioned media (Section 5.10). Receptor antagonists were used in the presence of growth enhancing media (MG63 and U2OS 72 hour conditioned media) in order to identify whether these cytokines contribute to OS growth. The CXC chemokine IL-8 has been found to signal via the CXCR1 and CXCR2 G-protein coupled receptors (Park et al., 2011b) (Section 1.4.5). In order to analyse the impact of IL-8 antagonists on the growth rate HOS and U2OS, cells were grown for 8 – 9 days and cell density was assessed using an MTT assay (Section 2.4.4). No significant decrease in growth was observed in conditioned or unconditioned media for either U2OS or HOS cells in response to 200 ng/ml of CXCR1 and CXCR2 antagonist antibodies (Figure 6.1). Increasing the concentration of the CXCR1 inhibitory antibody 10 fold to 2 µg/ml also had no significant effect on the growth rates of either HOS or U2OS (Figure 6.2). These findings suggest that the IL-8 present in U2OS and MG63 conditioned media is not responsible for the growth enhancement observed in HOS and U2OS proliferation (Section 5.7).

CCL-2 is specific for the G-protein coupled receptor CCR2 and CCR2 signal transduction can be inhibited using a specific CCR2 antagonist RS 504393 (Section 2.4.4). Using RS 504393 at a concentration of 1 µM had no significant effect on growth of HOS and U2OS cells when grown in unconditioned media and MG63 72 hour conditioned media (Figure 6.3). However, increasing the concentration to 10 µM significantly reduced the growth (Figure 6.3). These findings suggest that both HOS and U2OS utilise CCR2 signaling to enhance proliferation. In addition, the increased growth observed in U2OS and HOS cells in response to MG63 conditioned media (Section 5.7) is attributed to the expression of CCL-2 from MG63 cells. CCR2 antagonism reduced the growth of U2OS cells in response to U2OS conditioned media (Figure 6.4.A), however it had no significant effect on HOS proliferation in the presence of U2OS conditioned media (Figure 6.4.B).

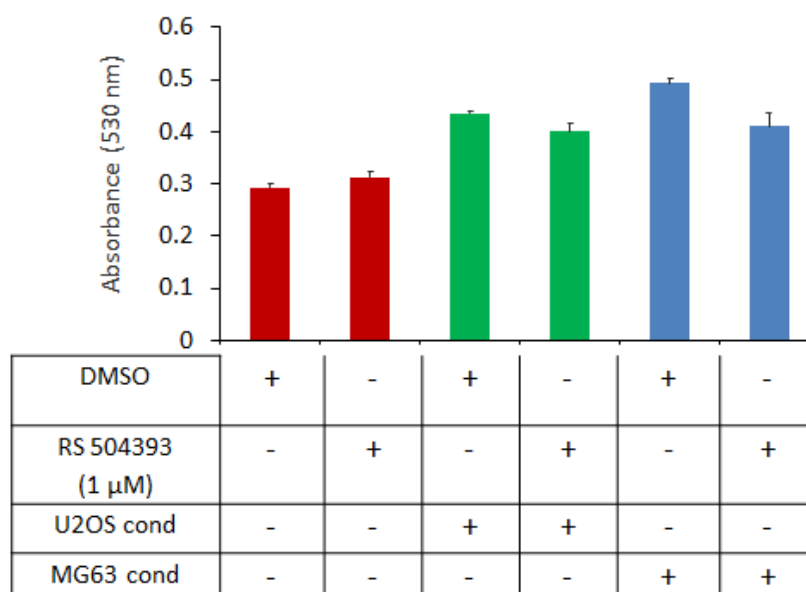
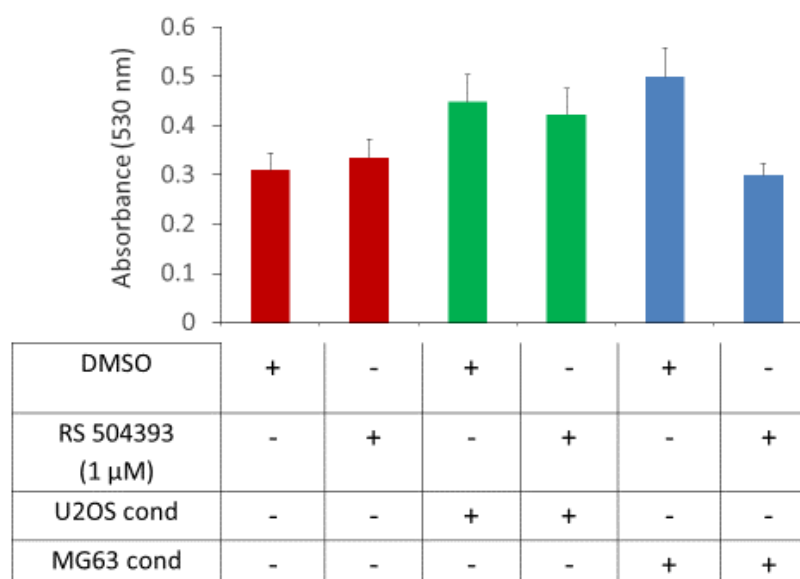


**(A) U2OS****(B) HOS**

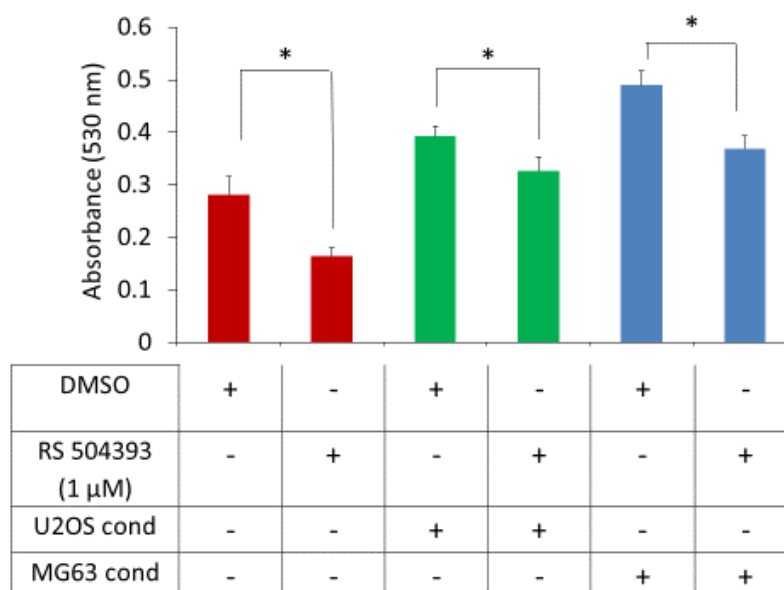
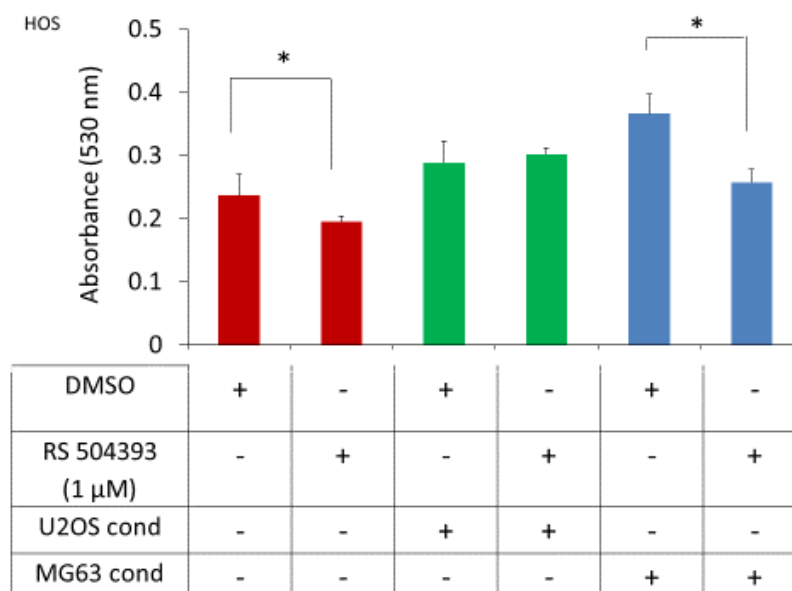
**Figure 6.1: IL-8 receptor antagonism of U2OS and HOS cells growth in unconditioned, U2OS and MG63 72 hour conditioned media in the presence or absence of 200 ng/ml CXCR1 and CXCR2 inhibitory antibodies.** U2OS (A) and HOS (B) cells were grown in unconditioned (red bars), U2OS conditioned (green bars) and MG63conditioned (blue bars) in the absence and presence of CXCR1 and CXCR2 antagonist antibodies (200 ng/ml). Data presented as mean and standard error, all samples repeated in sextuplicate in 3 separate experiments ( $n = 3$  independent replicates). Tukey's post hoc analysis used to assess significance by comparing no antagonist present to antagonist in unconditioned, U2OS conditioned and MG63 conditioned cells. No significant difference observed between conditions.

**(A) U2OS****(B) HOS**

**Figure 6.2: IL-8 receptor antagonism of U2OS and HOS cells growth in unconditioned, U2OS and MG63 72 hour conditioned media in the presence or absence of 2  $\mu\text{g/ml}$  CXCR1 inhibitory antibody.** To analyse the effect CXCR1 receptor antagonism upon OS growth U2OS (A) and HOS (B) cells were grown in unconditioned (red bars), U2OS conditioned (green bars) and MG63 blue bars in the absence and presence of CXCR1 antagonist antibodies (2  $\mu\text{g/ml}$ ). Data presented as mean and standard error, all samples repeated in sextuplicate in 3 separate experiments ( $n = 3$  independent replicates). Tukey's post hoc analysis used to assess significance by comparing to no antagonist present to antagonist in unconditioned, U2OS conditioned and MG63 conditioned cells. No significant difference observed between conditions.

**(A) U2OS****(B) HOS**

**Figure 6.3: RS 504393 CCR2 receptor antagonism (1  $\mu$ M) of U2OS and HOS cells growth in unconditioned, U2OS and MG63 72 hour conditioned media.** To analyse the effect CCR2 receptor antagonism upon OS growth U2OS (A) and HOS (B) cells were grown in unconditioned (red bars), U2OS conditioned (green bars) and MG63 (blue bars) in the absence and presence CCR2 antagonist (1  $\mu$ M). Data presented as mean and standard error, all samples repeated in sextuplicate in 3 separate experiments (n = 3 independent replicates). Unpaired T-test used to assess statistical significance by comparing to no antagonist present to antagonist in unconditioned, U2OS conditioned and MG63 conditioned cells. No significant difference observed between conditions.

**(A) U2OS****(B) HOS**

**Figure 6.4: CCR2 receptor antagonism (10  $\mu$ M) of U2OS and HOS cells growth in unconditioned, U2OS and MG63 72 hour conditioned media.** To analyse the effect CCR2 receptor antagonism upon OS growth U2OS (A) and HOS (B) cells were grown in unconditioned (red bars), U2OS conditioned (green bars) and MG63 conditioned (blue bars) in the absence and presence CCR2 antagonist (10  $\mu$ M). Data presented as mean and standard error, all samples repeated in sextuplicate in 3 separate experiments (n = 3 independent replicates). Significance calculated using an unpaired T-test (\*= < 0.05).

### 6.3 Growth reponse of HOS, MCF7 and MG63 cells to IL-8 and CCL-2

To establish whether CCL-2 or IL-8 enhanced growth when supplemented individually or when combined in unconditioned media, the colony size after exposure to 2 ng/ml of both cytokines was analysed. Both HOS and MCF7 did not respond to either cytokines when supplemented individually or when combined in to unconditioned media (Figure 6.5.A and B). In contrast MG63 responded to CCL-2 when used as a single supplement and produced a significant increase in colony size compared to unconditioned colonies and CCL-2 and IL-8 co-supplemented colonies (Figure 6.5.C).

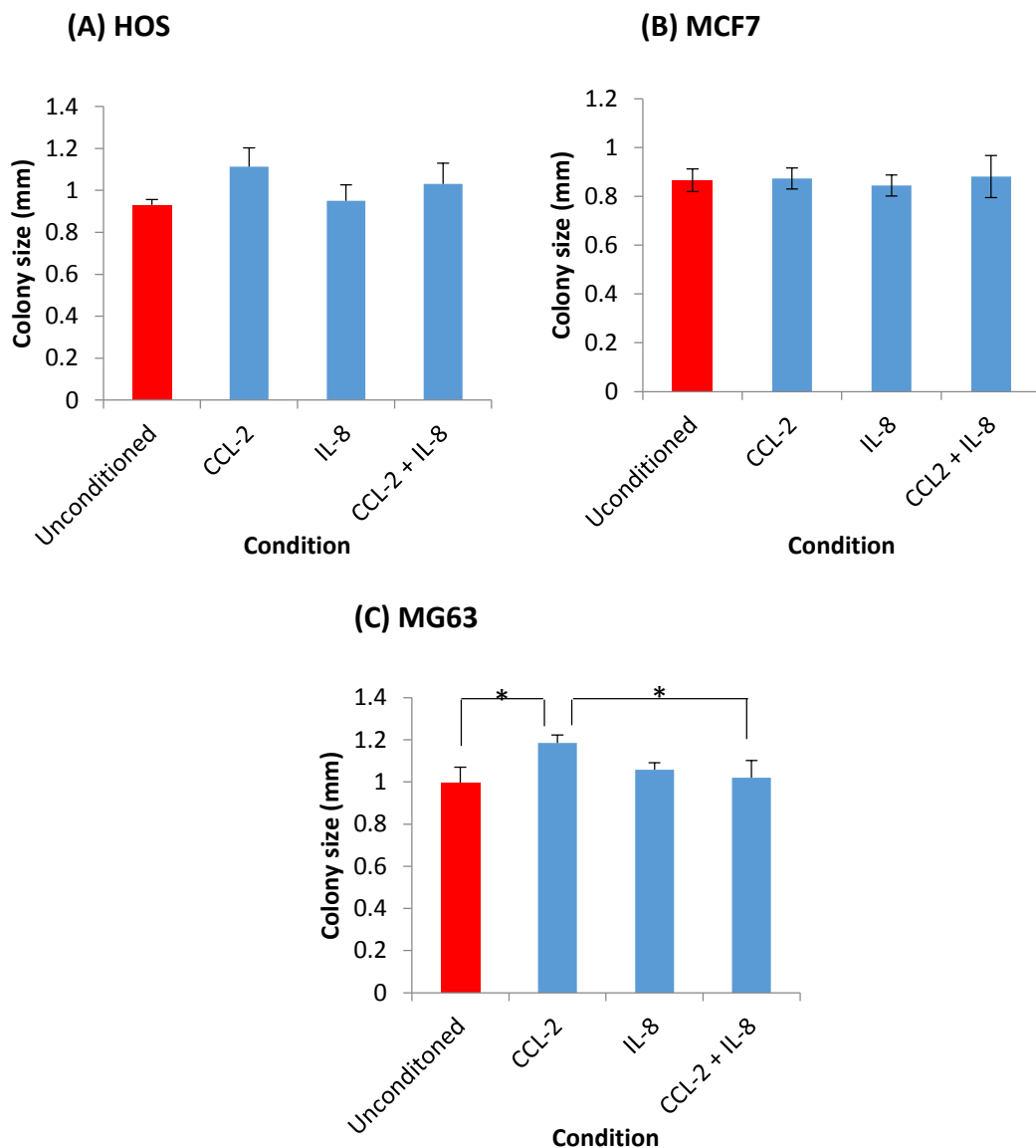


**Figure 6.5 Growth reponse of HOS, MCF7 and MG63 to CCL-2 and IL-8.** 2 ng/ml of IL-8, CCL-2 or IL-8 and CCL-2 was tested on HOS (A), MCF7 (B) and MG63 (C). Cells grown in 6 well dishes and colony size was assessed using ImageJ. Statistical significance assessed using Tukey's post hoc analysis (\* $p < 0.05$ ).

#### **6.4 Growth response of HOS and U2OS to recombinant CCL-2 in a 96 well growth assay**

The use of a CCR2 antagonist reduced the growth rates of both HOS and U2OS (Figure 6.4). To assess the effect of CCL-2 upon growth, recombinant CCL-2 was supplemented in to complete media and growth was assessed using a 96 well MTT assay (Section 2.4.3). CCL-2 used at a concentration of 10 ng/ml did not enhance the growth of either U2OS or HOS (Figures 6.5 and 6.6). An increased CCL-2 concentration of 100 ng/ml resulted in enhanced growth in U2OS (Figure 6.6) and HOS (Figure 6.7). Both HOS and U2OS cells were also grown in U2OS 72 hour conditioned media to compare the growth enhancement of the conditioned media to recombinant CCL-2. Both HOS and U2OS responded with increased growth in response to U2OS conditioned media as previously observed (Section 5.8). U2OS 72 hour conditioned media contains 22 ng/ml of CCL-2 according to the CCL-2 ELISA (Section 5.11). Recombinant CCL-2 at a concentration of 100 ng/ml did not enhance proliferation to the same degree as U2OS media, therefore, the lower concentration of CCL-2 secreted by U2OS suggests that either the recombinant protein has less activity compared to the native version expressed by U2OS or another growth factor is responsible for the increased proliferation.

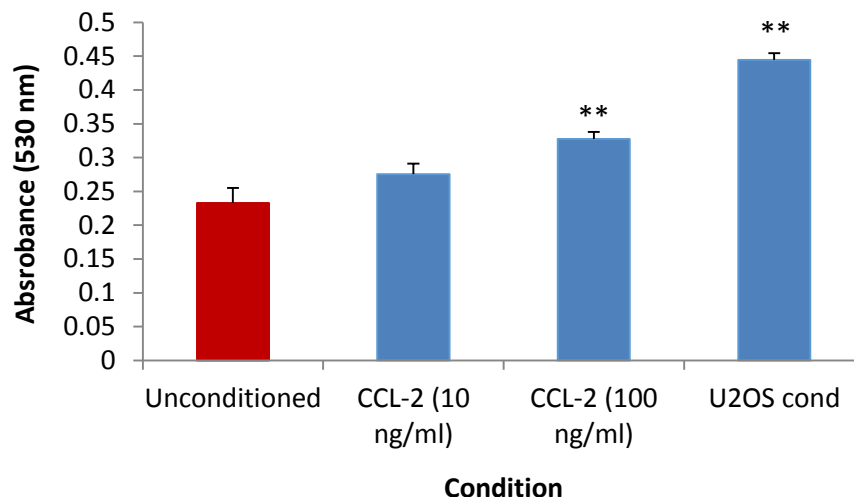


**Figure 6.6: Supplementation of recombinant CCL-2 in to complete media to assess the growth affect upon U2OS cells.** U2OS cells were exposed to 10 and 100 ng/ml recombinant CCL-2 and also U2OS 72 hour conditioned media (U2OS cond) for a growth comparison. 10 ng/ml CCL-2 had no effect on growth but 100 ng/ml increased growth. Data presented as mean and standard error, all samples repeated in sextruplicate in 3 separate experiments (n = 3 independent replicates). Significance calculated using Tukey's post hoc analysis by comparing to unconditioned cells (\*\*= <math>< 0.01</math>).

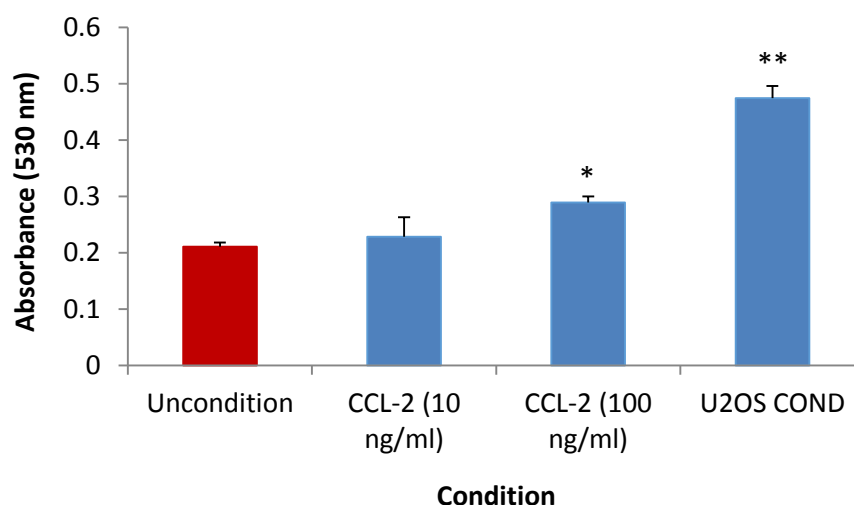


**Figure 6.7: Supplementation of recombinant CCL-2 in to complete media to assess the growth affect upon HOS cells.** HOS cells were exposed to 10 and 100 ng/ml recombinant CCL-2 and also U2OS 72 hour conditioned media (U2OS cond) for a growth comparison. CCL-2 at 10 and 100 ng/ml had no effect on growth but U2OS conditioned media increased growth. Data presented as mean and standard error, all samples repeated in sextruplicate in 3 separate experiments (n = 3 independent replicates). Significance calculated using Tukey's post hoc analysis by comparing to unconditioned cells (\*= <math>< 0.05</math>, \*\*= <math>< 0.01</math>).

### 6.5. Assessment of soft agarose colony formation in response to recombinant IL-8 and CCL-2 in the OS cell lines MG63 and U2OS

The soft agarose assay is an *in vitro* assay which has been found to replicate cancer growth rates observed *in vivo* (Courtenay, 1976), therefore, soft agarose colony formation represents an *in vitro* technique to assess the *in vivo* tumorigenicity of a cell line. MG63 and to a lesser extent U2OS have been demonstrated to produce colonies in soft agarose, whereas, HOS was unable to form colonies (Fawdar, 2010). Based upon these findings U2OS and MG63 were selected to be grown in the soft agarose assay in the presence of recombinant CCL-2 and IL-8 to assess the effect of these cytokines upon colony formation. According to ELISA results MG63 72 hour conditioned media contained the highest concentration of CCL-2 and IL-8 (Section 5.11) and therefore concentrations which replicated these were chosen (CCL-2 concentration of 36.4 ng/ml and IL-8 a concentration of 9 ng/ml). Colony formation was monitored over 12 – 15 days beyond this point a monolayer formed on the agarose and the media acidified (Section 2.2.5). MG63 cells were found to produce colonies of a greater size than U2OS and MG63 colonies were oval in shape unlike the irregular shapes produced by U2OS (Table 6.1). U2OS cells were found to produce a greater number of colonies in response to CCL-2 (Figure 6.8), which suggests that U2OS may rely on CCL-2 signaling to promote growth *in vivo*. MG63 cells did not respond to CCL-2 (Figure 6.9) suggesting that it may not be a universal growth factor in all OS tumours. Neither U2OS nor MG63 responded to IL-8 (Figures 6.9 and Figure 6.10), indicating that this cytokine does not have a role in soft agarose colony formation in U2OS and MG63.



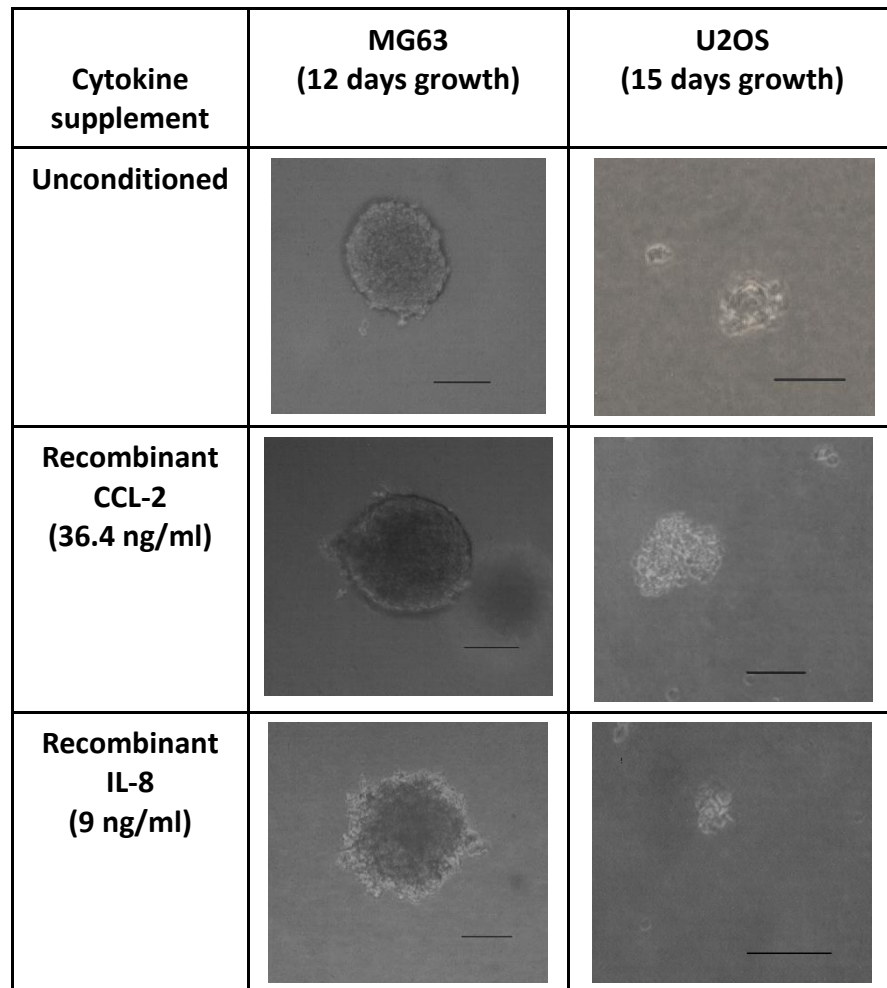


**Figure 6.8: Appearance of MG63 and U2OS soft agarose colonies formed in the absence and presence of recombinant CCL-2 and IL-8.** Cells seeded at a density of 1053 cells/cm<sup>2</sup> and grown for 12 – 15 days under standard culture conditions. Scale bars represent 100  $\mu$ M.

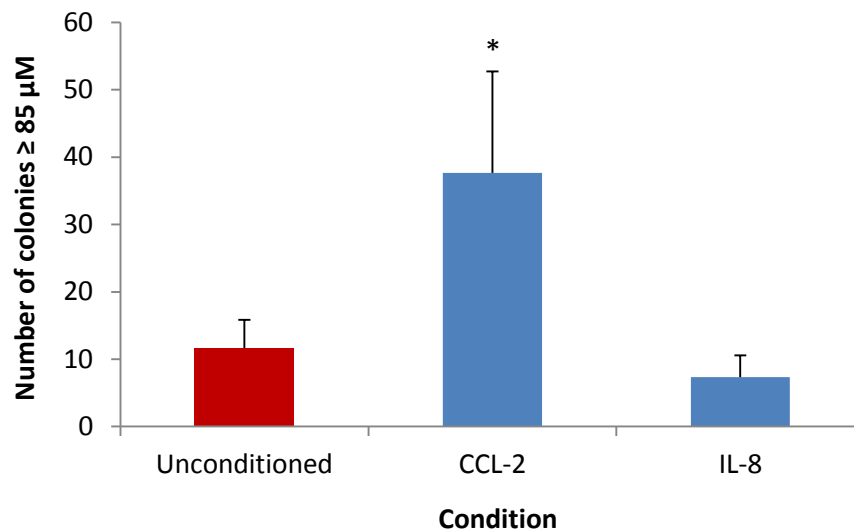


**Figure 6.9: Number of U2OS colonies present in the soft agarose assay in response to CCL-2 and IL-8.** U2OS cells were seeded at  $1 \times 10$  cells/6 well and allowed to grow for 15 days in the absence and presence of 36.4 ng/ml CCL-2 and 9 ng/ml IL-8. Colonies  $\geq 85 \mu\text{M}$  were counted and data presented as mean and standard deviation, all samples tested in triplicate ( $n = 3$ ). Significance calculated using Tukey's post hoc analysis by comparing CCL-2 to unconditioned and IL-8 (\* =  $<0.05$ ).

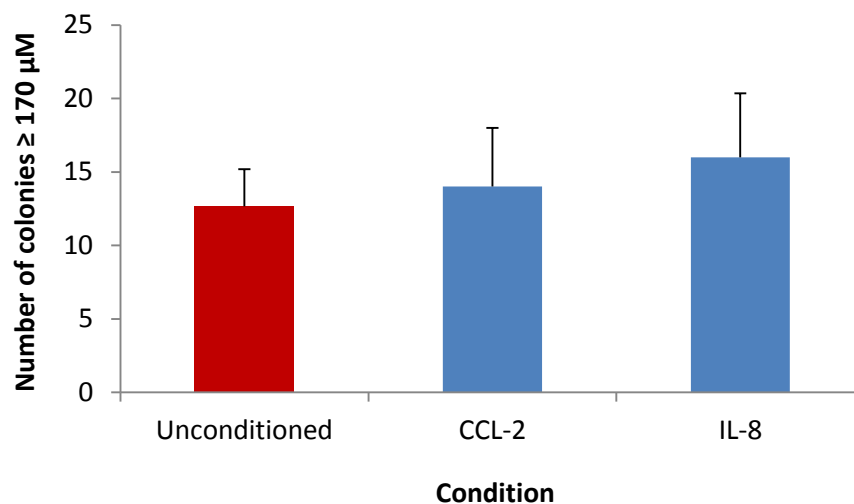


**Figure 6.10: Number of MG63 colonies present in the soft agarose assay in response to CCL-2 and IL-8.** MG63 cells were seeded at  $1 \times 10$  cells/6 well and allowed to grow for 12 days in the absence and presence of 36.4 ng/ml CCL-2 and 9 ng/ml IL-8. Colonies  $\geq 85 \mu\text{M}$  were counted and data presented as mean and standard deviation, all samples tested in triplicate ( $n = 3$ ). Tukey's post hoc analysis used to assess statistical significance, no significant difference observed.

### **6.6. Assessment of sarcosphere formation in response to recombinant IL-8 and CCL-2 in the OS cell line MG63**

The sarcosphere assay was originally proposed to select multi-potent neuronal cells (Reynolds et al., 1992), however, this assay has also been utilised to select for CSC which are able to grow within these serum depleted and low attachment conditions. OS cell lines have been screened for their sarcosphere forming ability, MG63 has been found to produce secondary sarcospheres (Section 3.7) so was used to identify if IL-8 or CCL-2 and any effect sarcosphere forming ability. A concentration of 2 ng/ml recombinant IL-8 or CCL-2 was supplemented in to growth media, which was chosen to reflect the concentration identified in U2OS 24 hour conditioned media (0.65 ng/ml IL-8 and 1.3 ng/ml CCL-2) (Section 5.11). U2OS 24 hour conditioned media was found to enhance growth in MG63 (Section 5.7), therefore, selecting a concentration higher than U2OS conditioned media could be hypothesised to increase MG63 sarcosphere formation.

Exposure of MG63 cells to IL-8 and CCL-2 did not alter the appearance of primary sarcospheres. In all conditions tested the primary sarcosphere appearance was oval shaped as was observed when grown in unconditioned media. However IL-8 and CCL-2 exposed sarcospheres presented a smoother appearance and individual cells within the spherical colony were less identifiable (Figure 6.11). Assessment of the size of these primary sarcospheres indicated that MG63 sarcospheres conditioned with IL-8 or CCL-2 did not have an increased size (Figure 6.12), suggesting that IL-8 and CCL-2 does not enhance the proliferation of primary sarcospheres or this was masked by the sarcospheres having a more compact shape. Secondary sarcospheres generated from all the conditions tested had a similar appearance which was characterised by a small colony size with individual cells clearly visible. However, IL-8 and CCL-2 conditioned cells produced colonies with a more spherical shape than the irregular shape of unconditioned colonies (Figure 6.11). Analysis of the sarcosphere forming efficiency of secondary sarcospheres showed that exposure to IL-8 and CCL-2 did not alter the sarcosphere forming efficiency of MG63 (Figure 6.13), suggesting that IL-8 and CCL-2 do not enhance the formation of sarcospheres in MG63.

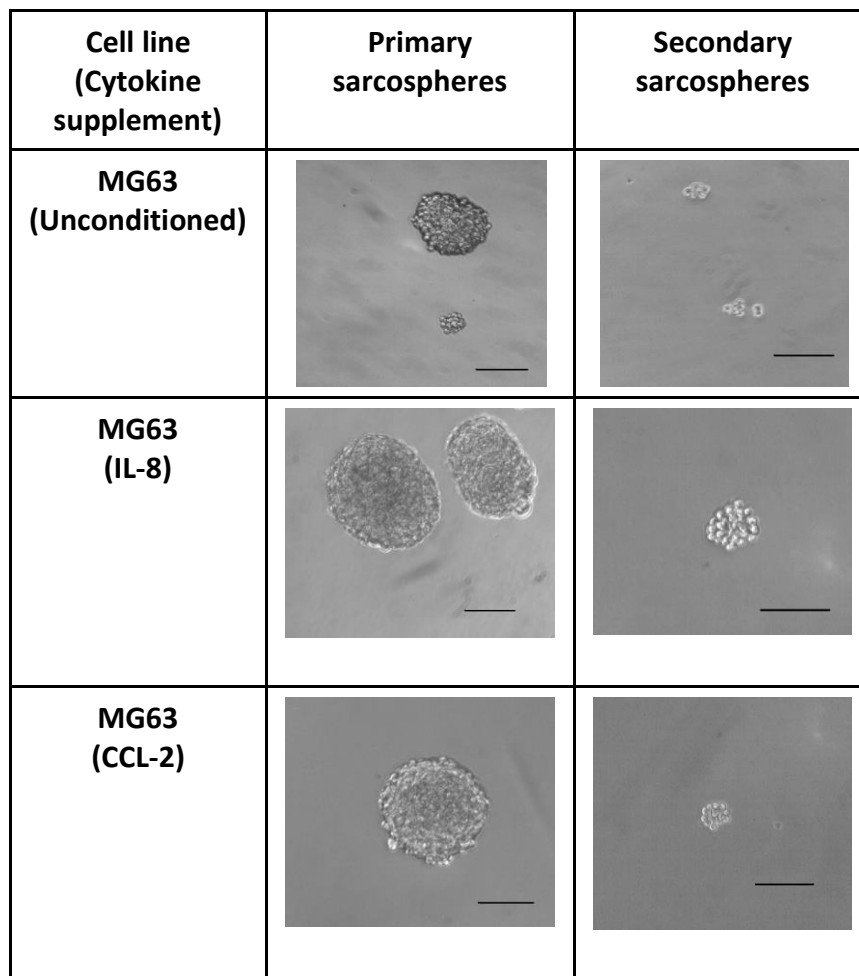


**Figure 6.11: Appearance of MG63 primary and secondary sarcosphere formed in the absence and presence of recombinant CCL-2 and IL-8.** MG63 cells seeded at a density of 1053 cells/cm<sup>2</sup> and grown for 7 days to form primary sarcospheres before passaging and re-seeding at 211 cells/cm<sup>2</sup> and allowing secondary sarcospheres to form over 7 days under standard culture conditions. 2 ng/ml of IL-8 and CCL-2 were supplemented in to sarcosphere media. Scale bars represent 100  $\mu$ M, images representative of 4 images.

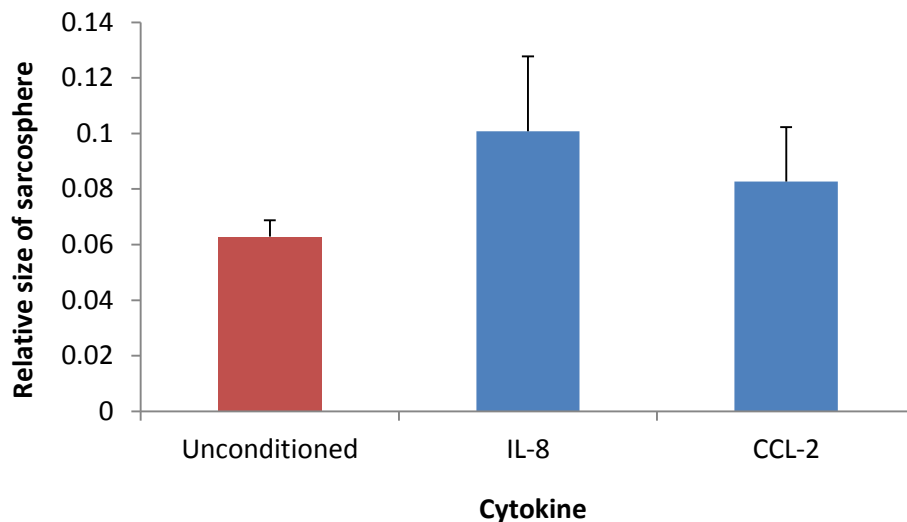


**Figure 6.12: Analysis of primary sarcosphere sizes in MG63 in response to IL-8 and CCL-2.** MG63 cells were either unconditioned (no cytokine) or exposed to either 2 ng/ml IL-8 or CCL-2, sarcosphere size assessed using ImageJ. All results repeated in triplicate (n = 3), presented as mean and standard deviation. Statistical significance was assessed using Tukey's post hoc analysis. No significance was observed when comparing all condition combinations.

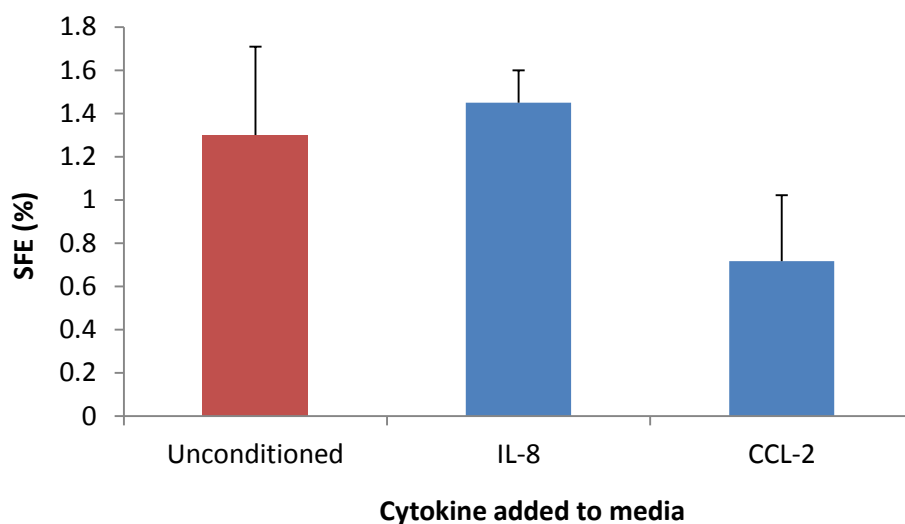


**Figure 6.13: Analysis of secondary sarcosphere forming efficiency of MG63 cells in response to IL-8 and CCL-2.** MG63 cells were treated with either unconditioned (no cytokine) media or media supplemented with either 2 ng/ml IL-8 or CCL-2. Sarcosphere forming efficiency (SFE), was assessed by counting each sarcosphere  $\geq 40 \mu\text{M}$ . All results repeated in triplicate (n = 3), presented as mean and standard deviation. Statistical significance was assessed using Tukey's post hoc analysis. No significance was observed when comparing all condition combinations.

### 6.7 Analysis of CXCR1, CXCR2 and CCR2 expression in OS cell lines and MCF7

IL-8 and CCL-2 have been identified as potential growth factors in OS cell lines (Section 5.11), therefore, identifying if the cell lines express the appropriate cognate receptors is necessary to evaluate whether receptor expression is linked to the observed proliferation response to conditioned media. IL-8 has been shown to signal via two different G-protein coupled receptors; CXCR1 and CXCR2 (Park et al., 2011b) (Section 1.4.5), whereas CCL-2 is specific to only one receptor CCR2 (Section 1.4.4). The expression level of each receptor expressed by the selected cell lines (HOS, MG63, U2OS and MCF7) was evaluated by, fixing cells and antibody staining for both surface and intracellular receptor expression which was evaluated using flow cytometry (Section 2.8.2).

Earlier findings indicated that the OS cell lines MG63 and U2OS respond with enhanced growth to all conditioned media apart from MCF7 media (Section 5.7). HOS only responded to MG63 and U2OS conditioned media. U2OS and MG63 conditioned media contained higher quantities of both cytokines compared to HOS conditioned media as determined by ELISA (Section 5.11). Therefore, it could be hypothesised that both U2OS and MG63 express higher levels of the growth factor receptor than HOS or MCF7, because they are able to respond to lower concentrations of the growth factor.

The CXCR1 expression profile did not fit the expected receptor expression pattern with all OS cell lines having a similar profile (Figure 6.14) with mean receptor expression values between 158.1 to 277.1 (Table 6.1). For CXCR2 the highest expression was observed in MCF7 with a mean expression value of 39, whilst HOS and U2OS expressed the lowest levels of the receptor of 9.5 and 9.7 respectively (Table 6.1). Expression levels of CXCR2 receptor did not therefore correlate with the observed growth in response to conditioned media. CCR2 receptor expression did fit the hypothesized receptor expression with U2OS and MG63 containing the largest mean expression of the receptors with 196.8 and 83.1 respectively (Table 6.1). In addition, MCF7 contained significantly less CCR2 expression than U2OS, (Table 6.1). The flow cytometry histogram of U2OS demonstrates the large proportion of cells positive for CCR2 in this cell line, demonstrating the high number of cells expressing this receptor.

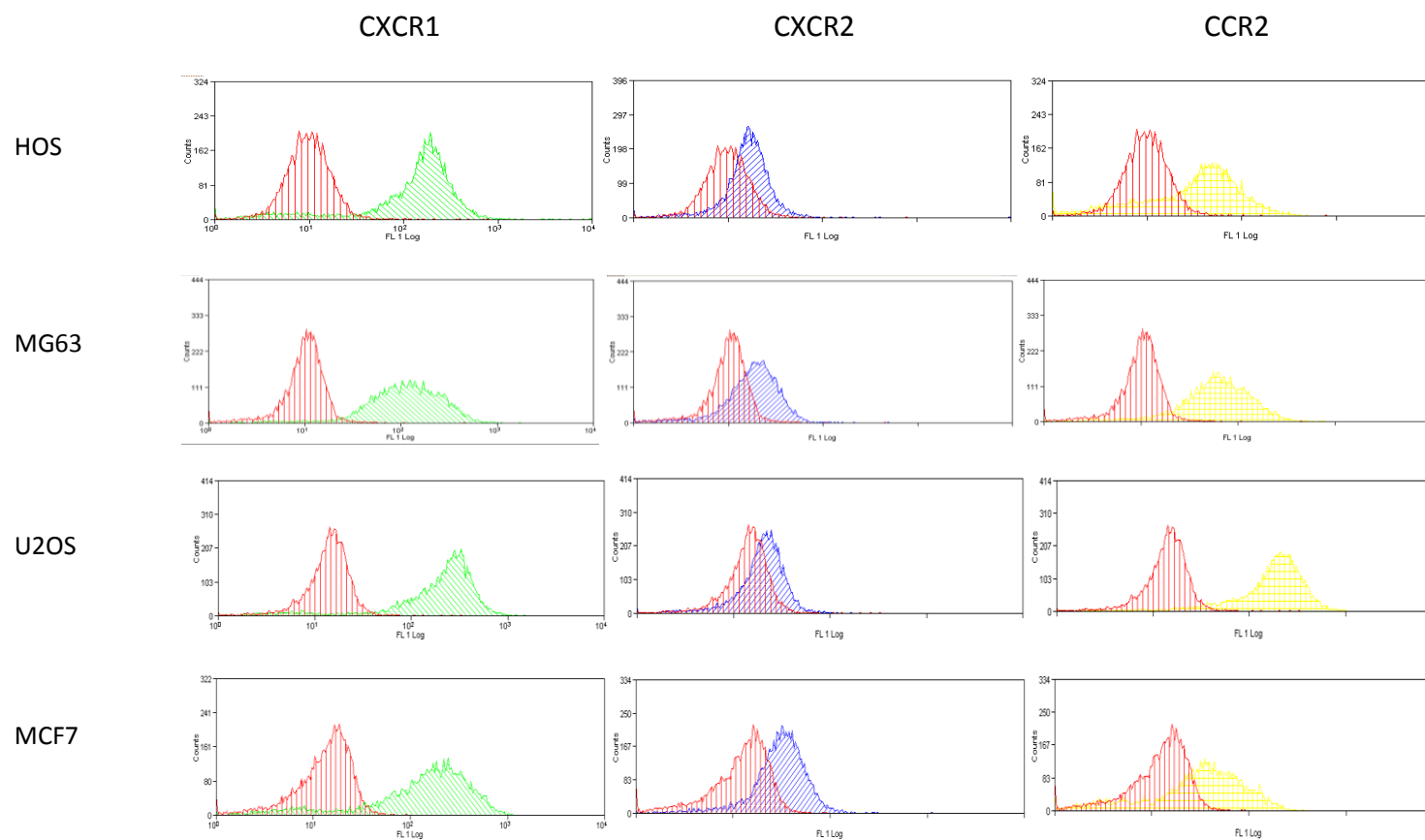


**Figure 6.14: Flow cytometry overlay analysis of CXCR1, CXCR2 and CCR2 expression from the cell lines HOS, MG63, U2OS and MCF7.** Cells stained with primary and secondary antibodies for the markers (Section 2.8.2), for analysis stained cells normalised to  $1 \times 10^4$  and dead cells and duplets (two cells passing through the laser at once) excluded. The control population of cells was stained with an isotype matched primary antibody and the same secondary antibody (red) as used for CXCR1 (green), CXCR2 (blue) and CCR2 (yellow) staining. The x axis on graphs represents cell counts and y axis FL1 Log ranging from  $10^0$  -  $10^4$ .

**Table 6.1: CXCR1, CXCR2 and CCR2 expression in the cell lines HOS, MG63, U2OS and MCF7.** The values indicate the difference in mean fluorescence between control populations (isotype matched primary antibody and the same secondary antibody used for analysis of CXCR1, CXCR2 and CCR2) and marker labelled population after removal of dead cells. Highlighted red indicates significant difference to expression in MCF7 (Significance Tukey's post hoc analysis \* < 0.01).

Cell line	CXCR1 expression ± std dev	CXCR2 expression ± std dev	CCR2 expression ± std dev
HOS	277.1 ± 196.2	9.5 ± 3.5	76.0 ± 54.8
MG63	172.0 ± 75.6	13.1 ± 6.3	83.1 ± 27.3
U2OS	295.5 ± 56.4	9.7 ± 6.8	196.8 ± 72.8*
MCF7	151.8 ± 40.1	39.0 ± 21.2	32.3 ± 16.0



### 6.8 RNA inference of CCL-2 gene expression in U2OS cells

In order to assess the role CCL-2 plays in OS proliferation CCL-2 gene expression was stably knocked down using RNA interference in the OS cell line U2OS. CCL-2 expression was suppressed using a retroviral based plasmid containing short hairpin RNA (shRNA) specific to CCL-2 (Section 2.6). To establish gene knockdown expression levels of CCL-2 were assessed using real time PCR, thermal melting curves of primers verified that the primers were binding to the same sequences within the cell lines (Appendix IV). The shRNA antisense sequences TTATAACAGCAGGTGACTGGG (knockdown 1) and TAAGGCATAATGTTTCACATC (knockdown 2), were found to reduce the presence of CCL-2 mRNA in the CCL-2 knockdown cell lines compared to cells infected with a plasmid containing a shRNA sequence which has no specificity to any mammalian genes (scrambled control).

The sequence used in knockdown 2 was more effective than knockdown 1, which is evident because less CCL-2 mRNA is present in the knockdown 2 cells compared to knockdown 1 (Figure 6.15). Conditioned media taken from the knockdown cells was tested using a CCL-2 ELISA (Section 2.5.2) to confirm if CCL-2 had been knocked down at the protein level. Conditioned media (24 hour) of the knocked down cell lines was found to contain 82 % less CCL-2 for knockdown 1 and 96 % less CCL-2 for knockdown 2 compared to the scrambled control cell line. U2OS wild-type cells (non-transduced) were found to contain a higher concentration of CCL-2 than scrambled control cells (Figure 6.15). The observed discrepancy of CCL-2 concentration between U2OS normal cells and empty vector control cells was not apparent in 72 hour conditioned media with both cell lines expressing approximately 22 ng/ml (Figure 6.17 and table 6.2). This finding confirms the CCL-2 mRNA levels observed in the cells lines correlate with CCL-2 expression at the protein level.

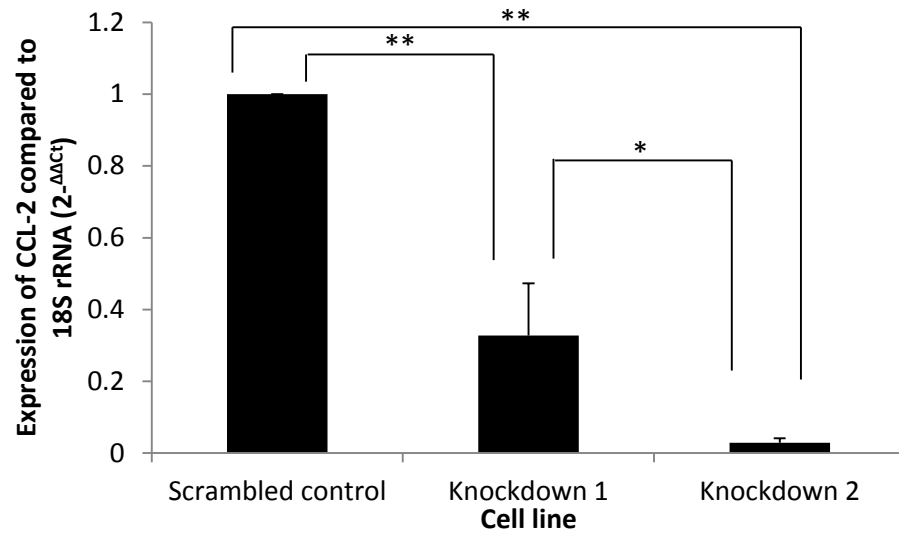


**Figure 6.15: Relative mRNA expression of CCL-2 compared to 18S rRNA expression from U2OS empty vector cells and CCL-2 knockdown 1 and 2 cells.** mRNA expression was calculated by subtracting  $\Delta Ct$  value of CCL-2 (target gene) from  $\Delta Ct$  of shRNA (calibrator gene) to produce  $\Delta\Delta Ct$ . Data presented as mean and standard deviation, all samples repeated in triplicate ( $n = 3$ ). Statistical significance calculated using Tukey's post hoc analysis (\* =  $< 0.05$ , \*\* =  $< 0.01$ ).

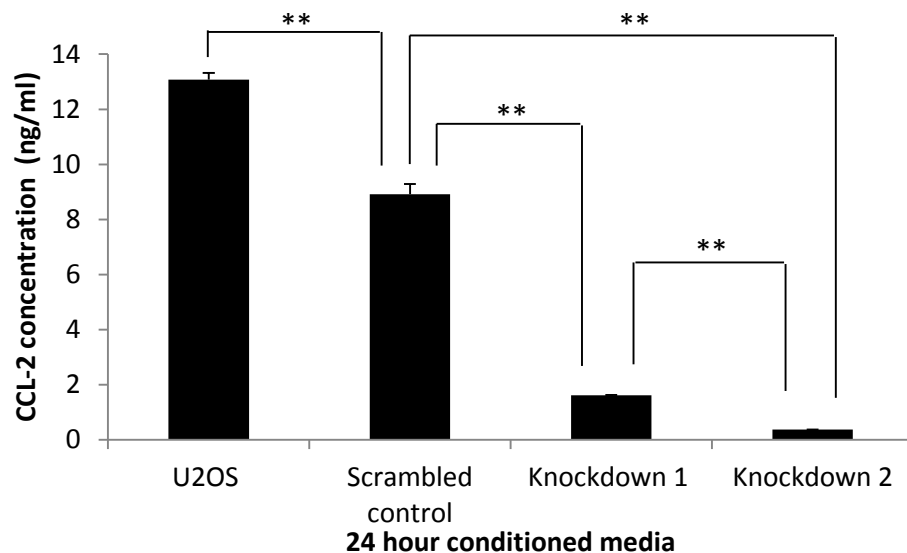


**Figure 6.16: Analysis of CCL-2 concentration of 24 hour conditioned media taken from normal U2OS cells along with U2OS CCL-2 knockdown lines.** A CCL-2 ELISA was used to obtain concentrations, data presented as mean and standard deviation, all samples repeated in triplicate ( $n = 3$ ). Statistical significance calculated using Tukey's post hoc analysis (\* =  $< 0.05$ , \*\* =  $< 0.01$ ).

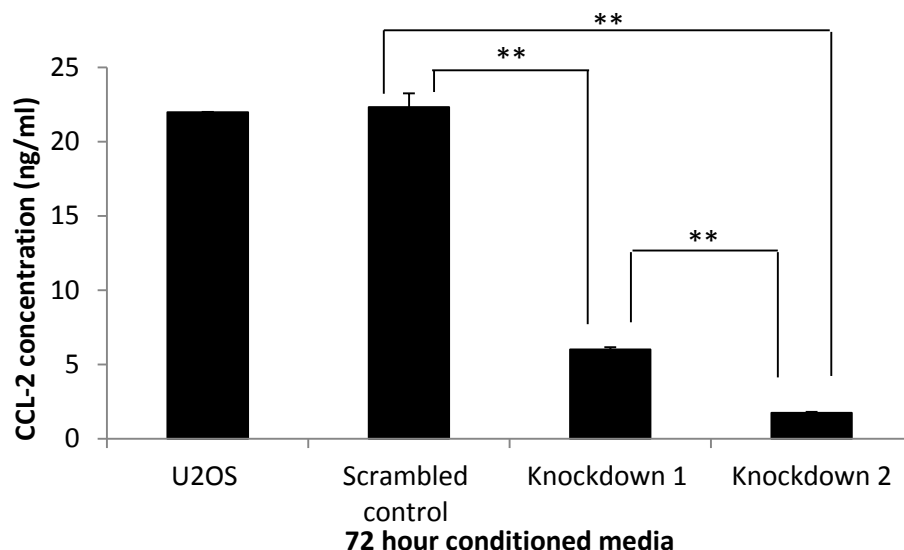


**Figure 6.17: Analysis of CCL-2 concentration of 72 hour conditioned media taken from normal U2OS cells along with U2OS CCL-2 gene knockdown cell lines.** A CCL-2 ELISA was used to obtain concentrations, data presented as mean and standard deviation, all samples repeated in triplicate (n = 3). Statistical significance calculated using Tukey's post hoc analysis (\*\*= <0.01).

**Table 6.2: Comparison of CCL-2 concentrations of conditioned media taken from U2OS cell, empty vector and knockdown 1 and 2 at 24 and 72 hours.** CCL-2 concentrations (ng/ml) established using an ELISA, all samples tested in triplicate. Statistical significance calculated by comparing to scrambled control CCL-2 concentration using Tukey's post hoc analysis (\*\*p = <0.01). Data presented as mean values ± standard deviation (std dev).

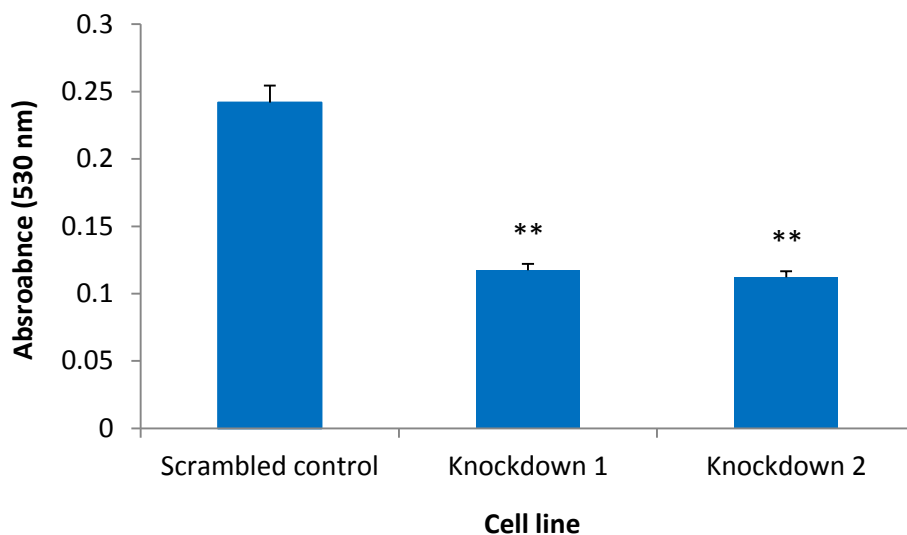
Conditioned media	CCL-2 24 hr concentration (ng/ml) ± std dev	CCL-2 72 hr concentration (ng/ml) ± std dev
Normal U2OS	13.1 ± 0.23 **	21.9 ± 0.24
Scrambled control	8.9 ± 0.38	22.3 ± 0.94
Knockdown 1	1.6 ± 0.01 **	6 ± 0.16 **
Knockdown 2	0.4 ± 0.01 **	1.7 ± 0.06 **

### 6.9 Assessment of the U2OS CCL-2 knockdown cell lines proliferation rate

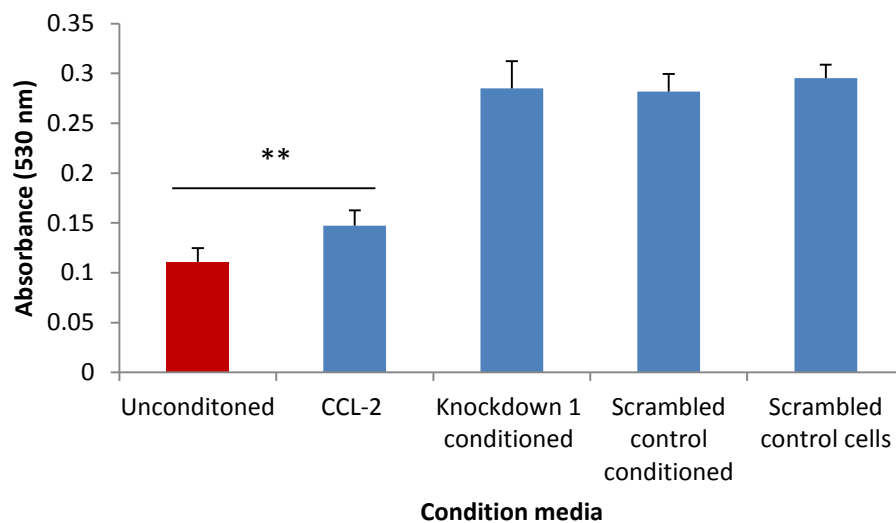
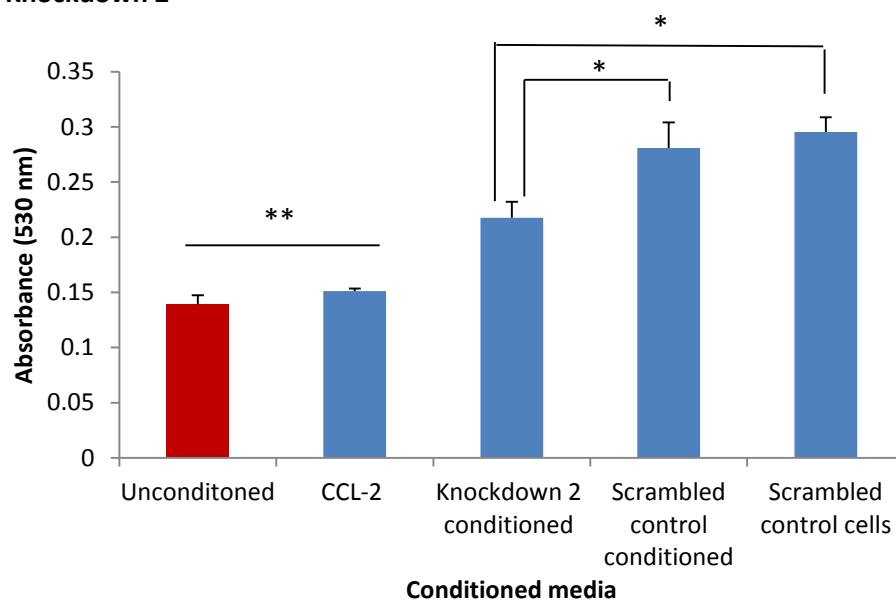
To assess whether knockdown of CCL-2 effects the proliferation rate of U2OS cells, CCL-2 knockdown cells were compared to U2OS empty vector control cells. Proliferation was assessed by seeding cells at 40 cells/96 well and growing for 8 days before staining with MTT and reading the absorbance at 530 nm (Section 2.4.3). The rate of growth of the scrambled control cells was found to be significantly faster than both U2OS CCL-2 knockdown 1 and 2. Interestingly although knockdown 2 cells were found to express less CCL-2 than knockdown 1 (Table 6.2), this had no impact the overall growth rate of the two knockdown cell lines with both producing similar similar growth rates (Figure 6.18). Supplementing recombinant CCL-2 in to complete media had no impact upon the growth rates of either knockdown cell line, however, growth of both cell lines in 72 hour empty vector conditioned media restored the growth rates to that observed in empty vector cells (Figure 6.19). Interestingly, the 72 hour conditioned media from knockdown 1 cells restored growth to the same level as the scrambled control conditioned cells (Figure 6.19.A), however, knockdown 2 cells grown in their own 72 hour conditioned media grew at a slower rate than empty vector conditioned cells (Figure 6.19.B). Knockdown 2 cells express less CCL-2 than knockdown 1 cells (Table 6.2), therefore, the reduced growth rate of knockdown 2 cells compared to scrambled control conditioned cells may be due to a lower concentration of CCL-2 in the conditioned media.

Recombinant CCL-2 supplemented in to unconditioned media did not alter the growth rates of either knockdown cell line. To identify if a CCR2 signaling co-factor is required for the growth promoting effect, recombinant CCL-2 was added to 24 hour and 72 hour conditioned media collected from knockdown 2 cells. In both knockdown cell lines no increase in growth was observed when supplementing recombinant CCL-2 in to 72 hour conditioned media. However, the 24 hour conditioned media supplemented with CCL-2 resulted in increased proliferation in knockdown 2 cells (Figure 6.20.B) but no change in growth was observed in the same conditions for knockdown 1 cells (Figure 6.19.A). This finding suggests that a co-factor may be required for the enhancement of growth in response to CCL-2, however, the increased proliferation observed at high recombinant CCL-2 concentrations (100 ng/ml) did not restore growth to the same level as knockdown 2 72 hour conditioned media which contains 1.7 ng/ml CCL-2. Therefore, another growth factor

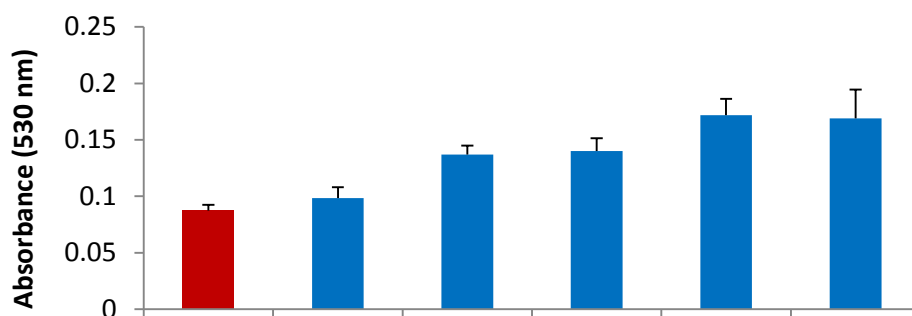
may also be responsible for the increased proliferation rates observed in response to U2OS conditioned media, as was indicated in the CCR2 antagonist growth experiments (Figure 6.6).



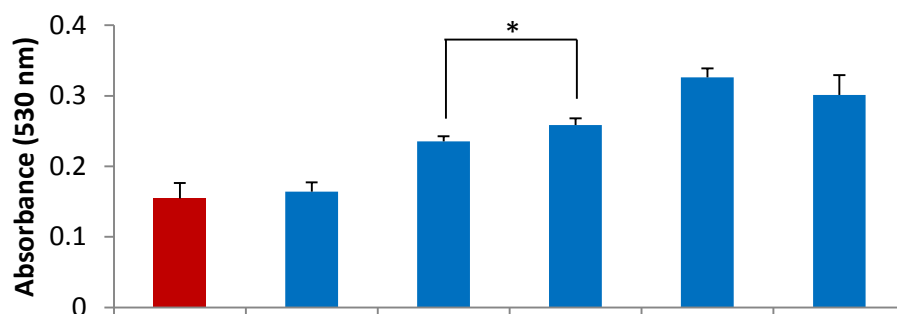
**Figure 6.18: Analysis of U2OS empty vector control and CCL-2 knockdown cell lines growth rates.** Cells grown seeded at a low density (40 cells/96 well) and grown for 8 day in 1.25  $\mu\text{g}/\text{ml}$  puromycin and assessing growth by staining with 1 mg/ml MTT and measuring absorbance at 530 nm. Data presented as mean and standard error, all samples repeated in octuplicate in four separate experiments ( $n = 3$  independent replicates). Statistical significance calculated using Tukey's post hoc analysis comparing to scrambled control absorbance (\*\*= <0.01).

**(A) Knockdown 1****(B) Knockdown 2**

**Figure 6.19: Assessment U2OS CCL-2 knockdown cell lines growth response to CCL-2 (100 ng/ml) and conditioned media from scrambled control and CCL-2 knockdown cell lines.** U2OS CCL-2 knockdown 1 (A) and knockdown 2 (B) cell lines were seeded at low density (50 cells/96 well) and grown in the presence of CCL-2 (100 ng/ml), 72 hour conditioned media taken from the same cell knockdown cell line as was grown, 72 hour empty vector conditioned media. Empty vector cells were also included to identify for a growth rate comparison. Data presented as mean and standard error, all conditions repeated in octuplicate in 3 separate experiment (n = 3 independent replicates). Statistical significance calculated using Tukey's post hoc analysis (\* = <math>< 0.05</math>, \*\* = <math>< 0.01</math>). Unconditioned and CCL-2 supplemented samples had a significantly lower absorbance than knockdown conditioned, scrambled control conditioned and scrambled control cells.

**(A) Knockdown 1**

CCL-2 (100 ng/ml)	-	+	-	+	-	+
24 hour knockdown 2 conditioned	-	-	+	+	-	-
72 hour knockdown 2 conditioned	-	-	-	-	+	+

**(B) Knockdown 2**

CCL-2 (100 ng/ml)	-	+	-	+	-	+
24 hour knockdown 2 conditioned	-	-	+	+	-	-
72 hour knockdown 2 conditioned	-	-	-	-	+	+

**Figure 6.20: The growth effect of supplementing CCL-2 in to knockdown 2 conditioned media upon knockdown 1 and 2 cell lines.** CCL-2 (100 ng/ml) was supplemented in to unconditioned media and conditioned media collected from knockdown 2 cells at 24 hours and 72 hours. U2OS CCL-2 knockdown 1 (A) and 2 (B) cell lines were used. Cells were seeded at 50 cells/96 well and grown for 8 days in standard cell culture conditions before staining with MTT. Data presented as mean and standard deviation, all conditions repeated in quadruplicate in 3 separate experiment (n = 3). Statistical significance calculated using an unpaired T-test (\* = <math>< 0.05</math>), comparing the addition of CCL-2 in unconditioned, knockdown 1 and 2 conditioned media.

### 6.10 U2OS CCL-2 knockdown cell lines in low attachment conditions

Growth of cancer cells within low attachment conditions has been found to replicate *in vivo* cancer growth (Courtenay, 1976). U2OS CCL-2 knockdown cell lines were grown within the soft agarose assay (Section 2.2.5) to assess whether CCL-2 expression effected colony formation in these conditions. The U2OS knockdown cell lines were grown in the absence and presence of recombinant CCL-2 (36.4 ng/ml). Cells grown in the presence of recombinant CCL-2 formed colonies which were in general larger in size and displayed a more oval appearance (Figure 6.21). An increased number of soft agarose colonies were formed by the scrambled control cells compared to the CCL-2 knockdown cell lines (Figure 6.22), which suggests that the of expression CCL-2 may enhance proliferation in anchorage independent conditions. This finding is supported by supplementation of recombinant CCL-2 (36.4 ng/ml) in to the soft agarose assay, which increased the number of colonies present in the scrambled control cells and knockdown 1 and 2 cells (Figure 6.23).



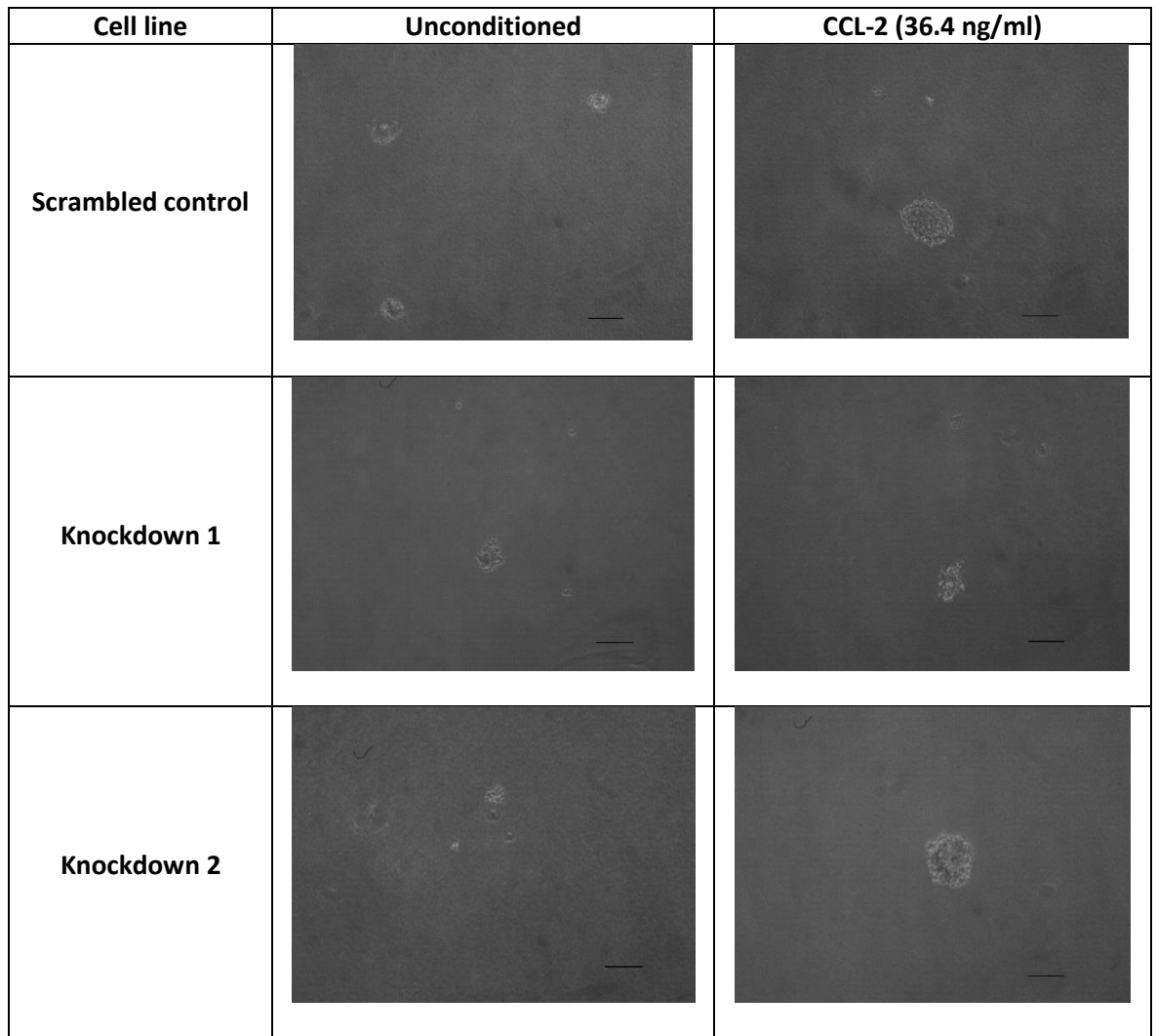


**Figure 6.21: Comparison of soft agarose colonies formed by U2OS CCL-2 knockdown cell lines and empty vector control in the absence (unconditioned) and presence of CCL-2 at 36.4 ng/ml.** Cells seeded at a density of 1053 cells/cm<sup>2</sup> and grown for 12 days under standard cell culture conditions Bar = 100 μM.

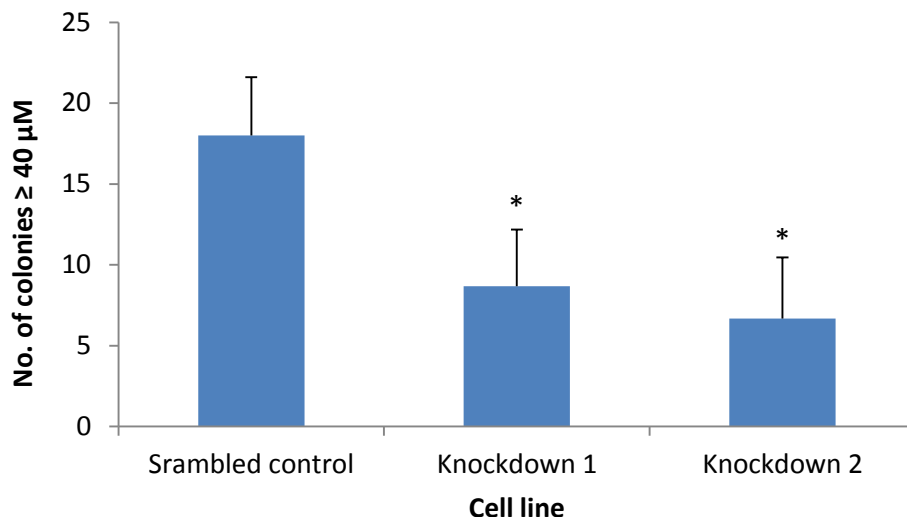


**Figure 6.22: Assessment of colonies formed by U2OS CCL-2 knockdown cell lines and empty vector control in the soft agarose assay.** Colonies  $\geq 40 \mu\text{M}$  were counted, data presented as mean and standard deviation, all conditioned tested in triplicate. Statistical significance calculated using unpaired T-test (\* =  $< 0.05$ ).

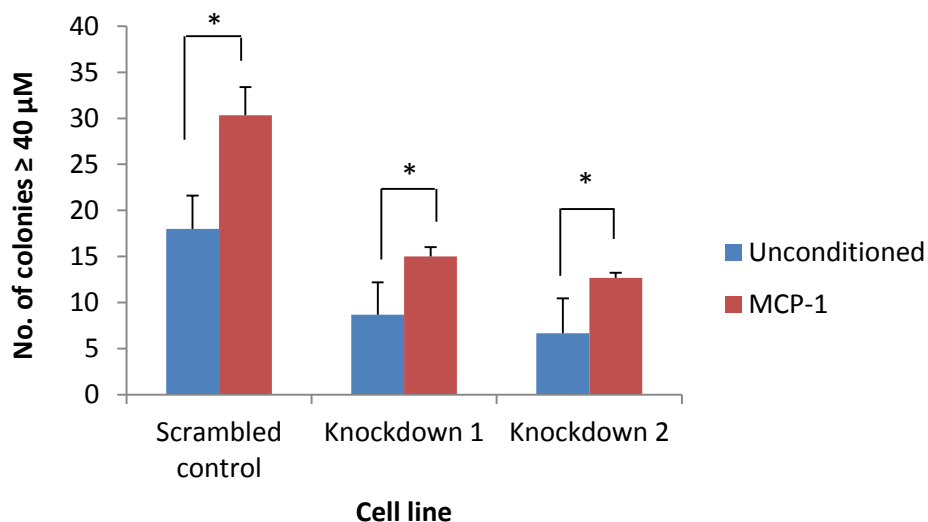


**Figure 6.23: Assessment of colonies formed by U2OS CCL-2 knockdown cell lines and empty vector control in the soft agarose assay.** Cell lines grown in the absence (unconditioned) or presence of CCL-2 (MCP-1) at 36.4 ng/ml. Colonies  $\geq 40 \mu\text{M}$  were counted, data presented as mean and standard deviation, all conditioned tested in triplicate. Statistical significance calculated using unpaired T-test (\* =  $< 0.05$ ).

### 6.11 Identification of genes with altered expression in U2OS cells in response to CCL-2 and U2OS conditioned media

Illumina gene microarrays were used in order to identify genes with altered expression in response to CCL-2 and U2OS conditioned media. U2OS cells were exposed to CCL-2 at a concentration of 36.4 ng/ml or U2OS conditioned for 8 days before RNA was extracted and analysed using an Illumina gene microarray (Section 2.7). This gene microarray analyses the expression level of all genes within the human genome. Samples were tested in triplicate, however, due to one array from the unconditioned cells and another from U2OS conditioned cells failing Bioconductor quality controls these samples were removed from analysis (Appendix V). Analysis of the remaining samples using Genespring (Agilent Technologies®) demonstrated that gene expression of unconditioned cells and CCL-2 exposed cells was similar whereas U2OS conditioned cells gene expression was clearly altered compared to unconditioned cells (Figure 6.24 and 6.25).

When comparing gene expression of CCL-2 treated cells to unconditioned cells, treated cells had a small number of genes (81) with an altered level of expression (Figure 6.25.A), whilst U2OS cells treated with conditioned media had a larger number of genes (857) with altered expression compared to the unconditioned cells (Figure 6.25.B). CCL-2 and U2OS conditioned cells shared 16 genes with altered expression (Figure 6.26). Annotation of these gene using NIH DAVID identified that these 16 genes were involved in transcription, producing a modified Fisher's exact test (EASE) score of 0.032 (Table 6.3). An EASE score of  $< 0.05$  is statistically significant (Huang et al., 2008), therefore, the assignment of these genes to transcription related processes is reliable. Annotation of genes with altered expression in CCL-2 compared to unconditioned cells, identified 14 genes with an EASE score of 0.0192 were associated with transcription regulation (Table 6.4). Annotation of genes with altered expression in response to U2OS conditioned media identified a number of different cellular functions. A highly significant EASE score of  $3 \times 10^{-4}$  was observed in genes associated with anti-apoptotic processes (Table 6.5) and also cancer signaling pathway associated genes (Table 6.6). Genes associated with cancer signaling were used to review published research to identify if any had been associated with CCL-2 signal transduction. Other genes which were found to be up-regulated in response to U2OS

conditioned media included genes involved with cell locomotion (Table 6.7), indicating that U2OS conditioned may enhance U2OS cell migration.

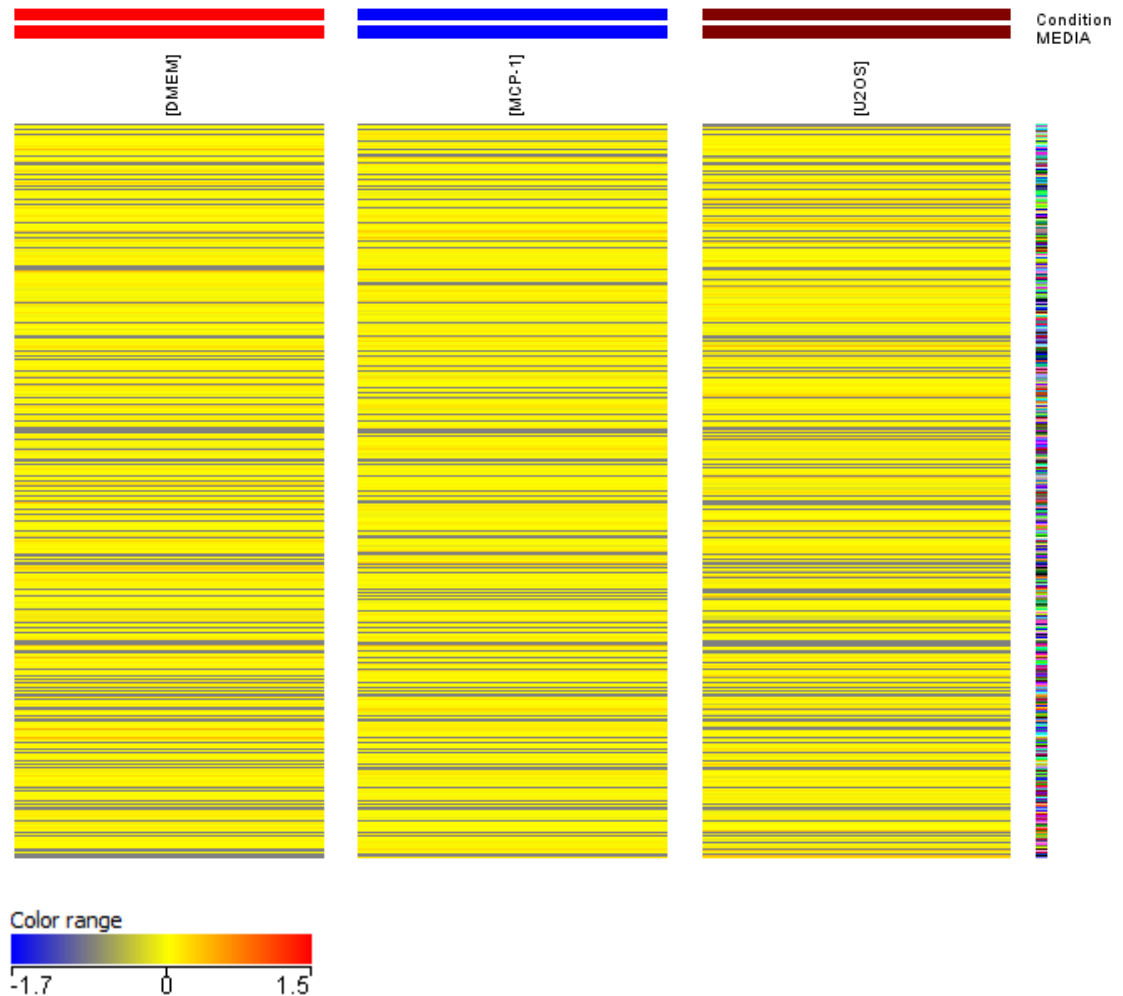
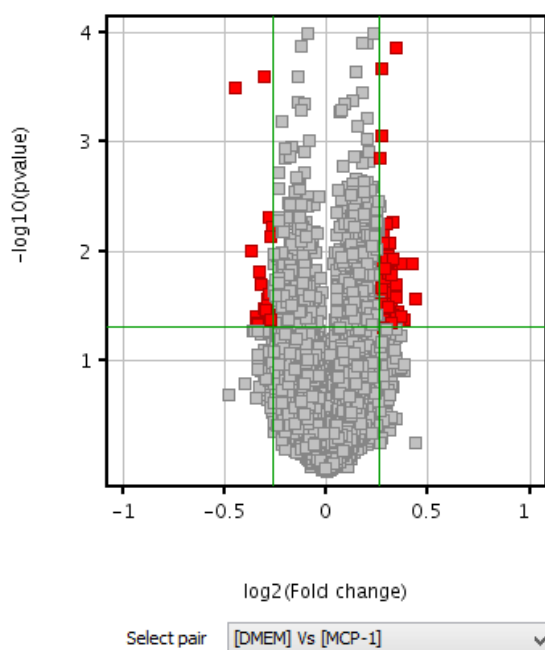


**Figure 6.24: Heatmap of genes expressed in U2OS cells in response to unconditioned (DMEM), CCL-2 (MCP-1) and U2OS conditioned media.** U2OS cells were seeded at 36 cells/cm<sup>2</sup> and grown either in unconditioned media or media supplemented with 36.4 ng/ml CCL-2 or U2OS 72 hour conditioned media for 7 days. Cell RNA was extracted and samples analysed using the genespring software to identify a 1.2 fold change in gene expression along with an unpaired T-test ( $p < 0.05$ ) to establish statistical significance.

(A) CCL-2 conditioned



(B) U2OS conditioned

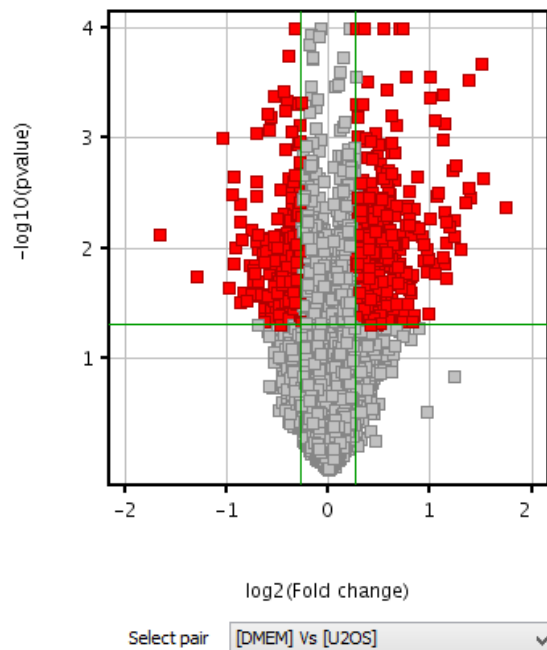


**Figure 6.25: Volcano plots of genes with altered expression in CCL-2 conditioned or U2OS conditioned cells compared to unconditioned cells.** Genes with altered expression in CCL-2 (A) and U2OS conditioned cells (B), were analysed using genespring to identify a 1.2 fold change in expression along with an unpaired T-test ( $p = <0.05$ ) to establish statistical significance.

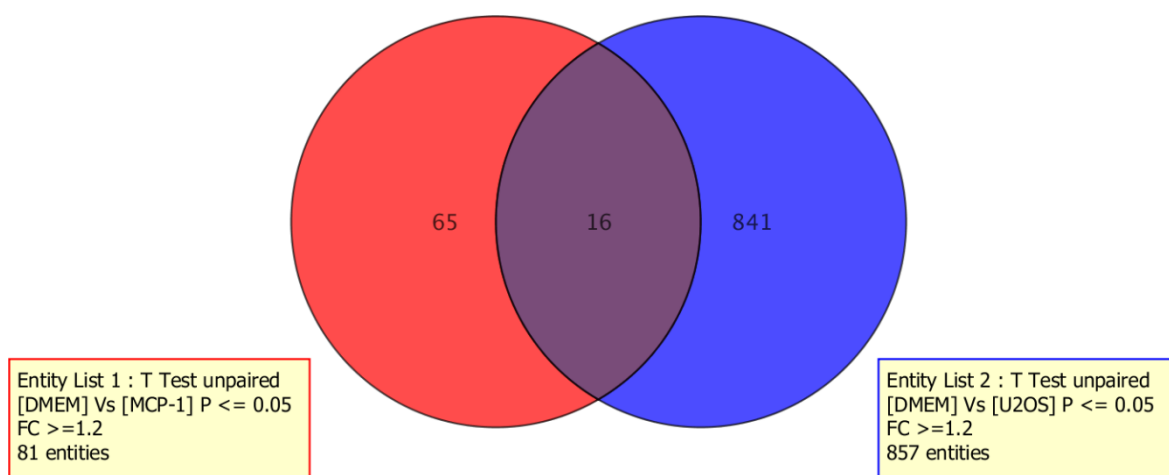


**Figure 6.26: Venn diagram of genes with altered expression compared to unconditioned cells in CCL-2 conditioned and U2OS conditioned cells.** In CCL-2 (red) 65 gene were found to have been altered and 841 in U2OS conditioned cells (blue) compared to unconditioned cells. CCL-2 and U2OS conditioned cells shared 16 genes which had the same alterations in expression compared to unconditioned cells.

**Table 6.3: Transcription genes with shared altered expression in U2OS cells in response to recombinant CCL-2 and U2OS conditioned media.** Using NIH DAVID genes were associated with transcription producing an EASE score of 0.032.

Gene	Protein description	Change in expression	Fold change
PRDM10	PR domain containing 10	Decreased	1.22
SNORA25	TATA box binding protein	Increased	1.22
POLR3G	Polymerase (RNA) III (DNA directed ) peptide	Decreased	1.21
TCEA2	Transcription elongation factor	Decreased	1.34
ZNF783	Zinc finger family member	Increased	1.21

**Table 6.4: Transcription genes with altered expression in U2OS cells in response to recombinant CCL-2.** Using NIH DAVID genes were associated with transcription producing an EASE score of 0.0192.

Gene	Protein description	Change in expression	Fold change
SOX17	SRY (sex determining region Y)-box 17RGHomo sapiens	Increased	1.22
SNORA25	TATA box binding protein	Increased	1.22
HES1	hairy and enhancer of split 1	Increased	1.25
MLL3	myeloid/lymphoid or mixed-lineage leukemia	Increased	1.24
ZNF783	Zinc finger family member	Increased	1.21

**Table 6.5: Apoptosis inhibiting genes with altered expression in U2OS cells in response to U2OS conditioned media.** Using NIH DAVID genes were associated with apoptosis inhibition producing an EASE score of  $3 \times 10^{-4}$ .

Gene	Protein description	Change in expression	Fold change
TAX1BP1	ax1 (human T-cell leukemia virus type I) binding protein	Increased	1.21
BIRC3	baculoviral IAP repeat-containing	Increased	1.65
CRYAB	crystallin, alpha	Increased	1.39
FOXC1	forkhead box	Increased	1.21
GCLC	glutamate-cysteine ligase, catalytic subunit	Increased	1.49
GSTP1	glutathione S-transferase	Increased	1.35

Table 6.5 continued overleaf.

**Table 6.5**

Gene	Protein description	Change in expression	Fold change
HSPBL2	heat shock 27kDa protein-like 2 pseudogene; heat shock 27kDa protein	Increased	1.20
NRG1	neuregulin	Increased	1.20
PIK3CA	phosphoinositide-3-kinase, catalytic, alpha polypeptide	Increased	1.22
RPS27	ribosomal protein S27a pseudogene 12;	Increased	1.28
SQSTM1	sequestosome	Increased	1.63
THBS1	thrombospondin	Increased	1.45
TNFAIP3	tumor necrosis factor, alpha-induced protein 3	Increased	1.22
UBB	ubiquitin	Increased	1.22

**Table 6.6: Cancer signaling genes with altered expression in U2OS cells in response to U2OS conditioned media.** Using NIH DAVID genes were associated with signaling in cancer cells producing an EASE score of  $4.5 \times 10^{-5}$ .

Gene	Protein description	Change in expression	Fold change
BCL2L1	BCL2-like 1	Decreased	1.35
TRAF1	TNF receptor-associated factor 1	Increased	2.00
ARNT2	aryl-hydrocarbon receptor nuclear translocator 2	Increased	1.26
AXIN2	axin 2	Increased	1.24
BIRC2	baculoviral IAP repeat-containing 2	Increased	1.37
BIRC3	baculoviral IAP repeat-containing 3	Increased	1.26
BMP4	bone morphogenetic protein 4	Decreased	1.64
CDH1	cadherin 1, type 1, E-cadherin	Increased	1.28
FGF1	fibroblast growth factor 1	Decreased	1.31
FGFR3	fibroblast growth factor receptor 3	Increased	1.25
FN1	fibronectin 1	Increased	1.20
FZD1	frizzled homolog 1	Increased	1.34
FZD6	frizzled homolog 6	Increased	1.26
GSTP	glutathione S-transferase pi 1	Increased	1.35
IKBKG	inhibitor of kappa light polypeptide gene enhancer in B-cells, kinase gamma	Increased	1.43

**Table 6.6 continued overleaf**

Table 6.6

Gene	Protein description	Change in expression	Fold change
ITGA3	integrin, alpha 3 (antigen CD49C, alpha 3 subunit of VLA-3 receptor)	Increased	1.48
ITGA6	integrin, alpha 6	Decreased	1.30
ITGAV	integrin, alpha V (vitronectin receptor, alpha polypeptide, antigen CD51)	Increased	1.27
IL-8	Interleukin 8	Increased	1.99
LAMA5	laminin, alpha 5	Decreased	2.05
LAMB1	laminin, beta 1	Decreased	1.33
LEF1	lymphoid enhancer- binding factor 1	Increased	1.27
MMP-9	matrix metalloproteinase 9	Increased	1.35
MAP2K2	mitogen-activated protein kinase kinase 2	Increased	1.32
PIK3CA	phosphoinositide-3- kinase, catalytic, alpha polypeptide	Increased	1.22
PDGFRB	phosphoinositide-3- kinase, catalytic, alpha polypeptide	Increased	1.49
PRKCA	protein kinase C, alpha	Increased	1.41
AKT1	v-akt murine thymoma viral oncogene homolog	Decreased	1.30
AKT3	v-akt murine thymoma viral oncogene homolog 3 (protein kinase B, gamma)	Increased	1.24
ETS1	v-ets erythroblastosis virus E26 oncogene homolog 1	Increased	1.27
FOS	v-fos FBJ murine osteosarcoma viral oncogene	Decreased	1.75
VEGFC	vascular endothelial growth factor C	Increased	1.42
Wnt5b	Wingless-type MMTV integration site, member 5B	Increased	1.33



**Table 6.7: Locomotion genes with altered expression in U2OS cells in response to U2OS conditioned media.** Using NIH DAVID genes were associated with cell locomotion producing an EASE score of  $3.2 \times 10^{-4}$ .

Gene	Protein description	Change in expression	Fold change
THY1	THY-1 cell surface antigen	Decreased	1.23
ADORA1	Adenosine A1 receptor	Decreased	1.24
CXCL16	Chemokine (C-X-C motif) ligand 16	Increased	1.44
F2RL1	Coagulation factor II (thrombin) receptor-like 1	Increased	1.24
HDAC9	Histone deacetylase 9	Increased	1.27
IL6ST	Interleukin 6 signal transducer (gp130, oncostatin M receptor)	Increased	1.21
IL-8	Interleukin 8	Increased	1.57
LAMA5	Laminin, alpha 5	Decreased	2.06
LAMB1	Laminin, beta 1	Decreased	1.33
MMP9	Matrix metalloproteinase 9 (gelatinase B, 92kDa gelatinase, 92kDa type IV collagenase)	Increased	1.35
PDGFRB	Platelet-derived growth factor, receptor polypeptide	Increased	1.49
SERPINE2	Serpin peptidase, clade E (nexin plasminogen activator inhibitor), member 2	Increased	1.61
SLIT2	slit homolog 2 (Drosophila)	Increased	1.31
SPAG9	Sperm associated antigen 9	Increased	1.21
THBS1	thrombospondin 1	Increased	1.45
TPM1	Tropomyosin 1 (alpha)	Increased	1.53
AKT1	v-akt murine thymoma viral oncogene homolog 1	Decreased	1.30
VEGFC	Vascular endothelial growth factor C	Increased	1.42

## 6.12 Discussion

In order to further elucidate the role that IL-8 and CCL-2 play in U2OS and HOS growth, receptor antagonists were used in the presence of growth enhancing conditioned media (MG63 and U2OS 72 hour conditioned media) to assess their impact upon proliferation. IL-8 has been found to signal via two receptors CXCR1 and CXCR2 (Park et al., 2011b), therefore, antagonist antibodies for both receptors were supplemented in to conditioned and unconditioned media. An initial experiment at 200 ng/ml demonstrated that the antibodies had no effect upon growth in unconditioned or conditioned media. Treating the human breast cancer cell line SUM159 using the same CXCR1 inhibiting antibody as used within this study at 10 µg/ml reduced cell viability by 95 % (Ginestier et al., 2010). Due to this finding the concentration of CXCR1 was increased by 10 fold to 2 µg/ml, however, even at this increased concentration no effect on the growth rate of HOS or U2OS cells was observed. This suggests that IL-8 signalling is not involved with the enhanced proliferation in response to conditioned media.

CCL-2 signals via the G-protein coupled receptor CCR2 (Deshmane et al., 2009) and therefore a specific CCR2 antagonist (RS 504393) was used which has a high affinity to selectively inhibiting CCL-2 binding to CCR2 (Mirzadegan et al., 2000, Cherney et al., 2008). RS 504393 when used at a concentration of 1 µM had no impact upon OS cell line proliferation, however increasing the concentration to 10 µM reduced the growth rate of both HOS and U2OS cells when grown in unconditioned and MG63 conditioned media. This finding suggests that HOS and U2OS cells both utilise CCR2 signalling for proliferation and MG63 conditioned media is reliant upon the presence of CCL-2 to enhance growth. The decreased growth observed in response to RS 504393 could be related to off target toxic effects, however, in the hamster ovary cell line (CHO) a RS 504393 concentration of 61 µM has been used and the cells are still able to migrate (Mirzadegan et al., 2000), therefore, the concentration of RS 504393 used within this study does not exceed *in vitro* published data. In addition U2OS conditioned growth enhancement was unaffected in both cell lines by RS 504393, suggesting that U2OS conditioned media contains additional growth factors, which compensates for the antagonism of CCR2.

In order to assess the growth enhancing potential of CCL-2, a commercially available recombinant CCL-2 was supplemented in to growth media. Findings show that recombinant CCL-2 did not increase the growth of either HOS or U2OS cells at 10 ng/ml. Increasing the concentration to 100 ng/ml did increase proliferation in U2OS and HOS cells. The increase in U2OS and HOS proliferation in response to 100 ng/ml CCL-2 was significantly less than the enhancement observed in response to U2OS 72 hour conditioned media. According to ELISA results this conditioned media contained 22 ng/ml CCL-2 which is less than the 100 ng/ml of recombinant protein used. The reduced activity of recombinant protein could indicate; recombinant CCL-2 has less bio-activity than the native protein, another growth factor is present within growth enhancing conditioned media or a co-stimulatory factor is required for CCL-2 increased proliferation. Another level of complexity has also been identified in CCL-2 signalling. Normally CCR2 homodimers form post ligand interaction which allows signal transduction, however, heterodimers can also form between CCR2 and CCR5. These receptor heterodimers along with their ligands have been found to activate cellular response in HEK293 cells at 10 – 100 fold lower ligand thresholds than when a single cytokine is used (Mellado et al., 2001). RANTES signals via the CCR5 receptor (Wang et al., 2012), RANTES was present in the conditioned media of all cell lines tested, therefore CCL-2 and RANTES could be signalling via CCR2-CCR5 heterodimeric receptors to increase proliferation in OS cell lines. If a heterodimeric CCR2 is present within U2OS and HOS it could explain why a receptor antagonist for CCR2 inhibits proliferation but supplementing the recombinant protein has no effect.

Soft agarose colony formation has been shown to be representative of *in vivo* cancer growth (Courtenay, 1976), and was used to identify if supplementing recombinant CCL-2 and IL-8 enhanced U2OS and MG63 colony formation. IL-8 did not alter colony formation in either cell line, which suggests that IL-8 does not contribute to non-adherent colony formation in these OS cell lines. CCL-2 was found to enhance soft agarose colony formation in U2OS cells but not MG63, therefore CCL-2 may represent an important factor in tumour formation *in vivo*, however, a mouse model of OS growth is required for conclusive evidence. The inability of CCL-2 to increase MG63 soft agarose colony formation highlights the heterogeneity of the OS cell lines. ELISA evaluation of MG63 72 hour conditioned media demonstrated that it contained significantly greater amounts of CCL-2 than U2OS

conditioned media. Therefore, it could be possible that increased expression of CCL-2 from this cell line may help to compensate for the lack of CCL-2 in the unconditioned cells and enhance proliferation.

Another assay which also selects cells able to grow in low attachment conditions is the spherical colony formation assay, however, this was originally utilised to select for multi-potent stem cells (Reynolds et al., 1992), IL-8 supplementation in breast cancer cell lines has been demonstrated to enhance sarcosphere forming ability through increased putative CSC replication (Tsuyada et al., 2012, Ginestier et al., 2010). Due to MG63 being able to form secondary sarcospheres it was tested to identify if recombinant CCL-2 or IL-8 would enhance sarcosphere formation. Both IL-8 and CCL-2 did not increase MG63 sarcosphere formation suggesting that CCL-2 or IL-8 do not increase the presence of putative CSC in MG63.

In order to assess whether the expression of IL-8 and CCL-2 receptors correlated with the observed sensitivity of the cell lines to growth enhancing conditioned media (MG63 and U2OS conditioned media). The cell lines HOS, MG63, U2OS and MCF7 were stained for receptor expression, cytokine receptors are frequently internalised in order to transduce a signal, in particular leukocyte CCR2 has been found to be rapidly internalised and a high rate of receptor recycling occurs (Volpe et al., 2012). Therefore intracellular expression of the receptors was tested to provide an accurate estimation of the receptors expressed by each cell line. CXCR1 was expressed to a high degree in the cell lines tested with no statistical difference in expression observed. For CXCR2 expression MCF7 was found to contain higher receptor CXCR2 expression than in the OS cell lines. Neither CXCR1 nor CXCR2 fitted the expected growth response to conditioned media, as U2OS and MG63 were found to be most responsive to the growth enhancement of the conditioned media, therefore, should have had a higher expression of a candidate growth receptor than HOS or MCF7. CCR2 however did fit this hypothesised expression pattern and MG63 and U2OS were found to express CCR2 at higher levels than HOS and MCF7. U2OS in particular was found to express the highest levels of CCR2, analysis of the flow cytometry histogram demonstrates that the receptor is expressed on almost all cells within this cell line. In prostate cancer enhanced CCR2 mRNA expression correlates with increased cell line

tumourigenicity, which is also supported by analysis of clinical tissue samples, whereby an increase in CCR2 was associated with an increased Gleason score (Lu et al., 2007). It would be of interest to identify if CCR2 expression also correlated with OS progression and to identify if highly expressing CCR2 cells have enhanced tumourigenic properties.

Short hairpin RNA (shRNA) is a method which has been found to inhibit gene expression, through viral transduction of plasmids into cells this allows stable integration of shRNA sequences into the genome with high efficiency (Brummelkamp and Bernards, 2003). In order to assess the RNA gene interference of CCL-2 two CCL-2 antisense sequences TTATAACAGCAGGTGACTGGG (knockdown 1) and TAAGGCATAATGTTTCACATC (knockdown 2) were transduced into U2OS cells and found to reduce the presence of CCL-2 mRNA. Analysis of the presence of CCL-2 mRNA using real time PCR found that CCL-2 mRNA was significantly lower in both knockdown cell lines compared to a scrambled control vector. Knockdown 1 CCL-2 mRNA was present at a lower level than knockdown 2 cells, suggesting that knockdown 1 expresses more CCL-2 than knockdown 2. To confirm that CCL-2 protein expression reflects the CCL-2 mRNA levels, conditioned media from these genetically manipulated cells was analysed using a CCL-2 ELISA. The same pattern of CCL-2 mRNA expression observed in the knockdown cell lines and scrambled control cells was replicated in the CCL-2 concentrations in 24 hour and 72 hour conditioned media. This finding shows that the RNA interference has inhibited the expression of CCL-2 and this inhibition has increased efficiency in the knockdown 2 cell line. When comparing the scrambled control CCL-2 expression with the normal U2OS cells, at 72 hours both cell lines expressed 22 ng/ml of CCL-2, however, at 24 hours normal cells express statistically more CCL-2. This discrepancy is unexpected, however, cell density of conditioned media was not standardised and was collected after cells had reached confluency. Therefore, the higher expression of normal cells at 24 hours could be attributed to a higher cell density compared to the scrambled control cells.

The proliferation of the knockdown cell lines was compared with the scrambled control cells to identify if decreasing CCL-2 expression affects U2OS growth. Findings show that both the knockdown 1 and 2 cells had a reduced proliferation rate compared to the control cells. However, although knockdown 2 cells expressed less CCL-2, this did not affect the

proliferation rate as both knockdown 1 and 2 produced the same amount of growth after 8 days. Recombinant CCL-2 and conditioned media were assessed to identify if they could increase the proliferation of knockdown 1 and 2 cells, conditioned media from scrambled control cells was able to return the growth rate of the both knockdown cells to same proliferation rate as empty vector cells. This finding indicates that the CCL-2 present within the empty vector conditioned media is able to increase the growth rate, interestingly knockdown 1 conditioned media increased growth to the same level as the scrambled control conditioned media.

The empty vector conditioned media contains 22 ng/ml of CCL-2 and knockdown 1 media contains 6 ng/ml CCL-2, this indicates that even though there is statistically a significant difference between the CCL-2 content of these conditioned media it has no impact upon growth. However, the lower concentration of 1.7 ng/ml found in 72 hour knockdown 2 conditioned media did produce a lower growth enhancement than empty vector 72 hour conditioned cells. This suggests that the CCL-2 content of conditioned media may have an effect upon cell growth, however, recombinant CCL-2 at 100 ng/ml had no effect upon the growth of either knockdown cell line. It is possible that either the recombinant CCL-2 does not produce the same proliferative response as the native cytokine in the conditioned media or alternatively a CCR2 signalling co-factor may be required for CCL-2 signal transduction. In order to identify whether a co-signalling molecule is required, the effect of adding 100 ng/ml recombinant CCL-2 into 24 hour and 72 hour knockdown 2 conditioned media was tested using both knockdown cell lines. No increase in growth was observed when adding recombinant CCL-2 in to 72 hour conditioned media, however, the effect in response to 24 hour conditioned media were contrasting for each cell line. Knockdown 1 had no growth enhancement, whereas knockdown 2 cells responded with increased growth in response to supplementing 100 ng/ml recombinant CCL-2 in to the conditioned media. The growth enhancement observed was not as high as occurred when cells were grown within 72 hour knockdown 2 conditioned media, therefore, supplementing 100 ng/ml of recombinant CCL-2 does not have the same effect as the presence of 1.7 ng/ml native CCL-2. These findings complicate the role CCL-2 plays in growth enhancement and suggest that either the recombinant CCL-2 used does not have the same effect as the native

form of CCL-2 produced by U2OS or alternatively there is another growth factor which is required.

The use of shRNA to inhibit CCL-2 expression could be causing off target effects which decrease growth, therefore producing misleading results indicating that CCL-2 is a OS growth factor. A scrambled control vector was used in this study, however, it is recommended that controls contain a sequence with a complimentary sequence except residues 2-7 or 2-8 from the 5' end. This produces an shRNA which has a similar sequence but unable to inhibit gene expression, allowing the assessment of off target effects of the shRNA to be accurately assessed (Cullen, 2006). The gold standard to test RNAi specific gene inhibition is through the use of RNAi knockdown, followed by restoring gene function using an RNAi resistant gene for the same function. This procedure can be achieved by using a gene from a different species which carries out the same function to restore the organism to the original phenotype (Rusconi et al., 2005). In order to identify if CCL-2 expression has been specifically inhibited in OS a functional complementary study would be required.

CCL-2 was found to play a central role in promoting growth in the soft agarose colony formation assay for both knockdown cell lines. Both knockdown 1 and 2 were found to produce statistically less colonies than the scrambled control cell line. In addition supplementation of recombinant CCL-2 at a concentration reflecting that found in MG63 72 hour conditioned media (36.4 ng/ml) enhanced the colony formation in both the scrambled control cell line and knockdown 1 and 2 cells. This demonstrates that recombinant CCL-2 does increase soft agarose colony formation, however, the inability to increase growth of the same cell lines in an adherent assay could be explained by the hierarchical nature of the cells which respond to CCL-2. Putative CSC in carcinomas which display EMT characteristics have been demonstrated to have an enhanced ability to form colonies in non-adherent *in vitro* conditions (Mani et al., 2008, Biddle et al., 2011), therefore, cells with similar EMT characteristics present in the U2OS knockdown and scrambled control cells lines may have enhanced sensitivity to CCL-2 than non-EMT cells. CCL-2 has been found to act as a chemoattractant for both prostate cancer and breast cancer cells, and is highly expressed by osteoblasts, therefore, has been hypothesised as a

mechanism by which these cancers commonly metastasise to the bone (Loberg et al., 2006, Molloy et al., 2009). Due to the high expression of CCL-2 from the OS cell lines it would appear contradictory to hypothesise that this is a chemoattractant for these metastatic OS cells, however, it may be a mechanism to increase the proliferation of OS EMT cells. The lungs are the primary site of OS secondary tumours (Jeffrey et al., 1975), CCL-2 is expressed by the lungs and has been demonstrated to increase carcinoma lung metastasis through the recruitment of monocytes which promote tumour growth (Lu and Kang, 2009). It could therefore be hypothesised that CCL-2 may be an important protein in the establishment of secondary OS tumours through the recruitment of monocytes.

Assessment of genes with altered expression in U2OS in response to recombinant CCL-2 and U2OS conditioned media was achieved using a gene microarray. An increase in proliferation was observed by U2OS normal cells in response to recombinant CCL-2, therefore, U2OS normal cells were tested for their response to the cytokine and conditioned media. Due to a replicate from the unconditioned and U2OS conditioned microarray not meeting quality controls these samples were removed from analysis. Therefore, unconditioned and U2OS conditioned gene expression were tested in duplicate which will compromise the results and decrease the sensitivity of gene expression analysis. A total of 81 genes had altered expression in response to recombinant CCL-2 compared to unconditioned cells, U2OS conditioned media cells had a more dramatic change in gene expression with 857 genes displaying changes. In order to identify if genes with changed expression in response to CCL-2 were also present in response to U2OS conditioned media, the gene expression between the two conditions was compared, 16 genes had shared altered expression. Although 16 genes is a small sample size, annotation of these genes using NIH DAVID found that they were statistically enriched in transcription regulation, of the 16 genes 5 are involved in transcription regulation. This indicates that the increased proliferation observed in response to recombinant CCL-2 and U2OS conditioned media may be attributed to enhanced transcription. However, a limitation of NIH DAVID is that it does not take into account whether a gene has been up or down regulated, of these 5 genes only 2 had increased expression. Therefore, the association of these genes with increased transcription is questionable.



In contrast to CCL-2, the 81 genes with changed expression in response to recombinant CCL-2 were also linked with transcription, however, 14 genes were identified all associated with transcription regulation and all had increased expression. *FOXC1* and *GSTP1* had increased expression in response to CCL-2 and loss of this gene in carcinoma cells decreased *in vitro* proliferation (Xu et al., 2012, Jin et al., 2012). Annotation of genes with altered expression in response to U2OS conditioned media identified a number of different cellular processes, including genes associated with inhibition of apoptosis, this indicates conditioned media may increase growth through suppression of cell death. In addition U2OS conditioned media may enhance resistance to chemotherapeutic agents. *GST1* which had increased expression in response to U2OS conditioned media has been associated with OS cis resistance *in vitro* and within clinical samples (Pasello et al., 2008). In OS IL-8 which was also increased in response to U2OS conditioned media has also been attributed to dox resistance (Rajkumar and Yamuna, 2008). Altered gene expression from U2OS conditioned media also identified an association with cell migration, indicating that the conditioning effect may also be promoting cell migration, however, further investigation will be required to substantiate this hypothesis.

The catalytic subunit of phosphoinositide-3-kinase (PIK3CA), was found up-regulated in response to U2OS conditioned media, and was associated with both anti-apoptotic and cell signalling processes. PI3K has been demonstrated as a signalling pathway utilised by CCR2 in prostate cancer to increase proliferation (Loberg et al., 2006). Interestingly when CCR2 forms a heterodimeric receptor complex with CCR5 and both receptors are activated by their respective ligands, this results in an increased and sustained activation of PI3K, compared to activation with CCL-2 alone (Mellado et al., 2001). Therefore, the enhancement in growth observed in response to U2OS conditioned media may be a consequence of intracellular signal transduction via PI3K and requires further investigation in OS proliferation.

In conclusion, the growth enhancing properties of conditioned media from the cell lines MG63 and in particular U2OS has been established. The growth factors secreted from U2OS are able to enhance growth in not only alternative OS cell lines but sarcoma cell lines and MCF7 as well, indicating the presence of a common cancer growth factor. IL-8 and CCL-2

were identified as candidate growth factors in growth enhancing conditioned media, further testing of IL-8 and CCL-2 signal transduction demonstrated that CCR2 inhibition is required for growth and this finding was confirmed through CCL-2 RNA interference in U2OS. Supplementing recombinant CCL-2 to assess growth resulted in enhanced growth of normal U2OS and HOS or U2OS at high concentrations (100 ng/ml) but had no impact upon U2OS CCL-2 knockdown cell lines. A co-stimulatory factor did not appear to be required for CCL-2 growth enhancement, however, CCR2 and CCR5 heterodimers have been demonstrated to enhance CCR2 response to CCL-2 when in the presence of RANTES (Mellado et al., 2001), therefore, supplementing both cytokines may be necessary to increase proliferation. Within non-adherent conditions (soft agarose assay) did consistently increase proliferation of U2OS cells. This indicates that a subset of cells within U2OS cell line are able to grow within low attachment conditions are sensitive to growth enhancement in response to CCL-2. Analysis of altered gene expression in response to CCL-2 suggests that the genes increase proliferation through up-regulation of transcription.

# **Chapter 7**

## **General Discussion, Conclusion and Future Work**

## 7.1 General discussion

This thesis is framed by three aims; to characterise putative CSC present in a panel of OS cell lines, identify if putative OS CSC contribute to chemotherapeutic drug resistance and to characterise OS signaling used to control growth.

Defining populations of putative CSC within OS cell lines was achieved by screening OS cells for ALDH and CD117 expression, both markers have been previously identified as OS CSC markers in a small number of cell lines (Wang et al., 2011, Adhikari et al., 2010). Both proteins were found to be heterogeneously expressed *in vitro* (Section 3.2) with CD117 expression ranging from a population of 0 % to 6.4 % and ALDH from 0.9 % to 60 % of cells. Cancer associated mutations have been demonstrated to enhance ALDH expression, loss of the tumour suppressor PTEN in mammary epithelial cells increased ALDH expression by 2 fold (Dull et al., 1998). OS tumours are characterised by a host of genetic abnormalities (Hansen, 2002), therefore the acquisition of these mutations during OS progression may result in the observed variations in ALDH expression between the cell lines. The OS cell lines tested are all able to recapitulate the colony hierarchies at low cell density (Section 3.5), however, the highly expressing ALDH cell lines (>10 % ALDH expression) contained ALDH positive cells within all the colony hierarchies not just the holoclones which are thought to originate from and contain CSC (Section 3.6). Therefore, if OS holoclones represent populations of OS CSC, as has been observed in carcinoma (Li et al., 2008), this makes ALDH an unsuitable CSC marker in these cell lines with an ALDH population greater than 10 % (143B, G292 and HOS). In contrast cell lines with lower ALDH expression (<10 % of cells) (MG63, SaOS-2 and MCF7) contained ALDH positive cells only within the holoclones, which indicates it has potential to function as a CSC marker in these cell lines, although further research is required to confirm the location of OS CSC within the colony hierarchies. This research will be aided by the use of multiple CSC markers for definitive identification of CSC, as has been utilised with the use of CD117 and stro-1 expression in the identification of OS CSC (Adhikari et al., 2010).

As part of the putative CSC characterisation cell lines were screened for epithelial and mesenchymal markers to evaluate the cellular origin of these cell lines. Results indicate

that all OS cell lines display a mesenchymal phenotype, this was evident from low e-cad expression (< 0.22 %) and high vimentin expression (> 90 %) (Section 3.3). These findings are suggestive of a mesenchymal cell origin of OS, which has been previously hypothesised (Tang et al., 2008), however, further conclusive evidence linking MSC to OS is required. One recent study demonstrated that human xenotransplanted MSC cells lacking *Rb* and *P53* could form OS tumours when grown upon calcified ceramic scaffolds in a murine model (Rubio et al., 2014). *P53* and *Rb* are common OS mutations but still present in only 62 % of OS tumours (Miller et al., 1996), therefore the finding by Rubio *et al* (2014) linking MSC to OS may not be representative of all OS tumours. CD44 is another protein highly expressed by MSC cells (Lee et al., 2004) and also OS cell lines, however, cells expressing CD44 and the epithelial marker e-cad had an enhanced primary sarcosphere forming ability (Section 3.7). A putative CSC population has been identified based upon a similar expression profile of CD44/e-cad in head and neck carcinoma cells *in vitro* (Biddle et al., 2011), therefore, it will be of interest to test OS cells expressing CD44<sup>+</sup>/e-cad<sup>+</sup> to analyse their CSC properties by FACS sorting and comparison of their sarcosphere forming ability.

To identify if putative OS CSC (based on ALDH expression) display enhanced chemo-resistance the effect of inhibiting ALDH activity was analysed using the ALDH inhibitor DEAB. OS ALDH expressing cells were previously shown to have an enhanced resistance to chemotherapeutics (Honoki et al., 2010), however, in Chapter 4 ALDH was found to comprise a chemo-resistant population in MG63 cells in response to MTX, U2OS cells in response to cisplatin and HOS cells in response to doxorubicin (Section 4.10). This finding indicates that ALDH expressing cells in different OS cell lines display resistance to opposing chemotherapeutics. If ALDH expressing cells do comprise a CSC population then the ability to successfully target them may require tailoring chemotherapeutic treatments strategies to individual patients.

Cell density dictates the *in vitro* population sizes of OS cells expressing ALDH, higher cell densities were observed to reduce ALDH expression (Section 4.7). *In vivo* conditions have been demonstrated to reduce the ALDH compared to *in vitro* culture conditions of the OS cell line OS99-1 (Wang et al., 2011), therefore, this reduction in ALDH expression could be attributed to an increase in cell density. Sarcospheres which has been shown to select for

the growth of OS cells with enhanced tumourigenicity (Rainusso et al., 2011), were found to contain more abundant ALDH expression in sarcospheres larger in size, which suggests that ALDH expressing cells may be driving growth in low attachment conditions (Section 3.8.1). CD117 expression was found to become reduced upon culture at low density (Section 3.6.2), therefore, CD117 may be increased in expression as cell density increases. These findings indicate a potential cell communication network, which controls CSC marker expression within a tumour and further elucidation of this network may help in the advancement of our understanding of OS progression.

In order to elucidate the paracrine growth factors utilised by OS conditioned media from a panel of sarcoma cell lines and MCF7 was tested. All the OS and sarcoma cell lines tested except for the *Ki-ras* transformed OS cell line 143B and its parental cell line HOS, secreted a paracrine factor which was found to enhance growth. The conditioned media from the cell line U2OS was found to also increase the growth of a fibrosarcoma cell line and breast carcinoma cell line (MCF7), suggesting the cytokine growth enhancement pathway may be common in both carcinomas and sarcomas. Alternatively, the paracrine growth factor may be an artifact of the cancer cells adaptation to *in vitro* conditions, which is common in cell lines derived from different cancer types.

The growth enhancement observed in the OS cell line U2OS in response to OS conditioned media increased growth by enhancing the presence of holoclone forming cells, indicating that an OS paracrine factor may enhance the CSC population. A similar observation has been observed in breast cancer in response to IL-8 (Singh et al., 2013), however analysis of IL-8 signaling in OS demonstrated it was not involved with OS proliferation. In order to identify candidate OS growth factors, the cytokines present in conditioned media of selected OS cell lines (HOS, U2OS and MG63) and MCF7 was analysed. The cytokines MIF, IL-5, IL-23, serpinE1 and RANTES were expressed by all four cell lines (Section 5.9). These cytokines have been associated with tumour progression either through mediating inflammation or promoting cell survival. Cytokines which have been found to mediate inflammatory responses include MIF, which promotes tumour formation through the suppression of immune response to cancer cells (Teng et al., 2010). IL-23 suppresses natural killer cell responses to cancer cells (Teng et al., 2010), and IL-5 and RANTES recruit

eosinophils during immune responses (Dubucquoi et al., 1994, Kameyoshi et al., 1992). SerpinE1 is important in tissue repair and has an anti-apoptotic role in fibrosarcoma and breast cancer cell lines (Fang et al., 2012).

CCL-2 was identified as a candidate growth factor and CCR2 antagonism (Section 6.2) and CCL-2 gene RNAi resulted in decreased proliferation of OS cell lines (Section 6.8). Supplementation of complete media with recombinant CCL-2 increased the growth rate of U2OS and HOS cells (Section 6.3) when used at a high concentration (100 ng/ml). The increase in proliferation in response to 100 ng/ml recombinant CCL-2 was lower than the increase in growth observed in response to U2OS 72 hour conditioned media (which according to ELISA results contained 22 ng/ml CCL-2). An explanation for this finding may be due to CCR2 heterodimers formed with CCR5, which can lead to intracellular signal transduction when both receptors are activated by their ligands CCL-2 and RANTES (Mellado et al., 2001, Sohy et al., 2009). Mellado *et al* (2001), identified that the heterodimeric receptor was able to enhance signal transduction by 10 – 100 fold compared to the monomeric CCR2 receptor via increased and sustained activation of phosphoinositide 3-kinase (PI3K). Therefore in order to increase proliferation in response to recombinant CCL-2 recombinant RANTES may also be required. Analysis of genes in U2OS cells with altered expression in response to U2OS conditioned media identified that PI3K catalytic gene (PIK3CA) was increased but not in response to recombinant CCL-2 (Section 6.10). Therefore, RANTES which is present in U2OS conditioned media (Section 5.10) may be enhancing proliferation when also in the presence of CCL-2, through PI3K signal transduction (Figure 7.1).

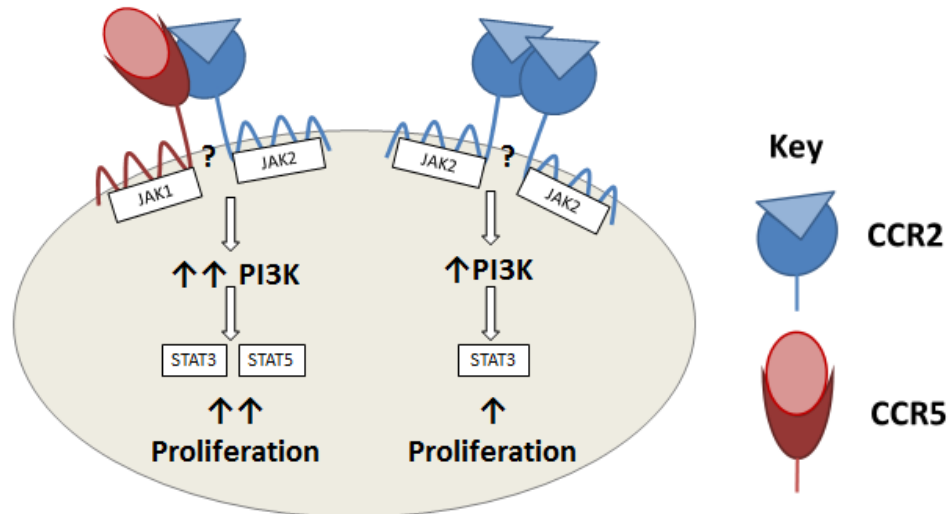


**Figure 7.1: Proposed signal transduction of homodimeric CCR2 and heterodimeric CCR2 and CCR5.** Based on Mellado *et al* (2001) findings CCR2 when bound to CCL-2 homodimerises and intracellular signal is proposed to activate JAK2, which leads to a moderate increase in PI3K and STAT3 activation and proliferation. Heterodimeric CCR2 and CCR5 which form after the binding to CCR2 to CCL-2 and CCR5 to RANTES are able to transduce intracellular signaling at 10 – 100 fold lower concentrations than the homodimeric receptor complex. Upon activation of the heterodimeric receptor complex signal is transduced via JAK1 and 2 which lead to an increased sustained activation of PI3K, which then activate both STAT3 and 5 and lead to increased proliferation.

CCL-2 was found to play a central role in colony formation in low attachment conditions (soft agarose colony formation), the presence of recombinant CCL-2 was shown to increase colony formation (Section 6.4) and knock-down of CCL-2 by RNAi was shown to decrease colony formation in U2OS cells (Section 6.8). *In vitro* carcinoma cells which demonstrate EMT characteristics have been shown to have enhanced ability to form colonies in low attachment conditions (Biddle *et al.*, 2011, Mani *et al.*, 2008). Cells present within the OS cell lines which have a mesenchymal phenotype may therefore have an enhanced sensitivity to CCL-2 possibly through the up-regulation of CCR2, which may also have a chemotactic role. In prostate cancer CCL-2 expression is associated with cancer progression (Izumi *et al.*, 2013) and has been shown to attract breast and prostate cancer cells to the bone (Loberg *et al.*, 2006, Molloy *et al.*, 2009). CCL-2 has been shown to attract the breast cancer cell line MDA-MB-231 to lungs in a mouse model due to CCL-2 expression from both the target organ and the cancer cells via recruitment of inflammatory monocytes (Qian *et al.*, 2011). These CCR2 expressing monocytes have been proposed to aid pulmonary breast



metastasis by facilitating cancer colonisation (Lu and Kang, 2009). The primary site of OS metastasis is the lungs (Jeffrey et al., 1975), therefore, CCL-2 expression from the lungs and OS cells may be attributing to its migration to the this organ and may provide a mechanism for reducing OS metastasis.

## 7.2 Conclusions

To conclude the findings within this thesis, the following novel observations have been made:

- The putative OS CSC markers ALDH and CD117 are heterogeneously expressed within 7 OS cell lines.
- The OS cell lines express mesenchymal markers vimentin and lack the epithelial marker e-cadherin.
- ALDH expression in the MG63 and MCF7 is decreased in response to increased cell density.
- The cell lines Cal72, G292, MG63, U2OS, SaOS-2, HT1080 and SKLNS1 were all found to secrete a factor which enhanced growth.
- Growth factors secreted by U2OS cells increase OS, sarcoma and MCF7 cell line proliferation.
- Cytokines secreted by OS cell lines are associated with inflammation.
- Cell line CCL-2 expression (measured by commercial ELISA) correlated with OS and MCF7 growth enhancement observed in response to conditioned media.
- CCR2 receptor antagonism and *CCL-2* RNA interference decrease U2OS proliferation.
- Genes with altered expression in response to recombinant CCL-2 are associated with transcription.
- Genes with increased expression following exposure to U2OS conditioned media were associated with cancer signaling pathways and cell migration.

To summarise, the data presented in this thesis characterised OS cells expressing putative CSC markers (ALDH and CD117) in a panel of 7 OS cell lines and MCF7. OS cell lines have been observed to secrete a paracrine growth factor, decreased proliferation has been observed in response to CCR2 antagonism and reduced CCL-2 expression. Genes associated with altered expression in response to CCL-2 signaling are associated with transcription, and U2OS conditioned media was found to express genes associated with cancer cell signaling pathways and cell locomotion.

### 7.3 Future work

In summary, future directions of this study could focus on the following aspects:

- Analysis of clonogenicity and spheroid forming ability of OS cells expressing CD44<sup>+</sup>/e-cad<sup>-</sup>. Flow assisted cell sorting (FACS) can be used to isolate OS cell line cells which express the phenotypes CD44<sup>+</sup>/e-cad<sup>-</sup>, CD44<sup>+</sup>/e-cad<sup>+</sup>, CD44<sup>-</sup>/e-cad<sup>+</sup> and CD44<sup>-</sup>/e-cad<sup>-</sup>. These four populations of cell can then be seeded at low density to assess clonogenicity through colony formation along with spheroid forming efficiency. This would confirm if CD44<sup>+</sup>/e-cad<sup>-</sup> cells have enhanced colony forming capabilities in both these assays.
- Cell sorting of OS ALDH expressing cells to identify if these cells have an enhanced chemotherapy resistance. ALDH expressing cells can be isolated using FACS and tested for resistance to cisplatin, doxorubicin and methotrexate by identifying the LD<sub>50</sub> concentrations for each drug.
- Improving CCL-2 knockdown through the use of an appropriate CCL-2 shRNA control, which utilises functional complementation to identify the effect of this upon OS proliferation. The murine chemokine MCP-5 shares 66 % sequence homology with human CCL-2 and carries out the chemotraction of leukocytes (Sarafi et al., 1997). OS cell lines transfected with murine MCP-5 can then have human CCL-2 expression reduced through RNAi. The expression of murine MCP-5 can be assessed to identify if CCL-2 RNAi has specific CCL-2 gene knockdown.
- CCR2 shRNA inhibition to identify the effect upon OS proliferation. To analyse the impact of reducing CCR2 expression upon OS cell lines, lentiviral shRNA particles can be generated and used to inhibit CCR2 expression. The growth of these CCR2 RNAi cell lines growth can then be assessed, along with the response of these cell lines to recombinant CCL-2 and conditioned media.
- Analysis of MG63 CCL-2 shRNA inhibition and effect upon cell proliferation. The impact of CCL-2 expression in the cell MG63 which highly expresses CCL-2 can be assessed through RNAi gene knockdown. Upon confirmation of CCL-2 gene knockdown the cells can be tested for proliferation rates and compared to the scrambled control cell line.

- Analyse effect of recombinant CCL-2 upon calcium influx in order to assess bio-activity in an alternative CCL-2 signal transduced pathway. To confirm the bio-activity of recombinant CCL-2, HEK293 cells transfected with CCR2 have been shown to respond to CCL-2 with an influx of intracellular calcium (Sarafi et al., 1997). Using the same system recombinant CCL-2 can be utilised upon HEK293 cells to assess the ability to recombinant CCL-2 to signal via CCR2.
- Assess the chemo active capabilities of CCL-2 on OS cell lines. In prostate cancer CCL-2 has been shown to act as a chemokine (Loberg et al., 2006), OS cells can be assessed for their ability to migrate towards CCL-2 using a transwell assay.

## Appendix

### I. Control images of confocal microscopy staining

To assess whether antibodies and reagents used to assess putative CSC marker expression (ALDH, CD117 and CD44) using confocal microscopy. Isotype control antibodies which had affinity only to murine proteins were also matched according to fluorescent label were tested to assess non-specific binding. Control antibodies were used at the same concentration as CSC marker antibodies (Section 2.8). For ALDH which is analysed using the BODIPY<sup>®</sup> aminoacetaldehyde, which is converted to a fluorescent molecule by ALDH, has been inhibited by the ALDH inhibitor DEAB. For all ALDH and CD44 isotype control images no non-specific binding can be observed for 143B when stained adherently (Figure I.A) or when grown under sarcosphere conditions (Figure I.B). No

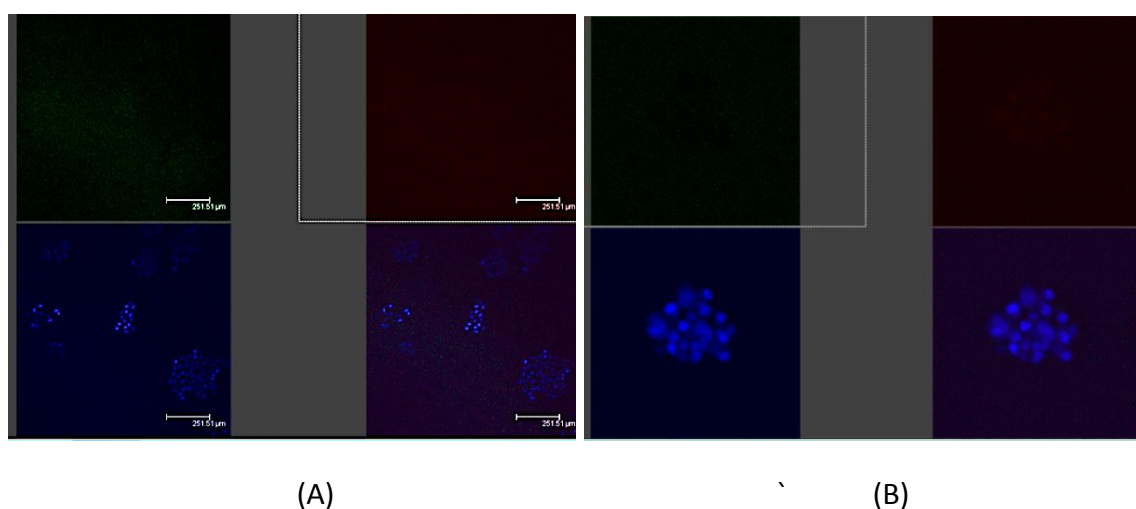


**Figure I: Negative control confocal microscopy images of ALDH and CD44 co-stained images.** (A) and (B) are representative images of 143B cells stained the ALDH (FITC) inhibitor DEAB and a CD44 isotype control and fluorescent label (PE) matched antibody when adherent (A) or grown under sarcosphere conditions (B). FITC fluorescence (green) can be observed in the top left panel, PE (red) in top right panel, bottom left indicates To-pro-3 fluorescence (blue) and an overlay in the bottom right panel.

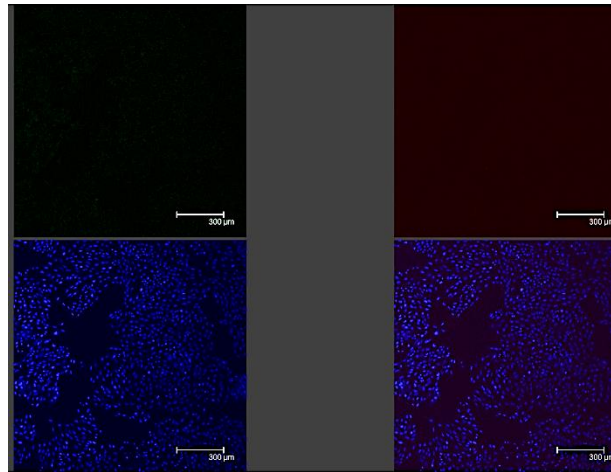


**Figure II: Negative control confocal microscopy image of CD117 and CD44 co-stained image.** Image is representative 143B cells stained the CD117 (FITC) and CD44 (PE) isotype control and fluorescent label matched antibody. FITC fluorescence (green) can be observed in the top left panel, PE (red) in top right panel, bottom left indicates To-pro-3 fluorescence (blue) and an overlay in the bottom right. (C) 143B representative image of adherent cells.

## II. Calibration curves to determine CCL-2 and IL-8 concentrations

To determine the concentration of IL-8 and CCL-2 in conditioned media (Section 2.5.2) a commercial ELISA kit (BioLegend) was used. For each experiment a calibration curve was constructed using a concentration of 0 – 500 pg/ml for CCL-2 and 0 – 1000 pg/ml for IL-8, each standard concentration was tested in triplicate. Absorbance readings at 570 nm were subtracted from 450 nm, and plotted as absorbance readings minus the blank absorbance (0 ng/ml) (Figure III). R<sup>2</sup> values varied from 0.98 – 0.99.

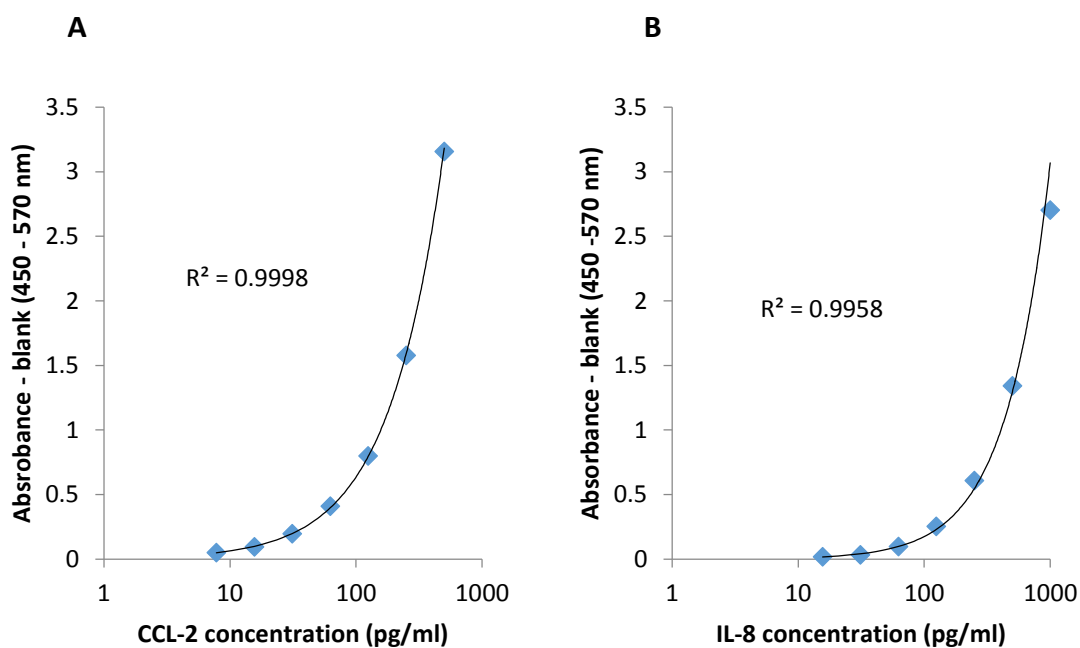


**Figure III: Calibration curves of CCL-2 and IL-8 concentration.** CCL-2 (A) and IL-8 (B) standards were prepared in triplicate (Section 2.5.2). Concentration of standards for CCL-2 was 0 – 500 pg/ml and IL-8 was 0 – 1000 pg/ml. Absorbance reading at 570 nm were subtracted from 450 nm readings and average blank reading were subtracted from standards. Average values were plotted and an excel power trendline was used to assess linearity.

### III. Real time PCR 18s rRNA and CCL-2 primer efficiencies

In order to assess the amplification efficiencies of the target gene (CCL-2) and endogenous reference gene (18s rRNA), both primers were tested using U2OS DNA concentrations of 0.16 – 100 ng/ml (Figure II). The amplification efficiencies of both primers was assessed using the by using the gradient of each primer DNA concentration curve, to calculate primer efficiency (E). An E value of 2 represents 100 % efficiency, CCL-2 primer produced an E value of 2.33 and 18s rRNA produced an E value of 2.11 (Table IV).

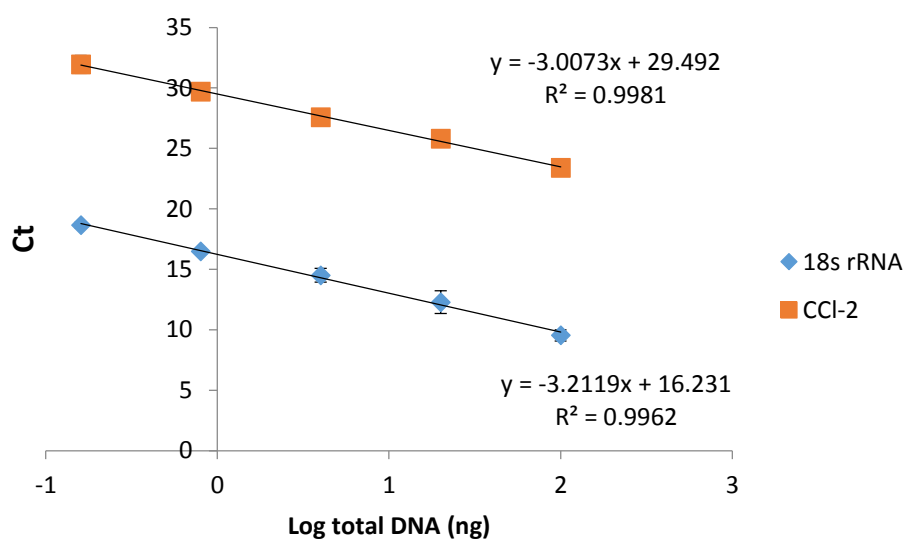


**Figure IV: Real time PCR primer efficiencies.** 18s rRNA and CCL-2 primers were used to assess DNA amplification for U2OS DNA concentrations at 0.16 – 100 ng/ml,  $\Delta$ Ct values were calculated, each primer was tested in triplicate for each DNA concentration. Data presented as mean and standard deviation.

**Table I: Primer efficiencies (E) for 18s rRNA and CCL-2.**

Primer	E value
18s rRNA	2.33
CCL-2	2.11



#### IV. Real time PCR melt curve

To assess the specificity of primers used for real time PCR (Section 2.7.3) CCL-2 gene expression analysis of U2OS CCL-2 RNAi cell lines, the temperature required to dissociate primer from the template strand was assessed. All cell lines were tested in triplicate, for the 18s rRNA primers melting temperatures varied from 76.5 – 76.7 °C (Figure V and table II) and CCL-2 primer melting concentration varied from 85.3 – 85.5 °C (Figure VI and table III). The due to the low concentration of CCL-2 present within knockdown 2 cell lines a melting temperature was not recorded because the peak was below the threshold. However, a small peak is visible for this cell line at 85.3 – 85.5 °C (Figure IV). All control samples which contained no DNA all did not produce a melting peak within the threshold.

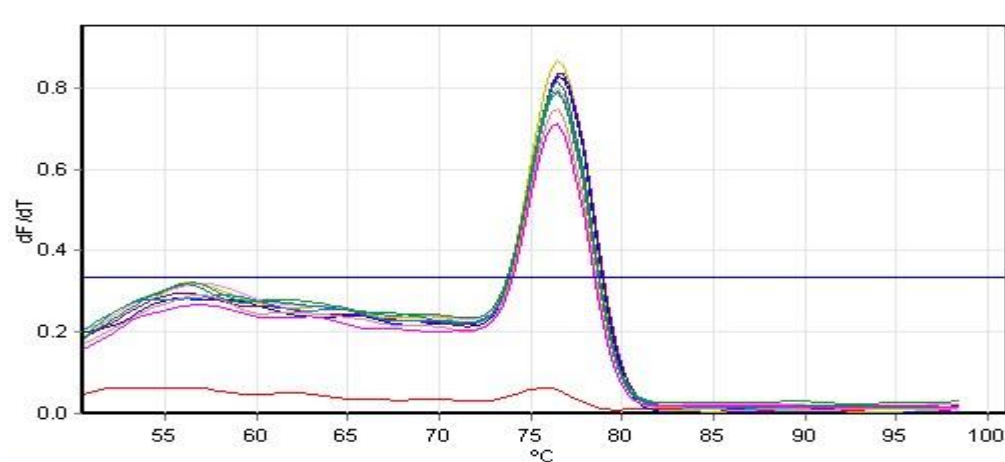


**Figure V: Melting curves of 18s rRNA primers.** U2OS cell knockdown cell lines were tested in triplicate using 100 ng of template DNA and 1  $\mu$ M of forward and reverse primers

**Table II: Melting temperatures of 18s rRNA primers tested with U2OS CCL-2 knockdown cell lines reverse transcribed RNA.**

Colour	Name	Temperature (°C)
Red	Neagtive control	
Yellow	Empty vec sample 1	76.5
Blue	Empty vec sample 2	76.5
Purple	Empty vec sample 3	76.7
Pink	Knockdown (1) sample 1	76.5
Light Blue	Knockdown (1) sample 2	76.5
Teal	Knockdown (1) sample 3	76.5
Light Red	Knockdown (2) sample 1	76.5
Green	Knockdown (2) sample 2	76.5
Magenta	Knockdown (2) sample 3	76.5

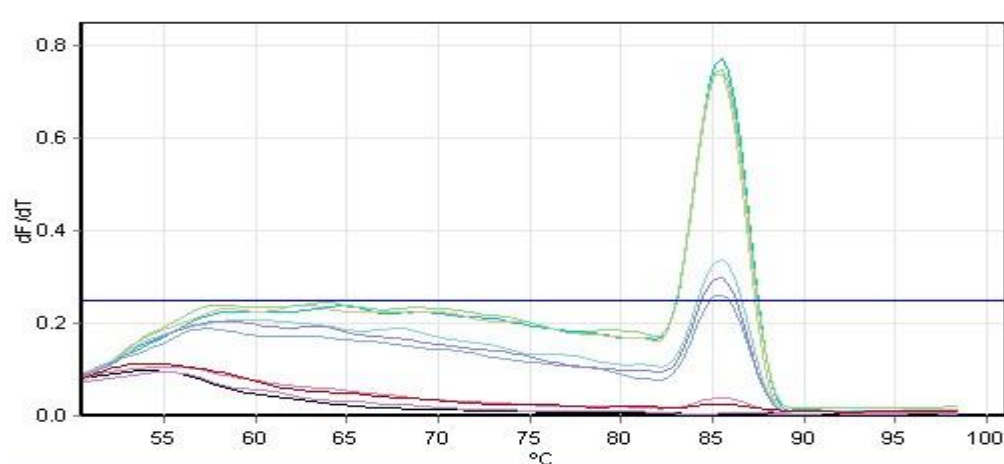


**Figure VI: Melting curves of CCL-2 primers.** U2OS cell knockdown cell lines were tested in triplicate using 100 ng of template DNA and 1  $\mu$ M of forward and reverse primers

**Table III: Melting temperatures of CCL-2 primers tested with U2OS CCL-2 knockdown cell lines reverse transcribed RNA.**

Colour	Name	Temperature (°C)
■	CCL-2 negative control	
■	Empty vec CCL-2 sample 1	85.5
■	Empty vec CCL-2 sample 2	85.3
■	Empty vec CCL-2 sample 3	85.5
■	Knockdown (1) sample 1	85.5
■	Knockdown (1) sample 2	85.5
■	Knockdown (1) sample 3	85.3
■	Knockdown (2) sample 1	Below threshold
■	Knockdown (2) sample 2	Below threshold
■	Knockdown (2) sample3	Below threshold

## V. Quality control of microarray data

In order to assess the suitability of all samples analysed using the affymetrix microarray (Section 2.7.4), samples were assessed using the R analysis package in the Bioconductor program. The software identified one of unconditioned sample (DMEM) and one of the U2OS conditioned samples did not have the same expression profiles as the other two samples tested in the same conditions. This was apparent when samples were analysed using a box plot of the fluorescence intensity (Figure VII), which is confirmed by the multi-dimensional plot (Figure VIII). Due to both these samples not conforming the expression observed in the other samples from the same conditions they were removed from analysis.

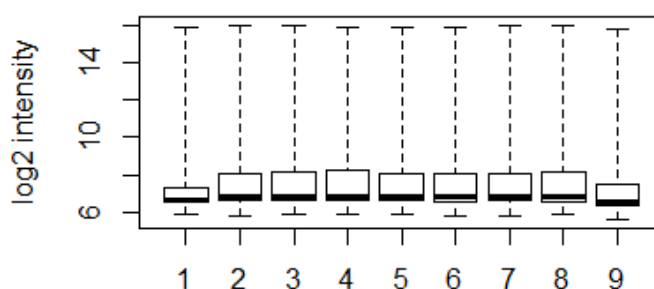


**Figure VII: Box plot of samples tested in using the affymetrix gene microarray.** Sample 1 (unconditioned) and sample 9 (U2OS conditioned media) do not correspond with the same box plot as the other samples.

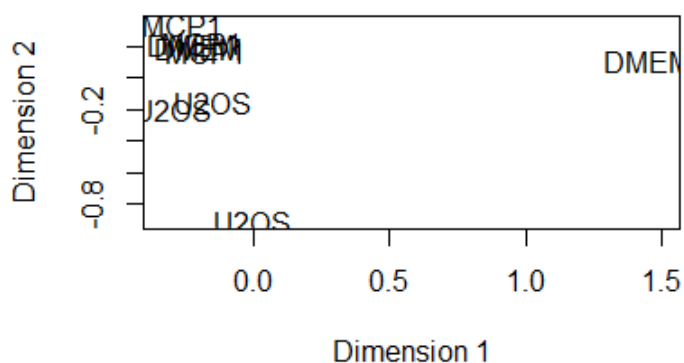


**Figure VIII: Multi-dimensional plot of genes expressed by microarray samples.** One sample from U2OS and another from DMEM do not have the same expression profile as the other samples so were removed from analysis.

## References

- ABKOWITZ, J., LINENBERGER, M., NEWTON, M., SHELTON, G., OTT, R. & GUTTORP, P. 1990. Evidence for the maintenance of hematopoiesis in a large animal by the sequential activation of stem-cell clones. *Proceedings of the National Academy of Sciences of the United States of America*, 87, 9062.
- ADHIKARI, A. S., AGARWAL, N., WOOD, B. M., PORRETTA, C., RUIZ, B., POCHAMPALLY, R. R. & IWAKUMA, T. 2010. CD117 and Stro-1 identify osteosarcoma tumor-initiating cells associated with metastasis and drug resistance. *Cancer Res*, 70, 4602-12.
- AEBI, S., KURDI-HAIDAR, B., GORDON, R., CENNI, B., ZHENG, H., FINK, D., CHRISTEN, R. D., BOLAND, C. R., KOI, M. & FISHEL, R. 1996. Loss of DNA mismatch repair in acquired resistance to cisplatin. *Cancer research*, 56, 3087-3090.
- AHMAD, A., ABOUKAMEEL, A., KONG, D., WANG, Z., SETHI, S., CHEN, W., SARKAR, F. H. & RAZ, A. 2011. Phosphoglucose isomerase/autocrine motility factor mediates epithelial-mesenchymal transition regulated by miR-200 in breast cancer cells. *Cancer Res*, 71, 3400-9.
- AIROLDI, I., MEAZZA, R., CROCE, M., DI CARLO, E., PIAZZA, T., COCCO, C., D'ANTUONO, T., PISTOIA, V., FERRINI, S. & CORRIAS, M. V. 2004. Low-dose interferon- $\gamma$ -producing human neuroblastoma cells show reduced proliferation and delayed tumorigenicity. *British Journal of Cancer*, 90, 2210-2218.
- AL-HAJJ, M., WICHA, M., BENITO-HERNANDEZ, A., MORRISON, S. & CLARKE, M. 2003. Prospective identification of tumorigenic breast cancer cells. *Proceedings of the National Academy of Sciences of the United States of America*, 100, 3983.
- ALISON, M. R., GUPPY, N. J., LIM, S. M. & NICHOLSON, L. J. 2010a. Finding cancer stem cells: are aldehyde dehydrogenases fit for purpose? *J Pathol*, 222, 335-44.
- ALISON, M. R., ISLAM, S. & WRIGHT, N. A. 2010b. Stem cells in cancer: instigators and propagators? *J Cell Sci*, 123, 2357-68.
- ALMOND, A. 2007. Hyaluronan. *Cell Mol Life Sci*, 64, 1591-6.
- ANDERSON, E. C. & WONG, M. H. 2010. Caught in the Akt: regulation of Wnt signaling in the intestine. *Gastroenterology*, 139, 718.
- ANGEL, P. & KARIN, M. 1991. The role of Jun, Fos and the AP-1 complex in cell-proliferation and transformation. *Biochimica et Biophysica Acta (BBA)-Reviews on Cancer*, 1072, 129-157.
- ANNINGA, J. K., GELDERBLUM, H., FIOCCO, M., KROEP, J. R., TAMINIAU, A. H., HOGENDOORN, P. C. & EGELER, R. M. 2011. Chemotherapeutic adjuvant treatment for osteosarcoma: where do we stand? *European Journal of Cancer*, 47, 2431-2445.
- ANSIEAU, S., BASTID, J., DOREAU, A., MOREL, A. P., BOUCHET, B. P., THOMAS, C., FAUVET, F., PUISIEUX, I., DOGLIONI, C., PICCININ, S., MAESTRO, R., VOELTZEL, T., SELMI, A., VALSESIA-WITTMANN, S., CARON DE FROMENTEL, C. & PUISIEUX, A. 2008. Induction of EMT by twist proteins as a collateral effect of tumor-promoting inactivation of premature senescence. *Cancer Cell*, 14, 79-89.
- ARUFFO, A., STAMENKOVIC, I., MELNICK, M., UNDERHILL, C. B. & SEED, B. 1990. CD44 is the principal cell surface receptor for hyaluronate. *Cell*, 61, 1303-13.
- ASKANAZY, M. 1907. *Die Teratome nach ihrem Bau, ihrem Verlauf, ihrer Genese und im Vergleich zum experimentellen Teratoid*, G. Fischer.
- ASSARAF, Y. G. 2007. Molecular basis of antifolate resistance. *Cancer Metastasis Rev*, 26, 153-81.
- AVIN, E., HAIMOVICH, J. & HOLLANDER, N. 2004. Anti-idiotypic x anti-CD44 bispecific antibodies inhibit invasion of lymphoid organs by B cell lymphoma. *The Journal of Immunology*, 173, 4736-4743.
- BARRANDON, Y. & GREEN, H. 1987. Three clonal types of keratinocyte with different capacities for multiplication. *Proceedings of the National Academy of Sciences of the United States of America*, 84, 2302.
- BASELGA, J. & SWAIN, S. M. 2009. Novel anticancer targets: revisiting ERBB2 and discovering ERBB3. *Nat Rev Cancer*, 9, 463-75.
- BAUMAN, S. J., WHINNA, H. C. & CHURCH, F. C. 2002. Serpins (serine protease inhibitors). *Current Protocols in Protein Science*, 21.7. 1-21.7. 14.
- BENNETT, C. N., OUYANG, H., MA, Y. L., ZENG, Q., GERIN, I., SOUSA, K. M., LANE, T. F., KRISHNAN, V., HANKENSON, K. D. & MACDOUGALD, O. A. 2007. Wnt10b increases postnatal bone formation by enhancing osteoblast differentiation. *J Bone Miner Res*, 22, 1924-32.

- BERDEL, W. E., DE VOS, S., MAURER, J., OBERBERG, D., VON MARSCHALL, Z., SCHROEDER, J. K., LI, J., LUDWIG, W. D., KREUSER, E. D., THIEL, E. & ET AL. 1992. Recombinant human stem cell factor stimulates growth of a human glioblastoma cell line expressing c-kit protooncogene. *Cancer Res*, 52, 3498-502.
- BERMAN, J. J. 2004. Tumor classification: molecular analysis meets Aristotle. *BMC Cancer*, 4, 10.
- BERTINO, J. R., GOKER, E., GORLICK, R., LI, W. W. & BANERJEE, D. 1996. Resistance Mechanisms to Methotrexate in Tumors. *Oncologist*, 1, 223-226.
- BIDDLE, A., LIANG, X., GAMMON, L., FAZIL, B., HARPER, L. J., EMICH, H., COSTEA, D. E. & MACKENZIE, I. C. 2011. Cancer stem cells in squamous cell carcinoma switch between two distinct phenotypes that are preferentially migratory or proliferative. *Cancer Res*, 71, 5317-26.
- BIELACK, S. S., KEMPF-BIELACK, B., DELLING, G., EXNER, G. U., FLEGE, S., HELMKE, K., KOTZ, R., SALZER-KUNTSCHIK, M., WERNER, M., WINKELMANN, W., ZOUBEK, A., JURGENS, H. & WINKLER, K. 2002. Prognostic factors in high-grade osteosarcoma of the extremities or trunk: an analysis of 1,702 patients treated on neoadjuvant cooperative osteosarcoma study group protocols. *J Clin Oncol*, 20, 776-90.
- BILEZIKIAN, J. P., RAISZ, L. G. & MARTIN, T. J. 2008. *Principles of Bone Biology, Two-Volume Set*, Academic Press.
- BODINE, P. V., ZHAO, W., KHARODE, Y. P., BEX, F. J., LAMBERT, A. J., GOAD, M. B., GAUR, T., STEIN, G. S., LIAN, J. B. & KOMM, B. S. 2004. The Wnt antagonist secreted frizzled-related protein-1 is a negative regulator of trabecular bone formation in adult mice. *Mol Endocrinol*, 18, 1222-37.
- BONNET, D. & DICK, J. E. 1997. Human acute myeloid leukemia is organized as a hierarchy that originates from a primitive hematopoietic cell. *Nat Med*, 3, 730-7.
- BOURGUIGNON, L. Y., SPEVAK, C. C., WONG, G., XIA, W. & GILAD, E. 2009. Hyaluronan-CD44 interaction with protein kinase C(epsilon) promotes oncogenic signaling by the stem cell marker Nanog and the Production of microRNA-21, leading to down-regulation of the tumor suppressor protein PDCD4, anti-apoptosis, and chemotherapy resistance in breast tumor cells. *J Biol Chem*, 284, 26533-46.
- BOYLE, W. J., SIMONET, W. S. & LACEY, D. L. 2003. Osteoclast differentiation and activation. *Nature*, 423, 337-42.
- BRULAND, Ø. & PIHL, A. 1997. On the current management of osteosarcoma. A critical evaluation and a proposal for a modified treatment strategy. *European Journal of Cancer*, 33, 1725-1731.
- BRUMMELKAMP, T. R. & BERNARDS, R. 2003. New tools for functional mammalian cancer genetics. *Nature Reviews Cancer*, 3, 781-789.
- BUNTING, K. & TOWNSEND, A. 1996. De novo expression of transfected human class 1 aldehyde dehydrogenase (ALDH) causes resistance to oxazaphosphorine anti-cancer alkylating agents in hamster V79 cell lines. *Journal of Biological Chemistry*, 271, 11884.
- BURGESS, T. L., QIAN, Y., KAUFMAN, S., RING, B. D., VAN, G., CAPPARELLI, C., KELLEY, M., HSU, H., BOYLE, W. J., DUNSTAN, C. R., HU, S. & LACEY, D. L. 1999. The ligand for osteoprotegerin (OPGL) directly activates mature osteoclasts. *J Cell Biol*, 145, 527-38.
- CALABRETTA, B. & PERROTTI, D. 2004. The biology of CML blast crisis. *Blood*, 103, 4010-4022.
- CAMP, R. L., SCHEYNIUS, A., JOHANSSON, C. & PURE, E. 1993. CD44 is necessary for optimal contact allergic responses but is not required for normal leukocyte extravasation. *The Journal of experimental medicine*, 178, 497-507.
- CANO, A., PEREZ-MORENO, M. A., RODRIGO, I., LOCASCIO, A., BLANCO, M. J., DEL BARRIO, M. G., PORTILLO, F. & NIETO, M. A. 2000. The transcription factor snail controls epithelial-mesenchymal transitions by repressing E-cadherin expression. *Nat Cell Biol*, 2, 76-83.
- CHAFFER, C. L., BRENNAN, J. P., SLAVIN, J. L., BLICK, T., THOMPSON, E. W. & WILLIAMS, E. D. 2006. Mesenchymal-to-epithelial transition facilitates bladder cancer metastasis: role of fibroblast growth factor receptor-2. *Cancer Res*, 66, 11271-8.
- CHAMBON, M., NIRDÉ, P., GLEIZES, M., ROGER, P. & VIGNON, F. 2003. Localization of BRCA1 protein in human breast cancer cells. *Breast cancer research and treatment*, 79, 107-119.
- CHANDAR, N., BILLIG, B., MCMASTER, J. & NOVAK, J. 1992. Inactivation of p53 gene in human and murine osteosarcoma cells. *British Journal of Cancer*, 65, 208.
- CHARAFE-JAUFFRET, E., GINESTIER, C., IOVINO, F., WICINSKI, J., CERVERA, N., FINETTI, P., HUR, M. H., DIEBEL, M. E., MONVILLE, F., DUTCHER, J., BROWN, M., VIENS, P., XERRI, L., BERTUCCI, F., STASSI, G., DONTU, G., BIRNBAUM, D. & WICHA, M. S. 2009. Breast cancer cell lines contain functional cancer stem cells with metastatic capacity and a distinct molecular signature. *Cancer Res*, 69, 1302-13.
- CHEN, J., LI, Y., YU, T. S., MCKAY, R. M., BURNS, D. K., KERNIE, S. G. & PARADA, L. F. 2012. A restricted cell population propagates glioblastoma growth after chemotherapy. *Nature*, 488, 522-6.

- CHEN, P.-L., CHEN, Y., BOOKSTEIN, R. & LEE, W.-H. 1990. Genetic mechanisms of tumor suppression by the human p53 gene. *Science*, 250, 1576-1580.
- CHEN, R. Z., PETTERSSON, U., BEARD, C., JACKSON-GRUSBY, L. & JAENISCH, R. 1998. DNA hypomethylation leads to elevated mutation rates. *Nature*, 395, 89-93.
- CHERNEY, R. J., MO, R., MEYER, D. T., NELSON, D. J., LO, Y. C., YANG, G., SCHERLE, P. A., MANDLEKAR, S., WASSERMAN, Z. R. & JEZAK, H. 2008. Discovery of disubstituted cyclohexanes as a new class of CC chemokine receptor 2 antagonists. *Journal of medicinal chemistry*, 51, 721-724.
- CHIOU, S. H., WANG, M. L., CHOU, Y. T., CHEN, C. J., HONG, C. F., HSIEH, W. J., CHANG, H. T., CHEN, Y. S., LIN, T. W., HSU, H. S. & WU, C. W. 2010. Coexpression of Oct4 and Nanog enhances malignancy in lung adenocarcinoma by inducing cancer stem cell-like properties and epithelial-mesenchymal transdifferentiation. *Cancer Res*, 70, 10433-44.
- CHUTE, J., MURAMOTO, G., WHITESIDES, J., COLVIN, M., SAFI, R., CHAO, N. & MCDONNELL, D. 2006. Inhibition of aldehyde dehydrogenase and retinoid signaling induces the expansion of human hematopoietic stem cells. *Proceedings of the National Academy of Sciences*, 103, 11707.
- CLARKE, M. F., DICK, J. E., DIRKS, P. B., EAVES, C. J., JAMIESON, C. H., JONES, D. L., VISVADER, J., WEISSMAN, I. L. & WAHL, G. M. 2006. Cancer stem cells--perspectives on current status and future directions: AACR Workshop on cancer stem cells. *Cancer Res*, 66, 9339-44.
- CORLESS, C. L., BARNETT, C. M. & HEINRICH, M. C. 2011. Gastrointestinal stromal tumours: origin and molecular oncology. *Nat Rev Cancer*, 11, 865-78.
- COTTERILL, S. J., WRIGHT, C. M., PEARCE, M. S. & CRAFT, A. W. 2004. Stature of young people with malignant bone tumors. *Pediatr Blood Cancer*, 42, 59-63.
- COURTENAY, V. D. 1976. A soft agar colony assay for Lewis lung tumour and B16 melanoma taken directly from the mouse. *British journal of cancer*, 34, 39.
- CREIGHTON, C. J., LI, X., LANDIS, M., DIXON, J. M., NEUMEISTER, V. M., SJOLUND, A., RIMM, D. L., WONG, H., RODRIGUEZ, A. & HERSCHKOWITZ, J. I. 2009. Residual breast cancers after conventional therapy display mesenchymal as well as tumor-initiating features. *Proceedings of the National Academy of Sciences*, 106, 13820-13825.
- CROCE, C. M. 2008. Oncogenes and cancer. *N Engl J Med*, 358, 502-11.
- CROKER, A. K. & ALLAN, A. L. 2012. Inhibition of aldehyde dehydrogenase (ALDH) activity reduces chemotherapy and radiation resistance of stem-like ALDHhiCD44(+) human breast cancer cells. *Breast Cancer Res Treat*, 133, 75-87.
- CULLEN, B. R. 2006. Enhancing and confirming the specificity of RNAi experiments. *Nature methods*, 3, 677-681.
- CURTIS, R. E., BOICE, J. D., JR., STOVALL, M., BERNSTEIN, L., GREENBERG, R. S., FLANNERY, J. T., SCHWARTZ, A. G., WEYER, P., MOLONEY, W. C. & HOOVER, R. N. 1992. Risk of leukemia after chemotherapy and radiation treatment for breast cancer. *N Engl J Med*, 326, 1745-51.
- DAI, C. Y. & ENDERS, G. H. 2000. p16 INK4a can initiate an autonomous senescence program. *Oncogene*, 19, 1613-22.
- DAMSKY, C. H., RICHA, J., SOLTER, D., KNUDSEN, K. & BUCK, C. A. 1983. Identification and purification of a cell surface glycoprotein mediating intercellular adhesion in embryonic and adult tissue. *Cell*, 34, 455-466.
- DEININGER, M. W., GOLDMAN, J. M., LYDON, N. & MELO, J. V. 1997. The tyrosine kinase inhibitor CGP57148B selectively inhibits the growth of BCR-ABL-positive cells. *Blood*, 90, 3691-8.
- DELORME, B., RINGE, J., GALLAY, N., LE VERN, Y., KERBOEUF, D., JORGENSEN, C., ROSSET, P., SENSEBE, L., LAYROLLE, P. & HAUPL, T. 2008. Specific plasma membrane protein phenotype of culture-amplified and native human bone marrow mesenchymal stem cells. *Blood*, 111, 2631.
- DEORAH, S., LYNCH, C. F., SIBENALLER, Z. A. & RYKEN, T. C. 2006. Trends in brain cancer incidence and survival in the United States: Surveillance, Epidemiology, and End Results Program, 1973 to 2001. *Neurosurg Focus*, 20, E1.
- DESHMANE, S. L., KREMLEV, S., AMINI, S. & SAWAYA, B. E. 2009. Monocyte chemoattractant protein-1 (MCP-1): an overview. *J Interferon Cytokine Res*, 29, 313-26.
- DEY, D., SAXENA, M., PARANJAPE, A. N., KRISHNAN, V., GIRADDI, R., KUMAR, M. V., MUKHERJEE, G. & RANGARAJAN, A. 2009. Phenotypic and functional characterization of human mammary stem/progenitor cells in long term culture. *PLoS One*, 4, e5329.
- DHARMACON. 2014. *Thermo Scientific The RNAi Consortium (TRC) Lentiviral shRNA technical manual* [Online]. Thermo scientific. [Accessed 11/05/2014 2014].

- DIGEL, W., STEFANIC, M., SCHONIGER, W., BUCK, C., RAGHAVACHAR, A., FRICKHOFEN, N., HEIMPEL, H. & PORZSOLT, F. 1989. Tumor necrosis factor induces proliferation of neoplastic B cells from chronic lymphocytic leukemia. *Blood*, 73, 1242-1246.
- DILLER, L., KASSEL, J., NELSON, C. E., GRYKA, M. A., LITWAK, G., GEBHARDT, M., BRESSAC, B., OZTURK, M., BAKER, S. J., VOGELSTEIN, B. & ET AL. 1990. p53 functions as a cell cycle control protein in osteosarcomas. *Mol Cell Biol*, 10, 5772-81.
- DOHERTY, R., HAYWOOD-SMALL, S., SISLEY, K. & CROSS, N. 2011. Aldehyde dehydrogenase activity selects for the holoclone phenotype in prostate cancer cells. *Biochemical and biophysical research communications*, 414, 801-807.
- DOMAGALA, W., STRIKER, G., SZADOWSKA, A., DUKOWICZ, A., HAREZGA, B. & OSBORN, M. 1994. p53 protein and vimentin in invasive ductal NOS breast carcinoma relationship with survival and sites of metastases. *European Journal of Cancer*, 30, 1527-1534.
- DRIESENS, G., BECK, B., CAAUWE, A., SIMONS, B. D. & BLANPAIN, C. 2012. Defining the mode of tumour growth by clonal analysis. *Nature*, 488, 527-30.
- DUBUCQUOI, S., DESREUMAUX, P., JANIN, A., KLEIN, O., GOLDMAN, M., TAVERNIER, J., CAPRON, A. & CAPRON, M. 1994. Interleukin 5 synthesis by eosinophils: association with granules and immunoglobulin-dependent secretion. *The Journal of experimental medicine*, 179, 703-708.
- DULL, T., ZUFFEREY, R., KELLY, M., MANDEL, R., NGUYEN, M., TRONO, D. & NALDINI, L. 1998. A third-generation lentivirus vector with a conditional packaging system. *Journal of virology*, 72, 8463-8471.
- ENTZ-WERLE, N., MARCELLIN, L., GAUB, M. P., GUERIN, E., SCHNEIDER, A., BERARD-MAREC, P., KALIFA, C., BRUGIERE, L., PACQUEMENT, H., SCHMITT, C., TABONE, M. D., JEANNE-PASQUIER, C., TERRIER, P., DIJOU, F., OUDET, P., LUTZ, P. & BABIN-BOILLETOT, A. 2005. Prognostic significance of allelic imbalance at the c-kit gene locus and c-kit overexpression by immunohistochemistry in pediatric osteosarcomas. *J Clin Oncol*, 23, 2248-55.
- ESTEY, E. & DOHNER, H. 2006. Acute myeloid leukaemia. *Lancet*, 368, 1894-907.
- FAN, S., SMITH, M. L., RIVERT, D. J., DUBA, D., ZHAN, Q., KOHN, K. W., FORNACE, A. J. & O'CONNOR, P. M. 1995. Disruption of p53 function sensitizes breast cancer MCF-7 cells to cisplatin and pentoxifylline. *Cancer research*, 55, 1649-1654.
- FAN, T.-J., HAN, L.-H., CONG, R.-S. & LIANG, J. 2005. Caspase family proteases and apoptosis. *Acta biochimica et biophysica Sinica*, 37, 719-727.
- FANG, H., PLACENCIO, V. R. & DECLERCK, Y. A. 2012. Protumorigenic activity of plasminogen activator inhibitor-1 through an antiapoptotic function. *Journal of the National Cancer Institute*, 104, 1470-1484.
- FARBER, S. & DIAMOND, L. K. 1948. Temporary remissions in acute leukemia in children produced by folic acid antagonist, 4-aminopteroyl-glutamic acid. *N Engl J Med*, 238, 787-93.
- FARBER, S., DIAMOND, L. K., MERCER, R. D., SYLVESTER JR, R. F. & WOLFF, J. A. 1948. Temporary remissions in acute leukemia in children produced by folic acid antagonist, 4-aminopteroyl-glutamic acid (aminopterin). *New England Journal of Medicine*, 238, 787-793.
- FAWDAR, S. B. 2010. *Characterisation of STRO-1 expression on human mesenchymal stem cells and identification of putative cancer stem cells in osteosarcoma: prevention by micronutrients*. Ph.D., University of Westminster.
- FEINBERG, A. P. & TYCKO, B. 2004. The history of cancer epigenetics. *Nat Rev Cancer*, 4, 143-53.
- FERRARI, S., BRICCOLI, A., MERCURI, M., BERTONI, F., PICCI, P., TIENGGHI, A., DEL PREVER, A. B., FAGIOLI, F., COMANDONE, A. & BACCI, G. 2003. Postrelapse survival in osteosarcoma of the extremities: prognostic factors for long-term survival. *Journal of Clinical Oncology*, 21, 710-715.
- FISCHER, O. M., HART, S., GSCHWIND, A. & ULLRICH, A. 2003. EGFR signal transactivation in cancer cells. *Biochem Soc Trans*, 31, 1203-8.
- FISHER, B., COSTANTINO, J. P., REDMOND, C. K., FISHER, E. R., WICKERHAM, D. L. & CRONIN, W. M. 1994. Endometrial cancer in tamoxifen-treated breast cancer patients: findings from the National Surgical Adjuvant Breast and Bowel Project (NSABP) B-14. *Journal of the National Cancer Institute*, 86, 527-537.
- FISHER, B., COSTANTINO, J. P., WICKERHAM, D. L., REDMOND, C. K., KAVANAH, M., CRONIN, W. M., VOGEL, V., ROBIDOUX, A., DIMITROV, N., ATKINS, J., DALY, M., WIEAND, S., TAN-CHIU, E., FORD, L. & WOLMARK, N. 1998. Tamoxifen for prevention of breast cancer: report of the National Surgical Adjuvant Breast and Bowel Project P-1 Study. *J Natl Cancer Inst*, 90, 1371-88.
- FORD, D., EASTON, D. F., BISHOP, D. T., NAROD, S. A. & GOLDFAR, D. E. 1994. Risks of cancer in BRCA1-mutation carriers. Breast Cancer Linkage Consortium. *Lancet*, 343, 692-5.



- FRANCHI, A., CALZOLARI, A. & ZAMPI, G. 1998. Immunohistochemical detection of c-fos and c-jun expression in osseous and cartilaginous tumours of the skeleton. *Virchows Arch*, 432, 515-9.
- FREUND, A., CHAUVEAU, C., BROUILLET, J. P., LUCAS, A., LACROIX, M., LICZNAK, A., VIGNON, F. & LAZENNEC, G. 2003. IL-8 expression and its possible relationship with estrogen-receptor-negative status of breast cancer cells. *Oncogene*, 22, 256-65.
- FRIEDENSTEIN, A. J., PIATETZKY, S., II & PETRAKOVA, K. V. 1966. Osteogenesis in transplants of bone marrow cells. *J Embryol Exp Morphol*, 16, 381-90.
- FRIEDL, P. & WOLF, K. 2003. Tumour-cell invasion and migration: diversity and escape mechanisms. *Nature Reviews Cancer*, 3, 362-374.
- FUNASAKA, T., HU, H., YANAGAWA, T., HOGAN, V. & RAZ, A. 2007. Down-regulation of phosphoglucose isomerase/autocrine motility factor results in mesenchymal-to-epithelial transition of human lung fibrosarcoma cells. *Cancer Res*, 67, 4236-43.
- GAO, S., NIELSEN, B. S., KROGDAHL, A., SØRENSEN, J. A., TAGESEN, J., DABELSTEEN, S., DABELSTEEN, E. & ANDREASEN, P. A. 2010. Epigenetic alterations of the SERPINE1 gene in oral squamous cell carcinomas and normal oral mucosa. *Genes, Chromosomes and Cancer*, 49, 526-538.
- GAYTHER, S. A., MANGION, J., RUSSELL, P., SEAL, S., BARFOOT, R., PONDER, B. A. J., STRATTON, M. R. & EASTON, D. 1997. Variation of risks of breast and ovarian cancer associated with different germline mutations of the BRCA2 gene. *Nature genetics*, 15, 103-105.
- GEORGE, M. & VAUGHAN, J. H. 1962. In vitro cell migration as a model for delayed hypersensitivity. *Experimental Biology and Medicine*, 111, 514-521.
- GERARD, N. P. & GERARD, C. 1991. The chemotactic receptor for human C5a anaphylatoxin.
- GIBBS, C., KUKUKOV, V., REITH, J., TCHIGRINOVA, O., SUSLOV, O., SCOTT, E., GHIVIZZANI, S., IGNATOVA, T. & STEINDLER, D. 2005. Stem-like cells in bone sarcomas: implications for tumorigenesis. *Neoplasia (New York, NY)*, 7, 967.
- GILLETTE, J. M., CHAN, D. C. & NIELSEN- PREISS, S. M. 2004. Annexin 2 expression is reduced in human osteosarcoma metastases. *Journal of cellular biochemistry*, 92, 820-832.
- GILLETTE, J. M., GIBBS, C. P. & NIELSEN-PREISS, S. M. 2008. Establishment and characterization of OS 99-1, a cell line derived from a highly aggressive primary human osteosarcoma. *In Vitro Cellular & Developmental Biology-Animal*, 44, 87-95.
- GINESTIER, C., HUR, M. H., CHARAFE-JAUFFRET, E., MONVILLE, F., DUTCHER, J., BROWN, M., JACQUEMIER, J., VIENS, P., KLEER, C. G., LIU, S., SCHOTT, A., HAYES, D., BIRNBAUM, D., WICHA, M. S. & DONTU, G. 2007. ALDH1 is a marker of normal and malignant human mammary stem cells and a predictor of poor clinical outcome. *Cell Stem Cell*, 1, 555-67.
- GINESTIER, C., LIU, S., DIEBEL, M. E., KORKAYA, H., LUO, M., BROWN, M., WICINSKI, J., CABAUD, O., CHARAFE-JAUFFRET, E. & BIRNBAUM, D. 2010. CXCR1 blockade selectively targets human breast cancer stem cells in vitro and in xenografts. *The Journal of clinical investigation*, 120, 485.
- GINESTIER, C., WICINSKI, J., CERVERA, N., MONVILLE, F., FINETTI, P., BERTUCCI, F. O., WICHA, M. S., BIRNBAUM, D. & CHARAFE-JAUFFRET, E. 2009. Retinoid signaling regulates breast cancer stem cell differentiation. *Cell cycle (Georgetown, Tex.)*, 8, 3297.
- GLINSKII, A. B., SMITH, B. A., JIANG, P., LI, X.-M., YANG, M., HOFFMAN, R. M. & GLINSKY, G. V. 2003. Viable circulating metastatic cells produced in orthotopic but not ectopic prostate cancer models. *Cancer research*, 63, 4239-4243.
- GLOBOCAN. 2014. *GLOBOCAN 2012: Estimated cancer incidence mortality and prevalence worldwide 2012* [Online]. Lyon, France: World health organisation. Available: <http://www.who.int/mediacentre/factsheets/fs297/en/> [Accessed 09/05 2014].
- GONG, C., YAO, H., LIU, Q., CHEN, J., SHI, J., SU, F. & SONG, E. 2010. Markers of tumor-initiating cells predict chemoresistance in breast cancer. *PLoS One*, 5, e15630.
- GONG, Y., SLEE, R. B., FUKAI, N., RAWADI, G., ROMAN-ROMAN, S., REGINATO, A. M., WANG, H., CUNDY, T., GLORIEUX, F. H., LEV, D., ZACHARIN, M., OEXLE, K., MARCELINO, J., SUWAIIRI, W., HEEGER, S., SABATAKOS, G., APTE, S., ADKINS, W. N., ALLGROVE, J., ARSLAN-KIRCHNER, M., BATCH, J. A., BEIGHTON, P., BLACK, G. C., BOLES, R. G., BOON, L. M., BORRONE, C., BRUNNER, H. G., CARLE, G. F., DALLAPICCOLA, B., DE PAEPE, A., FLOEGE, B., HALFHIDE, M. L., HALL, B., HENNEKAM, R. C., HIROSE, T., JANS, A., JUPPNER, H., KIM, C. A., KEPPLER-NOREUIL, K., KOHLSCHUETTER, A., LACOMBE, D., LAMBERT, M., LEMYRE, E., LETTEBOER, T., PELTONEN, L., RAMESAR, R. S., ROMANENGO, M., SOMER, H., STEICHEN-GERSDORF, E., STEINMANN, B., SULLIVAN, B., SUPERTI-FURGA, A., SWOBODA, W., VAN DEN BOOGAARD, M. J., VAN HUL, W., VIKKULA, M., VOTRUBA, M., ZABEL, B., GARCIA, T., BARON, R.,

- OLSEN, B. R. & WARMAN, M. L. 2001. LDL receptor-related protein 5 (LRP5) affects bone accrual and eye development. *Cell*, 107, 513-23.
- GRAVES, D. T., JIANG, Y. & VALENTE, A. J. 1999. Regulated expression of MCP-1 by osteoblastic cells in vitro and in vivo. *Histol Histopathol*, 14, 1347-54.
- GRAVES, D. T., JIANG, Y. L., WILLIAMSON, M. J. & VALENTE, A. J. 1989. Identification of monocyte chemotactic activity produced by malignant cells. *Science*, 245, 1490-3.
- GRIGOLO, B., ROSETI, L., LISIGNOLI, G., REMIDDI, G. & FACCHINI, A. 1999. Expression of different chemokines by human osteosarcoma cells in response to tumor necrosis factor-alpha. *Anticancer Res*, 19, 3093-8.
- GRIGORIADIS, A. E., SCHELLANDER, K., WANG, Z. Q. & WAGNER, E. F. 1993. Osteoblasts are target cells for transformation in c-fos transgenic mice. *J Cell Biol*, 122, 685-701.
- GRIMSHAW, M. J., COOPER, L., PAPAZISIS, K., COLEMAN, J. A., BOHNENKAMP, H. R., CHIAPERO-STANKE, L., TAYLOR-PAPADIMITRIOU, J. & BURCHELL, J. M. 2008. Mammosphere culture of metastatic breast cancer cells enriches for tumorigenic breast cancer cells. *Breast Cancer Res*, 10, R52.
- GUO, W., HEALEY, J. H., MEYERS, P. A., LADANYI, M., HUVOS, A. G., BERTINO, J. R. & GORLICK, R. 1999. Mechanisms of methotrexate resistance in osteosarcoma. *Clinical Cancer Research*, 5, 621-627.
- GUO, Y., ZI, X., KOONTZ, Z., KIM, A., XIE, J., GORLICK, R., HOLCOMBE, R. F. & HOANG, B. H. 2007. Blocking Wnt/LRP5 signaling by a soluble receptor modulates the epithelial to mesenchymal transition and suppresses met and metalloproteinases in osteosarcoma Saos-2 cells. *J Orthop Res*, 25, 964-71.
- HAGNER, N. & JOERGER, M. 2010. Cancer chemotherapy: targeting folic acid synthesis. *Cancer management and research*, 2, 293.
- HALAZONETIS, T. D., GEORGOPOULOS, K., GREENBERG, M. E. & LEDER, P. 1988. c-Jun dimerizes with itself and with c-Fos, forming complexes of different DNA binding affinities. *Cell*, 55, 917-24.
- HALL, P. & WATT, F. 1989. Stem cells: the generation and maintenance of cellular diversity. *Development*, 106, 619.
- HAMBURGER, A. & SALMON, S. E. 1977. Primary bioassay of human myeloma stem cells. *J Clin Invest*, 60, 846-54.
- HANAHAH, D. & WEINBERG, R. A. 2011. Hallmarks of cancer: the next generation. *Cell*, 144, 646-74.
- HANSEN, M. 2002. Genetic and molecular aspects of osteosarcoma. *JOURNAL OF MUSCULOSKELETAL AND NEURONAL INTERACTIONS*, 2, 554-560.
- HARADA, A., SEKIDO, N., AKAHOSHI, T., WADA, T., MUKAIDA, N. & MATSUSHIMA, K. 1994. Essential involvement of interleukin-8 (IL-8) in acute inflammation. *J Leukoc Biol*, 56, 559-64.
- HARPER, L. J., COSTEA, D. E., GAMMON, L., FAZIL, B., BIDDLE, A. & MACKENZIE, I. C. 2010. Normal and malignant epithelial cells with stem-like properties have an extended G2 cell cycle phase that is associated with apoptotic resistance. *BMC cancer*, 10, 166.
- HARRIS, N. L., JAFFE, E. S., DIEBOLD, J., FLANDRIN, G., MULLER-HERMELINK, H. K., VARDIMAN, J., LISTER, T. A. & BLOOMFIELD, C. D. 1999. The World Health Organization classification of neoplastic diseases of the hematopoietic and lymphoid tissues. Report of the Clinical Advisory Committee meeting, Airlie House, Virginia, November, 1997. *Ann Oncol*, 10, 1419-32.
- HATTINGER, C. M., REVERTER-BRANCHAT, G., REMONDINI, D., CASTELLANI, G. C., BENINI, S., PASELLO, M., MANARA, M. C., SCOTLANDI, K., PICCI, P. & SERRA, M. 2003. Genomic imbalances associated with methotrexate resistance in human osteosarcoma cell lines detected by comparative genomic hybridization-based techniques. *Eur J Cell Biol*, 82, 483-93.
- HAY, E. D. 2005. The mesenchymal cell, its role in the embryo, and the remarkable signaling mechanisms that create it. *Dev Dyn*, 233, 706-20.
- HEINRICH, M. C., CORLESS, C. L., DEMETRI, G. D., BLANKE, C. D., VON MEHREN, M., JOENSUU, H., MCGREEVEY, L. S., CHEN, C.-J., VAN DEN ABEELE, A. D. & DRUKER, B. J. 2003. Kinase mutations and imatinib response in patients with metastatic gastrointestinal stromal tumor. *Journal of Clinical Oncology*, 21, 4342-4349.
- HELD, M. A., CURLEY, D. P., DANKORT, D., MCMAHON, M., MUTHUSAMY, V. & BOSENBERG, M. W. 2010. Characterization of melanoma cells capable of propagating tumors from a single cell. *Cancer research*, 70, 388-397.
- HEMS, G. 1970. Aetiology of bone cancer and some other cancers in the young. *British Journal of Cancer*, 24, 208.
- HENDERSON, S. R., GUILIANO, D., PRESNEAU, N., MCLEAN, S., FROW, R., VUJOVIC, S., ANDERSON, J., SEBIRE, N., WHELAN, J., ATHANASOU, N., FLANAGAN, A. M. & BOSHOFF, C. 2005. A molecular map of mesenchymal tumors. *Genome Biol*, 6, R76.

- HENSLER, P. J., ANNAB, L. A., BARRETT, J. C. & PEREIRA-SMITH, O. M. 1994. A gene involved in control of human cellular senescence on human chromosome 1q. *Molecular and cellular biology*, 14, 2291-2297.
- HINES, S. J., ORGAN, C., KORNSTEIN, M. J. & KRYSTAL, G. W. 1995. Coexpression of the c-kit and stem cell factor genes in breast carcinomas. *Cell Growth Differ*, 6, 769-79.
- HOLOHAN, C., VAN SCHAEYBROECK, S., LONGLEY, D. B. & JOHNSTON, P. G. 2013. Cancer drug resistance: An evolving paradigm. *Nature Reviews Cancer*, 13, 714-726.
- HONOKI, K., FUJII, H., KUBO, A., KIDO, A., MORI, T., TANAKA, Y. & TSUJIUCHI, T. 2010. Possible involvement of stem-like populations with elevated ALDH1 in sarcomas for chemotherapeutic drug resistance. *Oncology reports*, 24, 501-505.
- HOWELL, A., CLARKE, R. B. & ANDERSON, E. 1997. Oestrogens, Beatson and endocrine therapy. *Endocrine-Related Cancer*, 4, 371-380.
- HUANG, D. W., SHERMAN, B. T. & LEMPICKI, R. A. 2008. Systematic and integrative analysis of large gene lists using DAVID bioinformatics resources. *Nature protocols*, 4, 44-57.
- HUANG, E., HYNES, M., ZHANG, T., GINESTIER, C., DONTU, G., APPELMAN, H., FIELDS, J., WICHA, M. & BOMAN, B. 2009. Aldehyde dehydrogenase 1 is a marker for normal and malignant human colonic stem cells (SC) and tracks SC overpopulation during colon tumorigenesis. *Cancer research*, 69, 3382.
- HUBER, M. A., AZOITEI, N., BAUMANN, B., GRÄNERT, S., SOMMER, A., PEHAMBERGER, H., KRAUT, N., BEUG, H. & WIRTH, T. 2004. NF- $\kappa$ B is essential for epithelial-mesenchymal transition and metastasis in a model of breast cancer progression. *Journal of Clinical Investigation*, 114, 569-581.
- HUSE, J. T. & HOLLAND, E. C. 2010. Targeting brain cancer: advances in the molecular pathology of malignant glioma and medulloblastoma. *Nat Rev Cancer*, 10, 319-31.
- HWANG-VERSLUES, W., KUO, W., CHANG, P., PAN, C., WANG, H., TSAI, S., JENG, Y., SHEW, J., KUNG, J. & CHEN, C. 2009. Multiple lineages of human breast cancer stem/progenitor cells identified by profiling with stem cell markers. *PLoS One*, 4, e8377.
- IWASAKI, H. & SUDA, T. 2009. Cancer stem cells and their niche. *Cancer science*, 100, 1166-1172.
- IZUMI, K., FANG, L. Y., MIZOKAMI, A., NAMIKI, M., LI, L., LIN, W. J. & CHANG, C. 2013. Targeting the androgen receptor with siRNA promotes prostate cancer metastasis through enhanced macrophage recruitment via CCL2/CCR2 induced STAT3 activation. *EMBO molecular medicine*, 5, 1383-1401.
- JAFFE, N., FREI, E., 3RD, TRAGGIS, D. & BISHOP, Y. 1974. Adjuvant methotrexate and citrovorum-factor treatment of osteogenic sarcoma. *N Engl J Med*, 291, 994-7.
- JAWAD, M. U., CHEUNG, M. C., CLARKE, J., KONIARIS, L. G. & SCULLY, S. P. 2011. Osteosarcoma: improvement in survival limited to high-grade patients only. *J Cancer Res Clin Oncol*, 137, 597-607.
- JEFFREE, G. M., PRICE, C. H. & SISSONS, H. A. 1975. The metastatic patterns of osteosarcoma. *British Journal of Cancer*, 32, 87.
- JEMAL, A., CENTER, M. M., DESANTIS, C. & WARD, E. M. 2010. Global patterns of cancer incidence and mortality rates and trends. *Cancer Epidemiology Biomarkers & Prevention*, 19, 1893-1907.
- JIA, S.-F., WORTH, L. L. & KLEINERMAN, E. S. 1999. A nude mouse model of human osteosarcoma lung metastases for evaluating new therapeutic strategies. *Clinical & experimental metastasis*, 17, 501-506.
- JIN, P., XIE, J., ZHU, X., ZHOU, C., DING, X. & YANG, L. 2012. Effect of gene GSTP1 silencing via shRNA transfection on androgen independent prostate cancer cell line Du145. *Journal of Central South University Medical sciences*, 37, 807-816.
- JOHRER, K., JANKE, K., KRUGMANN, J., FIEGL, M. & GREIL, R. 2004. Transendothelial migration of myeloma cells is increased by tumor necrosis factor (TNF)-alpha via TNF receptor 2 and autocrine up-regulation of MCP-1. *Clin Cancer Res*, 10, 1901-10.
- JONES, P. A. & BAYLIN, S. B. 2002. The fundamental role of epigenetic events in cancer. *Nat Rev Genet*, 3, 415-28.
- JOSEPH, N. & MORRISON, S. 2005. Toward an understanding of the physiological function of Mammalian stem cells. *Developmental cell*, 9, 173-183.
- KALLURI, R. & WEINBERG, R. A. 2009. The basics of epithelial-mesenchymal transition. *J Clin Invest*, 119, 1420-8.
- KAMEYOSHI, Y., DÖRSCHNER, A., MALLET, A., CHRISTOPHERS, E. & SCHRÖDER, J. 1992. Cytokine RANTES released by thrombin-stimulated platelets is a potent attractant for human eosinophils. *The Journal of experimental medicine*, 176, 587-592.
- KANTARJIAN, H., SAWYERS, C., HOCHHAUS, A., GUILHOT, F., SCHIFFER, C., GAMBACORTI-PASSERINI, C., NIEDERWIESER, D., RESTA, D., CAPDEVILLE, R. & ZOELLNER, U. 2002. Hematologic and cytogenetic

- responses to imatinib mesylate in chronic myelogenous leukemia. *New England Journal of Medicine*, 346, 645-652.
- KATIYAR, S. K., ROY, A. M. & BALIGA, M. S. 2005. Silymarin induces apoptosis primarily through a p53-dependent pathway involving Bcl-2/Bax, cytochrome c release, and caspase activation. *Mol Cancer Ther*, 4, 207-16.
- KATO, M., PATEL, M. S., LEVASSEUR, R., LOBOV, I., CHANG, B. H., GLASS, D. A., 2ND, HARTMANN, C., LI, L., HWANG, T. H., BRAYTON, C. F., LANG, R. A., KARSENTY, G. & CHAN, L. 2002. Cbfa1-independent decrease in osteoblast proliferation, osteopenia, and persistent embryonic eye vascularization in mice deficient in Lrp5, a Wnt coreceptor. *J Cell Biol*, 157, 303-14.
- KELLAND, L. 2007. The resurgence of platinum-based cancer chemotherapy. *Nature Reviews Cancer*, 7, 573-584.
- KLEIN, M. & SIEGAL, G. 2006. Anatomic and Histologic Variants. *Am J Clin Pathol*, 125, 555-581.
- KOK, S. H., HONG, C. Y., KUO, M. Y. P., WANG, C. C., HOU, K. L., LIN, Y. T., GALSON, D. L. & LIN, S. K. 2009. Oncostatin M-induced CCL2 transcription in osteoblastic cells is mediated by multiple levels of STAT-1 and STAT-3 signaling: An implication for the pathogenesis of arthritis. *Arthritis & Rheumatism*, 60, 1451-1462.
- KRAMER, K., HICKS, D. G., OPPENHEIMER, J., PALIS, J., ROSIER, R. N., FALLON, M. D. & COHEN, H. J. 1993. Epithelioid osteosarcoma of bone immunocytochemical evidence suggesting divergent epithelial and mesenchymal differentiation in a primary osseous neoplasm. *Cancer*, 71, 2977-2982.
- KÜHL, M., SHELD AHL, L. C., PARK, M., MILLER, J. R. & MOON, R. T. 2000. The Wnt/Ca<sup>+</sup> pathway: a new vertebrate Wnt signaling pathway takes shape. *Trends in genetics*, 16, 279-283.
- LAPIDOT, T., GRUNBERGER, T., VORMOOR, J., ESTROV, Z., KOLLET, O., BUNIN, N., ZAIZOV, R., WILLIAMS, D. & FREEDMAN, M. 1996. Identification of human juvenile chronic myelogenous leukemia stem cells capable of initiating the disease in primary and secondary SCID mice. *Blood*, 88, 2655.
- LAZEBNIK, Y. 2010. What are the hallmarks of cancer? *Nat Rev Cancer*, 10, 232-3.
- LEE, K. D., KUO, T. K. C., JACQUELINE, W. P., CHUNG, Y. F., LIN, C. T., CHOU, S. H., CHEN, J. R., CHEN, Y. P. & LEE, O. K. S. 2004. In vitro hepatic differentiation of human mesenchymal stem cells. *Hepatology*, 40, 1275-1284.
- LEE, Y. S., CHOI, I., NING, Y., KIM, N. Y., KHATCHADOURIAN, V., YANG, D., CHUNG, H. K., CHOI, D., LABONTE, M. J., LADNER, R. D., NAGULAPALLI VENKATA, K. C., ROSENBERG, D. O., PETASIS, N. A., LENZ, H. J. & HONG, Y. K. 2012. Interleukin-8 and its receptor CXCR2 in the tumour microenvironment promote colon cancer growth, progression and metastasis. *Br J Cancer*, 106, 1833-41.
- LEWIS, C., LEEK, R., HARRIS, A. & MCGEE, J. 1995. Cytokine regulation of angiogenesis in breast cancer: the role of tumor-associated macrophages. *Journal of leukocyte biology*, 57, 747-751.
- LI, A., DUBEY, S., VARNEY, M. L., DAVE, B. J. & SINGH, R. K. 2003. IL-8 directly enhanced endothelial cell survival, proliferation, and matrix metalloproteinases production and regulated angiogenesis. *J Immunol*, 170, 3369-76.
- LI, H., CHEN, X., CALHOUN-DAVIS, T., CLAYPOOL, K. & TANG, D. G. 2008. PC3 human prostate carcinoma cell holoclones contain self-renewing tumor-initiating cells. *Cancer Res*, 68, 1820-5.
- LI, N., YANG, R., ZHANG, W., DORFMAN, H., RAO, P. & GORLICK, R. 2009. Genetically transforming human mesenchymal stem cells to sarcomas. *Cancer*, 115, 4795-4806.
- LI, P. F., DIETZ, R. & VON HARSDORF, R. 1999. p53 regulates mitochondrial membrane potential through reactive oxygen species and induces cytochrome c-independent apoptosis blocked by Bcl-2. *The EMBO journal*, 18, 6027-6036.
- LI, W. W., FAN, J., HOCHHAUSER, D. & BERTINO, J. R. 1997. Overexpression of p21waf1 leads to increased inhibition of E2F-1 phosphorylation and sensitivity to anticancer drugs in retinoblastoma-negative human sarcoma cells. *Cancer Res*, 57, 2193-9.
- LI, Y., FLORES, R., YU, A., OKCU, M. F., MURRAY, J., CHINTAGUMPALA, M., HICKS, J., LAU, C. C. & MAN, T. K. 2011. Elevated expression of CXC chemokines in pediatric osteosarcoma patients. *Cancer*, 117, 207-217.
- LI, Y., LIANG, Q., WEN, Y. Q., CHEN, L. L., WANG, L. T., LIU, Y. L., LUO, C., LIANG, H., LI, M. & LI, Z. 2010. Comparative proteomics analysis of human osteosarcomas and benign tumor of bone. *Cancer Genetics and Cytogenetics*, 198, 97-106.
- LIPINSKI, M. M. & JACKS, T. 1999. The retinoblastoma gene family in differentiation and development. *Oncogene*, 18, 7873-82.
- LIPPITZ, B. E. 2013. Cytokine patterns in patients with cancer: a systematic review. *Lancet Oncol*, 14, e218-28.

- LIU, S., GINESTIER, C., OU, S. J., CLOUTHIER, S. G., PATEL, S. H., MONVILLE, F., KORKAYA, H., HEATH, A., DUTCHER, J., KLEER, C. G., JUNG, Y., DONTU, G., TAICHMAN, R. & WICHA, M. S. 2011. Breast cancer stem cells are regulated by mesenchymal stem cells through cytokine networks. *Cancer Res*, 71, 614-24.
- LOBERG, R. D., DAY, L. L., HARWOOD, J., YING, C., ST JOHN, L. N., GILES, R., NEELEY, C. K. & PIENTA, K. J. 2006. CCL2 is a potent regulator of prostate cancer cell migration and proliferation. *Neoplasia*, 8, 578-86.
- LOBERG, R. D., YING, C., CRAIG, M., DAY, L. L., SARGENT, E., NEELEY, C., WOJNO, K., SNYDER, L. A., YAN, L. & PIENTA, K. J. 2007. Targeting CCL2 with systemic delivery of neutralizing antibodies induces prostate cancer tumor regression in vivo. *Cancer Res*, 67, 9417-24.
- LOCKE, M., HEYWOOD, M., FAWELL, S. & MACKENZIE, I. 2005. Retention of intrinsic stem cell hierarchies in carcinoma-derived cell lines. *Cancer research*, 65, 8944.
- LOU, N., WANG, Y., SUN, D., ZHAO, J. & GAO, Z. 2010. Isolation of stem-like cells from human MG-63 osteosarcoma cells using limiting dilution in combination with vincristine selection. *Indian J Biochem Biophys*, 47, 340-7.
- LOUIS, D. N., OHGAKI, H., WIESTLER, O. D., CAVENEE, W. K., BURGER, P. C., JOUVET, A., SCHEITHAUER, B. W. & KLEIHUES, P. 2007. The 2007 WHO classification of tumours of the central nervous system. *Acta Neuropathol*, 114, 97-109.
- LU, X. & KANG, Y. 2009. Chemokine (CC motif) ligand 2 engages CCR2+ stromal cells of monocytic origin to promote breast cancer metastasis to lung and bone. *Journal of biological chemistry*, 284, 29087-29096.
- LU, Y., CAI, Z., XIAO, G., LIU, Y., KELLER, E. T., YAO, Z. & ZHANG, J. 2007. CCR2 expression correlates with prostate cancer progression. *Journal of cellular biochemistry*, 101, 676-685.
- LUEDER, G. T., JUDISCH, F. & O'GORMAN, T. W. 1986. Second nonocular tumors in survivors of heritable retinoblastoma. *Arch Ophthalmol*, 104, 372-3.
- LUU, H. H., KANG, Q., PARK, J. K., SI, W., LUO, Q., JIANG, W., YIN, H., MONTAG, A. G., SIMON, M. A. & PEABODY, T. D. 2005. An orthotopic model of human osteosarcoma growth and spontaneous pulmonary metastasis. *Clinical & experimental metastasis*, 22, 319-329.
- MA, S., CHAN, K., LEE, T., TANG, K., WO, J., ZHENG, B. & GUAN, X. 2008. Aldehyde dehydrogenase discriminates the CD133 liver cancer stem cell populations. *Molecular Cancer Research*, 6, 1146.
- MACKALL, C. L., MELTZER, P. S. & HELMAN, L. J. 2002. Focus on sarcomas. *Cancer Cell*, 2, 175-8.
- MACKENZIE, I. C. 2008. Cancer stem cells. *Ann Oncol*, 19 Suppl 5, v40-3.
- MAGNI, M., SHAMMAH, S., SCHIRO, R., MELLADO, W., DALLA-FAVERA, R. & GIANNI, A. 1996. Induction of cyclophosphamide-resistance by aldehyde-dehydrogenase gene transfer. *Blood*, 87, 1097.
- MANI, S. A., GUO, W., LIAO, M. J., EATON, E. N., AYYANAN, A., ZHOU, A. Y., BROOKS, M., REINHARD, F., ZHANG, C. C., SHIPITSIN, M., CAMPBELL, L. L., POLYAK, K., BRISKEN, C., YANG, J. & WEINBERG, R. A. 2008. The epithelial-mesenchymal transition generates cells with properties of stem cells. *Cell*, 133, 704-15.
- MARTELLI, L., DI MARIO, F., BOTTI, P., RAGAZZI, E., MARTELLI, M. & KELLAND, L. 2007. Accumulation, platinum-DNA adduct formation and cytotoxicity of cisplatin, oxaliplatin and satraplatin in sensitive and resistant human osteosarcoma cell lines, characterized by p53 wild-type status. *Biochem Pharmacol*, 74, 20-7.
- MATSUSHIMA, K., LARSEN, C. G., DUBOIS, G. C. & OPPENHEIM, J. J. 1989. Purification and characterization of a novel monocyte chemotactic and activating factor produced by a human myelomonocytic cell line. *J Exp Med*, 169, 1485-90.
- MCDONALD, S., GRAHAM, T., SCHIER, S., WRIGHT, N. & ALISON, M. 2009. Stem cells and solid cancers. *Virchows Archiv*, 455, 1-13.
- MEIJER, C., MULDER, N., HOSPERS, G., UGES, D. & DE VRIES, E. 1990. The role of glutathione in resistance to cisplatin in a human small cell lung cancer cell line. *British Journal of Cancer*, 62, 72.
- MELLADO, M., RODRÍGUEZ-FRADE, J. M., VILA-CORO, A. J., FERNÁNDEZ, S., MARTÍN DE ANA, A., JONES, D. R., TORÁN, J. L. & MARTÍNEZ-A, C. 2001. Chemokine receptor homo- or heterodimerization activates distinct signaling pathways. *The EMBO journal*, 20, 2497-2507.
- MENDEZ-FERRER, S., MICHURINA, T. V., FERRARO, F., MAZLOOM, A. R., MACARTHUR, B. D., LIRA, S. A., SCADDEN, D. T., MA'AYAN, A., ENIKOLOPOV, G. N. & FRENETTE, P. S. 2010. Mesenchymal and haematopoietic stem cells form a unique bone marrow niche. *Nature*, 466, 829-34.
- MIJII, L. N., PETRILLI, A. S., DI CESARE, S., ODASHIRO, A. N., BURNIER, M. N., JR., DE TOLEDO, S. R., GARCIA, R. J. & ALVES, M. T. 2011. C-kit expression in human osteosarcoma and in vitro assays. *Int J Clin Exp Pathol*, 4, 775-81.

- MILLER, C. W., ASLO, A., WON, A., TAN, M., LAMPKIN, B. & KOEFFLER, H. P. 1996. Alterations of the p53, Rb and MDM2 genes in osteosarcoma. *J Cancer Res Clin Oncol*, 122, 559-65.
- MINOTTI, G., MENNA, P., SALVATORELLI, E., CAIRO, G. & GIANNI, L. 2004. Anthracyclines: molecular advances and pharmacologic developments in antitumor activity and cardiotoxicity. *Pharmacological reviews*, 56, 185-229.
- MIRZADEGAN, T., DIEHL, F., EBI, B., BHAKTA, S., POLSKY, I., MCCARLEY, D., MULKINS, M., WEATHERHEAD, G. S., LAPIERRE, J.-M. & DANKWARDT, J. 2000. Identification of the binding site for a novel class of CCR2b chemokine receptor antagonists binding to a common chemokine receptor motif within the helical bundle. *Journal of Biological Chemistry*, 275, 25562-25571.
- MISCHEL, P. S., CLOUGHESY, T. F. & NELSON, S. F. 2004. DNA-microarray analysis of brain cancer: molecular classification for therapy. *Nat Rev Neurosci*, 5, 782-92.
- MITALIPOV, S. & WOLF, D. 2009. Totipotency, pluripotency and nuclear reprogramming. *Engineering of Stem Cells*, 185-199.
- MOFFAT, J., GRUENEBERG, D. A., YANG, X., KIM, S. Y., KLOEPFER, A. M., HINKLE, G., PIQANI, B., EISENHAURE, T. M., LUO, B. & GRENIER, J. K. 2006. A lentiviral RNAi library for human and mouse genes applied to an arrayed viral high-content screen. *Cell*, 124, 1283-1298.
- MOHSENY, A. B., MACHADO, I., CAI, Y., SCHAEFER, K.-L., SERRA, M., HOGENDOORN, P. C. W., LLOMBART-BOSCH, A. & CLETON-JANSEN, A.-M. 2011. Functional characterization of osteosarcoma cell lines provides representative models to study the human disease. *Laboratory Investigation*, 91, 1195-1205.
- MOLLOY, A. P., MARTIN, F. T., DWYER, R. M., GRIFFIN, T. P., MURPHY, M., BARRY, F. P., O'BRIEN, T. & KERIN, M. J. 2009. Mesenchymal stem cell secretion of chemokines during differentiation into osteoblasts, and their potential role in mediating interactions with breast cancer cells. *International Journal of Cancer*, 124, 326-332.
- MOREB, J. S., UCAR, D., HAN, S., AMORY, J. K., GOLDSTEIN, A. S., OSTMARK, B. & CHANG, L.-J. 2012. The enzymatic activity of human aldehyde dehydrogenases 1A2 and 2 (ALDH1A2 and ALDH2) is detected by Aldefluor, inhibited by diethylaminobenzaldehyde and has significant effects on cell proliferation and drug resistance. *Chemico-biological interactions*, 195, 52-60.
- MOREL, A.-P., LIÃ VRE, M., THOMAS, C. M., HINKAL, G., ANSIEAU, S. P. & PUISIEUX, A. 2008. Generation of breast cancer stem cells through epithelial-mesenchymal transition. *PloS one*, 3, e2888.
- MUELLER, M. M. & FUSENIG, N. E. 2004. Friends or foes - bipolar effects of the tumour stroma in cancer. *Nat Rev Cancer*, 4, 839-49.
- NAM, J. S., KANG, M. J., SUCHAR, A. M., SHIMAMURA, T., KOHN, E. A., MICHALOWSKA, A. M., JORDAN, V. C., HIROHASHI, S. & WAKEFIELD, L. M. 2006. Chemokine (C-C motif) ligand 2 mediates the prometastatic effect of dysadherin in human breast cancer cells. *Cancer Res*, 66, 7176-84.
- NEVE, R. M., CHIN, K., FRIDLAND, J., YEH, J., BAEHNER, F. L., FEVR, T., CLARK, L., BAYANI, N., COPPE, J. P., TONG, F., SPEED, T., SPELLMAN, P. T., DEVRIES, S., LAPUK, A., WANG, N. J., KUO, W. L., STILWELL, J. L., PINKEL, D., ALBERTSON, D. G., WALDMAN, F. M., MCCORMICK, F., DICKSON, R. B., JOHNSON, M. D., LIPPMAN, M., ETHIER, S., GAZDAR, A. & GRAY, J. W. 2006. A collection of breast cancer cell lines for the study of functionally distinct cancer subtypes. *Cancer Cell*, 10, 515-27.
- NIINAKA, Y., HARADA, K., FUJIMURO, M., ODA, M., HAGA, A., HOSOKI, M., UZAWA, N., ARAI, N., YAMAGUCHI, S., YAMASHIRO, M. & RAZ, A. 2010. Silencing of autocrine motility factor induces mesenchymal-to-epithelial transition and suppression of osteosarcoma pulmonary metastasis. *Cancer Res*, 70, 9483-93.
- NIWA, Y., AKAMATSU, H., NIWA, H., SUMI, H., OZAKI, Y. & ABE, A. 2001. Correlation of tissue and plasma RANTES levels with disease course in patients with breast or cervical cancer. *Clinical Cancer Research*, 7, 285-289.
- ODOUX, C., FOHRER, H., HOPPO, T., GUZIK, L., STOLZ, D. B., LEWIS, D. W., GOLLIN, S. M., GAMBLIN, T. C., GELLER, D. A. & LAGASSE, E. 2008. A stochastic model for cancer stem cell origin in metastatic colon cancer. *Cancer Res*, 68, 6932-41.
- OKITA, K., ICHISAKA, T. & YAMANAKA, S. 2007. Generation of germline-competent induced pluripotent stem cells. *Nature*, 448, 313-7.
- ORIMO, A., GUPTA, P. B., SGROI, D. C., ARENZANA-SEISDEDOS, F., DELAUNAY, T., NAEEM, R., CAREY, V. J., RICHARDSON, A. L. & WEINBERG, R. A. 2005. Stromal fibroblasts present in invasive human breast carcinomas promote tumor growth and angiogenesis through elevated SDF-1/CXCL12 secretion. *Cell*, 121, 335-348.

- ORSI, N. & TRIBE, R. 2008. Cytokine networks and the regulation of uterine function in pregnancy and parturition. *Journal of neuroendocrinology*, 20, 462-469.
- ORY, B., BLANCHARD, F., BATTAGLIA, S., GOUIN, F., REDINI, F. & HEYMANN, D. 2007. Zoledronic acid activates the DNA S-phase checkpoint and induces osteosarcoma cell death characterized by apoptosis-inducing factor and endonuclease-G translocation independently of p53 and retinoblastoma status. *Molecular pharmacology*, 71, 333-343.
- OTTAVIANO, L., SCHAEFER, K. L., GAJEWSKI, M., HUCKENBECK, W., BALDUS, S., ROGEL, U., MACKINTOSH, C., DE ALAVA, E., MYKLEBOST, O. & KRESSE, S. H. 2010. Molecular characterization of commonly used cell lines for bone tumor research: A trans European EuroBoNet effort. *Genes, Chromosomes and Cancer*, 49, 40-51.
- OWENS, M. A., HORTEN, B. C. & DA SILVA, M. M. 2004. HER2 amplification ratios by fluorescence in situ hybridization and correlation with immunohistochemistry in a cohort of 6556 breast cancer tissues. *Clin Breast Cancer*, 5, 63-9.
- PAPPA, A., BROWN, D., KOUTALOS, Y., DEGREGORI, J., WHITE, C. & VASILIOU, V. 2005. Human aldehyde dehydrogenase 3A1 inhibits proliferation and promotes survival of human corneal epithelial cells. *Journal of Biological Chemistry*, 280, 27998-28006.
- PARK, C. H., BERGSAGEL, D. E. & MCCULLOCH, E. A. 1971. Mouse myeloma tumor stem cells: a primary cell culture assay. *J Natl Cancer Inst*, 46, 411-22.
- PARK, J. H., LEE, Y. S. & KIM, S. H. 2011a. Depletion of Neuroguidin/CANu1 sensitizes human osteosarcoma U2OS cells to doxorubicin. *Biochemistry and Molecular Biology Reports*, 44, 46-51.
- PARK, S. H., CASAGRANDE, F., CHO, L., ALBRECHT, L. & OPELLA, S. J. 2011b. Interactions of interleukin-8 with the human chemokine receptor CXCR1 in phospholipid bilayers by NMR spectroscopy. *J Mol Biol*, 414, 194-203.
- PASELLO, M., MICHELACCI, F., SCIONTI, I., HATTINGER, C. M., ZUNTINI, M., CACCURI, A. M., SCOTLANDI, K., PICCI, P. & SERRA, M. 2008. Overcoming Glutathione S-Transferase P1-Related Cisplatin Resistance in Osteosarcoma. *Cancer research*, 68, 6661-6668.
- PATEL, S. A., NDBAHALIYE, A., LIM, P. K., MILTON, R. & RAMESHWAR, P. 2010. Challenges in the development of future treatments for breast cancer stem cells. *Breast Cancer (London)*, 2, 1-11.
- PEARCE, D., TAUSSIG, D., SIMPSON, C., ALLEN, K., ROHATINER, A., LISTER, T. & BONNET, D. 2005. Characterization of cells with a high aldehyde dehydrogenase activity from cord blood and acute myeloid leukemia samples. *Stem Cells*, 23, 752-760.
- PEREGO, P., CASERINI, C., GATTI, L., CARENINI, N., ROMANELLI, S., SUPINO, R., COLANGELO, D., VIANO, I., LEONE, R., SPINELLI, S., PEZZONI, G., MANZOTTI, C., FARRELL, N. & ZUNINO, F. 1999. A novel trinuclear platinum complex overcomes cisplatin resistance in an osteosarcoma cell system. *Mol Pharmacol*, 55, 528-34.
- PETRILLI, A. S., DE CAMARGO, B., FILHO, V. O., BRUNIERA, P., BRUNETTO, A. L., JESUS-GARCIA, R., CAMARGO, O. P., PENA, W., PERICLES, P., DAVI, A., PROSPERO, J. D., ALVES, M. T., OLIVEIRA, C. R., MACEDO, C. R., MENDES, W. L., ALMEIDA, M. T., BORSATO, M. L., DOS SANTOS, T. M., ORTEGA, J. & CONSENTINO, E. 2006. Results of the Brazilian Osteosarcoma Treatment Group Studies III and IV: prognostic factors and impact on survival. *J Clin Oncol*, 24, 1161-8.
- PICCART-GEHBART, M. J., PROCTER, M., LEYLAND-JONES, B., GOLDBIRSCHE, A., UNTCH, M., SMITH, I., GIANNI, L., BASELGA, J., BELL, R., JACKISCH, C., CAMERON, D., DOWSETT, M., BARRIOS, C. H., STEGER, G., HUANG, C. S., ANDERSSON, M., INBAR, M., LICHINITSER, M., LANG, I., NITZ, U., IWATA, H., THOMSEN, C., LOHRISCH, C., SUTER, T. M., RUSCHOFF, J., SUTO, T., GREATORREX, V., WARD, C., STRAEHLE, C., MCFADDEN, E., DOLCI, M. S. & GELBER, R. D. 2005. Trastuzumab after adjuvant chemotherapy in HER2-positive breast cancer. *N Engl J Med*, 353, 1659-72.
- PITTENGER, M. F., MACKAY, A. M., BECK, S. C., JAISWAL, R. K., DOUGLAS, R., MOSCA, J. D., MOORMAN, M. A., SIMONETTI, D. W., CRAIG, S. & MARSHAK, D. R. 1999. Multilineage potential of adult human mesenchymal stem cells. *Science*, 284, 143-7.
- POLLARD, J. W. 2004. Tumour-educated macrophages promote tumour progression and metastasis. *Nature Reviews Cancer*, 4, 71-78.
- POTAPOVA, I., PLOTNIKOV, A., LU, Z., DANILO, P., VALIUNAS, V., QU, J., DORONIN, S., ZUCKERMAN, J., SHLAPAKOVA, I. N. & GAO, J. 2004. Human mesenchymal stem cells as a gene delivery system to create cardiac pacemakers. *Circulation research*, 94, 952-959.
- PRASMICKAITE, L., ENGESÆTER, B. Ø., SKRBO, N., HELLENES, T., KRISTIAN, A., OLIVER, N. K., SUO, Z. & MÆLANDSMO, G. M. 2010. Aldehyde dehydrogenase (ALDH) activity does not select for cells with enhanced aggressive properties in malignant melanoma. *PLoS One*, 5, e10731.

- PRINCE, M. E., SIVANANDAN, R., KACZOROWSKI, A., WOLF, G. T., KAPLAN, M. J., DALERBA, P., WEISSMAN, I. L., CLARKE, M. F. & AILLES, L. E. 2007. Identification of a subpopulation of cells with cancer stem cell properties in head and neck squamous cell carcinoma. *Proc Natl Acad Sci U S A*, 104, 973-8.
- QIAN, B.-Z., LI, J., ZHANG, H., KITAMURA, T., ZHANG, J., CAMPION, L. R., KAISER, E. A., SNYDER, L. A. & POLLARD, J. W. 2011. CCL2 recruits inflammatory monocytes to facilitate breast-tumour metastasis. *Nature*, 475, 222-225.
- RAINUSSO, N., MAN, T.-K., LAU, C. C., HICKS, J., SHEN, J. J., YU, A., WANG, L. L. & ROSEN, J. M. 2011. Identification and gene expression profiling of tumor-initiating cells isolated from human osteosarcoma cell lines in an orthotopic mouse model. *Cancer biology & therapy*, 12, 278-287.
- RAJKUMAR, T. & YAMUNA, M. 2008. Multiple pathways are involved in drug resistance to doxorubicin in an osteosarcoma cell line. *Anti-cancer drugs*, 19, 257-265.
- REN, D., MINAMI, Y. & NISHITA, M. 2011. Critical role of Wnt5a-Ror2 signaling in motility and invasiveness of carcinoma cells following Snail-mediated epithelial-mesenchymal transition. *Genes Cells*, 16, 304-15.
- REN, R. 2005. Mechanisms of BCR-ABL in the pathogenesis of chronic myelogenous leukaemia. *Nat Rev Cancer*, 5, 172-83.
- REYA, T., MORRISON, S., CLARKE, M. & WEISSMAN, I. 2001. Stem cells, cancer, and cancer stem cells. *Nature*, 414, 105-111.
- REYNOLDS, B. A., TETZLAFF, W. & WEISS, S. 1992. A multipotent EGF-responsive striatal embryonic progenitor cell produces neurons and astrocytes. *The Journal of neuroscience*, 12, 4565-4574.
- REYNOLDS, B. A. & WEISS, S. 1992. Generation of neurons and astrocytes from isolated cells of the adult mammalian central nervous system. *science*, 255, 1707-1710.
- RHIM, J. S., PUTMAN, D. L., ARNSTEIN, P., HUEBNER, R. J. & MCALLISTER, R. M. 1977. Characterization of human cells transformed in vitro by N-methyl-N'-nitro-N-nitrosoguanidine. *International journal of cancer*, 19, 505-510.
- RIGGI, N., CIRONI, L., PROVERO, P., SUVÀ, M., KALOULIS, K., GARCIA-ECHEVERRIA, C., HOFFMANN, F., TRUMPP, A. & STAMENKOVIC, I. 2005. Development of Ewing's Sarcoma from Primary Bone Marrow-Derived Mesenchymal Progenitor Cells. *Cancer research*, 65, 11459.
- ROCHET, N., DUBOUSSET, J., MAZEAU, C., ZANGHELLINI, E., FARGES, M. F., DE NOVION, H. S., CHOMPRET, A., DELPECH, B., CATTAN, N., FRENAY, M. & GIOANNI, J. 1999. Establishment, characterisation and partial cytokine expression profile of a new human osteosarcoma cell line (CAL 72). *Int J Cancer*, 82, 282-5.
- ROOT, D. E., HACOEN, N., HAHN, W. C., LANDER, E. S. & SABATINI, D. M. 2006. Genome-scale loss-of-function screening with a lentiviral RNAi library. *Nature methods*, 3, 715-719.
- ROSENBERG, B., VAN CAMP, L. & KRIGAS, T. 1965. Inhibition of cell division in Escherichia coli by electrolysis products from a platinum electrode. *Nature*, 205, 698-699.
- ROSENBERG, B. & VANCAMP, L. 1969. Platinum compounds: a new class of potent antitumour agents. *Nature*, 222, 385-386.
- RUBIO, R., ABARRATEGI, A., GARCIA-CASTRO, J., MARTINEZ-CRUZADO, L., SUAREZ, C., TORNIN, J., SANTOS, L., ASTUDILLO, A., COLMENERO, I. & MULERO, F. 2014. Bone environment is essential for osteosarcoma development from transformed mesenchymal stem cells. *Stem Cells*.
- RUSCONI, F., DURAND-DUBIEF, M. & BASTIN, P. 2005. Functional complementation of RNA interference mutants in trypanosomes. *BMC biotechnology*, 5, 6.
- SALVATORI, L., CAPORUSCIO, F., VERDINA, A., STARACE, G., CRISPI, S., NICOTRA, M. R., RUSSO, A., CALOGERO, R. A., MORGANTE, E., NATALI, P. G., RUSSO, M. A. & PETRANGELI, E. 2012. Cell-to-cell signaling influences the fate of prostate cancer stem cells and their potential to generate more aggressive tumors. *PLoS One*, 7, e31467.
- SANTINI, M. T., ROMANO, R., RAINALDI, G., FILIPPINI, P., BRAVO, E., PORCU, L., MOTTA, A., CALCABRINI, A., MESCHINI, S. & INDOVINA, P. L. 2001. The relationship between <sup>1</sup>H-NMR mobile lipid intensity and cholesterol in two human tumor multidrug resistant cell lines (MCF-7 and LoVo). *Biochimica et Biophysica Acta (BBA)-Molecular and Cell Biology of Lipids*, 1531, 111-131.
- SARAFI, M. N., GARCIA-ZEPEDA, E. A., MACLEAN, J. A., CHARO, I. F. & LUSTER, A. D. 1997. Murine monocyte chemoattractant protein (MCP)-5: a novel CC chemokine that is a structural and functional homologue of human MCP-1. *The Journal of experimental medicine*, 185, 99-110.
- SAUER, B. 1987. Functional expression of the cre-lox site-specific recombination system in the yeast *Saccharomyces cerevisiae*. *Mol Cell Biol*, 7, 2087-96.
- SAWYERS, C. L. 1999. Chronic myeloid leukemia. *N Engl J Med*, 340, 1330-40.



- SCHAJOWICZ, F., SISSONS, H. & SOBIN, L. 1995. The World Health Organization's histologic classification of bone tumors. *Cancer*, 75, 1208-1214.
- SCHOPPET, M., PREISSNER, K. T. & HOFBAUER, L. C. 2002. RANK ligand and osteoprotegerin: paracrine regulators of bone metabolism and vascular function. *Arterioscler Thromb Vasc Biol*, 22, 549-53.
- SCIONTI, I., MICHELACCI, F., PASELLO, M., HATTINGER, C. M., ALBERGHINI, M., MANARA, M. C., BACCI, G., FERRARI, S., SCOTLANDI, K., PICCI, P. & SERRA, M. 2008. Clinical impact of the methotrexate resistance-associated genes C-MYC and dihydrofolate reductase (DHFR) in high-grade osteosarcoma. *Ann Oncol*, 19, 1500-8.
- SERRA, M., REVERTER-BRANCHAT, G., MAURICI, D., BENINI, S., SHEN, J.-N., CHANO, T., HATTINGER, C.-M., MANARA, M.-C., PASELLO, M. & SCOTLANDI, K. 2004. Analysis of dihydrofolate reductase and reduced folate carrier gene status in relation to methotrexate resistance in osteosarcoma cells. *Annals of oncology*, 15, 151-160.
- SHAPIRO, C. L., HARDENBERGH, P. H., GELMAN, R., BLANKS, D., HAUPTMAN, P., RECHT, A., HAYES, D. F., HARRIS, J. & HENDERSON, I. C. 1998. Cardiac effects of adjuvant doxorubicin and radiation therapy in breast cancer patients. *J Clin Oncol*, 16, 3493-501.
- SHI, S. & GRONTHOS, S. 2003. Perivascular niche of postnatal mesenchymal stem cells in human bone marrow and dental pulp. *J Bone Miner Res*, 18, 696-704.
- SICLARI, V. & QIN, L. 2010. Targeting the osteosarcoma cancer stem cell. *Journal of Orthopaedic Surgery and Research*, 5, 78.
- SIDDIK, Z. H. 2003. Cisplatin: mode of cytotoxic action and molecular basis of resistance. *Oncogene*, 22, 7265-7279.
- SIITONEN, S. M., KONONEN, J. T., HELIN, H. J., RANTALA, I. S., HOLLI, K. A. & ISOLA, J. J. 1996. Reduced E-cadherin expression is associated with invasiveness and unfavorable prognosis in breast cancer. *Am J Clin Pathol*, 105, 394-402.
- SIMONET, W. S., LACEY, D. L., DUNSTAN, C. R., KELLEY, M., CHANG, M. S., LUTHY, R., NGUYEN, H. Q., WOODEN, S., BENNETT, L., BOONE, T., SHIMAMOTO, G., DEROSE, M., ELLIOTT, R., COLOMBERO, A., TAN, H. L., TRAIL, G., SULLIVAN, J., DAVY, E., BUCAY, N., RENSHAW-GEGG, L., HUGHES, T. M., HILL, D., PATTISON, W., CAMPBELL, P., SANDER, S., VAN, G., TARPLEY, J., DERBY, P., LEE, R. & BOYLE, W. J. 1997. Osteoprotegerin: a novel secreted protein involved in the regulation of bone density. *Cell*, 89, 309-19.
- SIMPSON, C. D., ANYIWE, K. & SCHIMMER, A. D. 2008. Anoikis resistance and tumor metastasis. *Cancer letters*, 272, 177-185.
- SINGAL, P. K. & ILISKOVIC, N. 1998. Doxorubicin-induced cardiomyopathy. *N Engl J Med*, 339, 900-5.
- SINGH, A. B. & HARRIS, R. C. 2005. Autocrine, paracrine and juxtacrine signaling by EGFR ligands. *Cell Signal*, 17, 1183-93.
- SINGH, J. K., FARNIE, G., BUNDRED, N. J., SIMOES, B. M., SHERGILL, A., LANDBERG, G., HOWELL, S. J. & CLARKE, R. B. 2013. Targeting CXCR1/2 significantly reduces breast cancer stem cell activity and increases the efficacy of inhibiting HER2 via HER2-dependent and -independent mechanisms. *Clin Cancer Res*, 19, 643-56.
- SLADEK, N. E. 2003. Human aldehyde dehydrogenases: potential pathological, pharmacological, and toxicological impact. *J Biochem Mol Toxicol*, 17, 7-23.
- SOHY, D., YANO, H., DE NADAI, P., URIZAR, E., GUILLABERT, A., JAVITCH, J. A., PARMENTIER, M. & SPRINGAEL, J.-Y. 2009. Hetero-oligomerization of CCR2, CCR5, and CXCR4 and the protean effects of "selective" antagonists. *Journal of Biological Chemistry*, 284, 31270-31279.
- SOMMERS, C. L., BYERS, S. W., THOMPSON, E. W., TORRI, J. A. & GELMANN, E. P. 1994. Differentiation state and invasiveness of human breast cancer cell lines. *Breast Cancer Res Treat*, 31, 325-35.
- SONG, B., WANG, Y., TITMUS, M. A., BOTCHKINA, G., FORMENTINI, A., KORNMANN, M. & JU, J. 2010. Research Molecular mechanism of chemoresistance by miR-215 in osteosarcoma and colon cancer cells. *Mol Cancer*, 9, 96.
- SORLIE, T., PEROU, C. M., FAN, C., GEISLER, S., AAS, T., NOBEL, A., ANKER, G., AKSLEN, L. A., BOTSTEIN, D., BORRESEN-DALE, A. L. & LONNING, P. E. 2006. Gene expression profiles do not consistently predict the clinical treatment response in locally advanced breast cancer. *Mol Cancer Ther*, 5, 2914-8.
- SOULE, H., VAZQUEZ, J., LONG, A., ALBERT, S. & BRENNAN, M. 1973. A human cell line from a pleural effusion derived from a breast carcinoma. *Journal of the National Cancer Institute*, 51, 1409-1416.
- SPAETH, E. L., DEMBINSKI, J. L., SASSER, A. K., WATSON, K., KLOPP, A., HALL, B., ANDREEFF, M. & MARINI, F. 2009. Mesenchymal stem cell transition to tumor-associated fibroblasts contributes to fibrovascular network expansion and tumor progression. *PLoS One*, 4, e4992.

- SPRADLING, A., DRUMMOND-BARBOSA, D. & KAI, T. 2001. Stem cells find their niche. *Nature*, 414, 98-104.
- STAMENKOVIC, I., AMIOT, M., PESANDO, J. M. & SEED, B. 1989. A lymphocyte molecule implicated in lymph node homing is a member of the cartilage link protein family. *Cell*, 56, 1057-62.
- STEFANSKA, B., HUANG, J., BHATTACHARYYA, B., SUDERMAN, M., HALLETT, M., HAN, Z. G. & SZYF, M. 2011. Definition of the landscape of promoter DNA hypomethylation in liver cancer. *Cancer Res*, 71, 5891-903.
- STEINERT, P. M. & ROOP, D. R. 1988. Molecular and cellular biology of intermediate filaments. *Annual review of biochemistry*, 57, 593-625.
- STROHMEYER, T., PETER, S., HARTMANN, M., MUNEMITSU, S., ACKERMANN, R., ULLRICH, A. & SLAMON, D. J. 1991. Expression of the hst-1 and c-kit protooncogenes in human testicular germ cell tumors. *Cancer Res*, 51, 1811-6.
- SULZBACHER, I., BIRNER, P., TOMA, C., WICK, N. & MAZAL, P. R. 2007. Expression of c-kit in human osteosarcoma and its relevance as a prognostic marker. *Journal of clinical pathology*, 60, 804-807.
- TAKAHASHI, H., NAKAYAMA, R., HAYASHI, S., NEMOTO, T., MURASE, Y., NOMURA, K., TAKAHASHI, T., KUBO, K., MARUI, S. & YASUHARA, K. 2013. Macrophage Migration Inhibitory Factor and Stearoyl-CoA Desaturase 1: Potential Prognostic Markers for Soft Tissue Sarcomas Based on Bioinformatics Analyses. *PLoS One*, 8, e78250.
- TAKEBE, N., ZHAO, S.-C., ADHIKARI, D., MINEISHI, S., SADELAIN, M., HILTON, J., COLVIN, M., BANERJEE, D. & BERTINO, J. R. 2001. Generation of dual resistance to 4-hydroperoxycyclophosphamide and methotrexate by retroviral transfer of the human aldehyde dehydrogenase class 1 gene and a mutated dihydrofolate reductase gene. *Molecular Therapy*, 3, 88-96.
- TAKEICHI, M. 1995. Morphogenetic roles of classic cadherins. *Curr Opin Cell Biol*, 7, 619-27.
- TAMAI, K., SEMENOV, M., KATO, Y., SPOKONY, R., LIU, C., KATSUYAMA, Y., HESS, F., SAINT-JEANNET, J. P. & HE, X. 2000. LDL-receptor-related proteins in Wnt signal transduction. *Nature*, 407, 530-5.
- TANG, N., SONG, W., LUO, J., HAYDON, R. & HE, T. 2008. Osteosarcoma development and stem cell differentiation. *Clinical Orthopaedics and Related Research*®, 466, 2114-2130.
- TANG, Q. L., LIANG, Y., XIE, X. B., YIN, J. Q., ZOU, C. Y., ZHAO, Z. Q., SHEN, J. N. & WANG, J. 2011. Enrichment of osteosarcoma stem cells by chemotherapy. *Chin J Cancer*, 30, 426-32.
- TENG, M. W., ANDREWS, D. M., MCLAUGHLIN, N., VON SCHEIDT, B., NGIOW, S. F., MÖLLER, A., HILL, G. R., IWAKURA, Y., OFT, M. & SMYTH, M. J. 2010. IL-23 suppresses innate immune response independently of IL-17A during carcinogenesis and metastasis. *Proceedings of the National Academy of Sciences*, 107, 8328-8333.
- TERASHIMA, Y., ONAI, N., MURAI, M., ENOMOTO, M., POONPIRIYA, V., HAMADA, T., MOTOMURA, K., SUWA, M., EZAKI, T., HAGA, T., KANEGASAKI, S. & MATSUSHIMA, K. 2005. Pivotal function for cytoplasmic protein FROUNT in CCR2-mediated monocyte chemotaxis. *Nat Immunol*, 6, 827-35.
- THIERY, J. P. 2002. Epithelial-mesenchymal transitions in tumour progression. *Nat Rev Cancer*, 2, 442-54.
- THOMAS, D. M., CARTY, S. A., PISCOPO, D. M., LEE, J. S., WANG, W. F., FORRESTER, W. C. & HINDS, P. W. 2001. The retinoblastoma protein acts as a transcriptional coactivator required for osteogenic differentiation. *Mol Cell*, 8, 303-16.
- THORPE, C. J., SCHLESINGER, A. & BOWERMAN, B. 2000. Wnt signalling in *Caenorhabditis elegans*: regulating repressors and polarizing the cytoskeleton. *Trends in cell biology*, 10, 10-17.
- TIEMANN, F. & HINDS, P. W. 1998. Induction of DNA synthesis and apoptosis by regulated inactivation of a temperature-sensitive retinoblastoma protein. *Embo J*, 17, 1040-52.
- TIRINO, V. & DESIDERIO, V. 2008. Detection and characterization of CD133+ cancer stem cells in human solid tumours. *PLoS One*, 3, 3469.
- TSANG, W. P., HO, F. Y., FUNG, K. P., KONG, S. K. & KWOK, T. T. 2005. p53-R175H mutant gains new function in regulation of doxorubicin-induced apoptosis. *Int J Cancer*, 114, 331-6.
- TSUYADA, A., CHOW, A., WU, J., SOMLO, G., CHU, P., LOERA, S., LUU, T., LI, A. X., WU, X., YE, W., CHEN, S., ZHOU, W., YU, Y., WANG, Y. Z., REN, X., LI, H., SCHERLE, P., KUROKI, Y. & WANG, S. E. 2012. CCL2 mediates cross-talk between cancer cells and stromal fibroblasts that regulates breast cancer stem cells. *Cancer Res*, 72, 2768-79.
- TUDOR, D., LOCKE, M., OWEN-JONES, E. & MACKENZIE, I. C. 2004. Intrinsic patterns of behavior of epithelial stem cells. *J Investig Dermatol Symp Proc*, 9, 208-14.
- UCHINO, M., KOJIMA, H., WADA, K., IMADA, M., ONODA, F., SATOFUKA, H., UTSUGI, T. & MURAKAMI, Y. 2010. Nuclear beta-catenin and CD44 upregulation characterize invasive cell populations in non-aggressive MCF-7 breast cancer cells. *BMC cancer*, 10, 414.

- UMBAS, R., ISAACS, W. B., BRINGUIER, P. P., SCHAAFSMA, H. E., KARTHAUS, H. F., OOSTERHOF, G. O., DEBRUYNE, F. M. & SCHALKEN, J. A. 1994. Decreased E-cadherin expression is associated with poor prognosis in patients with prostate cancer. *Cancer Res*, 54, 3929-33.
- VACHON, E., MARTIN, R., PLUMB, J., KWOK, V., VANDIVIER, R. W., GLOGAUER, M., KAPUS, A., WANG, X., CHOW, C.-W. & GRINSTEIN, S. 2006. CD44 is a phagocytic receptor. *Blood*, 107, 4149-4158.
- VALENT, P., BONNET, D., DE MARIA, R., LAPIDOT, T., COPLAND, M., MELO, J. V., CHOMIENNE, C., ISHIKAWA, F., SCHURINGA, J. J., STASSI, G., HUNTLY, B., HERRMANN, H., SOULIER, J., ROESCH, A., SCHUURHUIS, G. J., WOHRER, S., AROCK, M., ZUBER, J., CERNY-REITERER, S., JOHNSEN, H. E., ANDREEFF, M. & EAVES, C. 2012. Cancer stem cell definitions and terminology: the devil is in the details. *Nat Rev Cancer*, 12, 767-75.
- VAN EWIJK, W., COFFMAN, R. C. & WEISSMAN, I. L. 1980. Immunoelectron microscopy of cell surface antigens: a quantitative analysis of antibody binding after different fixation protocols. *The Histochemical Journal*, 12, 349-361.
- VARDIMAN, J. W., THIELE, J., ARBER, D. A., BRUNNING, R. D., BOROWITZ, M. J., PORWIT, A., HARRIS, N. L., LE BEAU, M. M., HELLSTROM-LINDBERG, E., TEFFERI, A. & BLOOMFIELD, C. D. 2009. The 2008 revision of the World Health Organization (WHO) classification of myeloid neoplasms and acute leukemia: rationale and important changes. *Blood*, 114, 937-51.
- VARGO-GOGOLA, T. & ROSEN, J. M. 2007. Modelling breast cancer: one size does not fit all. *Nat Rev Cancer*, 7, 659-72.
- VERMEULEN, S. J., BRUYNEEL, E. A., VAN ROY, F. M., MAREEL, M. M. & BRACKE, M. E. 1995. Activation of the E-cadherin/catenin complex in human MCF-7 breast cancer cells by all-trans-retinoic acid. *Br J Cancer*, 72, 1447-53.
- VESELSKA, R., HERMANOVA, M., LOJA, T., CHLAPEK, P., ZAMBO, I., VESELY, K., ZITTERBART, K. & STERBA, J. 2008. Nestin expression in osteosarcomas and derivation of nestin/CD133 positive osteosarcoma cell lines. *BMC cancer*, 8, 300.
- VISVADER, J. E. & LINDEMAN, G. J. 2008. Cancer stem cells in solid tumours: accumulating evidence and unresolved questions. *Nat Rev Cancer*, 8, 755-68.
- VOLPE, S., CAMERONI, E., MOEPPS, B., THELEN, S., APUZZO, T. & THELEN, M. 2012. CCR2 acts as scavenger for CCL2 during monocyte chemotaxis. *PLoS One*, 7, e37208.
- VON SCHLIPPE, M., MARSHALL, J. F., PERRY, P., STONE, M., ZHU, A. J. & HART, I. R. 2000. Functional interaction between E-cadherin and alpha-v-containing integrins in carcinoma cells. *J Cell Sci*, 113 ( Pt 3), 425-37.
- WANG, L., PARK, P. & LIN, C. 2009. Characterization of stem cell attributes in human osteosarcoma cell lines. *Cancer biology & therapy*, 8.
- WANG, L., PARK, P., ZHANG, H., LA MARCA, F. & LIN, C. Y. 2011. Prospective identification of tumorigenic osteosarcoma cancer stem cells in OS99-1 cells based on high aldehyde dehydrogenase activity. *Int J Cancer*, 128, 294-303.
- WANG, S.-W., WU, H.-H., LIU, S.-C., WANG, P.-C., OU, W.-C., CHOU, W.-Y., SHEN, Y.-S. & TANG, C.-H. 2012. CCL5 and CCR5 interaction promotes cell motility in human osteosarcoma. *PLoS One*, 7, e35101.
- WANG, X. B., JIANG, X. R., YU, X. Y., WANG, L., HE, S., FENG, F. Y., GUO, L. P., JIANG, W. & LU, S. H. 2014. Macrophage inhibitory factor 1 acts as a potential biomarker in patients with esophageal squamous cell carcinoma and is a target for antibody-based therapy. *Cancer science*.
- WANG, Z. Q., LIANG, J., SCHELLANDER, K., WAGNER, E. F. & GRIGORIADIS, A. E. 1995. c-fos-induced osteosarcoma formation in transgenic mice: cooperativity with c-jun and the role of endogenous c-fos. *Cancer Res*, 55, 6244-51.
- WEAVER, V. M., PETERSEN, O. W., WANG, F., LARABELL, C. A., BRIAND, P., DAMSKY, C. & BISSELL, M. J. 1997. Reversion of the malignant phenotype of human breast cells in three-dimensional culture and in vivo by integrin blocking antibodies. *J Cell Biol*, 137, 231-45.
- WEBER, G. F., BRONSON, R. T., ILAGAN, J., CANTOR, H., SCHMITS, R. & MAK, T. W. 2002. Absence of the CD44 gene prevents sarcoma metastasis. *Cancer Research*, 62, 2281-2286.
- WEBSTER, G. A. & PERKINS, N. D. 1999. Transcriptional cross talk between NF-kB and p53. *Molecular and cellular biology*, 19, 3485-3495.
- WEINER, S., TRAUB, W. & WAGNER, H. D. 1999. Lamellar bone: structure-function relations. *Journal of structural biology*, 126, 241-255.
- WEISS, R. B. The anthracyclines: will we ever find a better doxorubicin? *Seminars in oncology*, 1992. 670-686.
- WEISSMAN, I. 2000. Stem Cells: Units of Development, Review Units of Regeneration, and Units in Evolution. *Cell*, 100, 157-168.
- WEN, P. Y. & KESARI, S. 2008. Malignant gliomas in adults. *N Engl J Med*, 359, 492-507.

- WESTLEY, B. & ROCHEFORT, H. 1980. A secreted glycoprotein induced by estrogen in human breast cancer cell lines. *Cell*, 20, 353-362.
- WILLIAMS, S. R., JIANG, Y., COCHRAN, D., DORSAM, G. & GRAVES, D. T. 1992. Regulated expression of monocyte chemoattractant protein-1 in normal human osteoblastic cells. *American Journal of Physiology-Cell Physiology*, 263, C194-C199.
- WU, P. K., CHEN, W. M., CHEN, C. F., LEE, O. K., HAUNG, C. K. & CHEN, T. H. 2009. Primary osteogenic sarcoma with pulmonary metastasis: clinical results and prognostic factors in 91 patients. *Japanese journal of clinical oncology*, 39, 514-522.
- XIE, X. K., YANG, D. S., YE, Z. M. & TAO, H. M. 2006. Recombinant antisense C-myc adenovirus increase in vitro sensitivity of osteosarcoma MG-63 cells to cisplatin. *Cancer Invest*, 24, 1-8.
- XU, Z.-Y., DING, S.-M., ZHOU, L., XIE, H.-Y., CHEN, K.-J., ZHANG, W., XING, C.-Y., GUO, H.-J. & ZHENG, S.-S. 2012. FOXC1 contributes to microvascular invasion in primary hepatocellular carcinoma via regulating epithelial-mesenchymal transition. *International journal of biological sciences*, 8, 1130.
- YAN, W., CHEN, Y., YAO, Y., ZHANG, H. & WANG, T. 2013. Increased invasion and tumorigenicity capacity of CD44+/CD24-breast cancer MCF7 cells in vitro and in nude mice. *Cancer cell international*, 13, 62.
- YANG, J., MANI, S. A. & WEINBERG, R. A. 2006. Exploring a new twist on tumor metastasis. *Cancer Res*, 66, 4549-52.
- YASUDA, H., SHIMA, N., NAKAGAWA, N., MOCHIZUKI, S. I., YANO, K., FUJISE, N., SATO, Y., GOTO, M., YAMAGUCHI, K., KURIYAMA, M., KANNO, T., MURAKAMI, A., TSUDA, E., MORINAGA, T. & HIGASHIO, K. 1998a. Identity of osteoclastogenesis inhibitory factor (OCIF) and osteoprotegerin (OPG): a mechanism by which OPG/OCIF inhibits osteoclastogenesis in vitro. *Endocrinology*, 139, 1329-37.
- YASUDA, H., SHIMA, N., NAKAGAWA, N., YAMAGUCHI, K., KINOSAKI, M., MOCHIZUKI, S., TOMOYASU, A., YANO, K., GOTO, M., MURAKAMI, A., TSUDA, E., MORINAGA, T., HIGASHIO, K., UDAGAWA, N., TAKAHASHI, N. & SUDA, T. 1998b. Osteoclast differentiation factor is a ligand for osteoprotegerin/osteoclastogenesis-inhibitory factor and is identical to TRANCE/RANKL. *Proc Natl Acad Sci U S A*, 95, 3597-602.
- YEN, C.-C. 2009. Osteosarcoma: is age an issue? *Journal of the Chinese Medical Association*, 72, 453-454.
- YOSHIMURA, T., MATSUSHIMA, K., TANAKA, S., ROBINSON, E. A., APPELLA, E., OPPENHEIM, J. J. & LEONARD, E. J. 1987. Purification of a human monocyte-derived neutrophil chemotactic factor that has peptide sequence similarity to other host defense cytokines. *Proc Natl Acad Sci U S A*, 84, 9233-7.
- YOUNGS, S. J., ALI, S. A., TAUB, D. D. & REES, R. C. 1997. Chemokines induce migrational responses in human breast carcinoma cell lines. *Int J Cancer*, 71, 257-66.
- YUAN, X., CURTIN, J., XIONG, Y., LIU, G., WASCHSMANN-HOGIU, S., FARKAS, D. L., BLACK, K. L. & JOHN, S. Y. 2004. Isolation of cancer stem cells from adult glioblastoma multiforme. *Oncogene*, 23, 9392-9400.
- ZACHARIAE, C. O., THESTRUP-PEDERSEN, K. & MATSUSHIMA, K. 1991. Expression and secretion of leukocyte chemotactic cytokines by normal human melanocytes and melanoma cells. *J Invest Dermatol*, 97, 593-9.
- ZAPPERI, S. & LA PORTA, C. A. 2012. Do cancer cells undergo phenotypic switching? The case for imperfect cancer stem cell markers. *Sci Rep*, 2, 441.
- ZHANG, M., BEHBOD, F., ATKINSON, R. L., LANDIS, M. D., KITTRELL, F., EDWARDS, D., MEDINA, D., TSIMELZON, A., HILSENBECK, S. & GREEN, J. E. 2008. Identification of tumor-initiating cells in a p53-null mouse model of breast cancer. *Cancer research*, 68, 4674-4682.
- ZHAO, Y., ZHANG, C.-L., ZENG, B.-F., WU, X.-S., GAO, T.-T. & ODA, Y. 2009. Enhanced chemosensitivity of drug-resistant osteosarcoma cells by lentivirus-mediated Bcl-2 silencing. *Biochemical and biophysical research communications*, 390, 642-647.
- ZIELSKE, S. P., SPALDING, A. C. & LAWRENCE, T. S. 2010. Loss of tumor-initiating cell activity in cyclophosphamide-treated breast xenografts. *Translational oncology*, 3, 149.
- ZOLLER, M. 2011. CD44: can a cancer-initiating cell profit from an abundantly expressed molecule? *Nat Rev Cancer*, 11, 254-67.

